

AD-A146 511

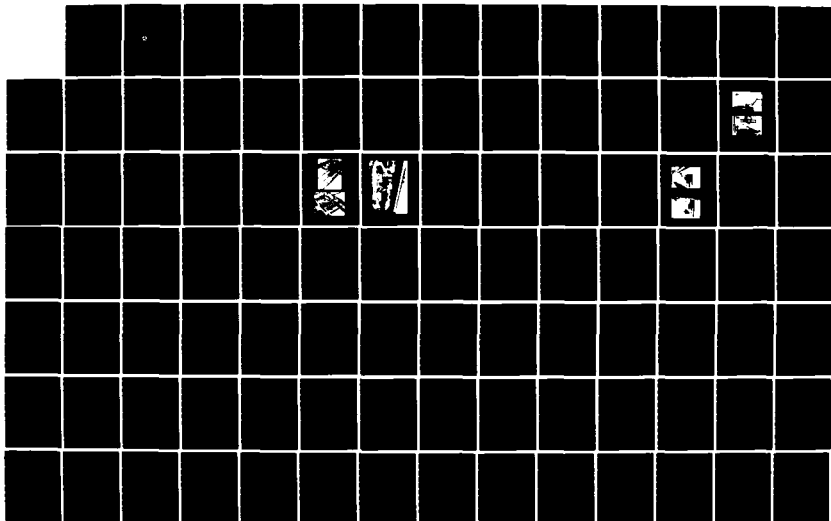
MODEL TESTS AND COMPUTER SIMULATIONS OF A 15-BARGE TOW
FOR THE UPPER MISS. (U) TRACOR HYDRONAUTICS INC LAUREL
MD R HATTON ET AL. JAN 84 TR-83011-2 USCG-D-10-84
DTCG23-82-C-20041

1/3

UNCLASSIFIED

F/G 9/2

NL





COPY RESOLUTION TEST CHART

14

AD-A146 511

Report No. CG-D-10-84

MODEL TESTS AND COMPUTER
SIMULATIONS OF A 15-BARGE TOW
FOR THE UPPER MISSISSIPPI RIVER



January 1976

This document is available to the U.S. public through the National
Technical Information Service, Springfield, Virginia 22161

DTIC
SELECTED
OCT 11 1984
E

Prepared for:

U.S. Department of Transportation
United States Coast Guard

Office of Research and Development
Washington, D.C. 20593

DTIC FILE COPY

64 1 10 1984

NOTICE

This document is disseminated under the sponsorship of the Department of Transportation in the interest of information exchange. The United States Government assumes no liability for its contents or use thereof.

The contents of this report do not necessarily reflect the official view or policy of the Coast Guard; and they do not constitute a standard, specification, or regulation.

This report, or portions thereof may not be used for advertising or sales promotion purposes. Citation of trade names and manufacturers does not constitute endorsement or approval of such products.

Technical Report Documentation Page


1. Report No. CG-D-10-84		2. Government Accession No. AD-A146 511		3. Recipient's Catalog No.																					
4. Title and Subtitle Model Tests and Computer Simulations of A 15-Barge Tow for the Upper Mississippi River		5. Report Date January 1984		6. Performing Organization Code																					
7. Author(s) Robert Hatton, Vladimir Ankudinov, and Roderick Barr		8. Performing Organization Report No. 83011-2		10. Work Unit No. (TRAIS)																					
9. Performing Organization Name and Address Tracor Hydronautics, Inc. 7210 Pindell School Road Laurel, Maryland 20707		11. Contract or Grant No. DTCG23-82-C-20041		13. Type of Report and Period Covered Technical Report Feb. 1983 - Dec. 1983																					
12. Sponsoring Agency Name and Address U. S. Coast Guard 2100 Second Street, SW Washington, D.C. 20543		14. Sponsoring Agency Code		15. Supplementary Notes																					
16. Abstract <p>→ A maneuvering model was developed, for a typical river tow, with experimentally determined hydrodynamic coefficients.</p> <p>The investigation included extensive model tests in both deep and shallow water, development of a method for predicting tow hydrodynamic coefficients, and simulations of tow behavior as a function of channel dimensions and potential obstacles to navigation.</p> <p>↑</p>																									
17. Key Words Model Tests Simulations Manuevering		18. Distribution Statement 		<table border="1"> <tr> <td colspan="2">Accession For</td> </tr> <tr> <td>NTIS GRA&I</td> <td><input checked="" type="checkbox"/></td> </tr> <tr> <td>DTIC TAB</td> <td><input type="checkbox"/></td> </tr> <tr> <td>Unannounced</td> <td><input type="checkbox"/></td> </tr> <tr> <td colspan="2">Justification</td> </tr> <tr> <td colspan="2">By _____</td> </tr> <tr> <td colspan="2">Distribution/ _____</td> </tr> <tr> <td colspan="2">Availability Codes</td> </tr> <tr> <td>Dist</td> <td>Avail and/or Special</td> </tr> <tr> <td>A-1</td> <td></td> </tr> </table>		Accession For		NTIS GRA&I	<input checked="" type="checkbox"/>	DTIC TAB	<input type="checkbox"/>	Unannounced	<input type="checkbox"/>	Justification		By _____		Distribution/ _____		Availability Codes		Dist	Avail and/or Special	A-1	
Accession For																									
NTIS GRA&I	<input checked="" type="checkbox"/>																								
DTIC TAB	<input type="checkbox"/>																								
Unannounced	<input type="checkbox"/>																								
Justification																									
By _____																									
Distribution/ _____																									
Availability Codes																									
Dist	Avail and/or Special																								
A-1																									
19. Security Classif. (of this report) UNCLASSIFIED		20. Security Classif. (of this page) UNCLASSIFIED		21. No. of Pages 294																					
				22. Price																					

TABLE OF CONTENTS

	Page
1.0 INTRODUCTION	1
2.0 DESCRIPTION OF PROTOTYPE AND MODEL	3
3.0 TEST EQUIPMENT, PROCEDURES AND TEST PROGRAM	7
4.0 REDUCTION AND PRESENTATION OF DATA	25
5.0 DEVELOPMENT OF THE MANEUVERING MODEL	71
6.0 SIMULATED MANEUVERS	87
7.0 CONCLUSIONS AND RECOMMENDATIONS	101
8.0 REFERENCES	105
 APPENDIX A - PLANAR MOTION MECHANISM TEST DATA FOR 7.5 FOOT (PROTOTYPE) DRAFT TOWBOAT WITH 15-BARGE TRAIN IN DEEP AND SHALLOW WATER	
 APPENDIX B - PLANAR MOTION MECHANISM TEST DATA FOR 9.0 FOOT (PROTOTYPE) DRAFT TOWBOAT WITH 15-BARGE TRAIN IN DEEP AND SHALLOW WATER	
 APPENDIX C - MATHEMATICAL MODEL, NON-DIMENSIONAL HYDRODYNAMIC COEFFICIENTS, AND METHODS OF ANALYSIS USED AT TRACOR HYDRONAUTICS FOR SURFACE SHIP MANEUVERING PREDICTIONS	
 APPENDIX D - NEAR-BANK AND WAVY-BOTTOM INTERACTION TEST DATA FOR 7.5 FOOT (PROTOTYPE) DRAFT TOWBOAT WITH 15-BARGE TRAIN	

LIST OF FIGURES

	Page
Figure 1 - Model Tow, Towboat and Fifteen Barges, in the HSMB	4
Figure 2 - HSMB Specifications	8
Figure 3 - Schematic of HSMB LAHPMM System	9
Figure 4 - Integrated Surface Ship Towing System Used for Resistance, Propulsion and LAHPMM Tests	10
Figure 5 - HSMB LAHPMM with Mariner Model Attached	11
Figure 6 - Swaying Carriage Servo-Ball-Bearing Jack Screw Drive System	12
Figure 7 - Sketch Showing Wing Dams and Banks in the HSMB	15
Figure 8 - The Wavy Bottom Installed on the Floor of the HSMB	17
Figure 9 - Variation of Lateral Force and Yawing Moment Coefficients with Distance From Banks for Water Depth/Draft Ratio of 1.17	56
Figure 10 - Variation of Lateral Force and Yawing Moment Coefficients with Distance From Banks for Water Depth/Draft Ratio of 1.5	57
Figure 11 - Variation of Y_v' and N_v' Coefficients With Distance From Banks for Water Depth/Draft Ratio of 1.17	60
Figure 12 - Variation of Y_v' and N_v' Coefficients With Distance From Banks for Water Depth/Draft Ratio of 1.5	61

LIST OF FIGURES

	Page
Figure 13 - Variation of Lateral Force and Yawing Moment Coefficients with Water Depth/Draft Ratio For Ahead Motion	64
Figure 14 - Variation of Lateral Force and Yawing Moment Coefficients with Water Depth/Draft Ratio For Astern Motion	65
Figure 15 - Variation of Lateral Force and Yawing Moment Rudder Coefficients with Water Depth/Draft Ratio for Ahead and Astern Motion	66
Figure 16 - Variation of Equilibrium Propulsion Advance Coefficients with Water Depth/Draft Ratio for Ahead and Astern Motion	67
Figure 17 - Model Force and Moment Coefficients for 7.5 Feet Draft and 9.0 Feet Draft Towboat/Barge Systems in Deep Water	74
Figure 18 - Assumed Variation of Towboat Command RPM With Throttle Setting Used in Maneuvering Simulations of 15 Barge Tow System	85
Figure 19 - Comparison of Simulation and Full Scale Data for Steady Turns	95
Figure 20 - Universal Stopping Curve for Tankers From Reference 11	98

LIST OF TABLES

	Page
Table 1 - Principal Geometric Characteristics of the 15-Barge Tow and Towboat with 7.5-Foot Draft	5
Table 2 - Principal Geometric Characteristics of the 15-Barge Tow and Towboat with 9.0-Foot Draft	6
Table 3 - Model Test Program for 15-Barge Tow and Towboat With 7.5-Foot Draft	18
Table 4 - Model Test Program for 15-Barge Tow and Towboat With 9.0-Foot Draft	23
Table 5 - Measured Nondimensional Hydrodynamic Coefficients for the 15-Barge Tow in Deep Water in Combination With a Towboat Operating at a 7.5 Foot Draft	26
Table 6 - Measured Nondimensional Hydrodynamic Coefficients for the 15-Barge Tow in Shallow Water, $H/T = 1.5$, in Combination With a Towboat Operating at a 7.5 Foot Draft	29
Table 7 - Measured Nondimensional Hydrodynamic Coefficients for the 15-Barge Tow in Shallow Water, $H/T = 1.17$, in Combination With a Towboat Operating at a 7.5 Foot Draft	32
Table 8 - Estimated Nondimensional Hydrodynamic Coefficients for the 15-Barge Tow in Shallow Water, $H/T = 1.5$, in Combination With a Towboat Operating at a 7.5 Foot Draft	40

LIST OF TABLES

	Page
Table 9 - Estimated Nondimensional Hydrodynamic Coefficients for the 15-Barge Tow in Shallow Water, $H/T = 1.17$, in Combination With a Towboat Operating at a 7.5 Foot Draft	43
Table 10 - Measured Nondimensional Hydrodynamic Coefficients for the 15-Barge Tow in Deep Water in Combination With a Towboat Operating at a 9.0 Foot Draft	47
Table 11 - Measured Nondimensional Hydrodynamic Coefficients for the 15-Barge Tow in Shallow Water, $H/T = 1.5$, in Combination With a Towboat Operating at a 9.0 Foot Draft	50
Table 12 - Lateral Force and Yawing Moment Coefficients Derived from Tests Past Wing Dams in Two Different Values of Water Depth/Draft	54
Table 13 - Axial Force, Lateral Force and Yawing Moment Coefficients Derived by Autocorrelation Analyses of Time Histories of Forces and Moments Acting on the Operation of the Tow Past Wing Dams	55
Table 14 - Rates of Change of Hydrodynamic Coefficients With Distance From Banks	62
Table 15 - Hydrodynamic Coefficients for Tests Over A Wavy or Irregular Bottom	63

LIST OF TABLES

	Page
Table 16 - Axial Force, Lateral Force, and Yawing Moment Coefficients for Tests Over A Wavy Bottom	69
Table 17 - Effective Water Depths Deduced From Tests Over A Wavy Bottom	82
Table 18 - Maneuvering Characteristics Derived From Calculations of Steady Turning Maneuvers for Tow in Deep and Shallow Water, 9.0 Foot Draft Towboat and 7.5 Foot Draft Towboat	88
Table 19 - Maneuvering Characteristics Derived From Calculations of Zig Zag Maneuvers for 15 Barge Tow with 9.0 Foot Draft Towboat	90
Table 20 - Stopping Characteristics Derived From Calculations of Stopping Maneuvers With 9.0-Foot Draft Towboat	91
Table 21 - Characteristics of River Tows	94
Table 22 - Comparison of Stopping Performance of Exxon Nashville and 15 Barge Tow - Deep Water No Current	97

DIRECTIONAL STABILITY AND CONTROL

The following nomenclature conforms to DTMB Report 1319 and NSRDC Report 2510 where applicable. The positive direction of axes, angles, forces, moments, and velocities are shown by the accompanying sketch.

Symbol	Nondimensional Form	Definition
a_i		Constant in quadratic fit to axial force equation $X'_{\beta-\delta=0} = f(\eta)$ for each of i^{th} segments where $i = 1, 2, 3, 4$; $a_i = X'_{uu}$ at $\eta = 0$ in appropriate segment
b_i		First order coefficient in quadratic fit to axial propeller force equation $X'_{\beta-\delta=0} = f(\eta)$ for each of i^{th} segments where $i = 1, 2, 3, 4$
c_i		Second order coefficient in quadratic fit to axial propeller force equation $X'_{\beta-\delta=0} = f(\eta)$ for each of i^{th} segments where $i = 1, 2, 3, 4$
AD	$AD' = \frac{AD}{L}$	Advance
CB		Center of buoyancy
CG		Center of mass of ship
D		Propeller diameter
D_s	$D_s' = \frac{D_s}{L}$	Steady-turning diameter
I_x'	$I_x' = \frac{I_x}{\frac{1}{2}\rho L^3}$	Moment of inertia of ship about x axis
I_y	$I_y' = \frac{I_y}{\frac{1}{2}\rho L^3}$	Moment of inertia of ship about y axis
I_z	$I_z' = \frac{I_z}{\frac{1}{2}\rho L^3}$	Moment of inertia of ship about z axis
J	$J = \frac{u}{nD}$	Propeller advance coefficient based on ship speed u
J_c	$J_c = \frac{u_c}{n_c D}$	Propeller advance coefficient at steady ship command speed u_c
k_x	$k_x' = \frac{k_x}{L}$	Radius of gyration of ship about x axis
k_y	$k_y' = \frac{k_y}{L}$	Radius of gyration of ship about y axis
k_z	$k_z' = \frac{k_z}{L}$	Radius of gyration of ship about z axis
L	$L' = 1$	Characteristic length; length between perpendiculars for commercial ships

Tracor Hydronautics

-X-

z_d	$z_d' = \frac{z_d}{L} = \frac{z_r - z_v}{L}$	Dynamic stability lever
z_r	$z_r' = \frac{z_r}{L} = \frac{N_r'}{Y_r' - n'}$	Damping lever
z_v	$z_v' = \frac{z_v}{L} = \frac{N_v'}{Y_v'}$	Static stability lever
n	$n' = \frac{n}{\frac{1}{2}\rho L^3}$	Mass of ship
N	$N' = \frac{N}{\frac{1}{2}\rho L^3 U^2}$	Hydrodynamic moment component about z axis (yawing moment)
N_0	$N_0' = \frac{N_0}{\frac{1}{2}\rho L^3 U^2}$	Yawing moment when $\beta = \delta r = 0$
N_r	$N_r' = \frac{N_r}{\frac{1}{2}\rho L^4 U}$	First order coefficient used in representing N as a function of r
$N_{r\eta}$	$N_{r\eta}' = \frac{N_{r\eta}}{\frac{1}{2}\rho L^4 U}$	First order coefficient used in representing N_r as a function of $(\eta-1)$
$N_{\dot{r}}$	$N_{\dot{r}}' = \frac{N_{\dot{r}}}{\frac{1}{2}\rho L^3}$	Coefficient used in representing N as a function of \dot{r}
$N_{r r}$	$N_{r r}' = \frac{N_{r r}}{\frac{1}{2}\rho L^3}$	Second order coefficient used in representing N as a function of r
$N_{r \delta r}$	$N_{r \delta r}' = \frac{N_{r \delta r}}{\frac{1}{2}\rho L^4 U}$	Coefficient used in representing $N_{\delta r}$ as a function of r
N_v	$N_v' = \frac{N_v}{\frac{1}{2}\rho L^3 U}$	First order coefficient used in representing N as a function of v
$N_{v\eta}$	$N_{v\eta}' = \frac{N_{v\eta}}{\frac{1}{2}\rho L^3 U}$	First order coefficient used in representing N_v as a function of $(\eta-1)$
$N_{\dot{v}}$	$N_{\dot{v}}' = \frac{N_{\dot{v}}}{\frac{1}{2}\rho L^3}$	Coefficient used in representing N as a function of \dot{v}
$N_{ v r}$	$N_{ v r}' = \frac{N_{ v r}}{\frac{1}{2}\rho L^4}$	Coefficient used in representing N_r as a function of v
$N_{v v}$	$N_{v v}' = \frac{N_{v v}}{\frac{1}{2}\rho L^3}$	Second order coefficient used in representing N as a function of v
$N_{v v \eta}$	$N_{v v \eta}' = \frac{N_{v v \eta}}{\frac{1}{2}\rho L^3}$	First order coefficient used in representing $N_{v v }$ as a function of $(\eta-1)$
$N_{\delta r}$	$N_{\delta r}' = \frac{N_{\delta r}}{\frac{1}{2}\rho L^3 U^2}$	First order coefficient used in representing N as a function of δr
$N_{\delta r\eta}$	$N_{\delta r\eta}' = \frac{N_{\delta r\eta}}{\frac{1}{2}\rho L^3 U^2}$	First order coefficient used in representing $N_{\delta r}$ as a function of $(\eta-1)$
n		Propeller revolution rate
n_0		Propeller revolution rate at steady command speed

Ordered revision number 1.00

Tracor Hydraulics

-X1-

O_y	$O_y' = \frac{O_y}{L}$	Overshoot width of path
O_ψ		Overshoot heading angle; measured from value at second execute
P		As subscript, meaning port.
R	$R' = \frac{R}{L}$	Steady-turning radius
r	$r' = \frac{rL}{U}$	Angular velocity component about z axis relative to fluid (yaw)
t	$t' = \frac{tL^2}{U^2}$	Angular acceleration component about z axis relative to fluid
S		As subscript, meaning starboard.
TD	$TD' = \frac{TD}{L}$	Tactical diameter
TR	$TR' = \frac{TR}{L}$	Transfer
t	$t' = \frac{tU}{L}$	Time
t_1	$t_1' = \frac{t_1 U}{L}$	Time at 1 th execute in an overshoot or zigzag maneuver
t_0	$t_0' = \frac{t_0 U}{L}$	Time at initiation of a maneuver
t_{90}	$t_{90}' = \frac{t_{90} U}{L}$	Time to reach 90-degree change of heading in a turn
t_{180}	$t_{180}' = \frac{t_{180} U}{L}$	Time to reach 180-degree change of heading in a turn
U	$U' = \frac{U}{U}$	Linear velocity of origin of body axes relative to fluid
U_A		Wind velocity
U_C		Linear velocity of current
U_R		Relative linear velocity of origin of body axis relative to fluid
u	$u' = \frac{u}{U}$	Component of U in direction of the x axis
\dot{u}	$\dot{u}' = \frac{\dot{u}L}{U^2}$	Time rate of change of u in direction of the x axis
u_0	$u_0' = \frac{u_0}{U}$	Command speed: steady value of ahead speed component u for a given propeller rpm for $\beta = 0$; sign changes with propeller reversal

Tracor Hydraulics

-xii-

u_c		Component of U_c in direction of x axis
u_p		Velocity at rudder due to motion and propeller race
u_R		Component of U_R in direction of x axis
v		Absolute speed in knots
v_o		Steady approach speed in knots
v_{90}		Speed in knots at 90-degree heading change in a turn
v_{180}		Speed in knots at 180-degree heading change in a turn
v	$v' = \frac{v}{U}$	Component of U in direction of the y axis
\dot{v}	$\dot{v}' = \frac{\dot{v}L}{U^2}$	Time rate of change of v in direction of the y axis
v_c		Component of U_c in direction of y axis
v_R		Component of U_R in direction of y axis
x	$x' = \frac{x}{L}$	Longitudinal body axis; also the coordinate of a point relative to the origin of body axes
x_B	$x_B' = \frac{x_B}{L}$	The x coordinate of CB
x_G	$x_G' = \frac{x_G}{L}$	The x coordinate of CG
x_o	$x_o' = \frac{x_o}{L}$	A coordinate of the displacement of CG relative to the origin of a set of fixed axes
X	$X' = \frac{X}{\frac{1}{2}\rho L^2 U^2}$	Hydrodynamic force component along x axis (longitudinal, or axial force)
x_A	$x_A' = \frac{x_A}{\frac{1}{2}\rho L^2 U_A^2}$	Acrodynamic force component along x axis
x_{rr}	$x_{rr}' = \frac{x_{rr}}{\frac{1}{2}\rho L^4}$	Second order coefficient used in representing X as a function of r . First order coefficient is zero
x_u	$x_u' = \frac{x_u}{\frac{1}{2}\rho L^3}$	Coefficient used in representing X as a function of u
x_{uu}	$x_{uu}' = \frac{x_{uu}}{\frac{1}{2}\rho L^3}$	Second order coefficient used in representing X as a function of u in the non-propelled case. First order coefficient is zero
x_{vr}	$x_{vr}' = \frac{x_{vr}}{\frac{1}{2}\rho L^3}$	Coefficient used in representing X as a function of the product vr

Tracor Hydronautics

-xiii-

X_{vv}	$X_{vv}' = \frac{X_{vv}}{\frac{1}{2}\rho L^2}$	Second order coefficient used in representing X as a function of v . First order coefficient is zero
$X_{vv\eta}$	$X_{vv\eta}' = \frac{X_{vv\eta}}{\frac{1}{2}\rho L^2}$	First order coefficient used in representing X_{vv} as a function of $(\eta-1)$
$X_{\delta r \delta r}$	$X_{\delta r \delta r}' = \frac{X_{\delta r \delta r}}{\frac{1}{2}\rho L^2 U^2}$	Second order coefficient used in representing X as a function of δr at $\eta = 0$. First order coefficient is zero
$X_{\delta r \delta r \eta \eta}$	$X_{\delta r \delta r \eta \eta}' = \frac{X_{\delta r \delta r \eta \eta}}{\frac{1}{2}\rho L^2 U^2}$	Second order coefficient used in representing $X_{\delta r \delta r}$ as a function of η
y	$y' = \frac{y}{L}$	Lateral body axis; also the coordinate of a point relative to the origin of body axes
y_B	$y_B' = \frac{y_B}{L}$	The y coordinate of CB
y_G	$y_G' = \frac{y_G}{L}$	The y coordinate of CG
y_p		Distance of port propeller from centerline
y_s		Distance of starboard propeller from centerline
y_o	$y_o' = \frac{y_o}{L}$	A coordinate of the displacement of CG relative to the origin of a set of fixed axes
Y	$Y' = \frac{Y}{\frac{1}{2}\rho L^2 U^2}$	Hydrodynamic force component along y axis (lateral force)
Y_o	$Y_o' = \frac{Y_o}{\frac{1}{2}\rho L^2 U^2}$	Lateral force when $\beta = \delta r = 0$
Y_A	$Y_A' = \frac{Y_A}{\frac{1}{2}\rho_A L^2 U_A^2}$	Aerodynamic force component along y axis
Y_r	$Y_r' = \frac{Y_r}{\frac{1}{2}\rho L^2 U}$	First order coefficient used in representing Y as a function of r
$Y_{r\eta}$	$Y_{r\eta}' = \frac{Y_{r\eta}}{\frac{1}{2}\rho L^2 U}$	First order coefficient used in representing Y_r as a function of $(\eta-1)$
$Y_{\dot{r}}$	$Y_{\dot{r}}' = \frac{Y_{\dot{r}}}{\frac{1}{2}\rho L^2}$	Coefficient used in representing Y as a function of \dot{r}
$Y_{r r }$	$Y_{r r }' = \frac{Y_{r r }}{\frac{1}{2}\rho L^2}$	Second order coefficient in representing Y as a function of r

Tracor Hydraulics

-xiv-

$Y_{ r \delta r}$	$Y_{ r \delta r}' = \frac{Y_{ r \delta r}}{\frac{1}{2}\rho L^3 U}$	Coefficient used in representing $Y_{\delta r}$ as a function of r
Y_v	$Y_v' = \frac{Y_v}{\frac{1}{2}\rho L^2 U}$	First order coefficient used in representing Y as a function of v
$Y_{v\eta}$	$Y_{v\eta}' = \frac{Y_{v\eta}}{\frac{1}{2}\rho L^2 U}$	First order coefficient used in representing Y_v as a function of $(\eta-1)$
Y_ϕ	$Y_\phi' = \frac{Y_\phi}{\frac{1}{2}\rho L^3}$	Coefficient used in representing Y as a function of ϕ
$Y_{v r }$	$Y_{v r }' = \frac{Y_{v r }}{\frac{1}{2}\rho L^3}$	Coefficient used in representing Y_v as a function of r
$Y_{v v }$	$Y_{v v }' = \frac{Y_{v v }}{\frac{1}{2}\rho L^2}$	Second order coefficient used in representing Y as a function of v
$Y_{v v \eta}$	$Y_{v v \eta}' = \frac{Y_{v v \eta}}{\frac{1}{2}\rho L^2}$	First order coefficient used in representing $Y_{v v }$ as a function of $(\eta-1)$
$Y_{\delta r}$	$Y_{\delta r}' = \frac{Y_{\delta r}}{\frac{1}{2}\rho L^2 U^2}$	First order coefficient used in representing Y as a function of δr
$Y_{\delta r\eta}$	$Y_{\delta r\eta}' = \frac{Y_{\delta r\eta}}{\frac{1}{2}\rho L^2 U^2}$	First order coefficient used in representing $Y_{\delta r}$ as a function of $(\eta-1)$
δ		Angle of drift
δ_r		Angle of drift relative to fluid
δ_F		Deflection of flanking rudder,
δ_S		Deflection of steering rudder
δ_{r_1}		Steady rudder angle at 1 th execute in an overshoot or zigzag maneuver; $1 = 1, 2, 3, \dots$
$\dot{\delta}_F$	$\dot{\delta}_F' = \frac{\dot{\delta}_F L}{U}$	Flanking rudder deflection rate
$\dot{\delta}_S$	$\dot{\delta}_S' = \frac{\dot{\delta}_S L}{U}$	Steering rudder deflection rate
η	$\eta = \frac{J_c}{J}$	Ship propulsion ratio; $\frac{u_c}{u} \cdot \frac{n}{n_c}$

Tracor Hydronautics

-XV-

ψ		Heading or yaw angle
ψ_1		Heading angle at 1 th execute in an overshoot or zigzag maneuver, measured from value at first execute; $i = 2, 3, \dots$
$\dot{\psi}$	$\dot{\psi}' = \dot{\psi} \frac{L}{U}$	Rate of change of heading
$\dot{\psi}_h$	$\dot{\psi}_h' = \dot{\psi}_h \frac{L}{U}$	Height of loop at neutral rudder angle from spiral maneuver
$\dot{\psi}_1$	$\dot{\psi}_1' = \dot{\psi}_1 \frac{L}{U}$	Rate of change of heading at 1 th execute in an overshoot or zigzag maneuver; $i = 2, 3, \dots$
ω	$\omega' = \frac{\omega L}{U}$	Frequency of oscillation

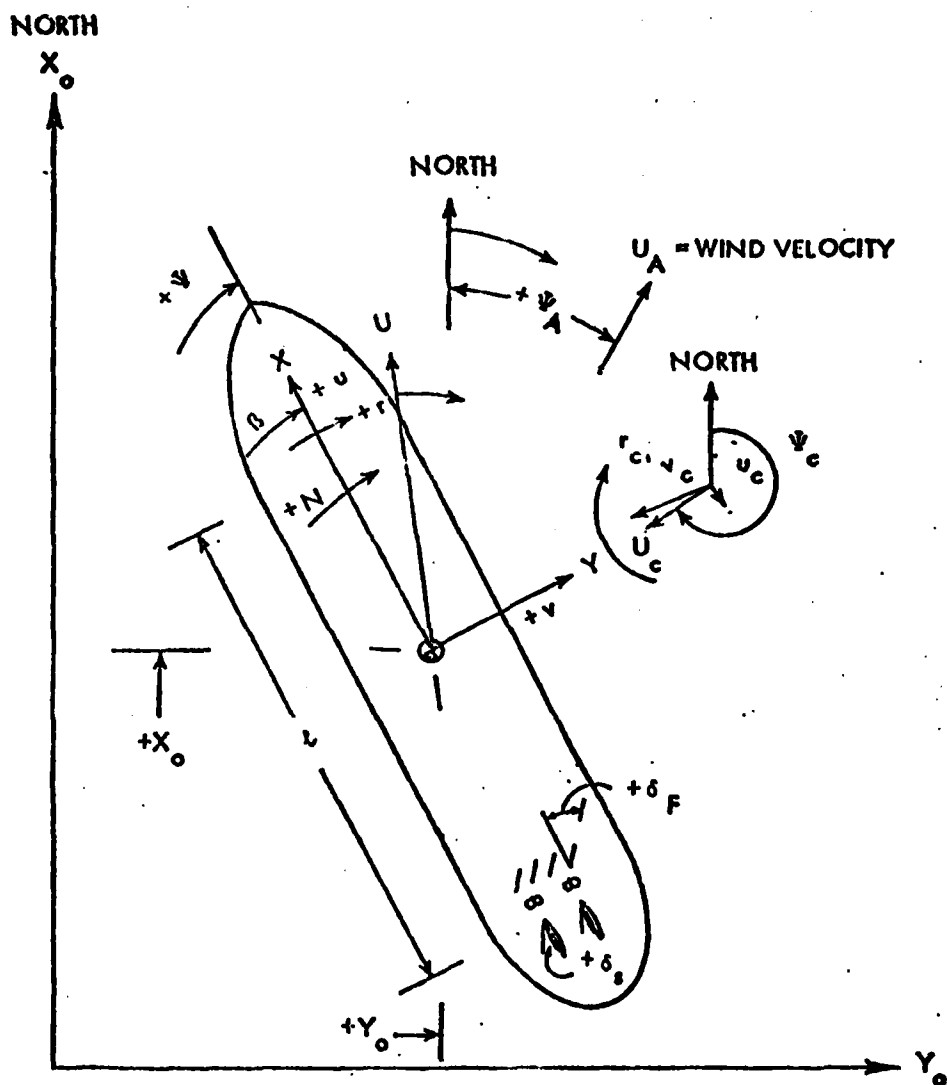


FIGURE - A-1 - SIGN CONVENTION FOR TWIN - SCREW SHIP MANEUVERING SIMULATION.

PLANAR MOTION MECHANISM TESTS

The following notation is used in discussions pertaining to LAHPMM testing and data reduction.

<u>Symbol</u>	<u>Definition</u>
K	Calibration constant millivolts per engineering unit.
n_d	Number of cycles of motion over which the signal is integrated during an LAHPMM test.
n	Propeller revolution rate, positive for direction of rotation corresponding to ahead motion.
T	Period of oscillatory motion of PMM.
U	Linear velocity of origin of body axes relative to fluid. Since $U = \sqrt{u^2 + v^2}$, U always is taken as a positive quantity.
U_c	Carriage Velocity.
x_s	Spacing of towing pivots in model. $x_s' = x_s/L$
1	Designates forward gage of pair.
2	Designates after gage of pair.

CURVE FITTING

The following notation is used in discussion of curve fit procedures.

<u>Symbol</u>	<u>Defintion</u>
a, b, c	Coefficients in expression of near-bank effects on lateral force and yaw moment.
a_i, b_i, c_i	Coefficients in expression of axial force as function of propeller loading.
a_w, b_w, c_w	Coefficients in expression of lateral force and yaw moment as functions of total vector velocity at rudder when rudder angle is zero.
d, e, f	Coefficients in expression of lateral force and yaw moment as functions of total vector velocity at rudder when drift vector velocity at rudder when drift is zero and rudder is deflected.
A_1, A_2, A_3, A_4	Coefficients in expression of hydrodynamic function changes with depth-to-draft ratio.

NEAR-BANK EFFECTS

The following notation is used in discussion of near-bank effects.

<u>Symbol</u>	<u>Definition</u>
a, b, c	Curve-fit coefficients defining F as function of \bar{B} , H, and T.
B	Beam of vessel.
F	General form representing hydrodynamic coefficient.
H	Water depth.
p	Subscript referring to port.
s	Subscript referring to starboard.
T	Vessel draft.
y	Distance between vessel and bank at water surface.
\bar{B}	Nondimensional bank distance parameter, $\bar{B} = B/y$.

Tracor Hydronautics

-XX-

SHALLOW WATER EFFECTS

The following notation is used in discussion of shallow water effects.

<u>Symbol</u>	<u>Definition</u>
A_1, A_2, A_3, A_4	Curve-fit coefficients defining R as a function of σ for each hydrodynamic coefficient.
H	Water Depth.
R	Ratio of hydrodynamic coefficient in shallow water to value in deep water.
T	Vessel Draft.
σ	Draft to Depth Ratio, T/H .

1.0 INTRODUCTION

Tracor Hydronautics, Incorporated has conducted for the U.S. Coast Guard, under Contract DTCG 23-82-C-20041, a study of the maneuverability of typical river tows in the Upper Mississippi River. This program was funded by the U.S. Army Corps of Engineers with technical and administrative assistance provided by the U.S. Coast Guard.

The investigation includes extensive model tests in both deep and shallow water, development of a method for predicting tow hydrodynamic coefficients, and simulations of tow behavior as a function of channel dimensions and potential obstacles to navigation.

The contract is divided into three basic phases. The first phase, the development of a method for predicting tow hydrodynamics and the use of this method to predict sets of coefficients for two typical tows, is presented in Reference 1. The second phase involves model tests in deep and shallow water, with and without banks and wing dams and with two towboat drafts (7.5 and 9.0 feet). Computer simulations of various maneuvers were made utilizing results of the model tests. These investigations are presented in this report. The third phase, describing results of the hands-on simulation studies, will be presented in a later report.

The primary objective of this second phase was to develop a maneuvering model, for a typical river tow, with experimentally determined hydrodynamic coefficients.

This report presents the model tests, the analyzed results of these tests, the mathematical models using these results, and simulated definitive maneuvers. The tests include tow hydrodynamics in deep water, water depth effects, bank effects,

Tracor Hydronautics

-2-

wing dam effects and wavy or irregular bottom effects. All results presented in this report are for a 3900 hp towboat and a tow of 15 loaded barges.

1.0 INTRODUCTION

Tracor Hydronautics, Incorporated is preparing for the U. S. Coast Guard, under Contract DTCG 23-82-C-20041, a study of the maneuverability of typical river tows in the Upper Mississippi River. This program is being jointly funded by the Coast Guard and the U. S. Army Corps of Engineers.

The investigation includes extensive model tests in both deep and shallow water, development of a method for predicting tow hydrodynamic coefficients, and simulations of tow behavior as a function of channel dimensions and potential obstacles to navigation.

The contract is divided into three basic phases. The first phase, the development of a method for predicting tow hydrodynamics and the use of this method to predict sets of coefficients for two typical tows, is presented in Reference 1. The second phase involves model tests in deep and shallow water, with and without banks and wing dams and with two towboat drafts (7.5 and 9.0 feet). Computer simulations of various maneuvers were made utilizing results of the model tests. These investigations are presented in this report. The third phase, describing results of the hands-on simulation studies, will be presented in a later report.

The primary objective of this second phase was to develop a maneuvering model, for a typical river tow, with experimentally determined hydrodynamic coefficients.

This report presents the model tests, the analyzed results of these tests, the mathematical models using these results, and simulated definitive maneuvers. The tests include tow hydrodynamics in deep water, water depth effects, bank effects,



FIGURE 1 - MODEL TOW, TOWBOAT AND FIFTEEN BARGES,
IN THE HSMB

Table 1

Principal Geometric Characteristics of the
15-Barge Tow and Towboat with 7.5 Foot Draft

	Full Scale	Model
Length of Tow and Towboat, LOA, feet*	1130.0	37.667
Beam of Tow, feet	105.0	3.500
Length of Towboat, LOA, feet	140.0	4.667
Beam of Towboat, feet	38.0	1.267
Draft of Tow, feet	9.0	0.300
Draft of Towboat, feet	7.5	0.250
Displacement, (feet) ³	930,250.0	34.454
Trim	Level	Level
Propeller Diameter, feet (Twin Screw)	8.5	0.283
Linear Scale Ratio	1.0	30.0

* Conversion from English to SI units

1 Foot = 0.3048 meters
 1 Horsepower = 1.0139 Horsepower
 = 0.7459 Kilowatts
 1 Pound = 4.448 Newtons
 1 Slug = 14.59 Kilograms mass
 1 Miles per hour = 0.5144 Meters per second

Table 2

Principal Geometric Characteristics of the
15-Barge Tow and Towboat with 9.0 Foot Draft

	Full Scale	Model
Length of Tow and Towboat, LOA, feet	1130.0	37.667
Beam of Tow, feet	105.0	3.500
Length of Towboat, LOA, feet	140.0	4.667
Beam of Towboat, feet	38.0	1.267
Draft of Tow, feet	9.0	0.300
Draft of Towboat, feet	9.0	0.300
Displacement, (feet) ³	937,580.0	34.725
Trim	Level	Level
Propeller Diameter (Twin Screw), feet	8.5	0.283
Linear Scale Ratio	1.0	30.0

3.0 TEST EQUIPMENT, PROCEDURES AND TEST PROGRAM

The experiments were conducted in the Hydronautics Ship Model Basin (HSMB), which is 420 feet long and 24 feet wide. A more detailed description is presented in Figure 2. The water depth in the basin during the deep water tests was 12.5 feet, while for the shallow water tests it was 5.4 and 4.2 inches for $H/T = 1.5$ and 1.17 respectively. The maneuvering tests were conducted using the HSMB Large Amplitude Horizontal Planar Motion Mechanism (LAHPMM) and Carriage No. 1. Reference 2 contains a detailed description of the LAHPMM system, including principles of operation and the data acquisition system

Figure 3 is a schematic drawing which shows the forced motion mechanism, towing arrangement, and dynamometry associated with the overall HSMB LAHPMM system. The forced motions are produced by means of a swaying carriage assembly which includes means both for setting discrete drift angles and for oscillating the model in yaw. The swaying carriage moves horizontally in a direction perpendicular to the basin centerline along a set of four rails mounted on a portable support frame which is rigidly clamped to the towing carriage. A strongback attached to the yawing tube provides the means for connecting the swaying carriage through the bearing and gage assemblies to the model. In this manner, the strongback is always aligned with the centerline of the model. Figure 4 presents a more detailed drawing of the LAHPMM attached to a ship model. Figures 5 and 6 are photographs of an actual installation.

For the static mode, the swaying carriage is first locked in place with the model aligned with the basin centerline; the drift angles are then set manually (with model at rest) by means



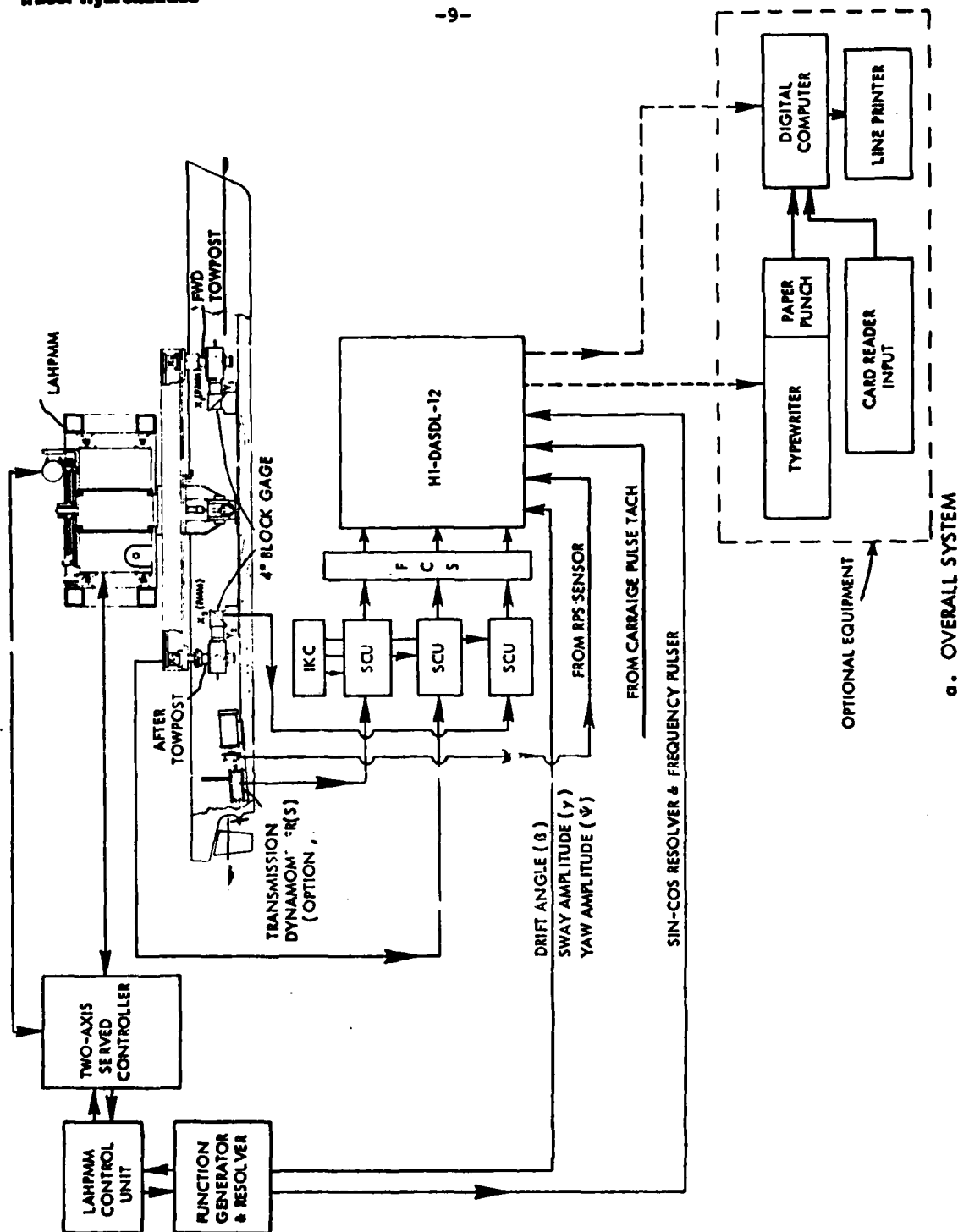
FIGURE 2 - HYDRONAUTICS SHIP MODEL BASIN SPECIFICATIONS

REPRINTED FROM:

INTERNATIONAL TOWING TANK CONFERENCE CATALOGUE OF FACILITIES
TOWING TANKS, SEAKEEPING AND MANEUVERING BASINS SECTION

HYDRONAUTICS, Incorporated 7210 Pindell School Rd. Laurel, Maryland 20810 (301) 776-7454 Telex: 8 7585		USA
Hydronautics Ship Model Basin (HSMB)		1968
DESCRIPTION OF CARRIAGES:	No. 1	No. 2
TYPE OF DRIVE SYSTEM AND TOTAL POWER:	Electro-Hydraulic, 56 kW (75 HP), (Both)	
MAXIMUM CARRIAGE SPEED:	6.1 m/s	10.7 m/s
WAVE GENERATION CAPABILITY: Regular and Irregular WAVEMAKER TYPE AND EXTENT: Wedge-type plunger BEACH TYPE AND LENGTH: Sloping grid METHOD OF IRREGULAR WAVE GENERATION: Sine-pot apparatus OTHER CAPABILITIES: Deep water test section (3.35 m dia. x 13.1 m deep)		
INSTRUMENTATION:	On-board real-time computer Data acquisition system	
MODEL SIZE:	2 10 m	
TESTS PERFORMED:	Surface ship resistance, powering, seakeeping - maneuvering Submarine resistance, powering, maneuvering Offshore structures tests	

HYDRONAUTICS
INCORPORATED



a. OVERALL SYSTEM

FIGURE 3 - SCHEMATIC OF HSMB LAHPMM SYSTEM

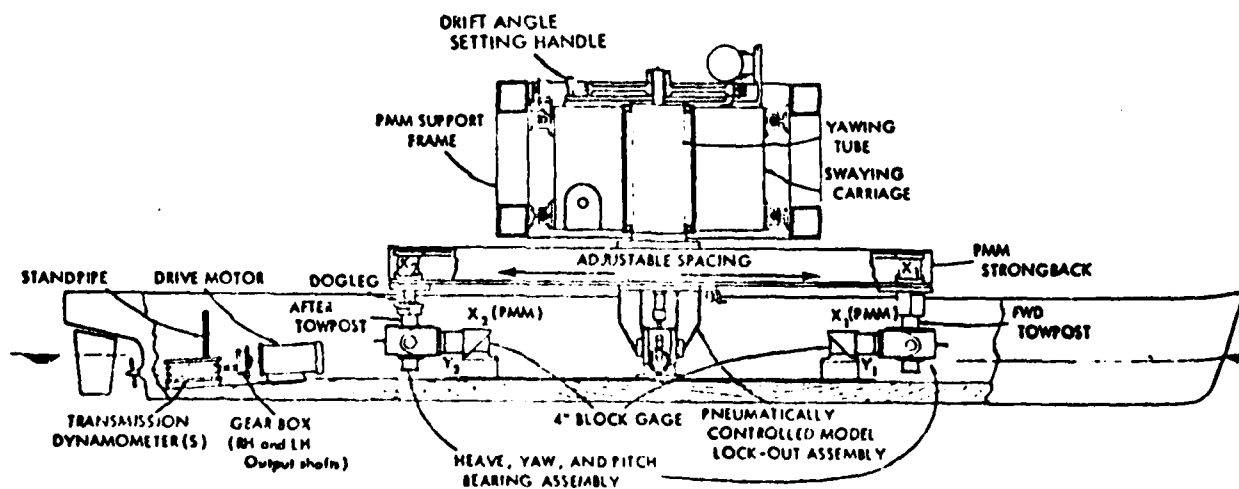
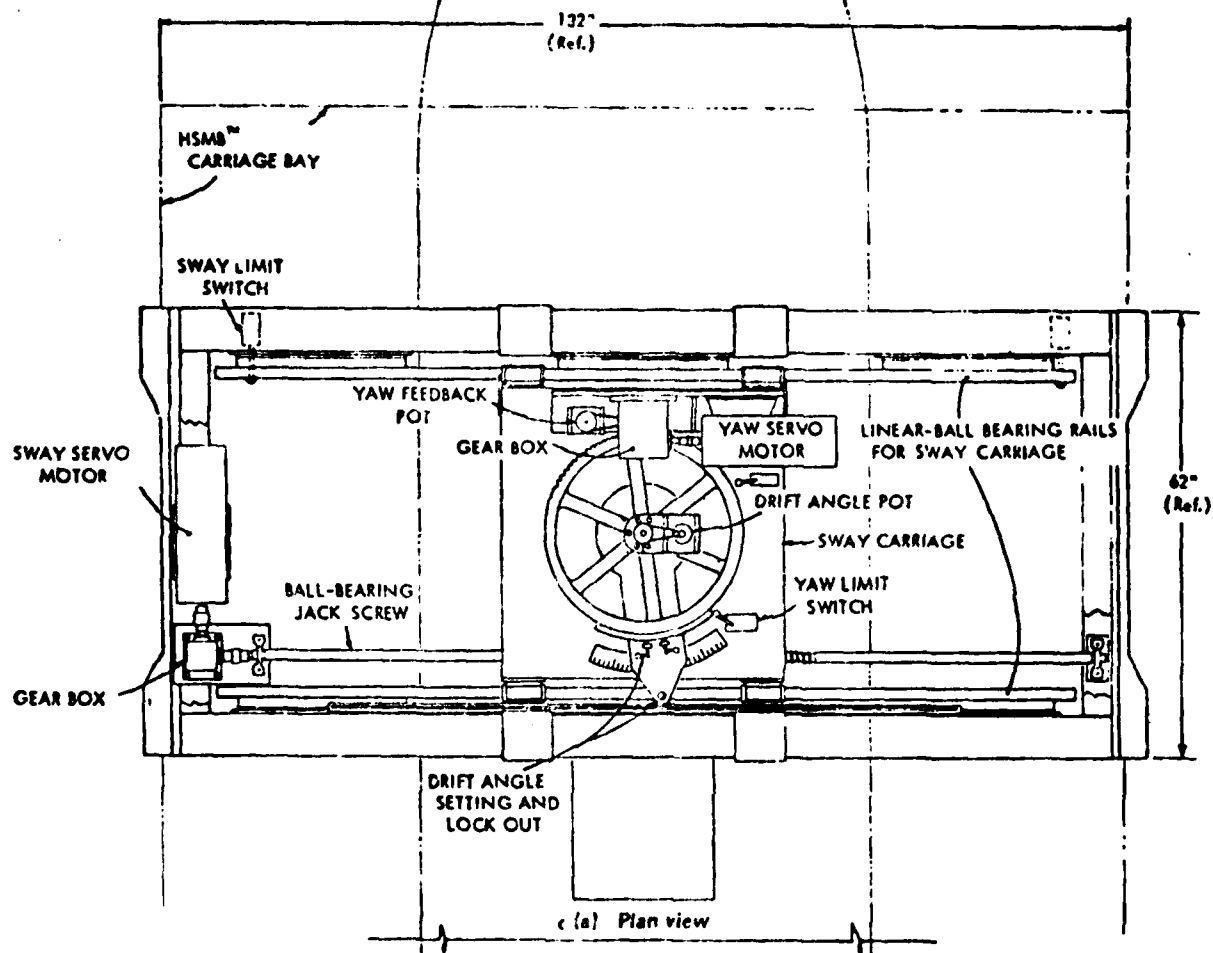
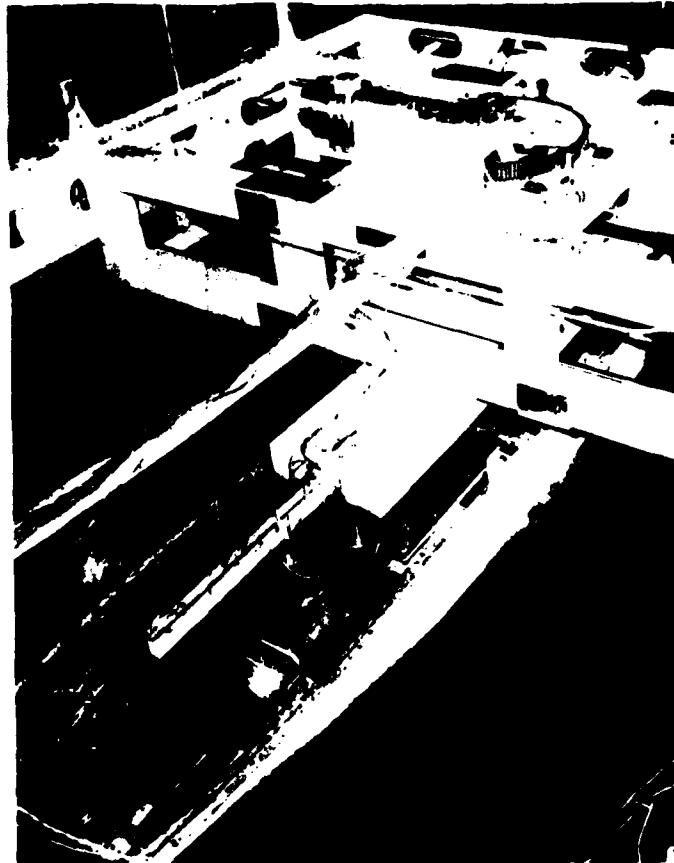
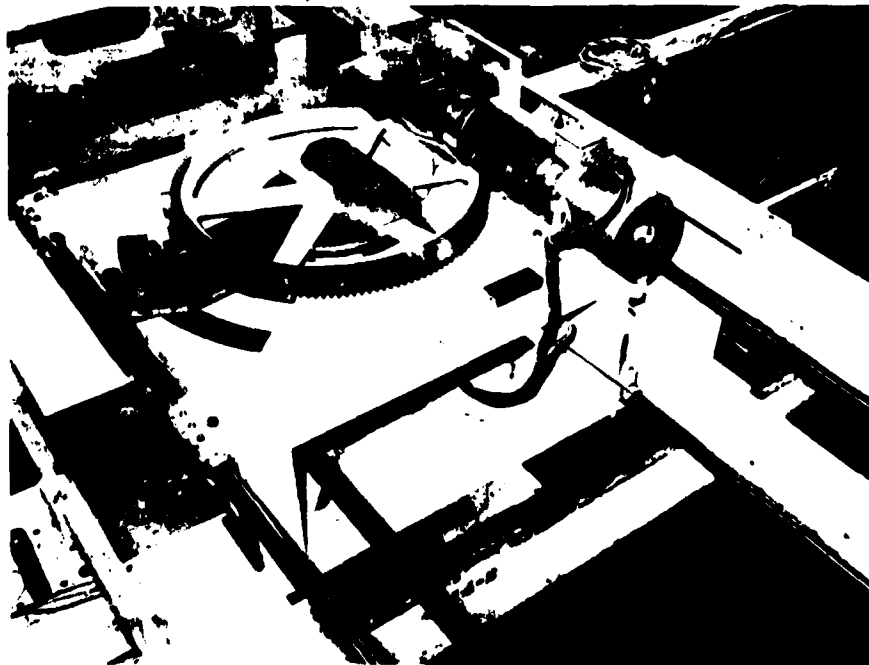


FIGURE 4 - INTEGRATED SURFACE SHIP TOWING SYSTEM USED FOR RESISTANCE, PROPULSION AND LAHPMM TESTS



a) View of LAHPMM Frame, Strong Back, Model and Propulsion System



b) Close-up View of Swaying Carriage, Yaw Servo and Sway Servo Systems

FIGURE 4 - HSMB LAHPMM WITH MARINER MODEL ATTACHED



FIGURE 5 - SWAYING CARRIAGE SERVO-BALL-BEARING JACK
CREW DRIVE SYSTEM

of a spring-loaded locking pin which can be set in 2-degree increments over a range of ± 30 degrees. For the oscillatory modes, the swaying carriage and yawing tube are independently actuated by separate DC servo-motor and control systems. Sinusoidal motions can thereby be produced which cover the following continuous ranges: frequencies from about 0.01 to 0.20 Hertz; linear (single) amplitudes up to 3 feet; and angular (single) amplitudes up to 30 degrees. For the pure swaying mode, the swaying carriage system is operated with the yawing tube system locked at the zero setting. For the yawing mode, the yawing tube is operated simultaneously at equal frequency with the swaying carriage, but with a 90-degree phase lag; the yawing amplitude setting is determined directly as a function of the swaying amplitude and carriage speed. The net result is to produce a pure yawing motion in which the model centerline is always tangent to the path. For yaw-sway coupling tests, the system is operated in what otherwise would be the pure yawing mode, but with a superimposed constant drift-angle setting.

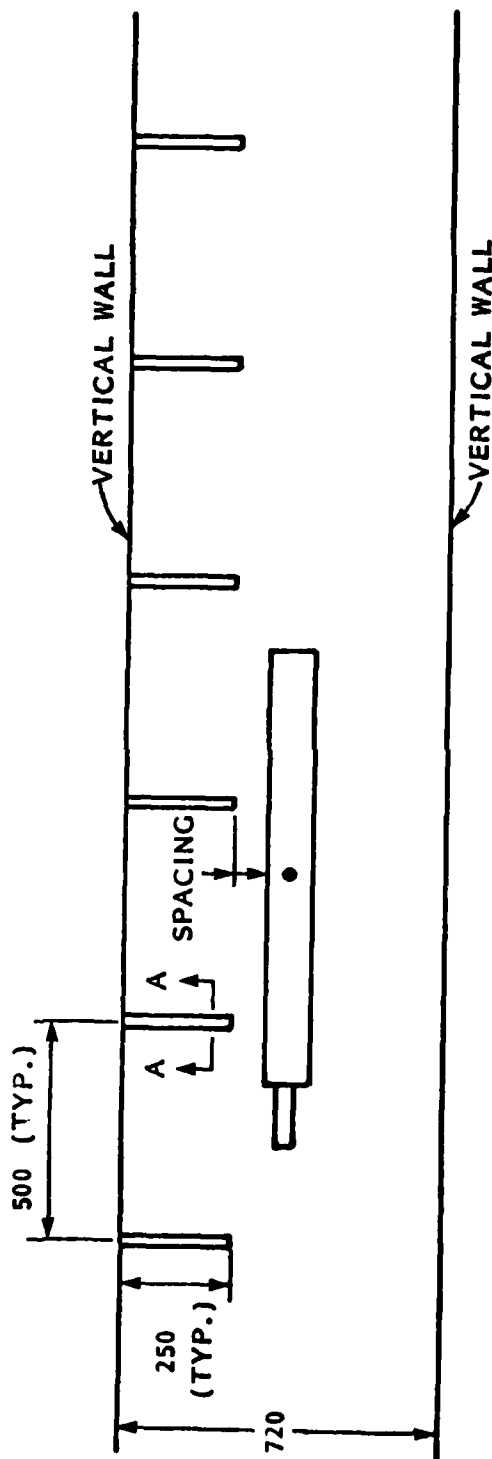
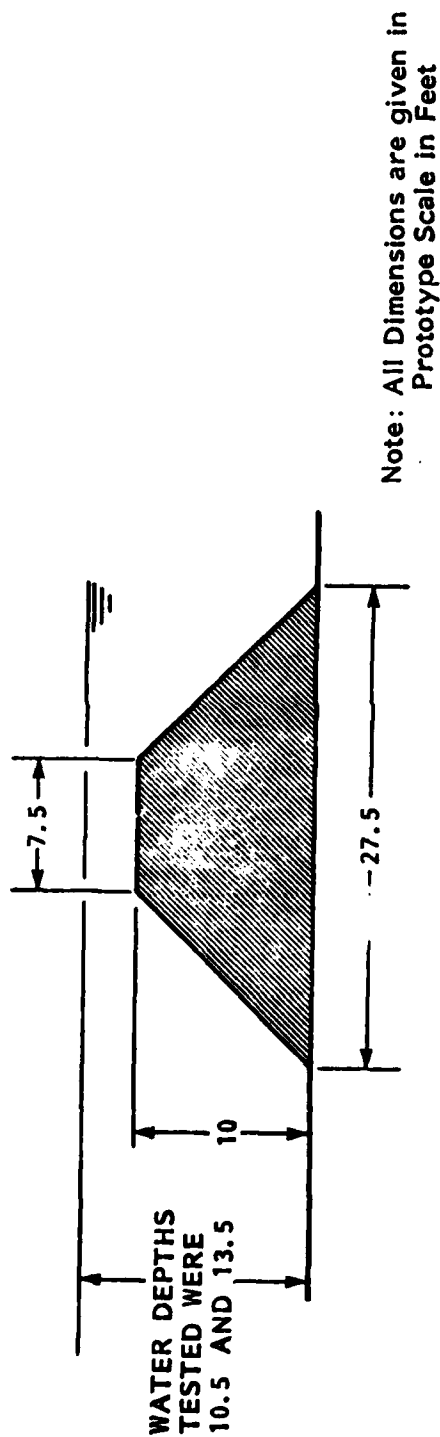
For the PMM tests of surface displacement ship models, each of the two gage assemblies consists of an X- and a Y-gage and the yaw bearing or gimbal. The arrangement allows the model to be free in heave and pitch while providing stiff restraint to longitudinal force, X, lateral force, Y, yawing moment, N, and roll moment, K. The base plates of the two gage assemblies are mounted in the model so that the gimbal centers are aligned and equidistant from the reference point or longitudinal center of gravity, LCG, location. In the case of surface ship models which are buoyant and free to trim, the LCG or reference point is the same for both model and prototype ship. Since the gages move with the model, they measure lateral force, Y, and longitudinal force, X, components with respect to a body axis system

(origin at model CG), as opposed to the lift-drag components associated with the fixed-axis system. With the PMM gage arrangement shown in Figure 4, the total Y-force exerted on the model is experienced as a pure reaction at each of the gimbal centers; the moment about each of these centers is zero. Thus, the total Y-force is equal to the vector sum of the forces measured by the Y_1 and Y_2 gages and, because of symmetry, the yawing moment, N , is equal to the vector difference between the Y_1 and Y_2 forces times the distance from that gimbal center to the CG. Similarly, the vector sum of the pure reaction forces measured for the X_1 and X_2 gages is equal to the total X-force, but since the reaction X-forces are aligned with the longitudinal axis, there is no contribution to the yawing moment.

For this test program, the X-gages used had a design range of ± 25 pounds and the Y-gages had a design range of ± 50 pounds.

The wing dam and bank tests were conducted in the same two water depths used for the shallow water tests. For these tests, wing dams and a 45° sloping bank were fabricated from galvanized steel sheet and placed on the tank floor. Figure 7 shows the wing dams and bank together with their arrangement in the model basin. Tests were carried out using the PMM sway table to set a desired spacing between model and bank (or wing dam), and a drift angle variation was then conducted for each spacing.

To measure model position in the freerunning tests, a lightweight pantograph arm was attached between towing carriage and model. The output from potentiometers mounted on the pantograph gave measures of model surge, sway and yaw motions relative to the carriage. A history of carriage position was obtained by integrating the carriage speed record and referencing the result to position pulses given by a photocell tripped by flags at several points along the run.



a. WING DAM ARRANGEMENT AND CROSS-SECTIONAL SKETCH

FIGURE 7 - SKETCH SHOWING WING DAMS AND BANKS IN THE HSMB

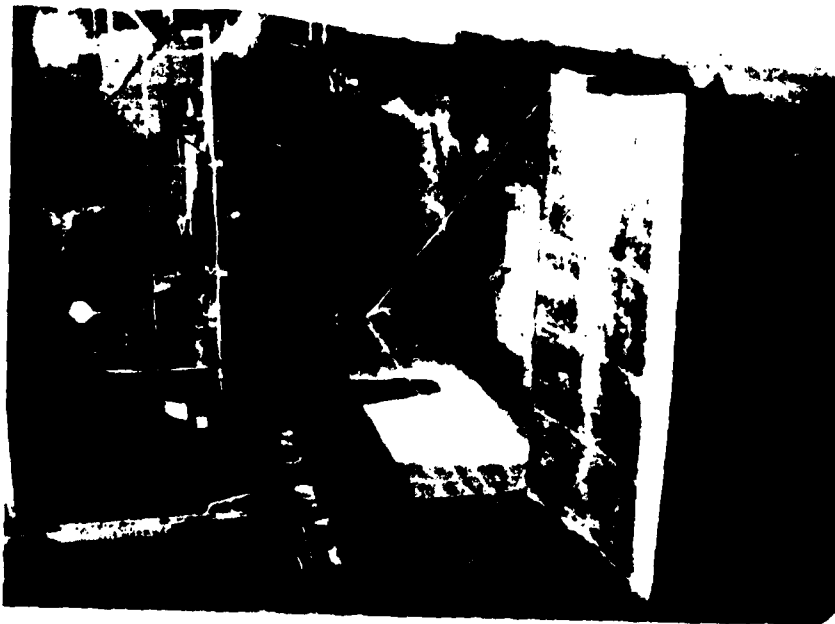
A wavy, or irregular, bottom was installed over a portion of the model basin floor to simulate typical observed bottom sand waves. The waves were made of galvanized sheet stiffened on the underside. To avoid flow of water under and through the structure, all seams were taped and data was taken only when the model was well clear of the edges of the irregular bottom. A prototype wave length of 250 feet was selected as representative of river bottom sand waves. The prototype wave height was five feet, and water depth over the crests was equal to 1.17 times tow draft. Figure 8(a) shows a single section about to be installed in the HSMB, while Figure 8(b) pictures the complete, installed wavy bottom.

The initial set of tests was conducted with the towboat ballasted to its design draft of 7.5 feet. An extensive program of Planar Motion Mechanism (PMM) tests was conducted in deep water, at two depths of shallow water, and over an irregular, wavy bottom. In addition, captive model and free-running model tests were conducted in shallow water to determine effects of banks and wing dams. The program is given in Table 3.

Additional work was conducted with the towboat ballasted to a draft of 9.0 feet, which was indicated by river pilots to be typical of normal operating practice. The purpose of these tests was to assess the differences in hydrodynamic coefficients due to a change in towboat draft and to provide a maneuvering mathematical model for the tow with the towboat at the more typical towboat operating draft. This set of tests included a limited program of PMM tests in deep water and the lesser of the two shallow water depths used in the tests with 7.5-foot towboat draft. This program is shown in Table 4.



b. COMPLETE INSTALLATION



a. SINGLE SECTION

FIGURE 8 - THE WAVY BOTTOM INSTALLED ON THE FLOOR OF THE HSMB

Table 3
Model Test Program for 15-Barge Tow and Towboat
With 7.5-Foot Draft

a) Deep Water PMM Tests

Test Type	Propulsion Ratio n	Drift Angle, Degrees β	Rudder Angle, Degrees δ
Ahead n Variation	$-\infty$ to ∞	0	0
Astern n Variation	$-\infty$ to ∞	0	0
Ahead β Variation	0,1,2	-2,0,2,4,6,8,10, 14,18	0
Astern β Variation	0,1,2	178,180,182,184, 186,188,190,194, 198	0
Ahead Main Rudder Variation	0,1,2, ∞	0	-5,0,5,10,15,20, 25,30,35
Astern Main Rudder Variation	-1	0	-5,0,5,10,15,20, 25,30,35
Ahead Flanking Rudder Variation	-2,-1	0	-5,0,5,10,15,20, 25,30,35
Astern Flanking Rudder Variation	0,1,2, ∞	0	-5,0,5,10,15,20, 25,30,35
Zero Speed Differential Thrust	$n_p = 0$ $n_s = \pm\infty$	0	0
Ahead Differ- ential Thrust	$n_p = 0$ $n_s = \pm 1$	0	0
Astern Differ- ential Thrust	$n_p = 0$ $n_s = \pm 1$	0	0

Table 3

Model Test Program for 15-Barge Tow and Towboat
With 7.5-Foot Draft

a) Deep Water PMM Tests - Continued

Test Type	Propulsion Ratio η	Drift Angle, Degrees β	Rudder Angle, Degrees δ
Ahead Pure Swaying	1	0	0
Astern Pure Swaying	1	0	0
Ahead Pure Yawing	1	0	0
Astern Pure Yawing	1	0	0
Ahead Yawing w/Drift Angle	1	4,8	0
Astern Yawing w/ Drift Angle	1	184,188	0

Table 3 (Continued)

Model Test Program for 15-Barge Tow and Towboat
With 7.5-Foot Draft

b) Shallow Water PMM Tests,
Depth/Draft = 1.50, 1.17

Test Type	Propulsion Ratio η	Drift Angle, Degrees β	Rudder Angle, Degrees δ
Ahead Variation	$-\infty$ to ∞	0	0
Astern Variation	$-\infty$ to ∞	0	0
Ahead Variation	0,1,2	-2,0,2,4,8,12	0
Astern Variation	0,1,2	-2,0,2,4,8,12	0
Ahead Main Rudder Variation	0,1,2,	0	-5,0,5,10,15,20, 25,30,35
Astern Main Rudder Variation	-1	0	-5,0,5,10,15,20, 25,30,35
Ahead Flanking Rudder Variation	-2,-1	0	-5,0,5,10,15,20 25,30,35
Astern Flanking Rudder Variation	0,1,2,	0	-5,0,5,10,15,20, 25,30,35
Ahead Pure Swaying	1	0	0
Astern Pure Swaying	1	0	0
Ahead Pure Yawing	1	0	0
Astern Pure Yawing	1	0	0
Ahead Yawing w/Drift Angle	1	2	0
Astern Yawing w/Drift Angle	1	182	0

Table 3 (Continued)
Model Test Program For 15-Barge Tow and Towboat
With 7.5-Foot Draft

c) Bank and Wing Dam Tests,
Depth/Draft = 1.50, 1.17

Test Type	Description
Captive Model Wing Dam Test	Variation of β and spacing between model and wing dam ends
Captive Model Bank Test	Variation of β and spacing between model and 45 degrees sloping bank
Free Running Bank and Wing Dam Tests	Model running free with rudder controlled, past 45-degrees sloping bank and wing dams, water depth/draft = 1.17 only

Table 3 (Concluded)

Model Test Program for 15-Barge Tow and Towboat
With 7.5-Foot Draft

d) PMM Tests Over Irregular Bottom

Test Type	Propulsion Ratio η	Drift Angle, Degrees β	Rudder Angle, Degrees δ
Ahead η Variation	-1 to 2	0	0
Astern η Variation	-1 to 2	0	0
Ahead β Variation	1	-2,0,2,4,6,8	0
Astern β Variation	1	-2,0,2,4,6,8	0
Ahead Main Rudder Variation	1	0	-5,0,5,10,15,20, 25,30,35
Astern Flanking Rudder Variation	1	0	-5,0,5,10,15,20 25,30,35

Table 4
Model Test Program for 15-Barge Tow and Towboat
With 9.0-Foot Draft

a) Deep Water PMM Tests

Test Type	Propulsion Ratio η	Drift Angle, Degrees β	Rudder Angle, Degrees δ
Ahead η Variation	-2 to 2	0	0
Astern η Variation	-2 to 2	0	0
Ahead β Variation	1	-2, 0, 2, 4, 6, 8, 10 12, 14, 16, 18	0
Astern β Variation	1	178, 180, 182, 184, 186, 188, 190, 192, 194, 196, 198	0
Ahead Main Rudder Variation	1, 2	0	-5, 0, 5, 10, 15, 20, 25, 30, 35
Astern Flanking Rudder Variation	2	0	-5, 0, 5, 10, 15, 20 25, 30, 35

Table 4 (Concluded)

Model Test Program for 15-Barge Tow and Towboat
With 9.0-Foot Draft

b) Shallow Water PMM Tests,
Depth/Draft = 1.17

Test Type	Propulsion Ratio n	Drift Angle, Degrees β	Rudder Angle, Degrees δ
Ahead n Variation	-2 to 2	0	0
Astern n Variation	-2 to 2	0	0
Ahead β Variation	1, 2	-2, 0, 2, 4, 6, 8	0
Astern β Variation	1	178, 180, 182, 184, 186, 188	0
Ahead Main Rudder Variation	1, 2	0	-5, 0, 5, 10, 15, 20, 25, 30, 35
Astern Main Rudder Variation	-2	0	-5, 0, 5, 10, 15, 20 25, 30, 35
Astern Flanking Rudder Variation	2	0	-5, 0, 5, 10, 15, 20 25, 30, 35

4.0 REDUCTION AND PRESENTATION OF DATA

The data obtained from the various tests were reduced and analyzed in accordance with standard model test procedures. In particular, the data derived from the Planar Motion Mechanism (PMM) tests have been reduced to nondimensional force and moment coefficients following the procedures and notation given in References 3 and 4.

The output data from the PMM tests were integrated values of force signals from two pairs of gages. At the conclusion of each run, integrated forces from the gages were combined to obtain longitudinal (X) force, lateral (Y) force, and yawing (N) moment. Nondimensionalization in accordance with standard notation yielded nondimensional forces X' , Y' , and moment N' which were plotted against appropriate test parameters. Data plots from this set of tests are presented in Appendices A and B. Hydrodynamic coefficients were derived from curve fits to these graphs as discussed in Appendix C. Table 5 presents the hydrodynamic coefficients for the 7.5-foot draft tow boat and 15 barge tow in the deep water condition. Table 6 presents the hydrodynamic coefficients for the same model configuration, but in shallow water, with the depth equal to 13.5 feet (full-scale), $H/T = 1.5$. Table 7 contains the hydrodynamic coefficients for the same configuration in shallow water where the depth was 10.5 feet (full-scale), $H/T = 1.17$.

One of the objectives of this study was to develop a maneuvering mathematical model for the tow. An aspect of this effort was to utilize the results given in Tables 5 to 7 in order to develop an algorithm that would modify deep water coefficients to obtain shallow water coefficients.

Measured Nondimensional Hydrodynamic Coefficients
for the 15-Barge Tow in Deep Water in Combination
With a Towboat Operating at a 7.5 Foot Draft

Coefficient	Ahead $u \geq 0$ $-30^\circ < \beta < 30^\circ$		$30^\circ \leq \beta \leq 150^\circ$ $210^\circ \leq \beta \leq 330^\circ$	Aft $u < 0$ $156^\circ \leq \beta \leq 210^\circ$	
	$n \geq 0$	$n < 0$		$n \leq 0$	$n > 0$
X_u'	-0.000022		-0.00051 -0.0072	-0.000022	
X_{vr}'	0.000207			0.000175	
X_{vv}'	-0.00061			-0.00067	
X_{rr}'	0.0			0.0	
$X_{\delta\delta}'$	-0.000244	0.0		0.0	0.000244
$X_{\delta F \delta F}'$	0.0	-0.000192		0.000192	0.0
$X_{vv\eta}$	0.0	0.0		0.0	0.0
Y_u'	-0.000397			-0.000372	
$Y_{\dot{r}}'$	-0.0000365			-0.0000273	
Y_r'	0.00047			-0.00009	
$Y_{r r}'$	-0.00028			-0.00027	
Y_v'	-0.00117			0.002478	
$Y_{v v}'$	-0.00505			0.002535	
$Y_{r\eta}$	0.000155	0.000155 Set $n=0$		-0.000208	-0.000208 Set $n=0$
$Y_{v\eta}$	-0.000338	-0.000339		0.000415	0.000415
$Y_{vv\eta}'$	0.0	0.0		0.0	0.0
$Y_{v r^2}'$	-0.00189			-0.00196	
Y_{δ}'	0.000008	0.000008		-0.000008	-0.000008
$Y_{\delta\delta}'$	0.000329	0.0		0.0	-0.000329
$Y_{\delta F}'$	0.0	0.00022		-0.00022	0.0
$Y_{\delta v}'$	0.0	0.0		0.0	0.0
$Y_{r v}'$	-0.000079	-0.000079		-0.000075	-0.000075

NOTE: Numerical values listed in center column are to be used as substitute values of the coefficients for the values of β in the center column header. Coefficients that are not assigned values in the center column remain unchanged throughout the β ranges listed in the first and third column header.

(Continued)

Coefficient	Ahead $u \geq 0$ $-30^\circ < \beta < 30^\circ$		$30^\circ \leq \beta \leq 150^\circ$ $210^\circ \leq \beta \leq 330^\circ$	Aster $u < 0$ $150^\circ \leq \beta \leq 210^\circ$	
N_y	0.000036		-0.0001 0.00029	-0.0000265	
N_z	-0.0000235			-0.0000189	
N_x	-0.000224			0.000254	
$N_{x z }$	-0.000101			-0.000137	
N_v	-0.00015			-0.000669	
$N_{v v }$	0.00054			-0.00016	
	$n \geq 0$	$n < 0$		$n \leq 0$	$n > 0$
$N_{x\eta}$	-0.000067	-0.00067 Set $n=0$		0.000098	0.000098 Set $n=0$
$N_{v\eta}$	0.000151	0.000151		-0.000123	-0.000183
$N_{v r 2'}$	0.000058			0.000087	
	$n \geq 0$	$n < 0$		$n \leq 0$	$n > 0$
N_a	-0.000004	-0.000004	0.000004	0.000004	
N_δ	-0.000171	0.0	0.0	0.000171	
$N_{\delta F}$	0.0	-0.000117	0.000117	0.0	
$N_{\delta v }$	0.0	0.0	0.0	0.0	
$N_{r v }$	-0.000257		-0.000231		
	$n \geq 0$	$n < 0$	$n \leq 0$	$n > 0$	
d_R	0.17	0.26	0.33	0.17	
c_R	0.13	0.27	0.145	0.08	
f_R	0.158	-0.094	0.094	-0.158	
d_A	0.0	0.0	0.0	0.0	
c_A	-0.065	-0.10	0.18	-0.155	
f_A	0.22	-0.175	0.175	-0.22	

NOTE: Numerical values listed in center column are to be used as substitute values of the coefficients for the values of β in the center column header. Coefficients that are not assigned values in the center column remain unchanged throughout the β ranges listed in the first and third column header.

Table 5
(Concluded)

Coefficient	$u \geq 0$	$u < 0$
a_1	-0.00031	0.000426
b_1	-0.00015 $1 \leq \eta \leq \infty$	0.00025 $1 \leq \eta \leq \infty$
c_1	0.00046	-0.000676
a_2	-0.00040	0.00045
b_2	-0.00002 $0 \leq \eta \leq 1$	-0.00010 $0 \leq \eta \leq 1$
c_2	0.00042	-0.00035
a_3	-0.00040	0.00045
b_3	0.00005 $-1 \leq \eta \leq 0$	-0.00041 $-1 \leq \eta \leq 0$
c_3	-0.00035	0.00095
a_4	-0.000465	0.00069
b_4	0.00020 $-\infty \leq \eta \leq -1$	0.00012 $-\infty \leq \eta \leq -1$
c_4	-0.000235	0.00132
m	0.185×10^7 pounds	SAME
I_z	0.1477×10^{12} pounds per foot ²	
L	1130. feet	
B	105. feet	
T	9. feet	
x_g	0.0 feet	
y_p	-10.5 feet	
y_a	10.5 feet	
D_p	8.5 feet	
u_a	4 knots	-4 knots
n_a	109.1 rpm	-165.5 rpm

Table 6

Measured Nondimensional Hydrodynamic Coefficients
for the 15-Barge Tow in Shallow Water, $H/T = 1.5$,
in Combination With a Towboat Operating at a 7.5 Foot Draft

Coefficient	Ahead $u \geq 0$ $-30^\circ < \beta < 30^\circ$		$30^\circ \leq \beta \leq 150^\circ$ $210^\circ \leq \beta \leq 330^\circ$	Astern $u < 0$ $150^\circ \leq \beta \leq 210^\circ$	
	$n \geq 0$	$n < 0$		$n \leq 0$	$n > 0$
X_u'	-0.000110		-0.00304 -0.0355	-0.000110	
X_{vr}'	0.00107			0.00084	
X_{vv}'	-0.00380			-0.00392	
X_{-rr}'	0.0			0.0	
$X_{\epsilon\delta}'$	-0.000299	0.0		0.0	0.000299
$X_{\delta F\delta F}'$	0.0	-0.00022		0.00022	0.0
X_{vvn}	0.0	0.0		0.0	0.0
Y_v'	-0.00198			-0.00189	
Y_r'	-0.000198			-0.000165	
Y_r'	0.00065			-0.00031	
$Y_r r '$	0.000135			0.00013	
Y_v'	-0.00754			0.01478	
$Y_v v '$	-0.0309			0.01892	
Y_{rn}	0.000552	0.000552		-0.00080	-0.00080
Y_{vn}	-0.001198	Set $n=0$ -0.001198		0.00175	Set $n=0$ 0.00175
Y_{vvn}'	0.0	0.0		0.0	0.0
$Y_{v r^2}'$	-0.00567			-0.00412	
Y_{δ}'	0.0000083	0.0000083		-0.0000083	-0.0000083
Y_{δ}'	0.000348	0.0		0.0	-0.000348
$Y_{\delta F}'$	0.0	0.000234		-0.000234	0.0
$Y_{\delta v }'$	0.0	0.0		0.0	0.0
$Y_{r v }'$	-0.00054	-0.00054		-0.00050	-0.00050

NOTE: Numerical values listed in center column are to be used as substitute values of the coefficients for the values of β in the center column header. Coefficients that are not assigned values in the center column remain unchanged throughout the β ranges listed in the first and third column header.

(Continued)

Coefficient	Ahead $u \geq 0$ $-30^\circ < \beta < 30^\circ$		$30^\circ \leq \beta \leq 150^\circ$ $210^\circ \leq \beta \leq 330^\circ$		Astern $u < 0$ $150^\circ \leq \beta \leq 210^\circ$	
N_v	0.000172		<div>-0.00198</div> <div>0.00145</div>		-0.000130	
N_f	-0.0000958				-0.0000817	
N_r	-0.000632				0.000742	
$N_r r $	-0.000332				-0.000386	
N_v	-0.001751				-0.00413	
$N_v v $	0.002272				-0.001475	
	$n \geq 0$	$n < 0$			$n \leq 0$	$n > 0$
$N_{r\eta}$	-0.000255	-0.000255 Set $n=0$			0.00039	0.00059 Set $n=0$
$N_{v\eta}$	0.000555	0.000555			-0.000795	-0.000795
$N_{v r}^2$	0.000113				0.000159	
	$n \geq 0$	$n < 0$			$n \leq 0$	$n > 0$
N_*	-0.000004	-0.000004			0.000004	0.000004
N_δ	-0.000169	0.0			0.0	0.000169
$N_{\delta F}$	0.0	-0.000117			0.000117	0.0
$N_\delta v $	0.0	0.0			0.0	0.0
$N_r v $	-0.00154				-0.00135	
	$n \geq 0$	$n < 0$			$n \leq 0$	$n > 0$
d_R	0.12	0.190			0.25	0.12
e_R	0.08	0.181			0.099	0.06
f_R	0.192	-0.129			0.129	-0.192
d_A	0.0	0.0			0.0	0.0
e_A	-0.0477	-0.0725			0.129	-0.111
f_A	0.267	-0.224	-0.267	0.224		

NOTE: Numerical values listed in center column are to be used as substitute values of the coefficients for the values of β in the center column header. Coefficients that are not assigned values in the center column remain unchanged throughout the β ranges listed in the first and third column header.

Table 6

(Concluded)

Coefficient	$u \geq 0$	$u \leq 0$
a_1	-0.000454	0.000151
b_1	-0.000297 $1 \leq n \leq \infty$	0.000924 $1 \leq n \leq \infty$
c_1	0.000751	-0.001075
a_2	-0.000695	0.000722
b_2	-0.000063 $0 \leq n \leq 1$	-0.000164 $0 \leq n \leq 1$
c_2	0.000756	-0.000558
a_3	-0.000695	0.000722
b_3	0.000060 $-1 \leq n \leq 0$	-0.000519 $-1 \leq n \leq 0$
c_3	-0.000411	0.001121
a_4	-0.000854	0.000885
b_4	-0.0001095 $-\infty \leq n \leq -1$	0.000918 $-\infty \leq n \leq -1$
c_4	-0.000368	0.002165
m	0.1866×10^7 pounds	same
I_z	0.1490×10^{12} pounds per foot ²	
L	1130 feet	
B	105 feet	
T	9 feet	
x_g	0 feet	
y_p	-10.5 feet	
y_g	10.5 feet	
D_p	8.5 feet	
u_e	4 knots	-2 knots
n_e	140.68 rpm	-124.9 rpm

Measured Nondimensional Hydrodynamic Coefficients
for the 15-Barge Tow in Shallow Water, $H/T = 1.17$,
in Combination With a Towboat Operating at a 7.5 Foot Draft

Coefficient	Ahead $u \geq 0$ $-30^\circ < \beta < 30^\circ$		$30^\circ \leq \beta \leq 150^\circ$ $210^\circ \leq \beta \leq 330^\circ$	Astern $u < 0$ $90^\circ \leq \beta \leq 270^\circ$	
	$n \geq 0$	$n < 0$		$n \leq 0$	$n > 0$
X_u'	-0.00022		-0.01169 -0.105	-0.00022	
X_{vr}'	0.00195			0.0019	
X_{vv}'	-0.0125			-0.0164	
X_{rr}'	0.0			0.0	
$X_{\delta\delta}'$ $X_{\delta F\delta F}'$ X_{vvr}	-0.000403	0.0		-0.0	0.000403
	0.0	-0.000314		0.000314	0.0
	0.0	0.0		0.0	0.0
Y_v'	-0.00409			-0.00371	
Y_f'	-0.00075			-0.00081	
Y_r'	0.00157			-0.00118	
$Y_r r '$	0.000546			0.000501	
Y_v'	-0.02696			0.0594	
$Y_v v '$	-0.0875			0.0417	
Y_{rn}' Y_{vn}' Y_{vvn}'	0.00215	0.00215 Set $n=0$		-0.00228	-0.00228 Set $n=0$
	-0.00554	-0.00554		0.00764	0.00764
	0.0	0.0		0.0	0.0
$Y_{v r^2}'$	-0.01953			-0.01787	
$Y_{\delta\delta}'$ Y_{δ}' $Y_{\delta F}'$ $Y_{\delta v }'$	$n \geq 0$	$n < 0$		$n \leq 0$	$n > 0$
	0.000008	0.000008		-0.000008	-0.000008
	0.000375	0.0		0.0	-0.000375
	0.0	0.00025		-0.00025	0.0
	0.0	0.0		0.0	0.0
$Y_{r v }'$	-0.00124	-0.00124		-0.00099	-0.00099

NOTE: Numerical values listed in center column are to be used as substitute values of the coefficients for the values of β in the center column header. Coefficients that are not assigned values in the center column remain unchanged throughout the β ranges listed in the first and third column header.

(Continued)

Coefficient	Ahead $u \geq 0$ $-30^\circ < \beta < 30^\circ$		$30^\circ \leq \beta \leq 150^\circ$ $210^\circ \leq \beta \leq 330^\circ$		Astern $u < 0$ $90^\circ \leq \beta \leq 270^\circ$	
	$n \geq 0$	$n < 0$			$n \leq 0$	$n > 0$
$N_{\frac{1}{2}}$	0.000574		-0.00249 0.00423		-0.000574	
$N_{\frac{1}{2}}$	-0.000164				-0.0001565	
$N_{\frac{1}{2}}$	-0.00131				0.001625	
$N_{\frac{1}{2}} r $	-0.000916				-0.00125	
$N_{\frac{1}{2}}$	-0.003581				-0.01429	
$N_{\frac{1}{2}} v $	0.01075				-0.00608	
$N_{\frac{1}{2}}$	-0.00098	-0.00098 Set $\eta=0$			0.00109 0.00109 Set $\eta=0$	
$N_{\frac{1}{2}}$	0.00255	0.00255			-0.00343 -0.00343	
$N_{\frac{1}{2}}r^2$	0.00072				0.000845	
$N_{\frac{1}{2}}$	$n \geq 0$	$n < 0$			$n \leq 0$ $n > 0$	
$N_{\frac{1}{2}}$	-0.000004	-0.000004			0.000004 0.000004	
$N_{\frac{1}{2}}$	-0.000165	0.0			0.0 0.000165	
$N_{\frac{1}{2}}F$	0.0	-0.000114			0.000114 0.0	
$N_{\frac{1}{2}} v $	0.0	0.0			0.0 0.0	
$N_{\frac{1}{2}} v $	-0.0322				-0.00253	
d_R	$n \geq 0$	$n < 0$			$n \leq 0$ $n > 0$	
e_R	0.08	0.13			0.17 0.08	
f_R	0.05	0.11			0.077 0.045	
d_A	0.24	-0.155			0.155 -0.24	
e_A	0.0	0.0			0.0 0.0	
f_A	-0.032	-0.06			0.11 -0.095	
e_A	0.34	-0.28			0.28 -0.34	

NOTE: Numerical values listed in center column are to be used as substitute values of the coefficients for the values of β in the center column header. Coefficients that are not assigned values in the center column remain unchanged throughout the β ranges listed in the first and third column header.

Table 7

(Concluded)

Coefficient	$u \geq 0$	$u \leq 0$
a_1	-0.001453	-0.00011
b_1	0.000187	0.00176
c_1	0.001266	-0.00165
	$1 \leq n \leq \infty$	$1 \leq n \leq \infty$
a_2	-0.001122	0.00127
b_2	-0.000373	-0.00022
c_2	0.001495	-0.00105
	$0 \leq n \leq 1$	$0 \leq n \leq 1$
a_3	0.001122	0.00127
b_3	0.000079	-0.00099
c_3	-0.000599	0.00154
	$-1 \leq n \leq 0$	$-1 \leq n \leq 0$
a_4	-0.001483	0.001892
b_4	-0.0002207	0.001988
c_4	-0.0005377	0.003896
	$-\infty \leq n \leq -1$	$-\infty \leq n \leq -1$
m	0.185×10^7 pounds	
I_x	0.1477×10^{12} pounds per foot ²	
L	1130. feet	
B	105. feet	
T	9. feet	
x_g	0 feet	
y_p	-10.5 feet	
y_g	10.5 feet	
D_p	8.5 feet	
u_e	4 knots	-4 knots
n_e	189.1 rpm	-331.8 rpm

The maneuvering model contains a set of coefficients for third order polynomials which define the variation of each hydrodynamic coefficient with water depth to vessel draft ratio. These polynomial coefficients are derived from the data for tests in deep and shallow water. The development of these coefficients for the tow is described below.

It was concluded in Reference 5 that shallow water corrections for ships could be expressed as a polynomial in ship draft to water depth ratio, σ :

$$R = A_4 + A_3 \sigma + A_2 \sigma^2 + A_1 \sigma^3 \quad [2]$$

where R is the ratio of coefficient values in shallow to deep water and where unknown coefficients A_4 , A_3 , A_2 , and A_1 are determined by the best fit to deep and shallow water data.

The data in Tables 5 to 7 were plotted against water depth/draft ratio, and it appeared that practically all shallow water effects became negligible for values of $H/T \geq 2.7 - 2.9$, which is approximately the same range of depth ratios found for the tanker forms in Reference 6. Therefore, it has been assumed that for all water depth/draft ratios larger than $H/T = 2.75$ ($\sigma \leq 0.3636$), the hydrodynamic coefficients will be the same as in deep water ($H/T = \infty$). This assumption allows the expression of shallow water correction coefficients, in the range of $H/T = 1.17$ to 2.75 , with good precision.

To make the curve fit more accurate and precise, a special numerical procedure to estimate coefficients A_4 , A_3 , A_2 , and A_1 has been developed. These four unknown coefficients were determined from four equations.

At water depth/draft ratio $H/T = 2.75$, or $\sigma = \sigma_0 = 0.3636$, the Equation [2] should be equal to one, and its derivative at this point should be equal to zero, resulting in two Equations [2a] and [2b]:

$$A_4 + A_3\sigma_0 + A_2\sigma_0^2 + A_1\sigma_0^3 = 1 \quad [2a]$$

$$A_3 + 2A_2\sigma_0 + 3A_1\sigma_0^2 = 0 \quad [2b]$$

Two additional equations were obtained to satisfy precisely the values of the shallow water correction coefficients at $H/T = 1.50$ ($\sigma = \sigma_1 = 0.6667$, and $R = R_1$) and at $H/T = 1.17$ ($\sigma = \sigma_2 = 0.8547$, and $R = R_2$).

Thus:

$$A_4 + A_3\sigma_1 + A_2\sigma_1^2 + A_1\sigma_1^3 = R_1 \quad [2c]$$

$$A_4 + A_3\sigma_2 + A_2\sigma_2^2 + A_1\sigma_2^3 = R_2 \quad [2d]$$

By solving the Equations [2a], [2b], [2c], and [2d], the unknown coefficients A_1 , A_2 , A_3 and A_4 were determined numerically:

$$A_1 = 21.786 R_2 - 57.06 R_1 + 35.272$$

$$A_2 = 10.823 R_1 - 10.823 - 1.3805 A_1$$

$$A_3 = -0.726 A_2 - 0.396 A_1$$

$$A_4 = 1 + 0.132 A_2 + 0.096 A_1$$

In order to represent adequately the variation of many coefficients with depth without changing the form of Equations [2a], [2b], [2c], and [2d] and requiring additional coefficients, some coefficients were expressed by a modified polynomial:

$$R = (A_4 + A_3\sigma + A_2\sigma^2 + A_1\sigma^3)^n \quad [3]$$

Where the factor n was chosen as the best fit to the shallow water data at $H/T = 1.5$ and $H/T = 1.17$. Conditions [2a] and [2b] at $H/T = 2.75$ were already satisfied by the appropriate procedure to determine A_1 , A_2 , A_3 and A_4 as explained earlier. A large number of sets of shallow water correction coefficients (more than 60) is required to model all coefficients.

There are required a total of ten sets of the coefficients $A_1(j)$, $A_2(j)$, $A_3(j)$, $A_4(j)$, $j = 1$ to 10:

$$A_1(j) = DE(1,j)$$

$$A_2(j) = DE(2,j)$$

$$j = 1 \text{ to } 10$$

$$A_3(j) = DE(3,j)$$

$$A_4(j) = DE(4,j)$$

As an example, the first three sets of values for $j = 1, 2, 3$, have the following values for the 7.5-foot towboat draft:

$$\underline{j = 1}$$

$$A_1 = DE(1,1) = -1.352$$

$$A_2 = DE(2,1) = 5.232$$

$$A_3 = DE(3,1) = -3.263$$

$$A_4 = DE(4,1) = 1.561$$

-38-

$$\underline{j = 2}$$

$$A_1 = DE (1,2) = 13.40$$

$$A_2 = DE (2,2) = -16.33$$

$$A_3 = DE (3,2) = 6.55$$

$$A_4 = DE (4,2) = 0.13$$

$$\underline{j = 3}$$

$$A_1 = DE (1,3) = 2.1757$$

$$A_2 = DE (2,3) = 3.796$$

$$A_3 = DE (3,3) = -3.618$$

$$A_4 = DE (4,3) = 1.710$$

These first three sets of shallow water correction coefficients are used to estimate three terms associated with tow resistance and propulsion as follows:

1. Propeller RPM to Longitudinal Speed Ratio, RPM/U (j = 1)

$$[URPMC(K)]_{\text{shallow water}} = \frac{RPM}{U(\text{ft/sec})} =$$

$$RPMC(K)_{\text{deep water}} \times [1.561 - 3.263\sigma + 5.232\sigma^2 - 1.352\sigma^3] \quad [4]$$

($\sigma = T/H$, draft/depth ratio; for $\sigma = \sigma_0 \geq 0.3636$, the square bracket is equal to one.)

K = 1 for ahead motion, K = 2 for astern motion

2. Resistance Term in First Quadrant (j = 2)

$$(1 < n = J_c/J < \infty), J = U/nD_p$$

$$[AP(1,1)]_{\text{shallow water}} = [AP(1,1)]_{\text{deep water}}$$

$$\times [0.13 + 6.55\sigma - 16.33\sigma^2 + 13.40\sigma^3] \quad [5]$$

3. Propeller Thrust Term in First Quadrant (j = 3)

$$[CP(1,1)]_{\text{shallow water}} = [CP(1,1)]_{\text{deep water}}$$

$$\times [1.710 - 3.618\sigma + 3.796\sigma^2 + 2.1757\sigma^4] \quad [6]$$

Tables 8 and 9 list shallow water hydrodynamic coefficients computed by application of the above correction process to deep water coefficients from Table 5. Accuracy of fit was validated by comparison of results in Tables 8 and 9 with the measured shallow water results summarized in Tables 6 and 7, respectively. A detailed comparison of results in these tables indicates that agreement is good to excellent for all coefficients and operating condition. The best agreement is obtained for ahead motion although agreement for astern motion is also quite good. Agreement at the two shallow water depths ($H/T = 1.5$ and 1.17) is comparable. It should also be noted that many forces (propulsion force, sway force due to sway velocity, etc.) consist of two or more components, each defined by a separate coefficient, and that a lack of agreement in one of these coefficients may have little effect on accuracy of the total force. Although accurate for the conditions covered by the tests, these corrections should not be extrapolated to shallow water conditions less than $H/T = 1.17$.

Table 8

Estimated Nondimensional Hydrodynamic Coefficients
for the 15-Barge Tow in Shallow Water, $H/T = 1.5$,
in Combination With a Towboat Operating at a 7.5 Foot Draft

Coefficient	Ahead $u \geq 0$ $-30^\circ < \beta < 30^\circ$		$30^\circ \leq \beta \leq 150^\circ$ $210^\circ \leq \beta \leq 330^\circ$		Astern $u < 0$ $150^\circ \leq \beta \leq 210^\circ$	
	$n \geq 0$	$n < 0$			$n \leq 0$	$n > 0$
X_u'	-0.000105		-0.00324 -0.0360		-0.000105	
X_{vr}'	0.00093				0.000808	
X_{vv}'	-0.00341				-0.00375	
X_{-rr}'	0.0				0.0	
$Z_{\delta\delta}'$	-0.000278	0.0			0.0	0.000278
$X_{\delta F \delta F}'$	0.0	-0.000218			0.000218	0.0
$X_{vv\eta}'$	0.0	0.0			0.0	0.0
$Y_{\dot{\theta}}'$	-0.00191				-0.00160	
$Y_{\dot{z}}'$	-0.000199				-0.000158	
Y_r'	0.000636				-0.000311	
$Y_{r x} $	0.000137				0.000132	
Y_v'	-0.00702				0.01594	
$Y_{v v} $	-0.0359				0.01853	
	$n \geq 0$	$n < 0$			$n \leq 0$	$n > 0$
$Y_{r\eta}'$	0.000550	0.000550 Set $n=0$			-0.000793	-0.000793 Set $n=0$
Y_{vn}'	-0.001294	-0.001294			0.00469	0.00169
$Y_{vv\eta}'$	0.0	0.0			0.0	0.0
$Y_{v r^2}'$	-0.00585				-0.00410	
	$n \geq 0$	$n < 0$			$n \leq 0$	$n > 0$
$Y_{\delta\delta}'$	0.00000852	0.00000852			-0.00000852	-0.00000852
Y_{δ}'	0.00350	0.0			0.0	-0.000350
$Y_{\delta F}'$	0.0	0.000233			-0.000233	0.0
$Y_{\delta v} $	0.0	0.0			0.0	0.0
$Y_{r v} $	-0.00055	-0.00055			-0.00052	-0.00052

NOTE: Numerical values listed in center column are to be used as substitute values of the coefficients for the values of β in the center column header. Coefficients that are not assigned values in the center column remain unchanged throughout the β ranges listed in the first and third column header.

Table 8

(Continued)

Coefficient	Ahead $u \geq 0$ $-30^\circ < \beta < 30^\circ$		$30^\circ \leq \beta \leq 150^\circ$ $210^\circ \leq \beta \leq 330^\circ$	Astern $u < 0$ $150^\circ \leq \beta \leq 210^\circ$	
	$n \geq 0$	$n < 0$		$n \leq 0$	$n > 0$
N_v	0.000176		-0.001165 0.001447	-0.000136	
N_z	-0.0000932			-0.0000751	
N_r	-0.000625			0.000709	
$N_{r r}$	-0.000321			-0.000425	
N_v	-0.00175			-0.00419	
$N_{v v}$	0.002279			-0.001447	
N_{rn}	-0.000238	-0.000238		0.000374	0.000374
N_{vn}	0.000576	0.000576		-0.000744	0.000744
$N_{v r}^2$	0.000102			0.000153	
N_a	-0.000004	-0.000004		0.000004	0.000004
N_δ	-0.000174	0.0		0.0	0.000174
$N_{\delta F}$	0.0	-0.000116	0.000116	0.0	
$N_{\delta v}$	0.0	0.0	0.0	0.0	
$N_{r v}$	-0.00155		-0.00139		
	$n \geq 0$	$n < 0$	$n \leq 0$	$n > 0$	
d_R	0.116	0.171	0.171	0.12	
e_R	0.08	0.170	0.09	0.06	
f_R	0.193	-0.126	0.126	-0.193	
d_A	0.0	0.0	0.0	0.0	
e_A	-0.0456	-0.0702	0.126	-0.1088	
f_A	0.271	-0.215	-0.271	0.215	

NOTE: Numerical values listed in center column are to be used as substitute values of the coefficients for the values of β in the center column header. Coefficients that are not assigned values in the center column remain unchanged throughout the β ranges listed in the first and third column header.

Tracor Hydronautics

-42-

Table 8

(Concluded)

Coefficient	$u \geq 0$	$u \leq 0$
a_1	-0.000452	0.000143
b_1	-0.000296	0.000921
c_1	0.000748	-0.001064
a_2	-0.000651	0.000732
b_2	-0.0001193	-0.000156
c_2	0.0007704	-0.000576
a_3	-0.000651	0.000732
b_3	0.000062	-0.000510
c_3	-0.000399	0.000891
a_4	-0.000853	0.000895
b_4	-0.000027	0.000901
c_4	-0.000341	0.002266
m	0.185×10^7 pounds	
I_z	0.1477×10^{12} pounds per foot ²	
L	1130. feet	
B	105. feet	
T	9. feet	
x_g	0.0 feet	
y_p	-10.5 feet	
y_o	10.5 feet	
D_p	8.5 feet	
u_o	4 knots	-2 knots
n_o	140.68 rpm	-124.9 rpm

Table 9

Estimated Nondimensional Hydrodynamic Coefficients
for the 15-Barge Tow in Shallow Water, $H/T = 1.17$,
in Combination With a Towboat Operating at a 7.5 Foot Draft

Coefficient	Ahead $u \geq 0$ $-30^\circ < \beta < 30^\circ$		$30^\circ \leq \beta \leq 150^\circ$ $210^\circ \leq \beta \leq 330^\circ$		Astern $u < 0$ $90^\circ \leq \beta \leq 270^\circ$	
	$n \geq 0$	$n < 0$			$n \leq 0$	$n > 0$
X_b'	-0.000224		-0.0117 -0.1051		-0.000224	
X_{vr}'	0.00195				0.00185	
X_{vv}'	-0.0124				-0.0144	
X_{-rr}'	0.0				0.0	
$X_{\delta\delta}'$	-0.000403	0.0			0.0	-0.000403
X_{vvr}'	0.0	-0.000317			0.000317	0.0
$X_{\delta F\delta F}'$	0.0	0.0			0.0	0.0
Y_b'	-0.00412				-0.00386	
Y_t'	-0.00073				-0.00065	
Y_r'	0.001618				-0.001181	
$Y_{r r}'$	0.000537				0.0005181	
Y_v'	-0.0269				0.05698	
$Y_{v v}'$	-0.08485				0.0294	
Y_{rn}'	0.00215	0.00215 Set $\eta=0$			-0.00220	-0.00220 Set $\eta=0$
Y_{vn}'	-0.00547	-0.00547			0.00764	0.00764
Y_{vvn}'	0.0	0.0			0.0	0.0
$Y_{v r 2}'$	-0.01974				-0.01716	
$Y_{\delta\delta}'$	0.0000091	0.0000091			-0.0000091	-0.0000091
Y_{δ}'	0.000375	0.0			0.0	0.000375
$Y_{\delta F}'$	0.0	0.0002509			-0.0002509	0.0
$Y_{\delta v}'$	0.0	0.0			0.0	0.0
$Y_{r v}'$	-0.00124	-0.00124			-0.00112	-0.00112

NOTE: Numerical values listed in center column are to be used as substitute values of the coefficients for the values of β in the center column header. Coefficients that are not assigned values in the center column remain unchanged throughout the β ranges listed in the first and third column header.

Table 9

(Continued)

Coefficient	Ahead $u \geq 0$ $-30^\circ < \beta < 30^\circ$		$30^\circ \leq \beta \leq 150^\circ$ $210^\circ \leq \beta \leq 330^\circ$	Astern $u < 0$ $90^\circ \leq \beta \leq 270^\circ$	
	$n \geq 0$	$n < 0$		$n \leq 0$	$n > 0$
N_y	0.000561		-0.00239 0.004232	-0.000443	
N_z	-0.0001659			-0.0001434	
N_r	-0.00136			0.00155	
$N_r r $	-0.000919			-0.00125	
N_v	-0.00357			-0.01442	
$N_v v $	0.010667			-0.006295	
	$n \geq 0$	$n < 0$		$n \leq 0$	$n > 0$
$N_{r\eta}$	-0.00093	-0.00093 Set $n=0$		0.00103	0.00103 Set $n=0$
$N_{v\eta}$	0.00244	0.00244		-0.00337	-0.00337
$N_{v r^2}$	0.00065			0.000885	
	$n \geq 0$	$n < 0$		$n \leq 0$	$n > 0$
N_a	-0.000004	-0.000004		0.000004	0.000004
N_δ	-0.000171	0.0	0.0	0.000171	
$N_{\delta F}$	0.0	-0.000117	0.000117	0.0	
$N_{\delta v }$	0.0	0.0	0.0	0.0	
$N_{r v }$	-0.00328		-0.00295		
	$n \geq 0$	$n < 0$	$n \leq 0$	$n > 0$	
d_R	0.0839	0.125	0.172	0.0839	
e_R	0.048	0.117	0.065	0.042	
f_R	0.24	-0.155	0.155	-0.24	
d_A	0.0	0.0	0.0	0.0	
e_A	-0.033	-0.053	0.097	-0.085	
f_A	0.338	-0.269	0.269	-0.338	

NOTE: Numerical values listed in center column are to be used as substitute values of the coefficients for the values of β in the center column header. Coefficients that are not assigned values in the center column remain unchanged throughout the β ranges listed in the first and third column header.

Table 9

(Concluded)

Coefficient	$u \geq 0$	$u \leq 0$
a_1	-0.001454	-0.000036
b_1	0.000189 $1 \leq n \leq \infty$	0.001759 $1 \leq n \leq \infty$
c_1	0.001265	-0.001723
a_2	-0.00110	0.001237
b_2	-0.000379 $0 \leq n \leq 1$	-0.000219 $0 \leq n \leq 1$
c_2	0.001479	-0.00102
a_3	-0.00110	0.001237
b_3	0.0000788 $-1 \leq n \leq 0$	-0.000997 $-1 \leq n \leq 0$
c_3	-0.000601	0.001273
a_4	-0.001487	0.00191
b_4	-0.000214 $-\infty \leq n \leq -1$	0.002063 $-\infty \leq n \leq -1$
c_4	-0.000596	0.003657
m	0.1866×10^7 pounds	Same
I_x	0.1490×10^{12} pounds per foot ²	
L	1130. feet	
B	105. feet	
T	9. feet	
x_g	0 feet	
y_p	-10.5 feet	
y_s	10.5 feet	
D_p	8.5 feet	
u_0	3 knots	-2 knots
n_0	144.0 rpm	-168.6 rpm

Table 10 presents the hydrodynamic coefficients for the nine-foot draft tow boat and fifteen barge tow in the deep water condition. Table 11 offers the hydrodynamic coefficients for this same model configuration except in shallow water where the depth is 13.5 feet (full scale), $H/T = 1.17$. For the nine-foot draft case, the shallow-water-depth-corrections were estimated using a modified procedure due to availability of data at only one finite water depth. As a result, coefficients based on the test data and based on the shallow-water-correction coefficients are identical at $H/T = 1.17$.

For the captive-model bank tests, only steady-state conditions were measured during the run. As a result, they were treated as a special case of PMM tests, and standard data analysis was performed. These data are contained in Appendix D. Data from captive model wing dam tests were expected to contain a series of transient forces generated by passage of the tow past the wing dam ends. To capture this effect, a digitized time history was made of model position, speed, and forces acting upon the model during each run. A preliminary analysis of the data showed that any transients due to wing dams were very small. The data were examined for energy as a function of frequency. A spectral analysis was performed using an autocorrelation routine developed for seakeeping studies at the HSMB.

The test data have been used to determine the change in lateral force and yawing moment from the wing dam, and to characterize the unsteady or time-varying forces acting on the tow during its passage by the set of six wing dams.

Table 10

Measured Nondimensional Hydrodynamic Coefficients
for the 15-Barge Tow in Deep Water in Combination
With a Towboat Operating at a 9.0 Foot Draft

Coefficient	Ahead $u \geq 0$ $-30^\circ < \beta < 30^\circ$		$30^\circ \leq \beta \leq 150^\circ$ $210^\circ \leq \beta \leq 330^\circ$		Astern $u < 0$ $150^\circ \leq \beta \leq 210^\circ$	
	$n \geq 0$	$n < 0$			$n < 0$	$n > 0$
x_u'	-0.000025		-0.00051 -0.0072		-0.000025	
x_{vr}'	0.000275				0.00025	
x_{vv}'	-0.00095				-0.00087	
x_{rr}'	0.0				0.0	
$x_{\delta\delta}'$	-0.000244	0.0			0.0	0.000244
$x_{\delta F \delta F}'$	0.0	-0.000192			0.000192	0.0
$x_{vv\eta}'$	0.0	0.0			0.0	0.0
y_u'	-0.000403				-0.000381	
$y_{\dot{x}}'$	-0.0000383				-0.0000315	
y_r'	0.00047				-0.00009	
$y_{r r} '$	-0.00028				-0.00027	
y_v'	-0.00117				0.002478	
$y_{v v} '$	-0.00505				0.00175	
	$n > 0$	$n < 0$			$n \leq 0$	$n > 0$
$y_{r\eta}'$	0.0015	0.000155 Set $n=0$			-0.000208	-0.000208 Set $n=0$
$y_{v\eta}'$	-0.000339	-0.000339			0.000415	0.000415
$y_{vv\eta}'$	0.0	0.0			0.0	0.0
$y_{v r^2}'$	-0.00189				-0.00196	
	$n > 0$	$n < 0$			$n \leq 0$	$n > 0$
$y_{\dot{x}}'$	0.000008	0.000008			-0.000008	-0.000008
y_{δ}'	0.000329	0.0			0.0	-0.000329
$y_{\delta F}'$	0.0	0.00022			-0.00022	0.0
$y_{\delta v} '$	0.0	0.0	0.0	0.0		
$y_{r v} '$	-0.000075	-0.000075	-0.000071	-0.000071		

NOTE: Numerical values listed in center column are to be used as substitute values of the coefficients for the values of β in the center column header. Coefficients that are not assigned values in the center column remain unchanged throughout the β ranges listed in the first and third column header.

Table 10

(Continued)

Coefficient	Ahead $u \geq 0$ $-30^\circ < \beta < 30^\circ$		$30^\circ \leq \beta \leq 150^\circ$ $210^\circ \leq \beta \leq 330^\circ$	Astern $u < 0$ $150^\circ \leq \beta \leq 210^\circ$	
N_v	0.000038		-0.0010 0.00027	-0.0000320	
N_r	-0.0000249			-0.0000205	
N_r	-0.000224			0.000254	
$N_r r $	-0.000101			-0.000137	
N_v	-0.000163			-0.000655	
$N_v v $	0.000445			-0.000110	
	$n \geq 0$	$n < 0$		$n \leq 0$	$n > 0$
$N_{r\eta}$	-0.000067	-0.000067 Set $\eta=0$		0.000098	0.000098 Set $\eta=0$
$N_{v\eta}$	0.000151	0.000151		-0.000183	-0.000183
$N_{v r^2}$	0.000055			0.000079	
	$n \geq 0$	$n < 0$		$n \leq 0$	$n > 0$
N_δ	-0.000004	-0.000004		0.000004	0.000004
N_δ	-0.000171	0.0		0.0	0.000171
$N_{\delta F}$	0.0	-0.000117		0.000117	0.0
$N_{\delta v }$	0.0	0.0		0.0	0.0
$N_{r v }$	-0.000257			-0.000231	
	$n \geq 0$	$n < 0$		$n \leq 0$	$n > 0$
d_R	0.17	0.26		0.33	0.17
e_R	0.13	0.27		0.145	0.08
f_R	0.158	-0.094		0.094	-0.158
d_A	0.0	0.0		0.0	0.0
e_A	-0.065	-0.10		0.18	-0.155
f_A	0.22	-0.175		0.175	-0.22

NOTE: Numerical values listed in center column are to be used as substitute values of the coefficients for the values of β in the center column header. Coefficients that are not assigned values in the center column remain unchanged throughout the β ranges listed in the first and third column header.

Table 10

(Concluded)

Coefficient	$u \geq 0$	$u < 0$
a_1	-0.00032	0.00057
b_1	-0.00018	0.00020
c_1	0.00050	-0.00077
a_2	-0.00040	0.00047
b_2	-0.00006	-0.00010
c_2	0.00056	-0.00037
a_3	-0.00040	0.00047
b_3	-0.00005	-0.00041
c_3	-0.00045	0.00126
a_4	-0.00053	0.00073
b_4	0.00002	0.00015
c_4	-0.00025	0.00156
m	0.1866×10^7 pounds	same
I_g	0.1490×10^{12} pounds per foot ²	
L	1130. feet	
B	105. feet	
T	9. feet	
x'_g	0 feet	
y_p	-10.5 feet	
y_e	10.5 feet	
D_p	8.5 feet	
u_e	4 knots	-4 knots
n_e	113.8 rpm	-187.6 rpm

Measured Nondimensional Hydrodynamic Coefficients
for the 15-Barge Tow in Shallow Water, $H/T = 1.17$
in Combination With a Towboat Operating at a 9.0 Foot Draft

Coefficient	Ahead $u \geq 0$ $-30^\circ < \beta < 30^\circ$		$30^\circ \leq \beta \leq 150^\circ$ $210^\circ \leq \beta \leq 330^\circ$		Astern $u < 0$ $90^\circ \leq \beta \leq 270^\circ$	
	$n > 0$	$n < 0$			$n < 0$	$n > 0$
X_u'	-0.000255				-0.000254	
X_{vr}'	0.00259				0.00236	
X_{vv}'	-0.01927				-0.01764	
X_{-rr}'	0.0				0.0	
$X_{\delta\delta}'$	-0.000403	0.0			-0.0	0.000403
X_{vvR}'	0.0	-0.000314			-0.000314	0.0
Y_u'	-0.004189				-0.00396	
Y_z'	-0.000753				-0.00062	
Y_r'	0.001618				-0.001181	
$Y_{r r}'$	0.000537				0.0005181	
Y_v'	-0.0269		-0.0117		0.05698	
$Y_{v v}'$	-0.08485		-0.1051		0.0294	
Y_{rn}'	0.00215	0.00215 Set $n=0$			-0.00228	0.00228 Set $n=0$
Y_{vn}'	-0.00554	-0.00554			0.00764	0.00764
Y_{vvn}'	0.0	0.0			0.0	0.0
Y_{vr}^2'	-0.01974				-0.01716	
Y_a'	0.0000091	0.0000091			-0.0000091	-0.0000091
Y_δ'	0.000375	0.0			0.0	-0.000375
$Y_{\delta F}'$	0.0	0.0002509			-0.0002509	0.0
$Y_{\delta v}'$	0.0	0.0			0.0	0.0
$Y_{r v}'$	-0.00118	-0.00118			-0.00111	-0.00111

NOTE: Numerical values listed in center column are to be used as substitute values of the coefficients for the values of β in the center column header. Coefficients that are not assigned values in the center column remain unchanged throughout the β ranges listed in the first and third column header.

Table 11

(Continued)

Coefficient	Ahead $u \geq 0$ $-30^\circ < \beta < 30^\circ$		$30^\circ \leq \beta \leq 150^\circ$ $210^\circ \leq \beta \leq 330^\circ$	Aster $u < 0$ $90^\circ \leq \beta \leq 270^\circ$	
N_z	0.00059		-0.00239 0.00394	-0.000497	
N_x	-0.000176			-0.000144	
N_y	-0.00136			0.00154	
$N_{r r}$	-0.000919			-0.00125	
N_v	-0.00389			-0.01093	
$N_{v v}$	0.00649			0.00224	
	$n > 0$	$n < 0$		$n < 0$	$n > 0$
$N_{z\eta}$	-0.00093	-0.00093 Set $\eta=0$		0.00103	0.00103 Set $\eta=0$
$N_{v\eta}$	0.00244	0.00244		-0.00337	-0.00337
$N_{v r}^2$	0.00056			0.00080	
	$n > 0$	$n < 0$	$n < 0$	$n > 0$	
N_a	-0.000004	-0.000004	0.000004	0.000004	
N_δ	-0.000174	0.0	0.0	0.000171	
N_{δ_F}	0.0	-0.000114	0.000114	0.0	
$N_{\delta v}$	0.0	0.0	0.0	0.0	
$N_{r v}$	-0.00328		-0.00295		
	$n > 0$	$n < 0$	$n < 0$	$n > 0$	
d_R	0.0839	0.105	0.172	0.0839	
e_R	0.048	0.117	0.065	0.042	
f_R	0.24	-0.155	0.155	-0.24	
d_A	0.0	0.0	0.0	0.0	
e_A	-0.034	-0.0523	0.0951	-0.082	
f_A	0.338	-0.269	0.269	-0.338	

NOTE: Numerical values listed in center column are to be used as substitute values of the coefficients for the values of β in the center column header. Coefficients that are not assigned values in the center column remain unchanged throughout the β ranges listed in the first and third column header.

Table 11

(Concluded)

Coefficient	$u \geq 0$	$u \leq 0$
a_1	-0.00144	-0.0000025
b_1	0.000279	0.001407
c_1	0.001164	-0.001405
	$1 \leq \eta \leq \infty$	$1 \leq \eta \leq \infty$
a_2	-0.000926	0.001088
b_2	-0.000169	-0.0002189
c_2	0.001095	-0.000869
	$0 \leq \eta \leq 1$	$0 \leq \eta \leq 1$
a_3	-0.000926	0.001088
b_3	-0.0000749	-0.000997
c_3	-0.000715	0.000786
	$-1 \leq \eta \leq 0$	$-1 \leq \eta \leq 0$
a_4	-0.001227	0.001429
b_4	-0.000178	0.001719
c_4	-0.000517	0.003161
	$-\infty \leq \eta \leq -1$	$-\infty \leq \eta \leq -1$
m	0.1866×10^7 pounds	
I_s	0.1490×10^{12} pounds per foot ²	
L	1130. feet	
B	105. feet	
T	9. feet	
x'_s	0. feet	
y_p	-10.5 feet	
y'_s	10.5 feet	
D_p	8.5 feet	
u_∞	3 knots	-3 knots
n_∞	150 rpm	-248.2 rpm

Table 12 presents lateral force and yawing moment coefficients derived from tests at water depth/draft ratios of 1.17 and 1.5. This table includes coefficients for tow-to-end-of-wing-dam clearances of 0.5 and 1.0 tow beams, and coefficients for tests with no wing dams, which correspond approximately to an infinite tow-to-wing-dam spacing.

Table 13 presents results of autocorrelation analysis of the time histories of forces acting on the tow during operation past the wing dams. Also, Table 13 presents mean and root mean square (rms) values for nondimensional axial force, lateral force, and yawing moment.

From the values in Table 13, the variation of mean and rms forces with clearance from the ends of the wing dams at varying water depths and drift angles can be determined. Variations with drift angle can only be determined with reasonable accuracy for a water depth to draft ratio of 1.17 and tow-to-wing-dam clearances of 0.5 and 1.0 beams. The values of hydrodynamic coefficients, Y_v' and N_v' , determined from the mean values in Table 13, are in good agreement with the values given in Table 12.

Data derived from the tests with one 45-degree sloping bank, and water depths where H/T equal to 1.50 and 1.17, are presented in Appendix D. These data have been analyzed to determine the variation of steady sway force and yaw moment with distance from banks.

Figures 9 and 10 present the variation of nondimensional lateral sway force and yawing moment with the bank distance parameter \bar{B} (defined and used as η in Reference 4). This parameter \bar{B} is defined for these tests by

Table 12

Lateral Force and Yawing Moment Coefficients Derived
From Tests Past Wing Dams in Two Different Values of
Water Depth/Draft

Water Depth/ Draft Ratio	Spacing/ Beam Ratio	Y_v'	N_v'
1.17	0.5	-0.023	-0.0034
	1.0	-0.025	-0.0033
	"	-0.027	-0.0036
1.50	0.5	-0.0091	-0.0024
	1.0	-0.0100	-0.0014
	"	-0.0079	-0.0018

Table 13

Axial Force, Lateral Force and Yawing Moment Coefficient Derived by
Autocorrelation Analyses of Time Histories of Forces and Moments
Acting on the Operation of the Tow Past Wing Dams

Water Depth	Clearance to Dam	Drift Angle, β	$X' \times 10^3$		$Y' \times 10^3$		$N' \times 10^3$	
			mean	rms	mean	rms	mean	rms
1.17T	0.287B	0	-0.20	5.15	0.46	3.03	0.20	0.36
1.17T	1.0B	0	-0.14	4.51	0.52	2.91	0.08	0.30
		2	-0.27	5.89	1.04	3.26	0.17	0.36
		4	-0.46	5.38	2.33	3.01	0.35	0.42
		8	-0.51	6.38	4.47	4.40	0.62	0.63
1.17T	1.0B	-8	-0.81	4.70	-3.88	3.24	-0.45	0.43
		-4	-0.25	5.57	-1.32	2.96	-0.16	0.33
		-2	-0.30	5.59	-0.40	2.86	-0.01	0.30
	0.5B	-4	-0.37	5.38	-0.96	3.10	-0.06	0.38
		-2	-0.08	6.08	-0.20	3.03	0.10	0.46
		0	-0.04	6.38	0.64	3.22	0.17	0.45
		2	-0.56	4.72	1.45	3.30	0.28	0.40
		4	-0.62	5.07	2.24	3.07	0.41	0.35
	1.375B	0	-0.20	4.47	0.41	3.08	0.20	0.42
1.5T	0.287B	0	-0.18	2.77	-0.03	2.19	0.05	0.21
	0.5B	-4	-0.48	3.08	-0.48	2.40	-0.14	0.21
		0	-0.37	3.23	0.03	2.30	0.07	0.24
		4	-0.51	3.10	0.79	2.17	0.19	0.22
	1.0B	-4	-0.47	3.01	-0.52	2.12	-0.13	0.19
		0	-0.20	2.80	-0.07	2.08	0.04	0.18
		4	-0.53	3.25	0.95	2.06	0.12	0.25

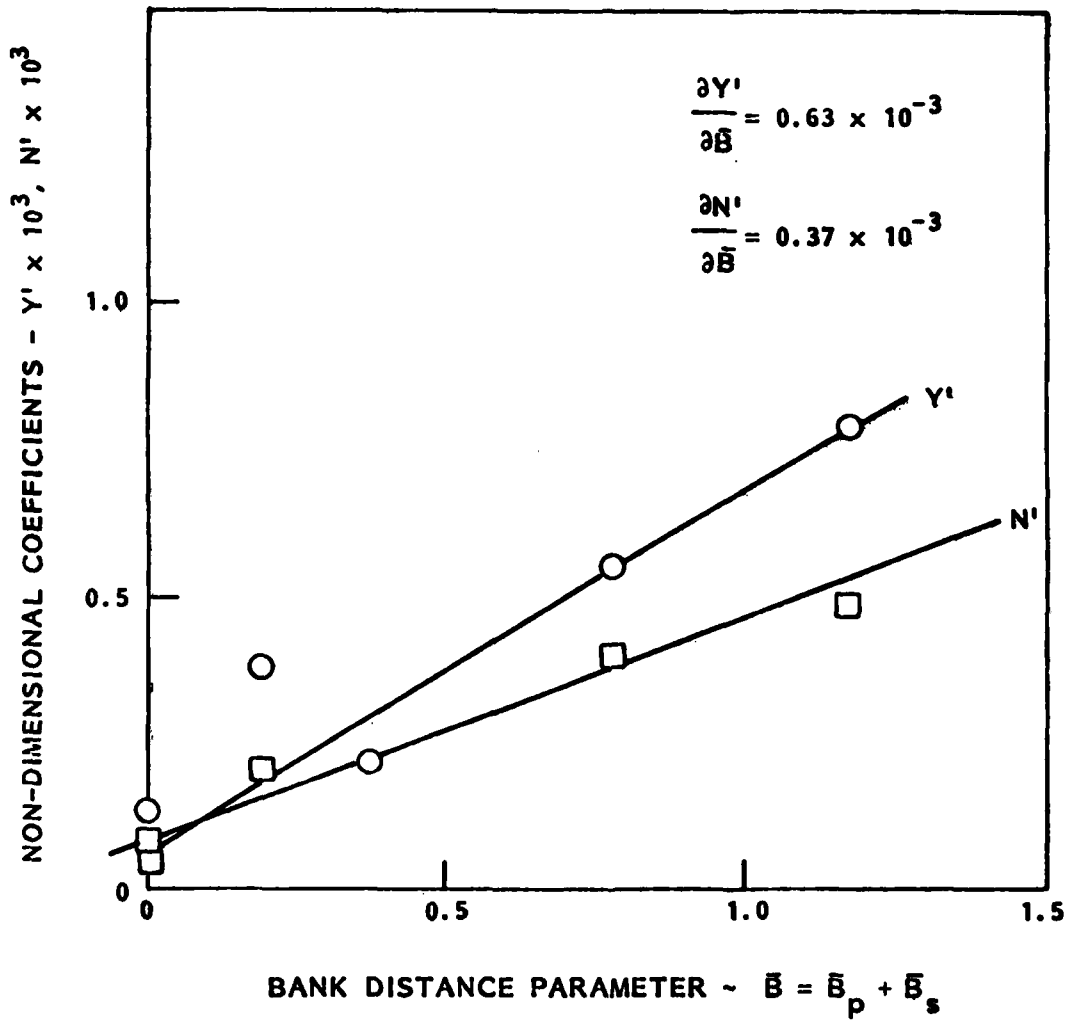


FIGURE 9 - VARIATION OF LATERAL FORCE AND YAWING MOMENT COEFFICIENTS WITH DISTANCE FROM BANKS FOR WATER DEPTH/DRAFT RATIO OF 1.17

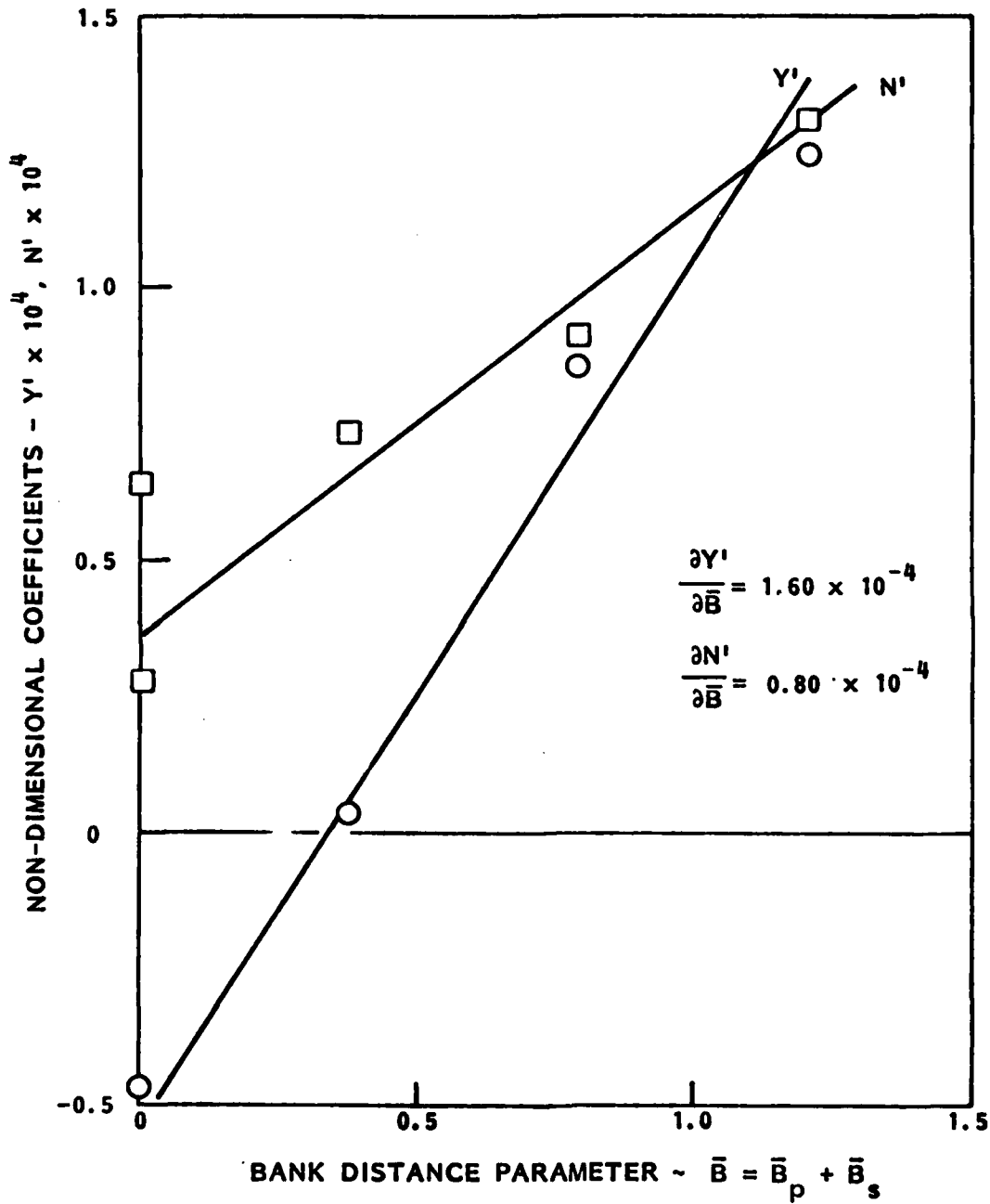


FIGURE 10- VARIATION OF LATERAL FORCE AND YAWING MOMENT COEFFICIENTS WITH DISTANCE FROM BANKS FOR WATER DEPTH/DRAFT RATIO OF 1.5

$$\begin{aligned}\bar{B} &= \bar{B}_s + \bar{B}_p \\ &= \frac{B}{y_s} + \left(1 - \frac{1}{2} \frac{T}{H}\right) \frac{B}{y_p} + \frac{1}{2} \frac{T}{H} \frac{B}{(y_p - 0.707 H)}\end{aligned}\quad [7]$$

where B is tow beam (105-foot for the prototype),

T is tow draft (9-foot for the prototype),

H is water depth,

y is distance from tow to bank at water surface,

and the subscripts p and s denote port and starboard, respectively.

In all tests, the starboard bank was the starboard tank wall and the port bank was the 45-degree bank placed on the tank bottom. Values of sway force and yawing moment for a zero value of \bar{B} were obtained from tests in shallow water with no bank, where the model was equidistant from the tank walls, and hence $\bar{B}_p = -\bar{B}_s$.

No bank effects were measured in the deep water tests. Bank effects were measured only for the original test configuration, with 7.5-foot towboat draft. As the towboat beam is much smaller than the beam of the tow (38 feet versus 105 feet), any bank influence should depend almost entirely on barge geometry, and hence the increase in towboat draft should have little or no effect on the results.

Because the bank was continuous and the model moved parallel to the bank, no unsteady forces due to the banks were expected and no unsteady forces were recorded.

The variation of the sway hydrodynamic coefficients, Y_v' and N_v' , with bank spacing parameter, \bar{B} , are plotted for

depth draft ratios of 1.17 and 1.50 in Figures 11 and 12, respectively. These figures show that there is an essentially linear variation of Y_v' and N_v' with \bar{B} . The rates of change of Y_v' and N_v' with respect to \bar{B} are given in Table 14.

PMM tests conducted over a wavy bottom were not expected to show a significant variation of forces with model position relative to wave crests and troughs. The primary data acquisition and analysis arrangements were thus the same as for ordinary PMM tests. Force time histories were recorded, however, and several runs analyzed by spectral analysis to test the above-mentioned hypothesis. The results of these tests are given in Appendix D. The test data were averaged and the resulting values were nondimensionalized by tow length and speed. The resulting force coefficients were used to determine lateral force, axial force, and yawing moment coefficients. In addition, spectral analyses of test data from several runs were carried out to determine mean and rms values.

Hydrodynamic coefficients determined from time averages of data for ahead and astern motion tests over the wavy bottom are given in Table 15. These include coefficients for static drift angle tests, main and flanking rudder angle tests and propulsion or η -variation tests. The self-propulsion advance coefficients, J_C , were determined from the propulsion tests; all other tests over the wavy bottom were carried out for these values of J_C .

The coefficients Y_v' , $Y|v|'$, $N_v|v|'$, Y_{δ_r}' , and N_{δ_r}' , determined from the static drift angle and rudder deflection tests over the wavy bottom, are compared with the values of these coefficients determined from tests with a flat bottom (the bottom of the HSMB) in Figures 13 to 16. The data were plotted on log-log scale to reflect the fact that these coefficients generally vary as a power of the depth/draft ratio. In these

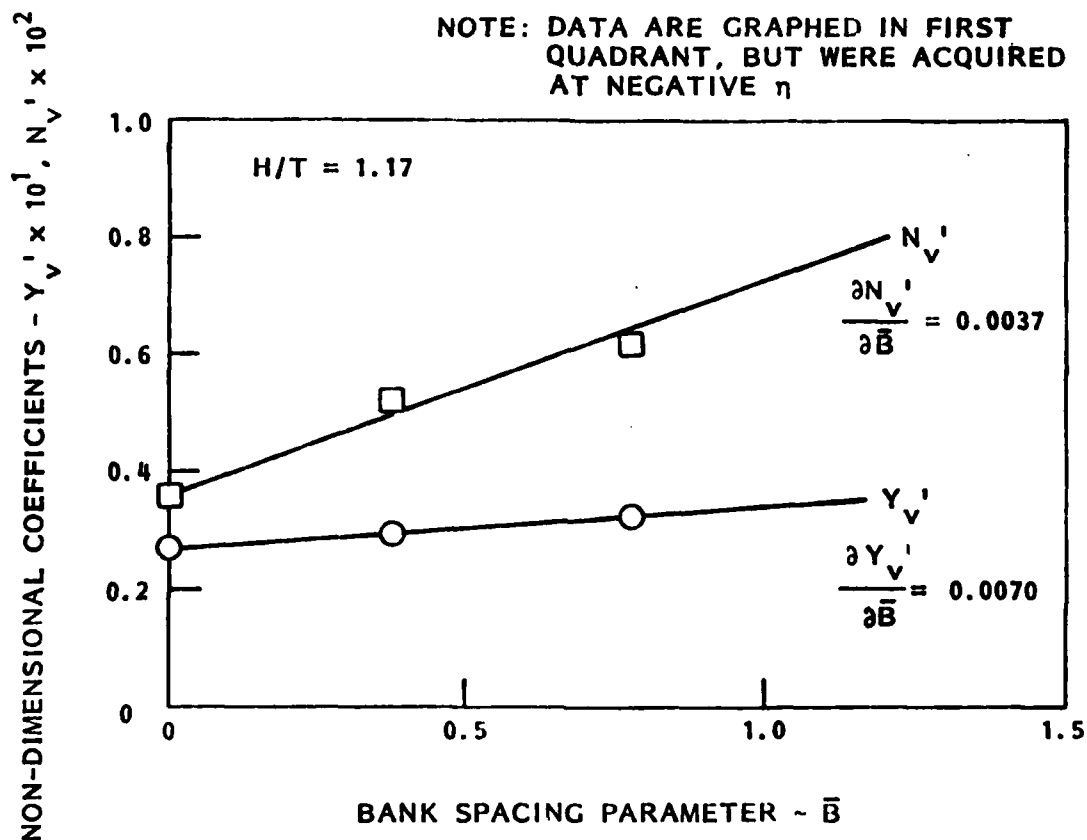


FIGURE 11- VARIATION OF Y_V' AND N_V' COEFFICIENTS WITH DISTANCE FROM BANKS FOR WATER DEPTH/DRAFT RATIO OF 1.17

NOTE: DATA ARE GRAPHED IN FIRST QUADRANT, BUT WERE ACQUIRED AT NEGATIVE η

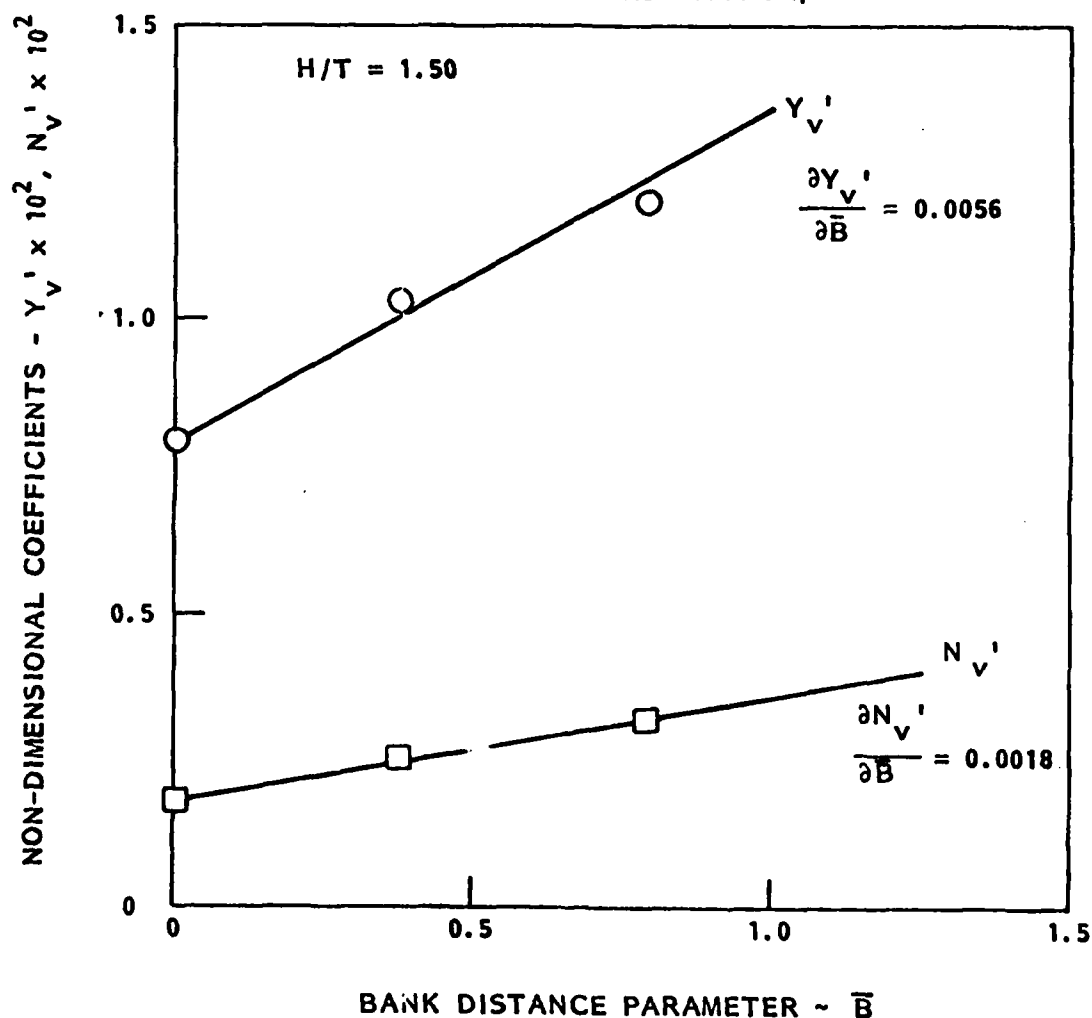


FIGURE 12- VARIATION OF Y_v' AND N_v' COEFFICIENTS WITH DISTANCE FROM BANKS FOR WATER DEPTH/DRAFT RATIO OF 1.50

Table 14
Rates of Change of Hydrodynamic Coefficients
With Distance From Banks

Water Depth- Draft Ratio	Y_V'	$\frac{\partial Y_V'}{\partial B}$	N_V'	$\frac{\partial N_V'}{\partial B}$
1.17	-0.0270	0.0070	-0.00357	0.0037
1.50	-0.0079	0.0056	-0.00175	0.0018

Table 15
Hydrodynamic Coefficients for Tests
Over a Wavy or Irregular Bottom

I. <u>Ahead Motion</u>	
Y_v'	= -0.00646
$Y_v v '$	= -0.0319
N_v'	= -0.00188
$N_v v '$	= -0.00191
J_c	= 0.303
$Y_{\delta_r \text{ main}}'$	= 0.000402
$N_{\delta_r \text{ main}}'$	= -0.000257
II. <u>Astern Motion</u>	
L_v'	= +0.0107
$Y_v v '$	= -0.0372
N_v'	= -0.00286
$N_v v '$	= -0.00948
J_c	= 0.156
$Y_{\delta_r \text{ flank}}'$	= -0.00099
$N_{\delta_r \text{ flank}}'$	= 0.000592

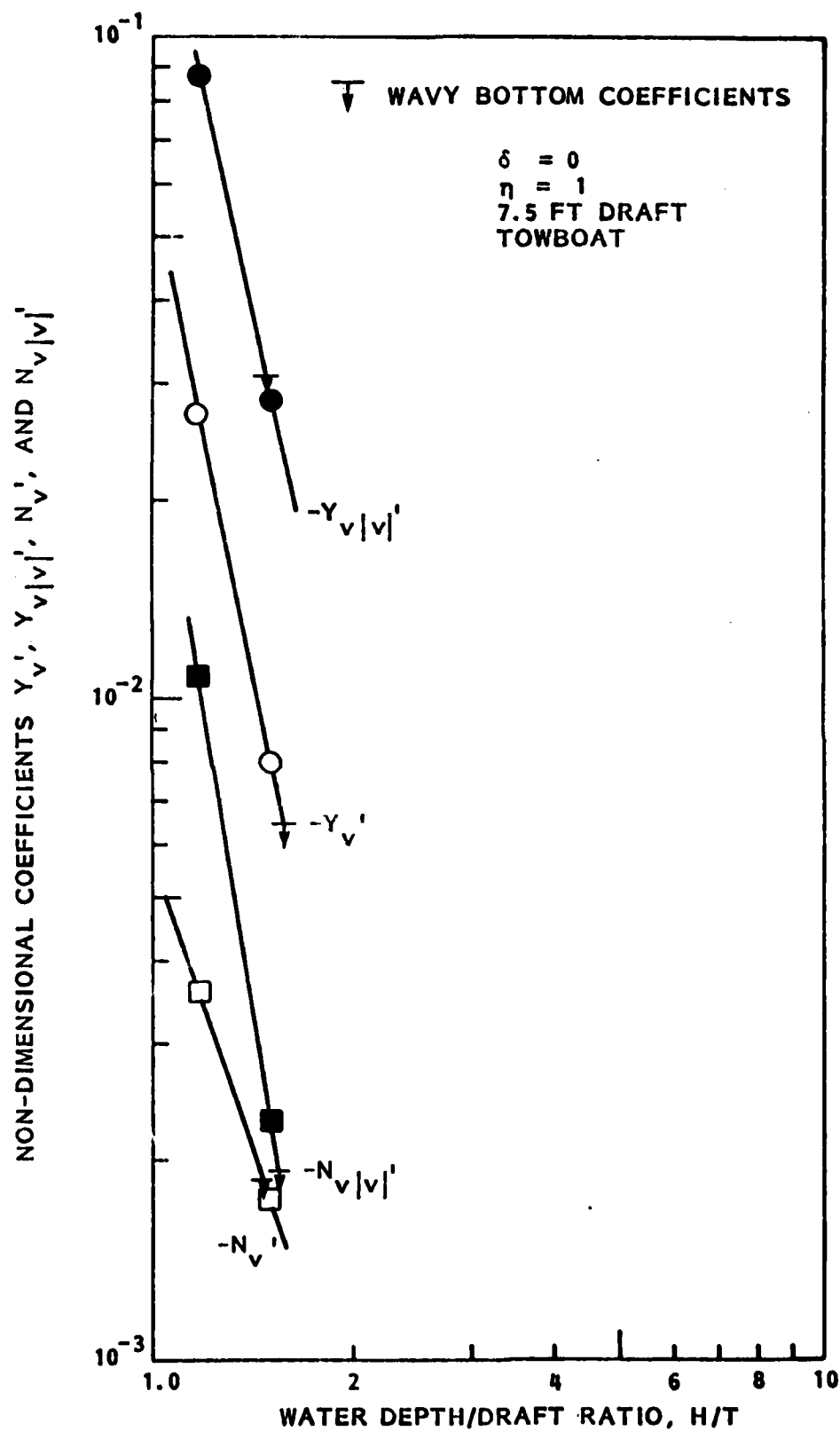


FIGURE 13- VARIATION OF LATERAL FORCE AND YAWING MOMENT COEFFICIENTS WITH WATER DEPTH/DRAFT RATIO FOR AHEAD MOTION

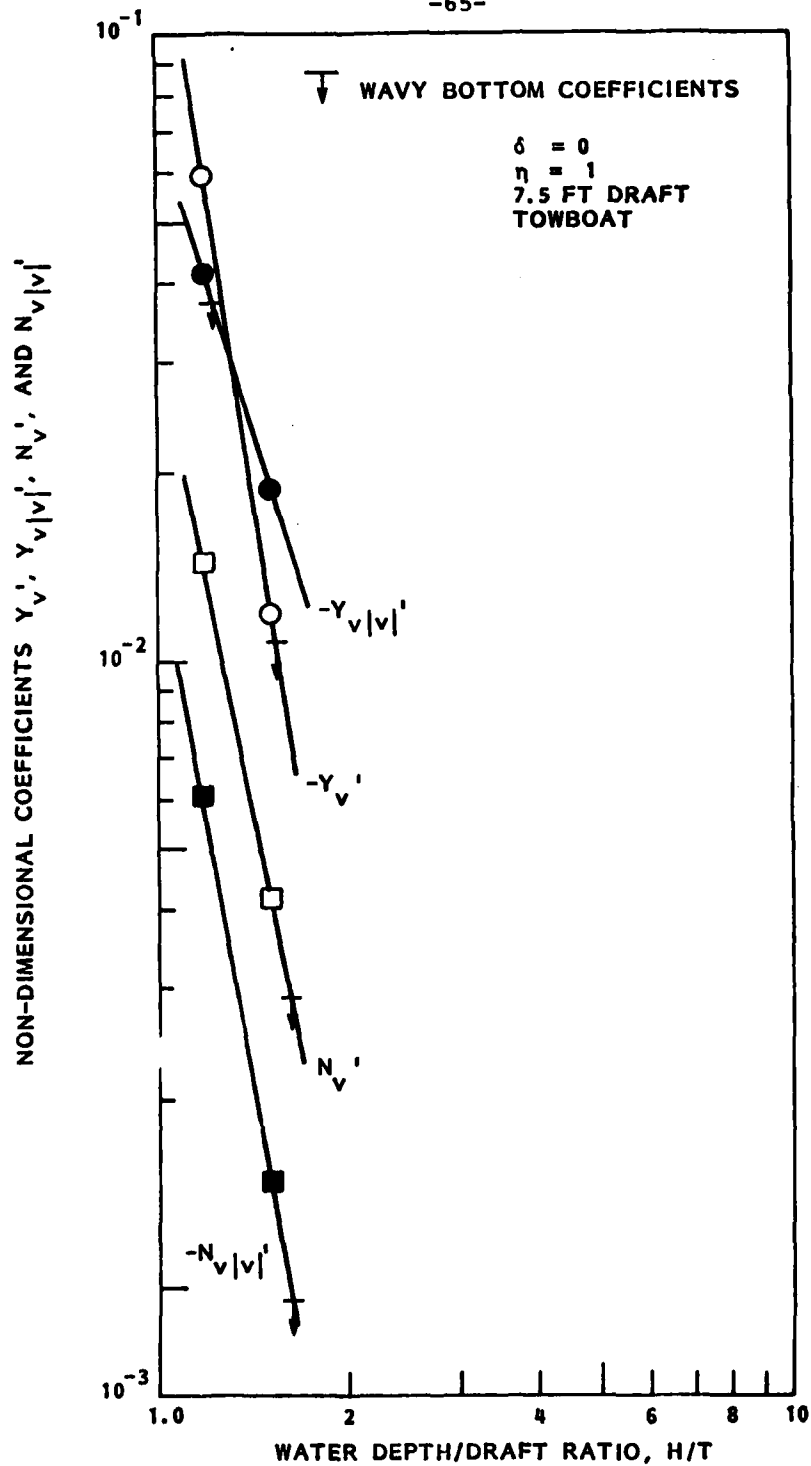


FIGURE 14- VARIATION OF LATERAL FORCE AND YAWING MOMENT COEFFICIENTS WITH WATER DEPTH/DRAFT RATIO FOR ASTERN MOTION

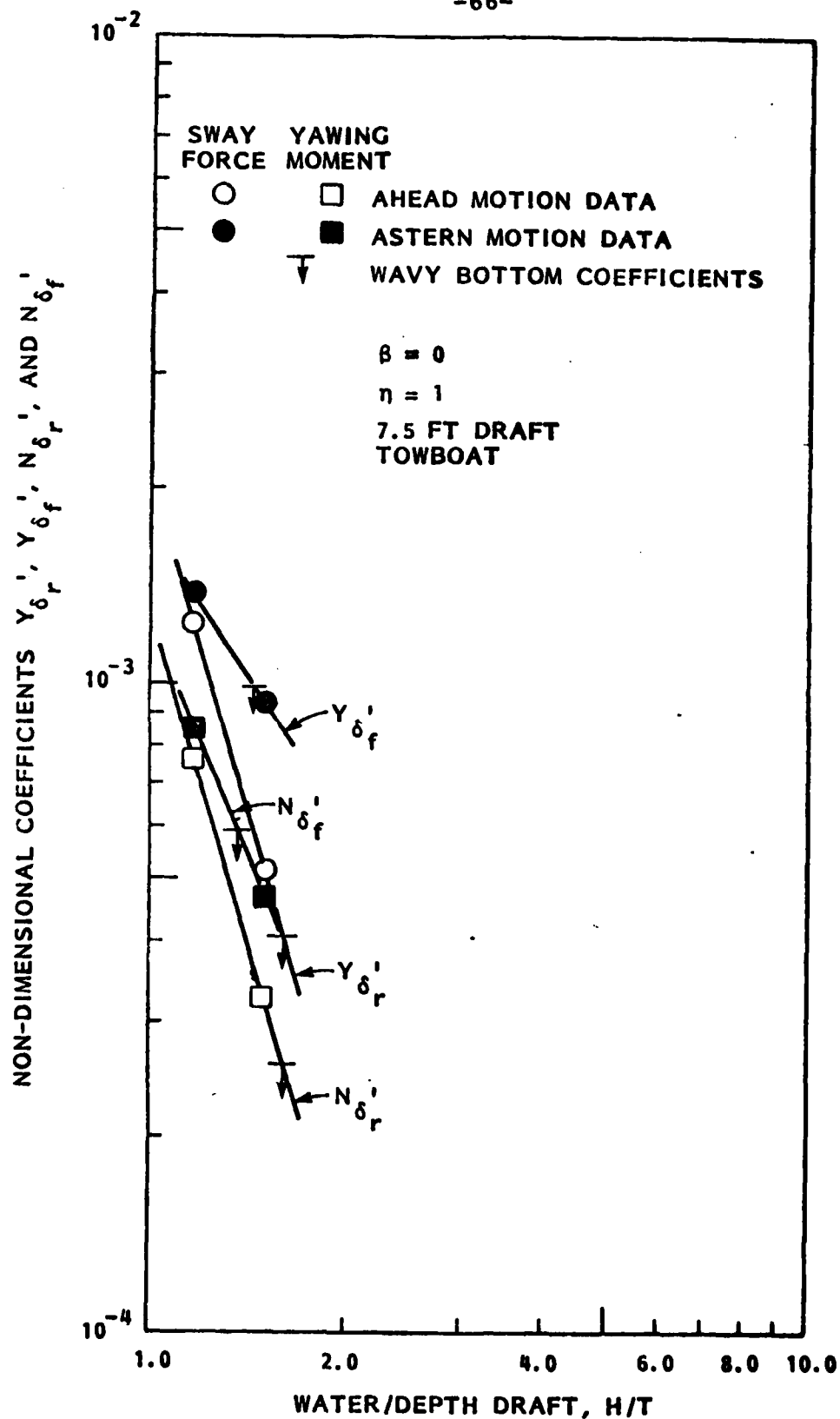


FIGURE 15- VARIATION OF LATERAL FORCE AND YAWING MOMENT RUDDER COEFFICIENTS WITH WATER DEPTH/DRAFT RATIO FOR AHEAD AND ASTERN MOTION

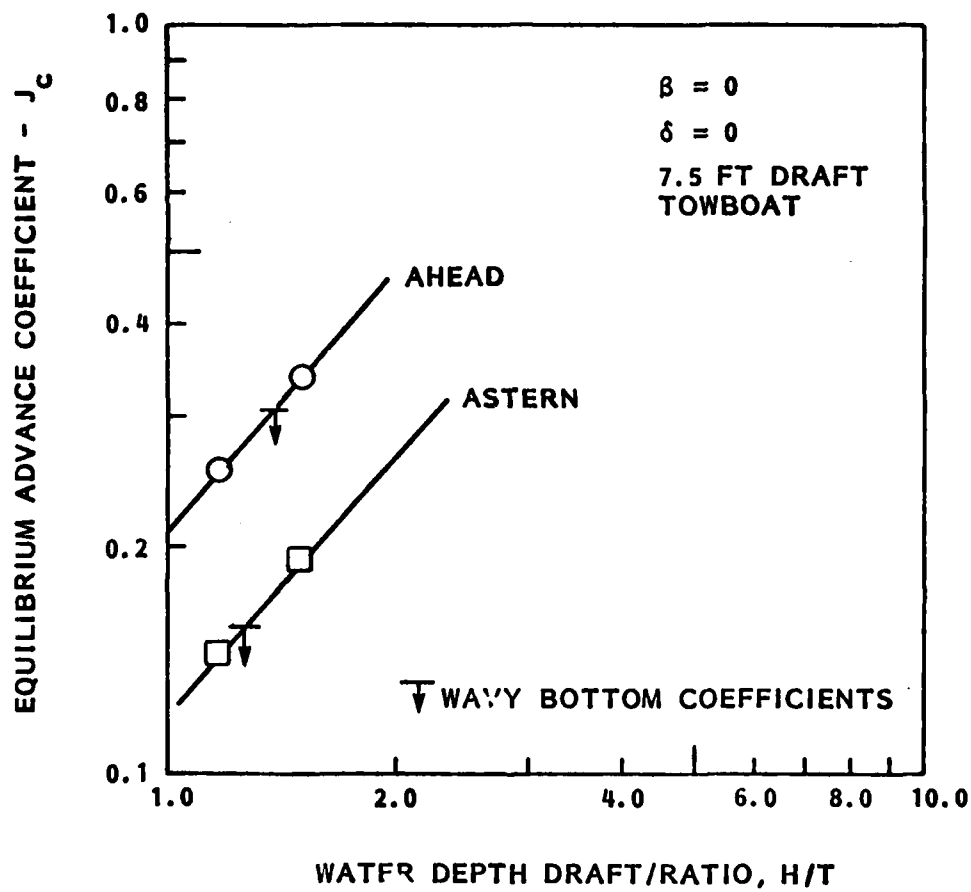


FIGURE 16 - VARIATION OF EQUILIBRIUM PROPULSION ADVANCE COEFFICIENTS WITH WATER DEPTH/DRAFT RATIO FOR AHEAD AND ASTERN MOTION

figures, the values of the coefficients for the wavy bottom were noted on a straight line connecting data points for the two flat bottom cases ($H/T = 1.17$ and 1.50) to indicate an "effective" water depth.

The mean and rms values of X' , Y' , and N' determined from the spectral analysis of the data obtained in the tests over a wavy bottom are presented in Table 16. The mean values of Y' and N' given in this table are generally very similar to the values determined from time-averaging of measured forces during the tests, and the resulting hydrodynamic coefficients (Y_v' , N_v' , etc.) are very similar to those determined from the time-averaged forces.

Figure D.13 of Appendix D contains a sample track plot from a free running model test past a series of wing dams. This figure illustrates the small effect of the wing dams on track of the tow.

Table 16
Axial Force, Lateral Force and Yawing Moment
Coefficients for Tests Over a Wavy Bottom

Direction of Motion	Drift Angle	Rudder Angle	$X' \times 10^3$		$Y' \times 10^3$		$N' \times 10^3$	
			mean	rms	mean	rms	mean	rms
Ahead	0	0	-0.49	4.26	0.04	0.65	0.01	0.10
	6	0	-0.42	4.06	1.02	1.36	0.18	0.22
	0	25	-0.49	4.81	-0.20	0.76	0.14	0.13
Astern	180	0	0.33	2.79	-0.36	0.64	-0.06	0.11
	186	0	-0.32	2.96	-1.41	1.11	0.47	0.20
	180	25	-0.06	2.95	-0.48	0.84	0.28	0.18

5.0 DEVELOPMENT OF THE MANEUVERING MODEL

A complete maneuvering model (see Appendix C) for the tow was developed which accounted, as appropriate, for:

- Squat
- Water Depth
- Bank Proximity
- Wing Dam Proximity
- Wavy or Irregular Bottom Geometry
- Engine Dynamics

The basic maneuvering model and software developed by Tracor Hydronautics, and used in the U.S. Coast Guard Simulator, include methods for modeling the effect of finite water depth and banks, but not the effect of wing dams or a wavy bottom. The required shallow water coefficients were developed in the section on Reduction and Presentation of Data.

As noted in Section 3.0, the model tow was free in heave and pitch. The effect of squat (sinkage and trim) was thus, except for the possible presence of viscous scale effects, properly modeled in the tests. For the model scale employed, such scale effects were estimated to be small. The one factor which was not, and could not, be modeled was the deformation of the relatively soft river bottom, which can be important at higher speeds and power levels. For extreme combinations of power and speed, with large resulting squat, a towboat can essentially dig itself into the river bottom. The bottom of the HSMB is rigid. It was assumed that the simulation model would not be applied to cases where significant bottom deformation occurs.

The PMM test data for the 7.5-foot draft towboat, deep water and shallow water conditions (depth/draft ratio, $H/T = 1.5$ and 1.17) are presented in Appendix A of this report. The second set of PMM test data for the 9.0-foot draft towboat in deep water and shallow water ($H/T = 1.17$ only) is given in Appendix B of this report. All these data were reduced to nondimensional hydrodynamic coefficients used in ship motion maneuvering equations in accordance with standard practices described in Reference 3. Some specific features of the very large body of data obtained should be particularly noted.

1. The resistance and propulsion coefficients for both sets of tests (7.5-foot draft and 9.0-foot draft towboats) are quite similar, with differences in the range of 5-7 percent, and are also similar to earlier analytical predictions for the 15-barge tow, Reference 1, particularly for ahead motion. At the test speed, the X' -force, as a function of propulsion ratio for the 9.0-foot draft towboat/barge system, was slightly lower (by 4-6 percent) than that achieved by the tow with 7.5-foot draft towboat. This may be due to the increase in towboat hull resistance at the 9.0-foot draft. Dependence of the resistance and propulsion coefficients on water depth was quite similar for both sets of data, and, as a result, the shallow water correction coefficients for terms a_1 , b_1 , and c_1 , which define the difference between resistance and thrust, were quite similar for the two drafts. It should be noted that for the shallow water tests, the scatter of test data was larger than that in deep water.

2. Measured forces and moments in deep water show effects of stalling for main rudder angles greater than 28 to 30 degrees. In shallow water, the stall starts somewhat earlier, at about 25 degrees. Flanking rudders operating in ship astern motion have a tendency to stall at even smaller rudder angles, about 20 to 22 degrees. The coefficients used in the simulation equation assume linear dependence of force and moment with rudder angle. Thus, these coefficients have been determined by a curve fit which averages all measured data up to and slightly beyond the observed stall angle.

3. Measured values of lateral forces and yawing moment are clearly nonlinear functions of the drift angle (see Figure 17). At drift angles larger than 6 to 7 degrees, these forces and moments are significantly influenced by cross-flow drag, which is proportional to velocity squared.

Comparisons of these test data for the 7.5-foot and 9.0-foot draft towboat tests within their linear range show that both sets of data are similar, and differences between them are in the range of the experimental scatter. Physically, this is the expected result because the barges, which dominate lateral force and yaw moment, had the same draft in both tests.

The results of curve fitting the test data using both linear and square absolute terms are presented by the hydrodynamic coefficients X_{vv}' , Y_v' , $Y_v|v|'$, N_v' and $N_v|v|'$ in Tables 5 to 11.

The differences between the two sets of data for the 7.5-foot draft and 9.0-foot drafts, for the deep water case, are basically in the nonlinear coefficients X_{vv}' and

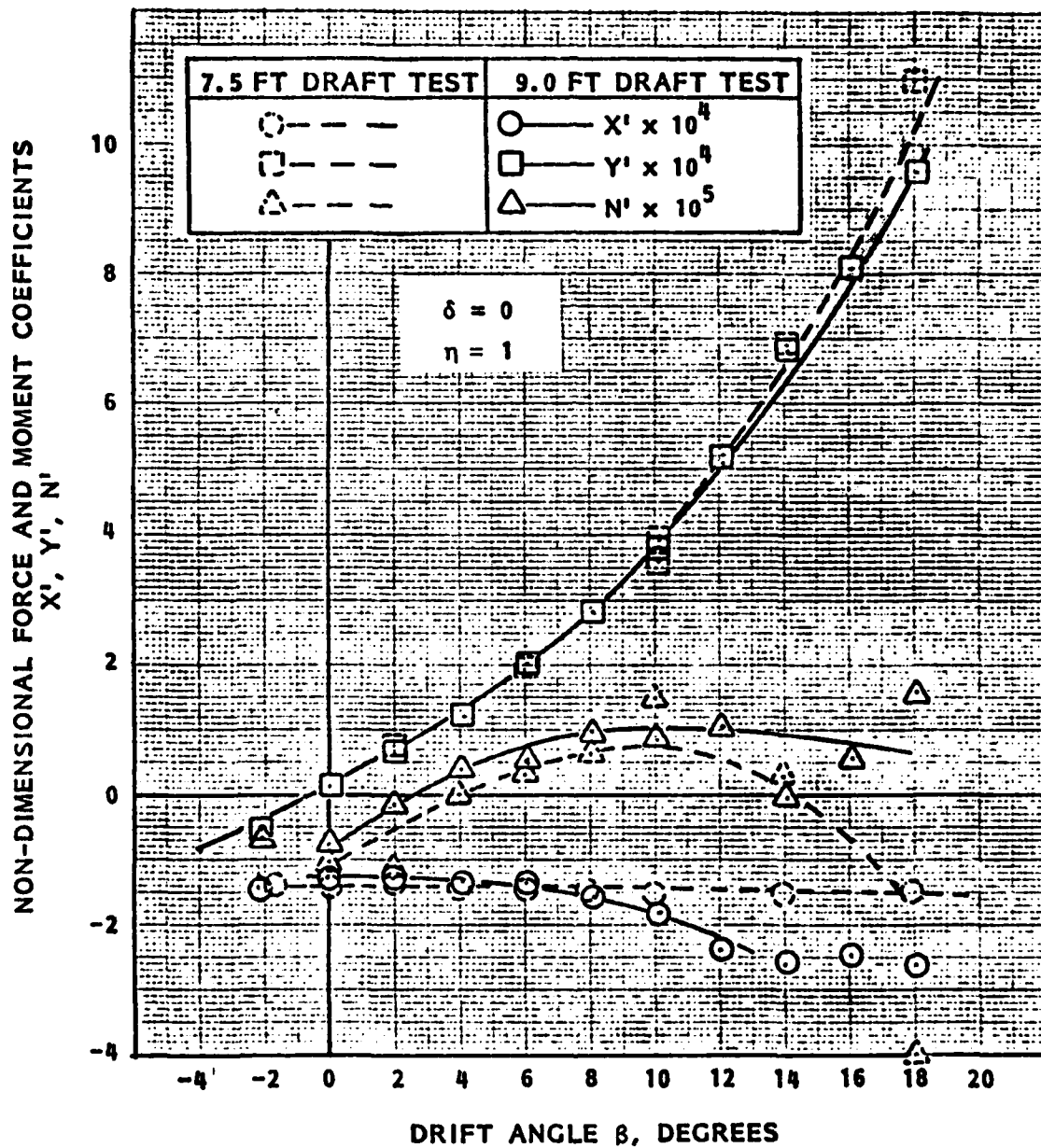


FIGURE 17 - MODEL FORCE AND MOMENT COEFFICIENTS FOR 7.5 FEET DRAFT AND 9.0 FEET DRAFT TOWBOAT/BARGE SYSTEMS IN DEEP WATER

$N_v|v|'$ for both ahead and astern motions. This trend was also detected in shallow water conditions with a depth/draft ratio of 1.17. For instance, the coefficient X_{vv}' was larger by 20-30 percent for the 9.0-foot draft towboat than for the 7.5-foot draft towboat for both deep and shallow water conditions, perhaps due to additional vortex shedding arising from the greater draft. Assuming this to be the case, it was decided to increase the coefficient X_{vr}' for the 9.0-foot draft towboat by 20-25 percent compared with its value for the 7.5-foot draft towboat.

4. Inertia and cross-coupling nonlinear coefficients were determined from the data for dynamic PMM tests in pure sway and yaw and dynamic tests in yaw with the fixed drift angles for the first river barge tow (with the 7.5-foot draft towboat) in deep and shallow water. For the river tow with 9.0-foot draft towboat, the inertia and cross-coupling nonlinear coefficients were estimated from the test data for the 7.5-foot draft towboat with suitable empirical corrections for the change in draft. The nonlinear cross-coupling coefficients for the 9.0-foot draft set were estimated from the data for 7.5-foot draft with corrections based on the underwater lateral area and the center of pressure associated with this area. These corrections were generally quite small and were in the range of 5-7 percent of the total value.

The final sets of the hydrodynamic coefficients obtained from the test data with the 7.5-foot draft towboat in deep and shallow water are given in Tables 5 to 7. Tables 8 and 9 show the hydrodynamic coefficients in

shallow water, depth/draft ratio, $H/T = 1.5$ and 1.17 , obtained by the curve fitting from the deep water results. They are quite close to the coefficients derived from the original test data.

The resulting set of hydrodynamic coefficients for the river tow with 9.0-foot draft towboat in deep water and shallow water ($H/T = 1.17$) are presented in Tables 10 and 11. It should be noted that in this case the test program in shallow water was quite limited. The derived curve fitting the hydrodynamic coefficients used exactly the data derived from the shallow water model tests where $H/T = 1.17$. Thus, for the shallow water case, for the 9.0-foot towboat, the table represents both the model test data and shallow water curve fitting from the deep water condition.

Measured steady lateral forces and yaw moments acting on the tow at zero drift angle and zero rudder angle in proximity to a bank are shown in Figures 9 and 10 to be an essentially linear function of the bank clearance parameter, \bar{B} . Comparable data for conventional ships, as presented in Reference 4, also exhibit a nearly linear variation of these forces with \bar{B} .

From curve fits to the data of Figures 9 and 10, slopes of the lateral force and yawing moment curves have been determined to be:

H/T	$\partial Y' / \partial \bar{B}$	$\partial N' / \partial \bar{B}$
1.17	0.00063	0.00037
1.50	0.00016	0.00008

AD-A146 511

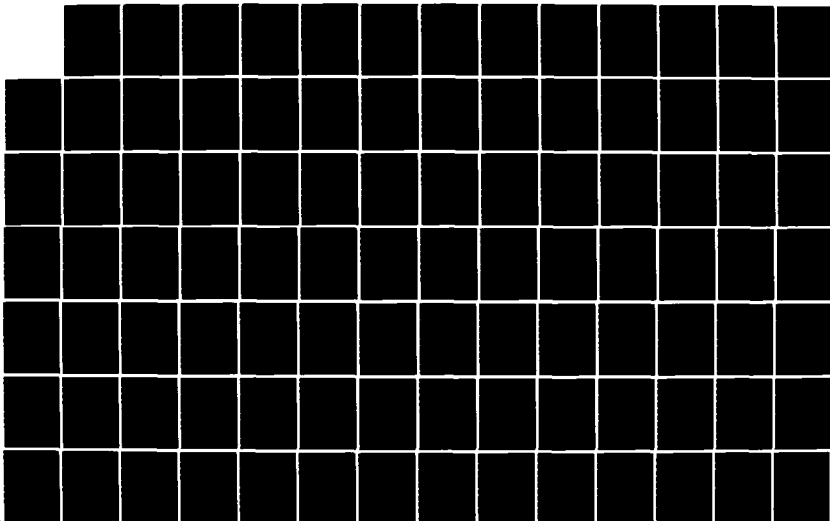
MODEL TESTS AND COMPUTER SIMULATIONS OF A 15-BARGE TOW
FOR THE UPPER MISS. (U) TRACOR HYDRONAUTICS INC LAUREL
MD R HATTON ET AL. JAN 84 TR-83011-2 USCG-D-10-84
DTCG23-82-C-20041

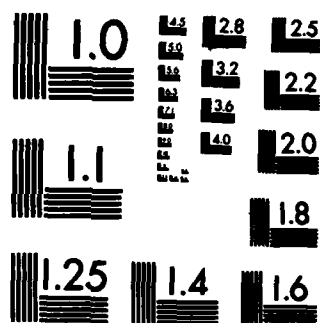
2/3

UNCLASSIFIED

F/G 9/2

NL





COPY RESOLUTION TEST CHART

These results are much different than the results for ships given in Reference 4, even when the differences in the length-draft ratios of the tow (126) and the ship (15) are taken into account. The forces for the tow are generally much smaller than those for the ship, but show a much greater variation with water depth/draft ratio, H/T . This greater dependence of H/T is probably due to the much greater beam/draft ratio of the tow.

It was decided to retain the basic form for modeling bank effects given in Reference 4:

$$F = a \cdot \bar{B} \cdot \left(\frac{b}{H/T}\right)^c$$

where the empirical constants a , b and c depend on vessel geometry and are generally different for lateral force and yawing moment. As bank effect data were not available for deep water, it was necessary to estimate a water depth beyond which bank effects were not dependent on H/T .

Based on the measured variation of $\partial Y'/\partial \bar{B}$ and $\partial N'/\partial \bar{B}$ with H/T , and the variation of other hydrodynamic forces with \bar{B} , it was assumed that depth effects were important only for $H/T < 2$. A value of 2.0 was therefore assumed for b for both Y' and N' . Using this value of b , the resulting expressions for Y' and N' for the tow are:

$$Y' = 0.000033\bar{B} \left(\frac{2}{H/T}\right)^{5.5} \quad \text{for } H/T < 2$$

$$= 0.000033\bar{B} \quad \text{for } H/T \geq 2$$

$$N' = 0.000014\bar{B} \left(\frac{2}{H/T}\right)^{6.15} \quad \text{for } H/T < 2$$

$$= 0.000014\bar{B} \quad \text{for } H/t > 2$$

While these expressions are identical in form to those given for ships in Reference 4, they exhibit several notable differences. The present exponents for the depth effect are some 4.5 times larger than those for ships (1.2 and 1.4), and the ratio of N' to Y' for the tow (approximately 0.5) is much larger than the same ratio for the ships (approximately 0.16). The large ratio of N' to Y' for the tow was not expected, but is clearly exhibited by all of the test data.

Figures 11 and 12 show that the hydrodynamic coefficients Y_V' and N_V' have an essentially linear variation with B . The sensitivity of these forces to B is larger for the smaller water depth ($H/T = 1.17$), as would be expected.

From the test data, it is not possible to determine the effect of bank proximity, or \bar{B} , on any other ship added mass or damping coefficients. It is considered undesirable, for reasons discussed in Reference 4, to consider the effect of bank proximity only on two coefficients or terms. The results in Figures 11 and 12 clearly indicate the need to conduct additional tests to determine the effect of bank proximity on other important hydrodynamic coefficients, and to modify the simulation equations and software, as necessary, to reflect these effects.

To illustrate the magnitude of the effect of bank proximity on Y_V' and N_V' , required operating drift and rudder angles for steady state operation parallel to a bank have been calculated including and neglecting the effect of \bar{B} on these coefficients. For a water depth/draft ratio of 1.5 and a clearance from the tow to a single bank of 0.5 tow beams, the required drift and rudder angles change by 0.65 and 1.0 degrees, respectively. Somewhat larger changes will be found for smaller water

depths. These results indicate that neglecting the variation of hydrodynamic coefficients with distance to the bank, although measureable, will probably not cause large errors in predicted tow maneuvering.

The results presented in Table 12 indicate that the clearance between the vessel and the end of the wing dams has, on average, only a small effect on the sway hydrodynamic coefficients, Y_v' and N_v' . For the depth/draft ratio of 1.17, the values of Y_v' and N_v' decrease slightly with decreasing clearance. There are less clearly defined trends for the depth/draft ratio of 1.5, although, on average, values of Y_v' and N_v' increase somewhat with decreasing clearance. Based on these results, it is not considered appropriate to model the effect of wing dam clearance or proximity on hydrodynamic coefficients in predicting vessel maneuvering.

Table 13 indicates that there are no significant and consistent variations of the mean values of X' , Y' , and N' with wing dam clearance at zero drift angle and a given water depth. The small finite values of Y' and N' at zero drift angle are probably due primarily to the off tank centerline location of the tow in these tests.

Table 14 also indicates that there are no significant variations of the rms values of X' , Y' and N' with wing dam clearance for either test depth. Rms values do show a significant variation with depth, however. Rms values show no significant and consistent variations with drift angle, increasing with increasing drift angle in some cases and decreasing with drift angle in other cases.

The spectral analyses of the unsteady force data indicated that much of the energy associated with these forces is at frequencies which are much greater than the wing dam frequency of encounter (0.064 - 0.080 Hertz). This indicates that these unsteady forces arise primarily from a source other than the hydrodynamic influence of the wing dams. However, the rms sway forces for a depth/draft ratio of 1.5 in Table 13 are larger than those for operation over a wavy bottom of comparable depth, as presented in Table 16. This could indicate that the waterway geometry does have some influence on unsteady sway forces.

It was concluded that the measured unsteady forces are due primarily to sources other than the presence of the wing dams, and much of the energy of these unsteady forces is at high frequencies which cannot affect vessel maneuvering. It is thus proposed not to include unsteady forces due to wing dam proximity in any prediction of tow maneuvering.

In actual tow operations, the effect of wing dams on tow behavior and maneuvering is often found to be significant, particularly with high river flows and currents. Discussions with pilots indicated that the effect of the wing dams was probably due primarily to the lateral flows near the ends of the dams produced by interactions of current and wing dams. Current velocities were not simulated in the model tests and hence such effects were not present in the model tests. This appears to be the reason why wing dam effects measured in the model tests were not significant.

The results for the sideslip and rudder tests in the presence of the wavy or irregular bottom, indicate two important effects of this bottom on vessel hydrodynamics. The first is an

effect on the propulsion, as defined by the equilibrium or self-propulsion advance coefficient, J_C . The second is the effect on the static hydrodynamic coefficients, Y_V' , N_V' , Y_{δ_r}' , N_{δ_r}' , for ahead and astern motion.

The overall effect of the wavy bottom is the existence of a typical or "effective" water depth for the static hydrodynamic coefficients. This "effective" water depth is the water depth with a uniform bottom for which a given coefficient is equal in value to that measured with the wavy bottom. A second effect is the unsteady forces acting on the tow due to the irregular bottom, and the magnitude of these forces relative to the mean forces. The magnitudes of these effects are discussed below.

Figures 13 to 16 indicate that for operation over the tested wavy bottom, almost all measured coefficients reflect an "effective" water depth between 1.35 and 1.60 drafts. The average values of these effective depths are summarized for various coefficient groups in Table 17.

From these results, it appears that a typical effective depth for all sideslip and rudder coefficients is 1.5 drafts and a typical effective depth for the propulsion J_C 's is about 1.35 drafts. The overall average effective depth for all coefficients is 1.44 drafts. The geometric average water depth for the tested wavy bottom was 1.44 drafts. Thus, the average values of effective water depth and geometric water depth are essentially identical. The effective depth for the sideslip coefficients is not dependent on direction of tow motion, while for the rudder and propulsion coefficients the effective depth is smaller for astern motion than for ahead motion. This difference is possibly due to the longitudinal asymmetry of the bottom "waves."

Table 17

Effective Water Depths Deduced
From Tests Over a Wavy Bottom

Coefficient Group	Effective Water Depth (in Tow Drafts)		
	Ahead	Astern	Both
Drift - Y_v' , N_v' , $Y_v v '$, $N_v v '$	1.5	1.5	1.5
Rudder, Y_{δ_r}' , N_{δ_r}'	1.6	1.4	1.5
Propulsion - J_c	1.4	1.27	1.34
All Coefficients	1.5	1.39	1.44

From these results it was concluded that the effective water depth of a wavy or irregular bottom can be suitably represented by using the average bottom water depth.

The rms values of unsteady surge force coefficient, X' , given in Table 16 for tests over a wavy bottom appear rather large. Most of the energy in the unsteady force spectra is at frequencies much higher than the bottom wave encounter frequency (0.13 Hertz), and rms values show no clear dependence on drift angle or rudder angle. It is thus not clear if these unsteady forces are directly related to passage of the tow over the wavy bottom.

The rms values of Y' and N' given in Table 4 are comparable in magnitude to the mean values at the tested finite drift angle (6 degrees) and rudder angle (25 degrees). The rates of change of the rms values with respect to drift and rudder angle are, on average, about 50 and 30 percent of the rates of change of the mean or average values, for ahead and astern motions, respectively.

Further investigation of the unsteady forces which occur during operation over a wavy bottom are needed to determine the significance of these forces for ship maneuverability and controllability. Based on the available results, it is recommended that unsteady forces be neglected in predicting vessel behavior when operating over an irregular bottom.

In preliminary simulations of the river tow with 7.5-foot draft towboat, engine dynamics were simulated by assuming a constant rate of change of rpm with time over the full range of propeller rpm's (from +190 to -190 rpm). A rate equal to 7.0 rpm/sec was selected as a representative rate from the available trial data performed by Exxon for different towboats, Reference 7.

In the final simulations, the modeling of engine dynamics was modified to reflect more accurately dynamics of the engine and clutch for this particular towboat design. From information supplied by St. Louis Ship, the average rate of change of rpm was specified to be 15.0 rpm/sec.

The engine dynamics model was modified to reflect known behavior and operating limits of the engines used on the towboat. It was determined that the minimum possible engine operating rpm corresponds to 70 propeller rpm. It is thus only possible to achieve propeller rpms between +70 and +190 or between -70 and -190, except for the case when the engine is declutched, and the propeller rpm is essentially zero. It was assumed that the engine was declutched when the commanded rpm is less than 10. The new engine dynamics model therefore limits command rpms as shown in Figure 18, or:

if:	$ n_c < 10$	set $n_c = 0$	engine declutched
if:	$10 \leq n_c < 70$	set $ n_c = 70$	unpermissible engine command
if:	$ n_c \geq 70$	set $n_c = n_c$	normal operating engine

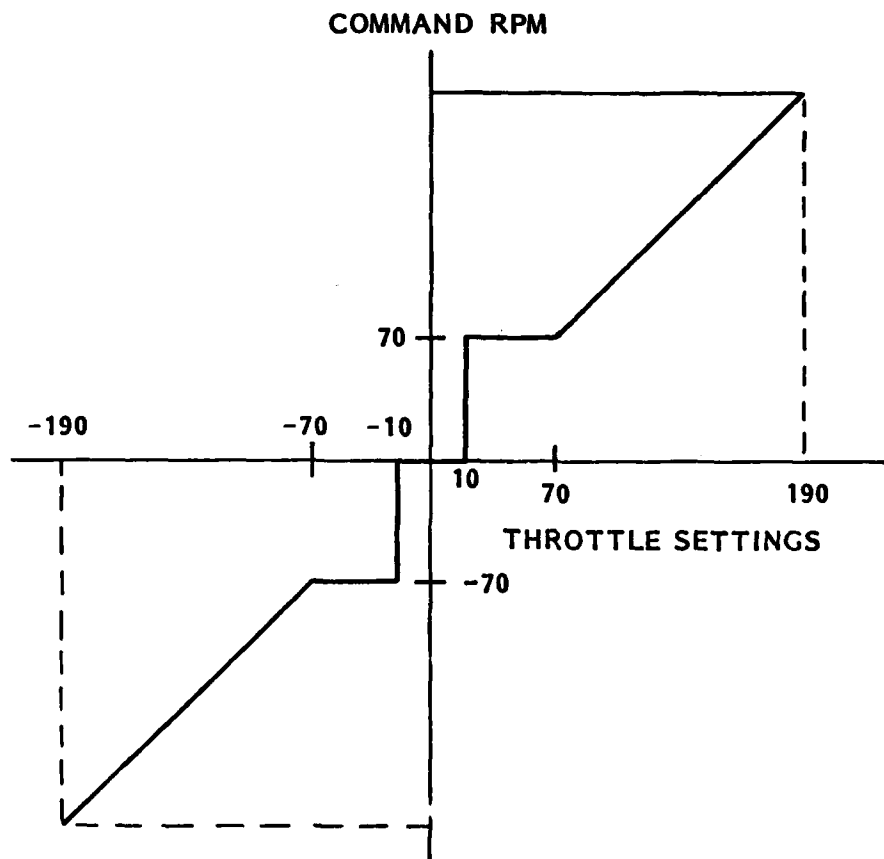


FIGURE 18 - ASSUMED VARIATION OF TOWBOAT COMMAND RPM WITH THROTTLE SETTING USED IN MANEUVERING SIMULATIONS OF 15 BARGE TOW SYSTEM

6.0 SIMULATED MANEUVERS

Results of the PMM tests and analysis provide a complete mathematical model capable of simulating arbitrary maneuvers of the 15-barge river tow in deep and shallow waters, for ahead and astern motions and for all variations of rudder angles (main and flanking rudders) and propeller rpm's (see Appendix C).

For the purpose of evaluating the turning and handling characteristics of the river tow in deep and shallow waters using the maneuvering simulation procedure, the so-called definitive maneuver approach was used (Reference 8). A standard turning maneuver with maximum rudder angle of 35 degrees, a 20 x 20 zig-zag maneuver, and a crash stop maneuver were performed for deep water conditions and in shallow water for depth/draft ratios, $H/T = 1.5$ and $H/T = 1.17$.

The simulations were made only for ahead motion at an approach speed of 4.6 mph (tow with 7.5-foot draft towboat) and 3.45 mph (for both tows, 7.5-foot and 9.0-foot draft towboat). Numerical values of coefficients used in these simulations have been presented in Tables 5 to 11. Simulations were performed with both measured shallow-water values and values derived by applying shallow water corrections to deep water test data. Computer printouts of several simulation runs are summarized in Tables 18 to 20. Analysis of these maneuvers allows certain conclusions to be drawn as described below.

Turning Maneuvers - Turning maneuvers provide quantitative measures of the effectiveness of the rudder in producing steady turning characteristics. Numerical measures obtained from the simulated turning maneuvers are presented in Table 18. There are no available models or trial data for this tow, but a

Table 18
 Maneuvering Characteristics Derived from Calculations of
 Steady Turning Maneuvers For Tow in Deep and Shallow Water,
 9.0-Foot Draft Towboat

Depth/Draft Ratio H/T	Approach Speed MPH	Rudder Angle Degrees	Advance Feet	Transfer Feet	Tactical Diameter Feet	Steady Turning Diameter Feet	Percent Loss of Speed in Steady Turns	Drift Angle in Steady Turns, Degrees
"	3.45	35	2892	1315	3401	-	38.33	19.01
1.5	3.45	35	2874	1982	4228	-	29.35	5.11
1.17	3.45	35	2950	2356	4870	-	27.33	2.30

Table 18 (Concluded)

Maneuvering Characteristics Derived from Calculations of
Steady Turning Maneuvers For Tow in Deep and Shallow Water,
7.5-Foot Draft Towboat

Depth/Draft Ratio H/T	Approach Speed MPH	Rudder Angle Degrees	Advance Feet	Transfer Feet	Tactical Diameter Feet	Steady Turning Diameter Feet	Percent Loss of Speed in Steady Turns	Drift Angle in Steady Turns, Degrees
∞	3.45	35	3173	1530	3906	-	34.33	17.66
1.5	3.45	35	3126	2241	4763	-	25.70	4.70
1.17	3.45	35	3294	2735	5643	-	27.33	2.02

Table 19
 Maneuvering Characteristics Derived From Calculations of
 Zig Zag Maneuvers For 15 Barge Tow With 9.0 Foot Draft Towboat

Depth/Draft Ratio, H/T	Approach Speed MPH	Rudder Angle	Time to Reach Execute Heading Change (Deg)	Overshoot Angle (Deg)	Total Heading Change (Deg)	Width of Path at Execute (Ft)	Overshoot Width of Path (Ft)	Total Width of Path (Ft)	Reach (sec)	Second Overshoot Heading Angle (Deg)	Third Overshoot Heading Angle (Deg)	Period (sec)
-	3.45	20	330	2.92	22.92	78	666	744	800	2.88	2.85	1520
1.5	3.45	20	355	2.61	22.61	170	628	798	840	2.56	2.59	1600
1.17	3.45	20	410	1.27	21.27	265	495	760	880	1.28	1.26	1730

Table 20
Stopping Characteristics Derived From Calculations of
Stopping Maneuver With 9.0-Foot Draft Towboat

Water Depth Feet	Depth/Draft Ratio H/T	Approach Speed MEH	Approach RPM	Astern RPM	Stopping Time Sec.	Stopping Reach Feet
Deep	∞	3.45	85.0	150	330	800
20.0	2.22	3.45	89.4	150	340	815
13.5	1.5	3.45	104.4	150	415	956
10.5	1.17	3.45	150	150	480	1021

comparison of deep water turning characteristics of this tow with characteristics of other tows (scaled to the dimensions of this tow, Reference 9) from Exxon test data, Reference 7, shows that this tow has very good turning characteristics. The tow with the 7.5-foot draft towboat has a nondimensional tactical diameter, D_T/L , of 3.45. With a 9.0-foot draft towboat, the tactical diameter is even smaller and equals only 3.01 ship lengths.

It should be noted that speed variation has little influence on turning characteristics. In shallow water, the tow showed increased directional stability, and therefore, compared with the deep water case, all linear characteristics are basically increased by a factor of 1.5 to 1.65 for depth/draft ratio, $H/T = 1.17$. For instance, a comparison of the tactical diameter of the deep water and shallow water case, $H/T = 1.17$, shows that the tactical diameter for ahead turning in shallow water is approximately 1.6 times that in deep water, which is also quite typical for full-form ships like tankers (Reference 5).

Also, due to the increased directional stability of the tow in shallow water, the relative loss of speed in the turn and the steady-state drift angle decrease significantly. Speed loss, in percent, changes from 38.33 in deep water to 27.33 for $H/T = 1.17$, and drift angle, in degrees, changes from 19.01 in deep water to 2.14 in shallow water. Turn rate changes approximately inversely to the tactical diameter.

Zig-Zag Maneuvers - Numerical measures for ahead 20-20 zig-zag maneuvers at 3.45 mph approach speed are given in Table 19. Due to the great stability of the tow in deep water, the overshoot heading angles are quite small (in the range from 2.9 to 3.25 degrees). In shallow water, the overshoot heading

angles are even smaller than those in deep water (in the range from 2.5 to 1.3 degrees) due to the increased stability of the ship in shallow water. A significant time is required to reach the execute heading angles.

Stopping Maneuver - The main numerical measures for crash stopping maneuvers are shown in Table 20.

The maximum astern rpm for these simulations was 150. It takes about five minutes to stop the 15-barge river tow from 3.45 mph ahead speed. In shallow water, under the same initial conditions, it takes longer to stop the tow than in deep water.

Validation of Maneuvering Performance - There are no full-scale maneuvering trial data available for the 15 barge tow and towboat used in this study. In fact, at this time about the only available river tow maneuvering trial data are presented in Reference 7. This reference, which presents work carried out for the Corps of Engineers, describes a full-scale test program conducted in the Baton Rouge area on the lower Mississippi using three different tow boats. The first tow included the towboat "Exxon Memphis," a twin screw Kort nozzle towboat designed to push an integrated oil barge tow. The second series of tests were performed using the "Exxon Nashville" and the Exxon Lake Charles, both open wheel towboats. The "Exxon Memphis" and "Exxon Nashville" were identical vessels with the exception of the Kort nozzles, while the "Exxon Lake Charles" had about 2/3 of their installed power.

The characteristics of the "Exxon Nashville" and its tow and the 15 barge tow of this study are given in Table 21.

Table 21
Characteristics of River Tows

Item	15 Barge Tow and Towboat	Exxon Nashville and Tow
Length of Tow and Towboat		
• LOA, feet	1130	1160
• Beam of tow, feet	105	54
• Length of Towboat, LOA, feet	140	120
• Beam of Towboat, feet	38	34
• Draft of Tow, feet	9.0	9.25
• Draft of Towboat, feet	9.0	9.0
• Displacement, Short ton	29,300	16,293
• Propeller Diameter, feet	8.5	8.5
• Installed BHP	3800	3300

The Exxon Nashville tow differs from the 15 barge tow of this study primarily in the overall beam of the tow (54' versus 105') and in the total displacement (16,293 versus 24,300 short tons). The towboats are similar in size and installed power.

Turning Performance - Figure 19 shows the average speed loss, drift angle (β) in degrees, and yaw rate ($\dot{\psi}$) in degrees per second for the three tested Exxon tows and the 15 barge tow in a steady turn using a 15 degree rudder angle. The trial data were obtained by averaging values for 60 second periods during 6 minutes of a constant sudden angle turn. The trial data were obtained at the full-power condition but the approach speeds varied between 7.2 and 6.3 MPH. For the 15 barge tow case the approach speed was 7.7 MPH. In all cases the water was deep.

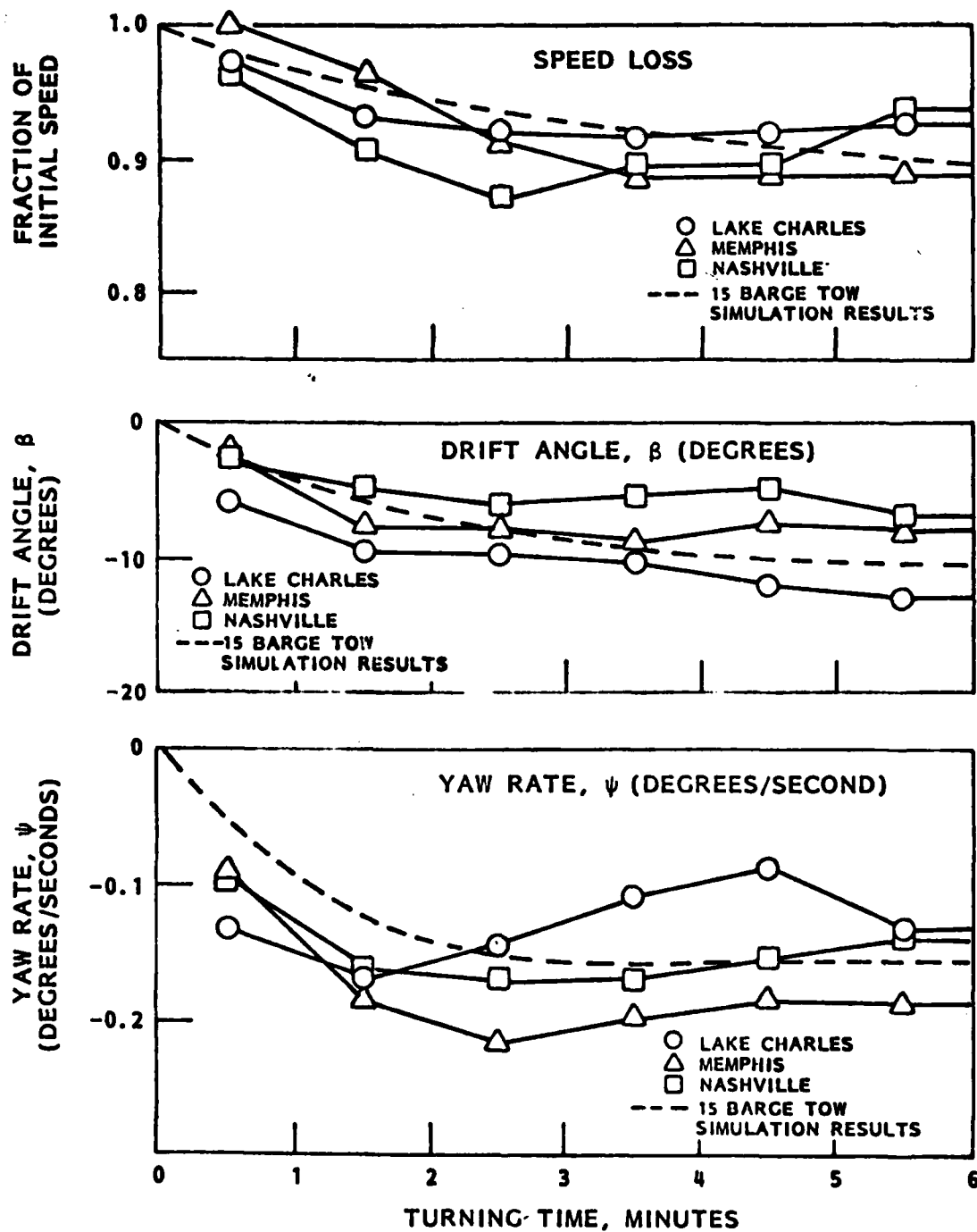


FIGURE 19 - COMPARISON OF SIMULATION AND FULL SCALE DATA FOR STEADY TURNS

Figure 19 shows that the turning characteristics of the three tows in the trials and the simulated 15 barge tow are very similar. This is to be expected in that turning performance is primarily a function of rudder size, power, overall length, and draft. These measures are all similar between the three trial tows and the 15 barge tow. Thus, within the limits of the trial data available, it may be concluded that the turning performance of the simulated 15 barge tow is as expected.

Stopping Performance - It is more difficult to make valid comparisons of stopping performance of the Exxon Nashville tow and the 15 barge tow than it is to compare their turning performance. This is because stopping performance is a function of approach speed, displacement, astern horsepower, and propeller diameter and efficiency. Also, the stopping trials were conducted either with or against a significant current and thus for comparison purposes the results must be corrected to still water values.

A down-river stopping maneuver of the Exxon Nashville (Run 2, Reference 5) has been corrected to the zero current condition and to include the thirty-second time lag reported for full ahead to full astern. The results for the Exxon Nashville and the 15 barge tow are given in Table 22.

Table 22
Comparison of Stopping Performance
of Exxon Nashville and 15 Barge Tow -
Deep Water No Current

Item	Exxon Nashville and Tow	15 Barge Tow and Towboat
Approach Speed	9.12 MPH	7.72 MPH
Astern Power, BHP	3300	2200
Astern RPM	201	150
Propeller Diameter	8.5 ft.	8.5 ft.
Head Reach, ft.	1670±150	2264
Time to Stop, Seconds	260	508

In both cases the stopping maneuvers were started from the nominal full-power speed in deep water. In the simulation for the 15 barge tow the astern RPM was limited to 150 (out of 190 maximum) which limits the astern power to about 2200 BHP. This was done for consistency with the simulated stopping maneuver results given in Table 20.

Clarke and Wellman (Reference 11) proposed universal stopping performance curves for large ships in which stopping distance is related to approach speed, displacement, astern power, and propeller diameter. The data for the river tows given in Table 22 has been converted to the Clarke parameters, and the results, along with the Clarke curve and data, are presented in Figure 20. The results for the tows are close to the theoretical curve and within the band of data for large ships. This indicates that the stopping performance of the 15 barge tow is basically similar to the Exxon Nashville trial performance when allowance is made for the difference in power, displacement, and approach speed.

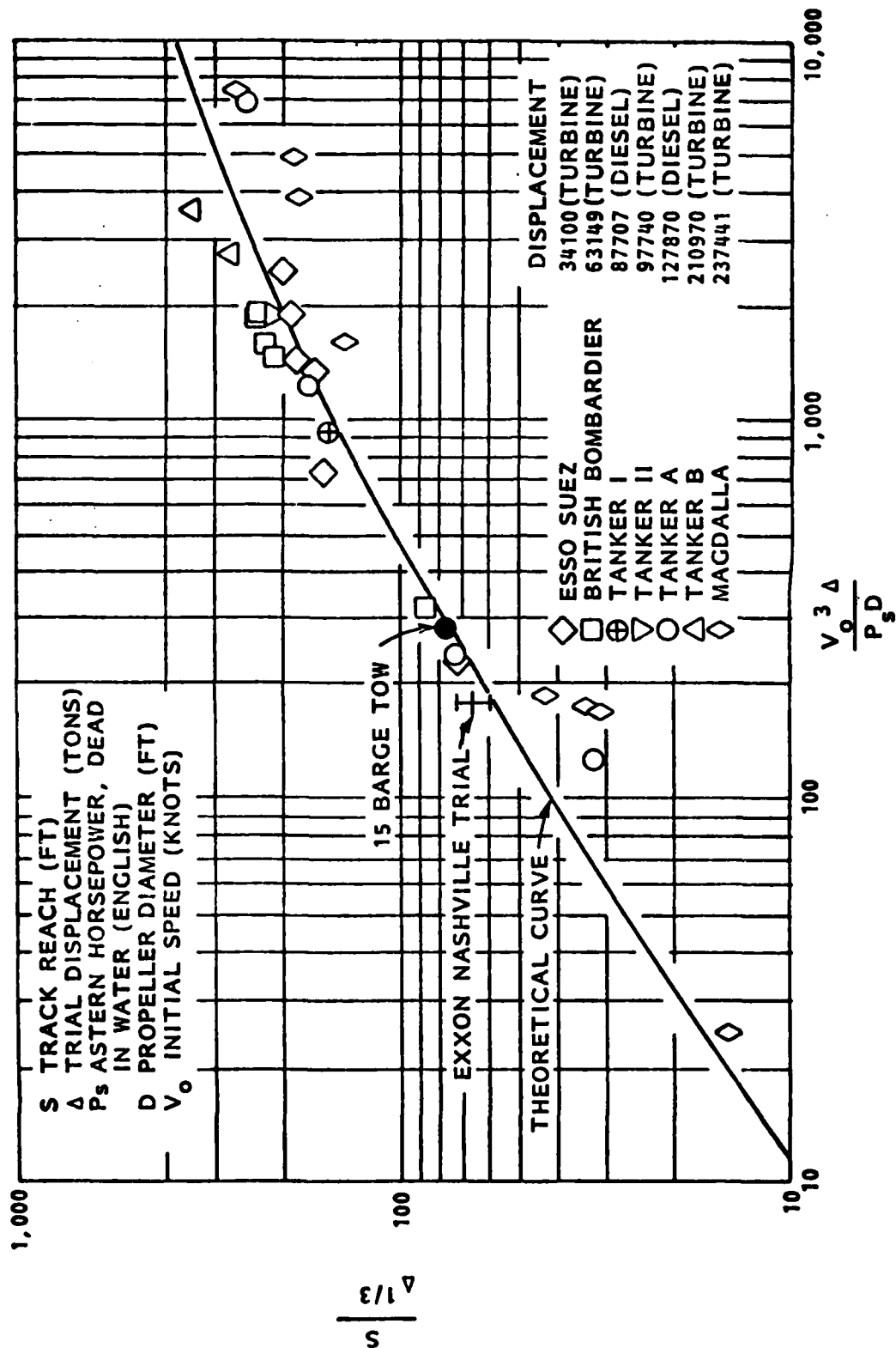


FIGURE 20 - UNIVERSAL STOPPING CURVE FOR TANKERS FROM REFERENCE 11

Based on the above comparison of the maneuvering performance of the simulated 15 barge tow and the measured maneuvering performance of the Exxon Nashville, it may be concluded that for deep water conditions the simulation gives the expected results. There are no full-scale trial data on shallow water effects on river tow maneuvering performance. The effects due to shallow water shown by the simulation are consistent with full-scale data on shallow water effects on large ship maneuvering.

7.0 CONCLUSIONS AND RECOMMENDATIONS

This report presents the results and analysis of a captive model test program and free running tests of a 15-barge tow in deep and shallow water, and computer simulations. The program included tests with models of a sloping bank, a series of wing dams, and an irregular or wavy bottom.

From the tests, complete sets of hydrodynamic coefficients for maneuvering simulations in ahead and astern maneuvers were obtained and a set of maneuvering simulations was performed. The following conclusions have been drawn:

1. The primary objective of the task was achieved. The mathematical model, simulating a typical river tow in the upper Mississippi, was developed and the hydrodynamic coefficients were obtained experimentally. Resultant definitive maneuvers demonstrated the validity of the system.
2. The test results for the tows with 7.5-foot and 9.0-foot draft towboats in deep and shallow water are very consistent. These data should thus provide a good basis for developing reliable hydrodynamic models of the tow maneuvering in deep and shallow water.
3. Increasing towboat draft from 7.5 to 9.0 feet resulted in generally small changes or no changes in most hydrodynamic coefficients. The primary measured effect of increasing towboat draft was to decrease the self-propulsion advance coefficients, an indication of an increase in required power at a given tow speed. This result would indicate the probable need for lower operating speeds in very shallow

water with the deeper towboat draft to avoid excessive squat and a tendency of the towboat to dig itself into the river bottom.

4. Shallow water effects on the surge-sway-yaw hydrodynamic coefficients were expressed by a modified third order polynomial with constant coefficients. A special curve fitting procedure allowed fitting the shallow water PMM test data with significant accuracy (typically four to five percent). Maneuvering simulations performed with hydrodynamic coefficients obtained from the shallow water data, and those performed with shallow water corrections to deep water data, show results that are practically identical, with differences in the range of two percent. Therefore, shallow water correction coefficients can be used with confidence down to depth/draft ratios of about 1.15 - 1.17. It is not recommended that these correction coefficients be used for $H/T < 1.15$.
5. From the results of simulated definitive maneuvers, it appears that the tow is directionally stable in ahead motion in deep water conditions, and becomes even more stable in shallow water. Tow handling characteristics in ahead motion turns, zig-zags, and crash stopping maneuvers are apparently satisfactory. The shallow water effect on the maneuvering performance of the tow is in general agreement with shallow water effects determined in previous studies. However, even in the shallowest water depth ($H/T = 1.17$), the tow is quite responsive to rudder deflection.

- 6.. Lateral forces and yawing moments on the tow in bank proximity are basically as expected, and decrease rapidly with increasing distance from the bank. In bank proximity, the bow turns away from the bank while the tow is sucked into the bank.
7. Bank proximity has a significant effect on Y_v' and N_v' coefficients. However, since the effect of bank proximity on other coefficients is not known, it is not considered appropriate to modify the maneuvering simulation to include only these effects.
8. Proximity of the tow to the ends of a series of wing dams did not have a significant effect on the hydrodynamic forces acting on the tow, perhaps because the tests were conducted with no current and a relatively wide river. A more significant effect would undoubtedly occur with current modeled.
9. The primary effect on maneuvering performance of operation of the tow over a wavy or irregular bottom appears to be that the effective water depth is the average geometric depth of the bottom. There is some difference in this effective depth for ahead and astern motion, probably due to the asymmetry of the wavy bottom used in the tests. The tests did not quantify any significant unsteady or transient forces due to passage of the tow over the sharp crests of the bottom "waves."

As a recommendation for future studies, it would be desirable to extend the experimental and analytical analysis of the bank effects to include the approach of the tow to the bank with different headings, influence of sway and yaw

velocities and accelerations on the hydrodynamic forces and influence of the bank configuration. In the same context, the interactions between the tow and other passing or standing ships should also be investigated.

8.0 REFERENCES

1. Ankudinov, V. and Barr, R. A., "Estimation of Hydrodynamic Maneuvering Models for Six and Fifteen Barge River Tows," HYDRONAUTICS, Incorporated Technical Report 83011-1, December 1982.
2. Altmann, R. J. and Goodman, A., "Description and Generation of Large-Amplitude Horizontal Planar Motion Mechanism," HYDRONAUTICS Incorporated Technical Manual 8099-1, May 1982.
3. Goodman, A., et al, "Experimental Techniques and Methods of Analysis Used at HYDRONAUTICS for Surface Ship Maneuvering Predictions," HYDRONAUTICS, Incorporated Technical Report 7600-1, June 1976.
4. Ankudinov, V. and Barr, R. A., "Bank and Channel Effects in Ship Maneuvering: Definition of Calculations Procedures," HYDRONAUTICS, Incorporated Technical Report 8048-3, Volume III, March 1980.
5. Barr, R. A., Miller, E. R., Jr., Lee, F. C., Ankudinov, V. and Van Dyke, P., "Maneuvering of Tankers at Deep Water Ports, HYDRONAUTICS, Incorporated Technical Report 8009-3, February 1981.
6. Gertler, M., Miller, E. R., Jr., and Ankudinov, V., "Shallow-Water Maneuverability Characteristics of MARAD Systematic Series for Large Full-Form Merchant Ships," HYDRONAUTICS, Incorporated Technical Report 7568-1, August 1977.
7. Schulz, Roger M., "River Tow Behavior in Waterways," Technical Report H-10-17, Exxon Test Program Report I, Prepared for the U.S. Army Corps of Engineers, October 1978.
8. Panel M-19 (Ship Trials) of the SNAME Ship Machinery Committee, "Code for Sea Trials-1973," SNAME Technical and Research Code C-2, 1974.
9. Eda, H., "Barge Trains in a Coastal Seaway, Part III Directional Stability and Control," Davidson Laboratory Report SIT-DL-70-1537, June 1970.

10. Miller, Eugene R., Jr., "The Prediction of River Tow Maneuvering Performance," HYDRONAUTICS, Incorporated Technical Report 7786-1, May 1978.
11. Clarke, D. and Wellman, F., "The Stopping of Large Tankers and Feasibility of Using Auxiliary Breaking Devices," Transactions of the RIMA, Vol. 113, 1977.

Tracor Hydronautics

APPENDIX A

PLANAR MOTION MECHANISM TEST DATA FOR 7.5 FOOT (PROTOTYPE) DRAFT
TOWBOAT WITH 15-BARGE TRAIN IN DEEP AND SHALLOW WATER

Tracor Hydraulics

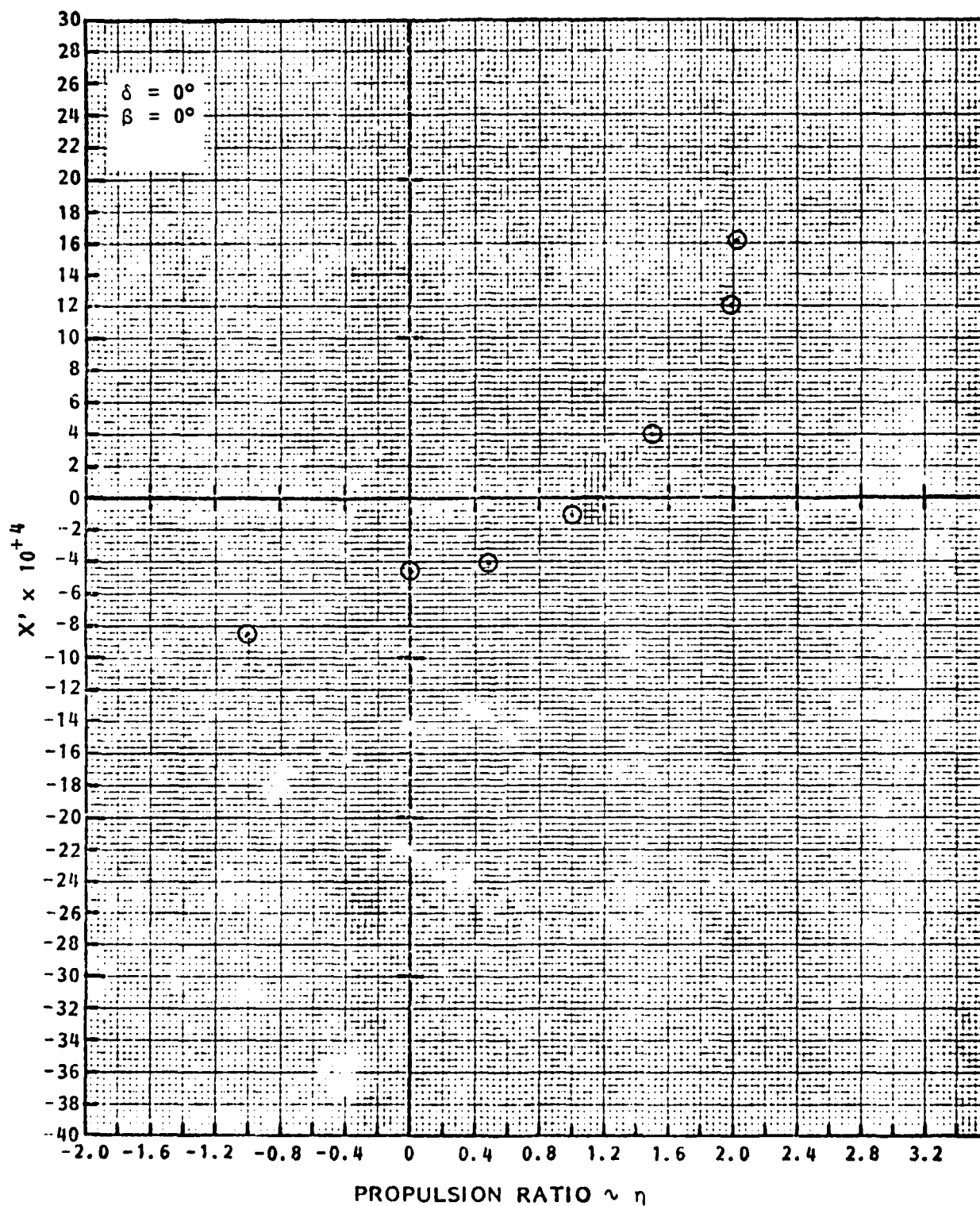


FIGURE A.1 - AXIAL FORCE COEFFICIENT AS FUNCTION OF PROPULSION RATIO η FOR AHEAD MOTION IN DEEP WATER

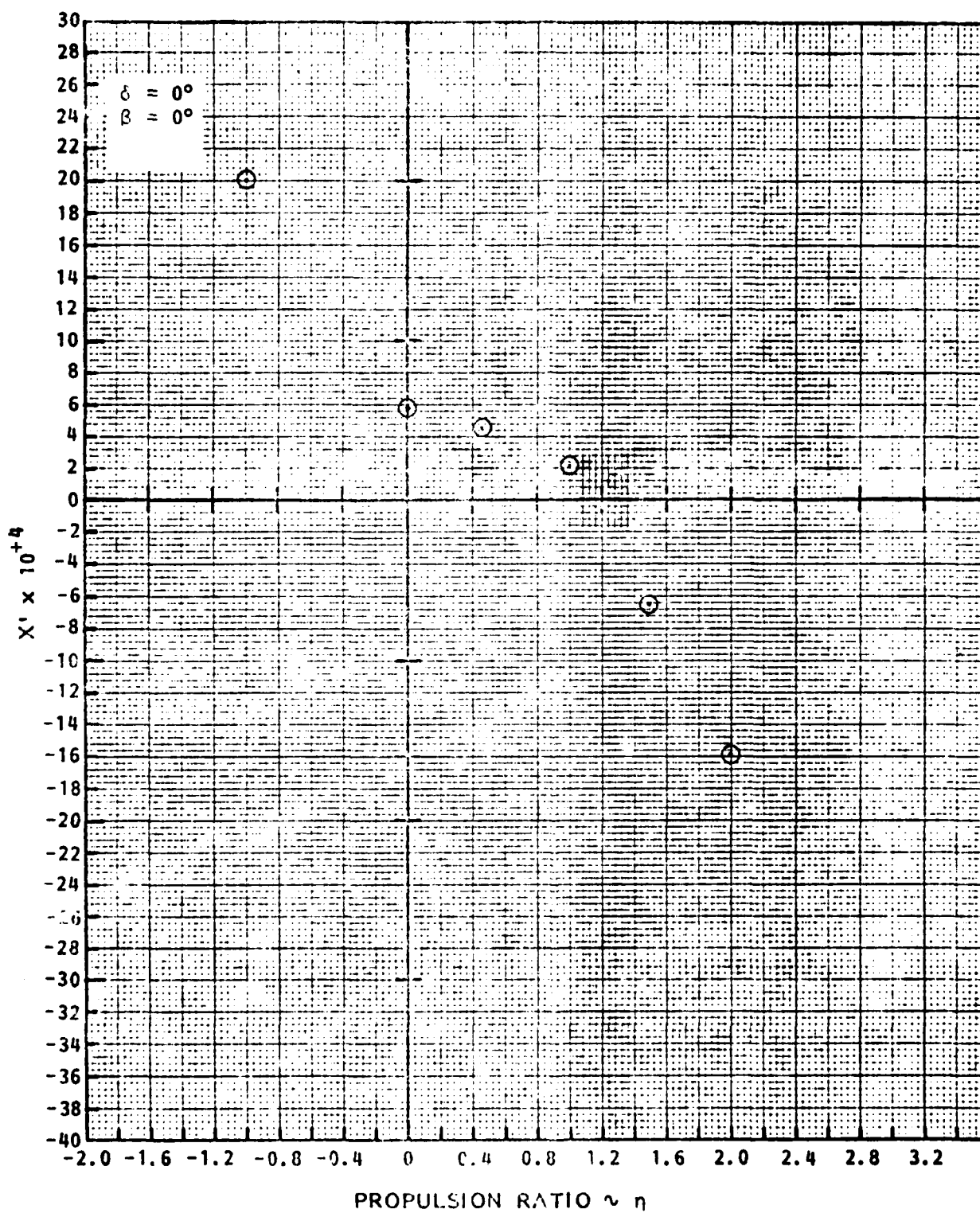


FIGURE A.2 - AXIAL FORCE COEFFICIENT AS FUNCTION OF PROPULSION RATIO η FOR ASTERN MOTION IN DEEP WATER

Tracer Hydronautics

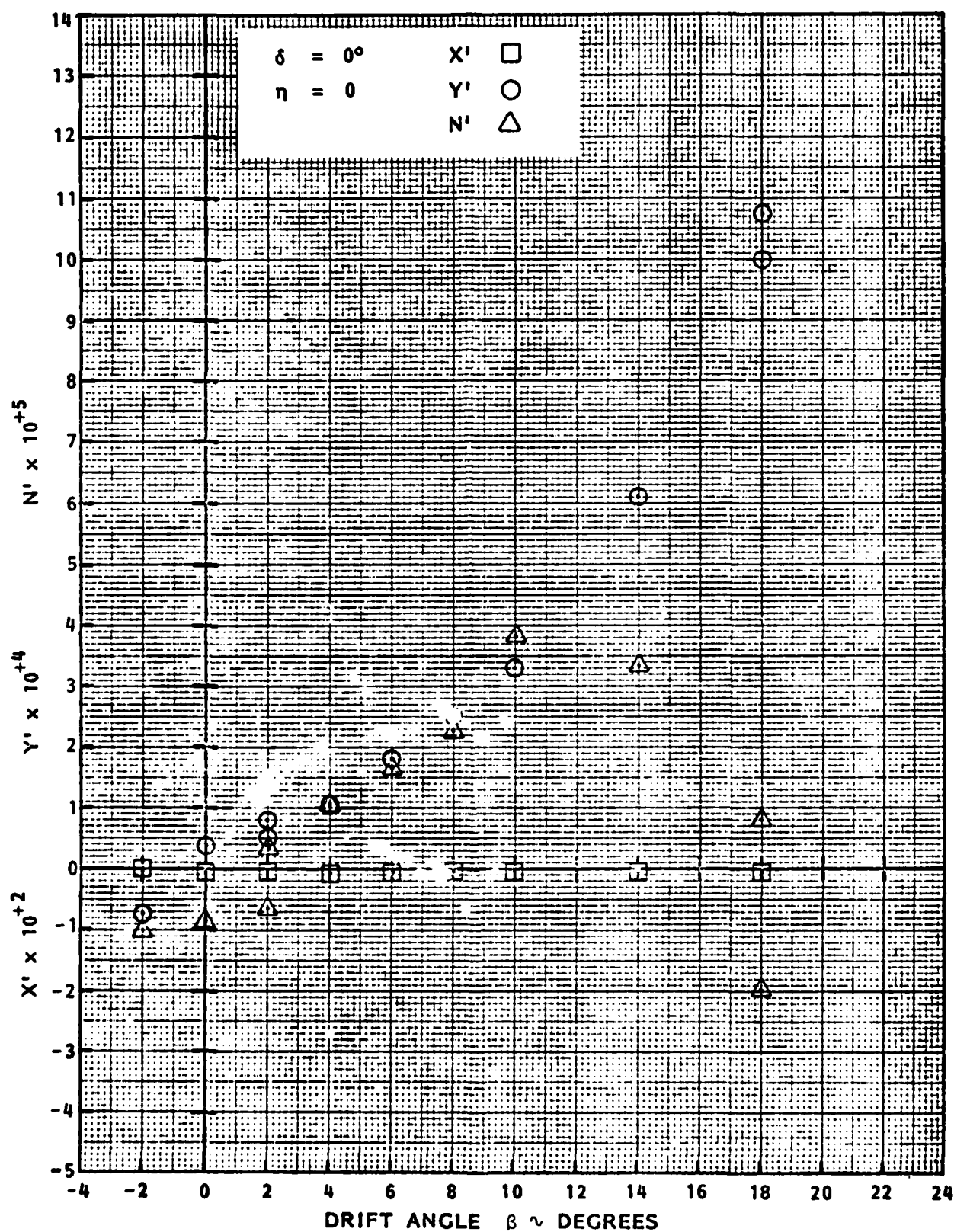


FIGURE A.3 - AXIAL FORCE, LATERAL FORCE, AND YAW MOMENT COEFFICIENTS AS FUNCTIONS OF DRIFT ANGLE β FOR AHEAD MOTION AT $\eta = 0$ IN DEEP WATER

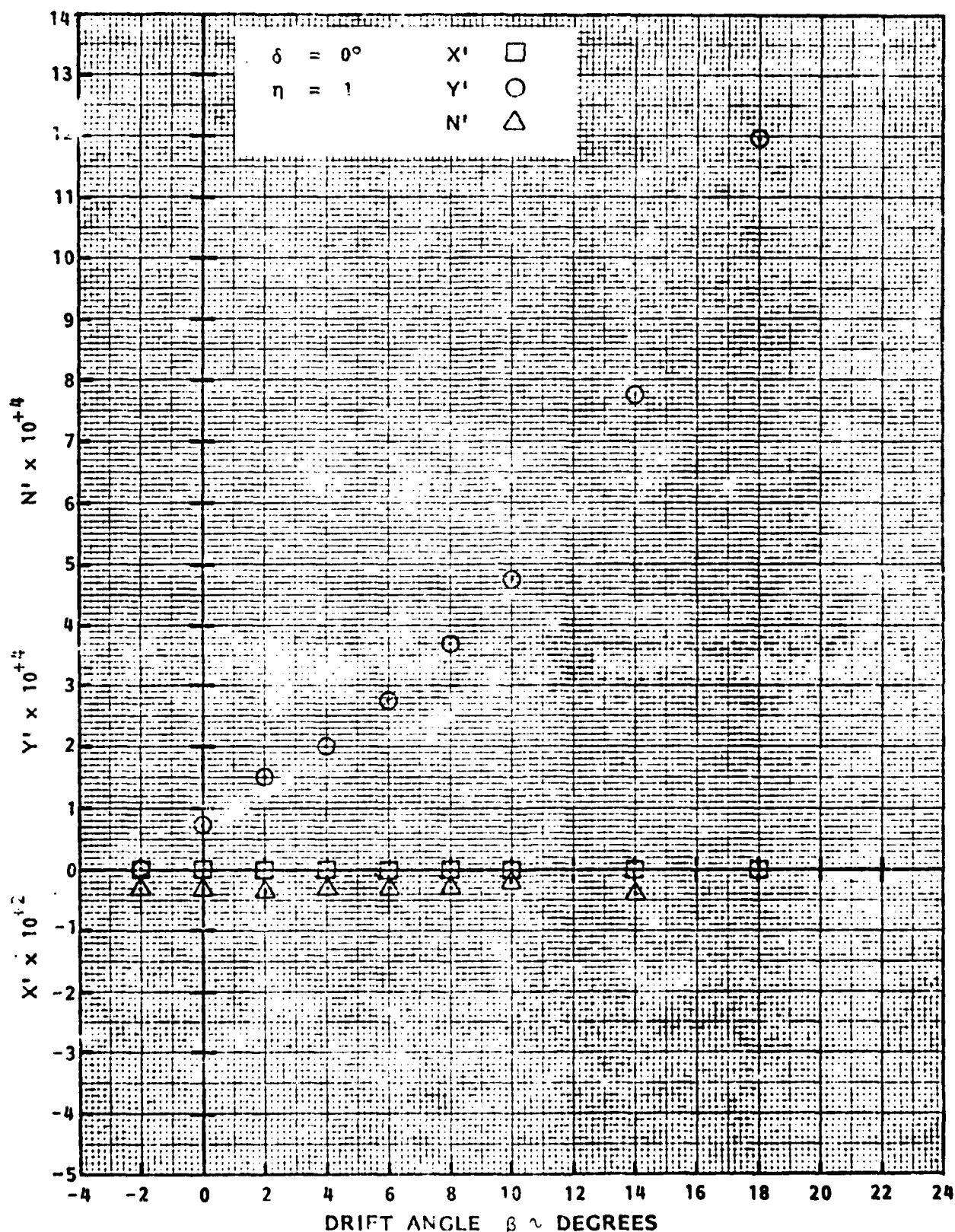


FIGURE A.4 - AXIAL FORCE, LATERAL FORCE, AND YAW MOMENT COEFFICIENTS AS FUNCTIONS OF DRIFT ANGLE β FOR AHEAD MOTION AT $\eta = 1$ IN DEEP WATER

Tracor Hydronautics

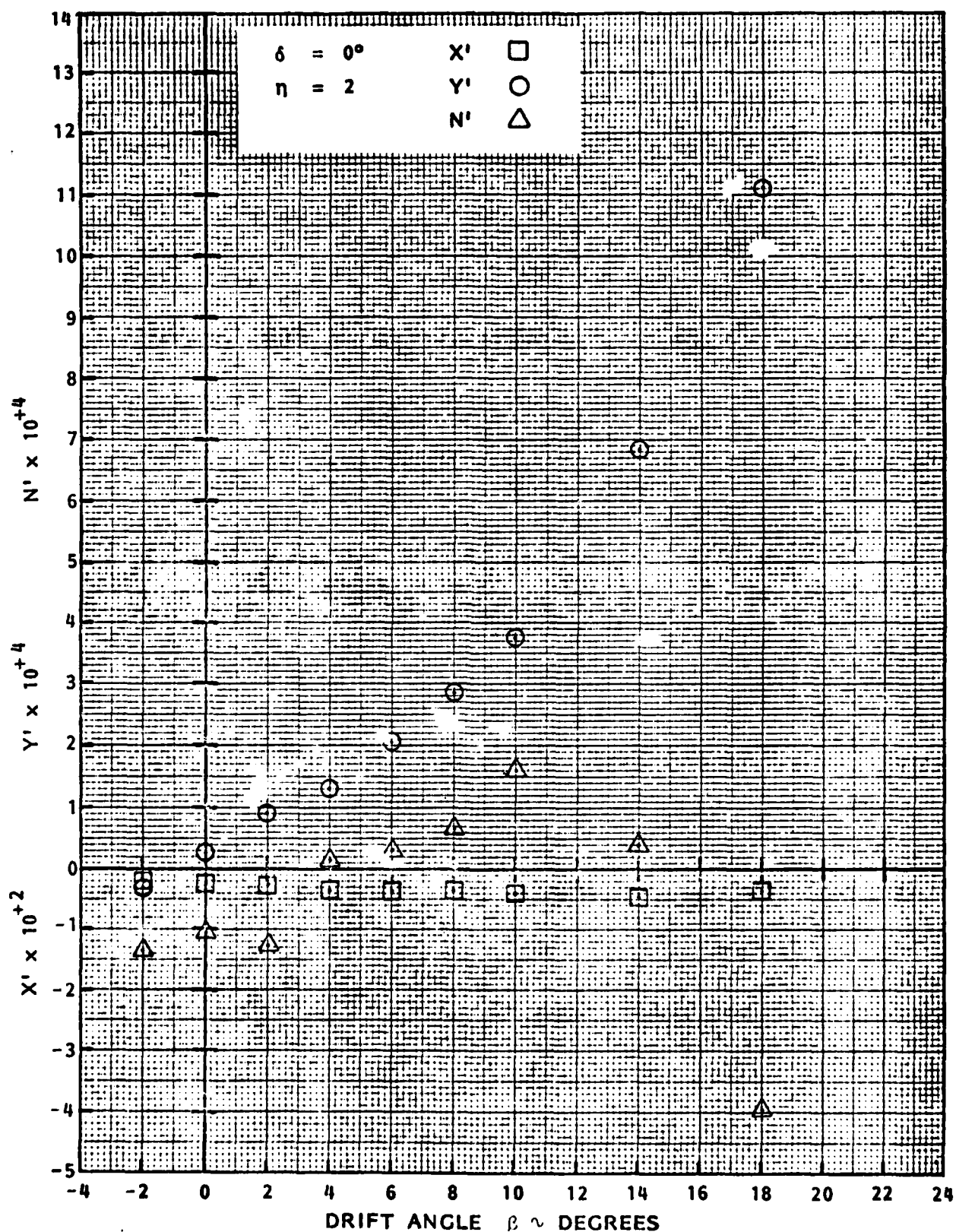


FIGURE A.5 - AXIAL FORCE, LATERAL FORCE, AND YAW MOMENT COEFFICIENTS AS FUNCTIONS OF DRIFT ANGLE β FOR AHEAD MOTION AT $\eta = 2$ IN DEEP WATER

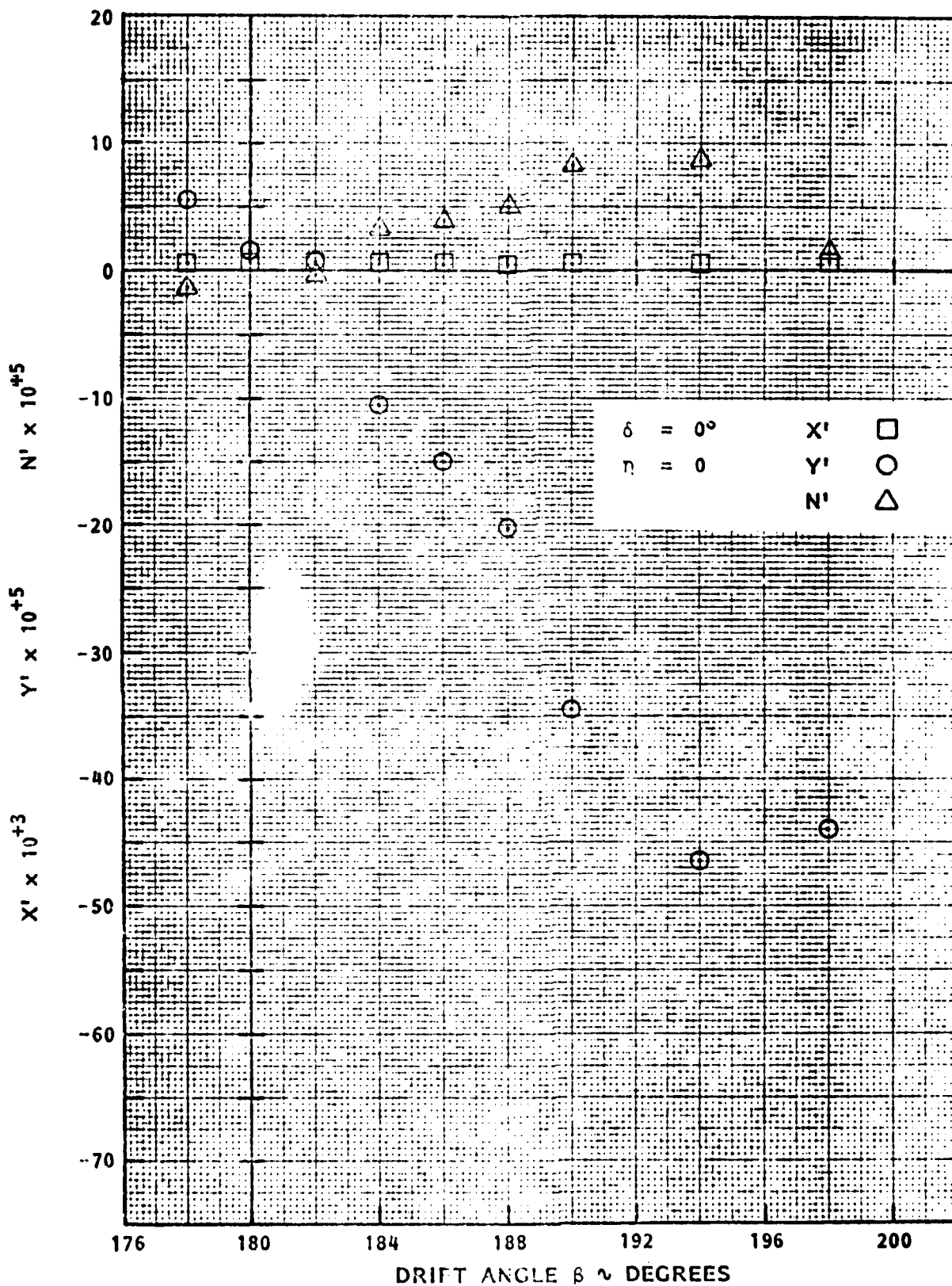


FIGURE A.6 - AXIAL FORCE, LATERAL FORCE, AND YAW MOMENT COEFFICIENTS AS FUNCTIONS OF DRIFT ANGLE β FOR ASTERN MOTION AT $\eta = 0$ IN DEEP WATER

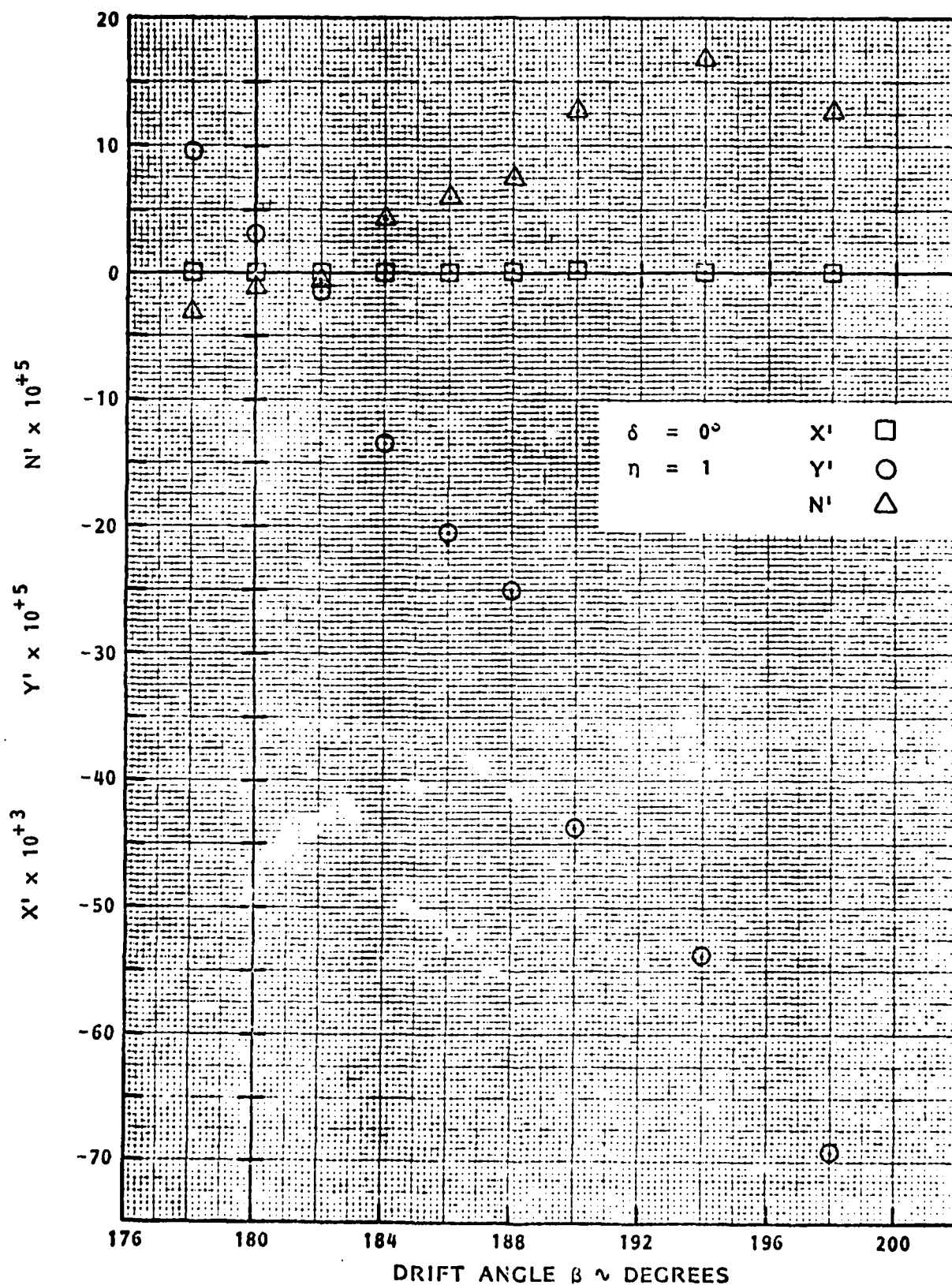


FIGURE A.7 - AXIAL FORCE, LATERAL FORCE, AND YAW MOMENT COEFFICIENTS AS FUNCTIONS OF DRIFT ANGLE β FOR ASTERN MOTION AT $\eta = 1$ IN DEEP WATER

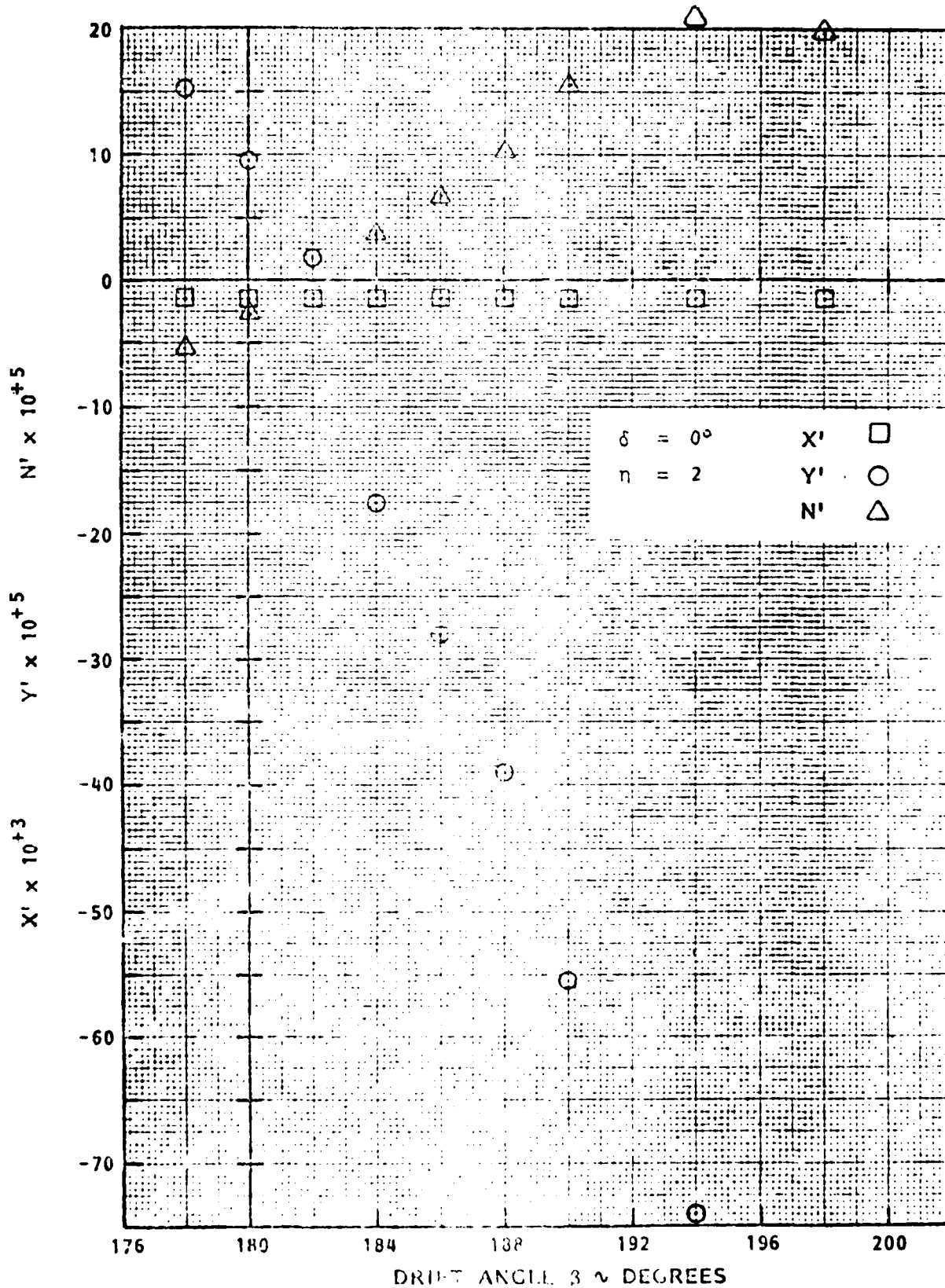


FIGURE A.3 - AXIAL FORCE, LATERAL FORCE, AND YAW MOMENT COEFFICIENTS AS FUNCTIONS OF DRIFT ANGLE δ FOR ASTERN MOTION AT $\eta = 2$ IN DEEP WATER

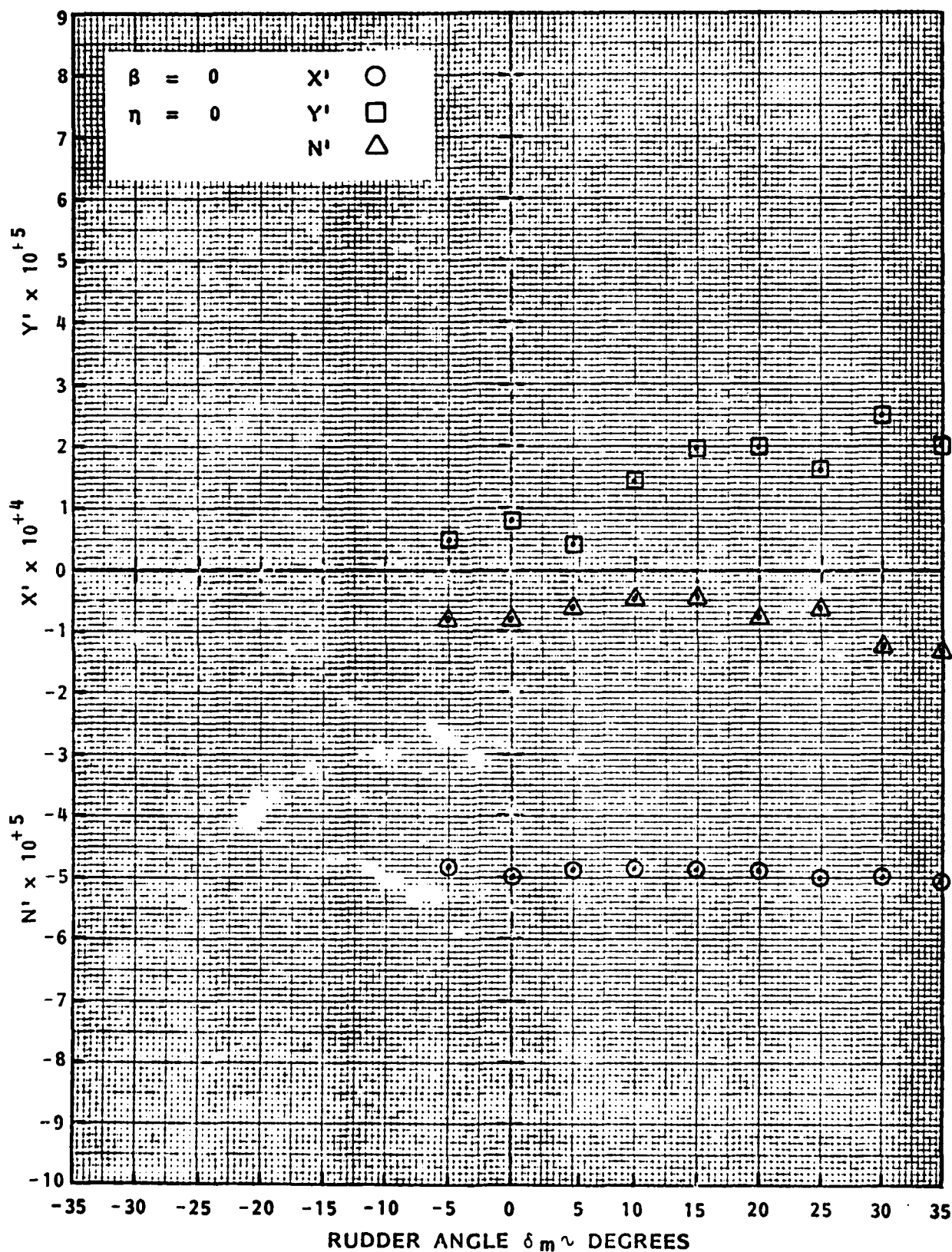


FIGURE A.9 - AXIAL FORCE, LATERAL FORCE AND YAW MOMENT COEFFICIENTS AS FUNCTIONS OF MAIN RUDDER ANGLE δ_m FOR AHEAD MOTION AT $\eta = 0$ IN DEEP WATER

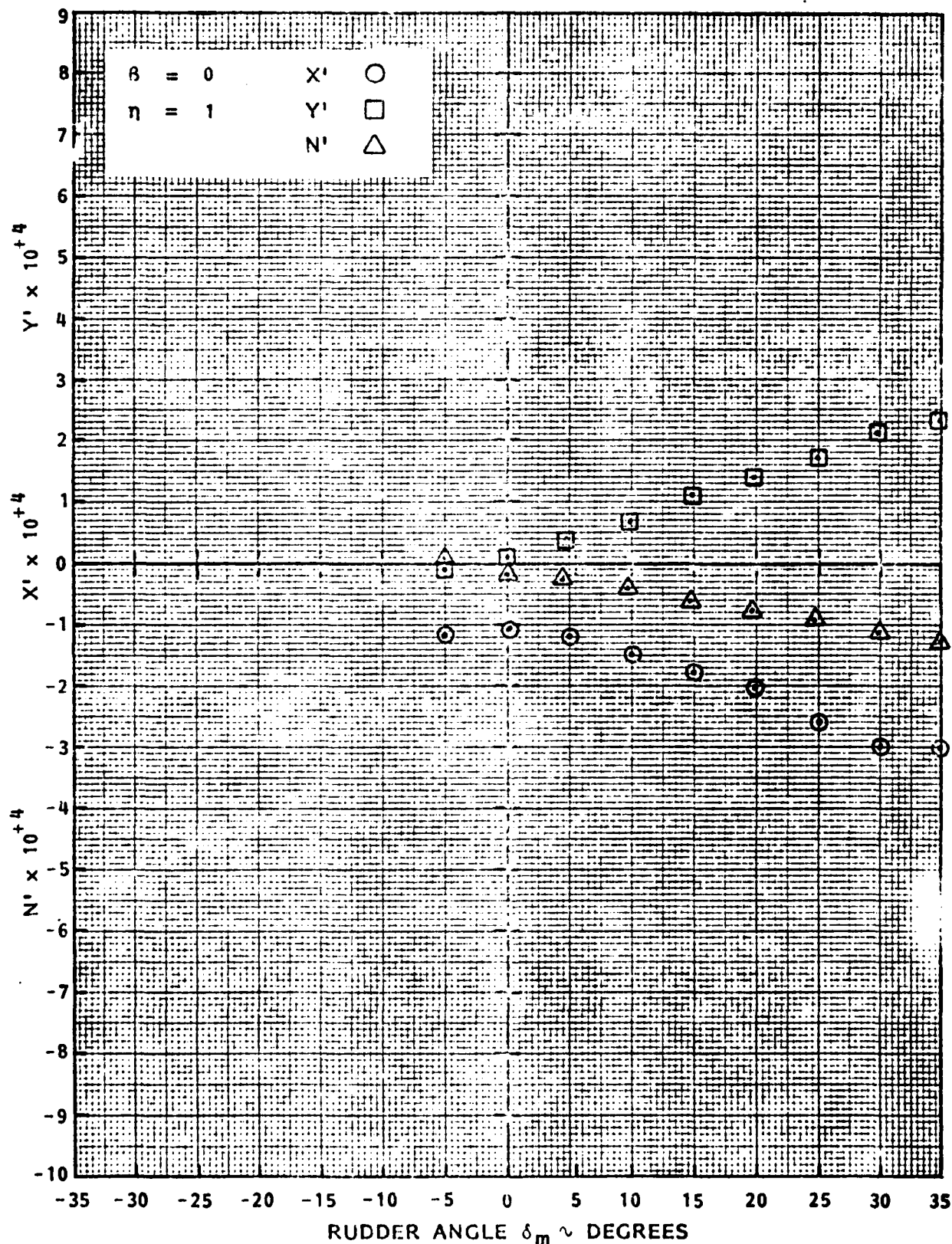


FIGURE A.10 - AXIAL FORCE, LATERAL FORCE AND YAW MOMENT COEFFICIENTS AS FUNCTIONS OF MAIN RUDDER ANGLE δ_m FOR AHEAD MOTION AT $\eta = 1$ IN DEEP WATER

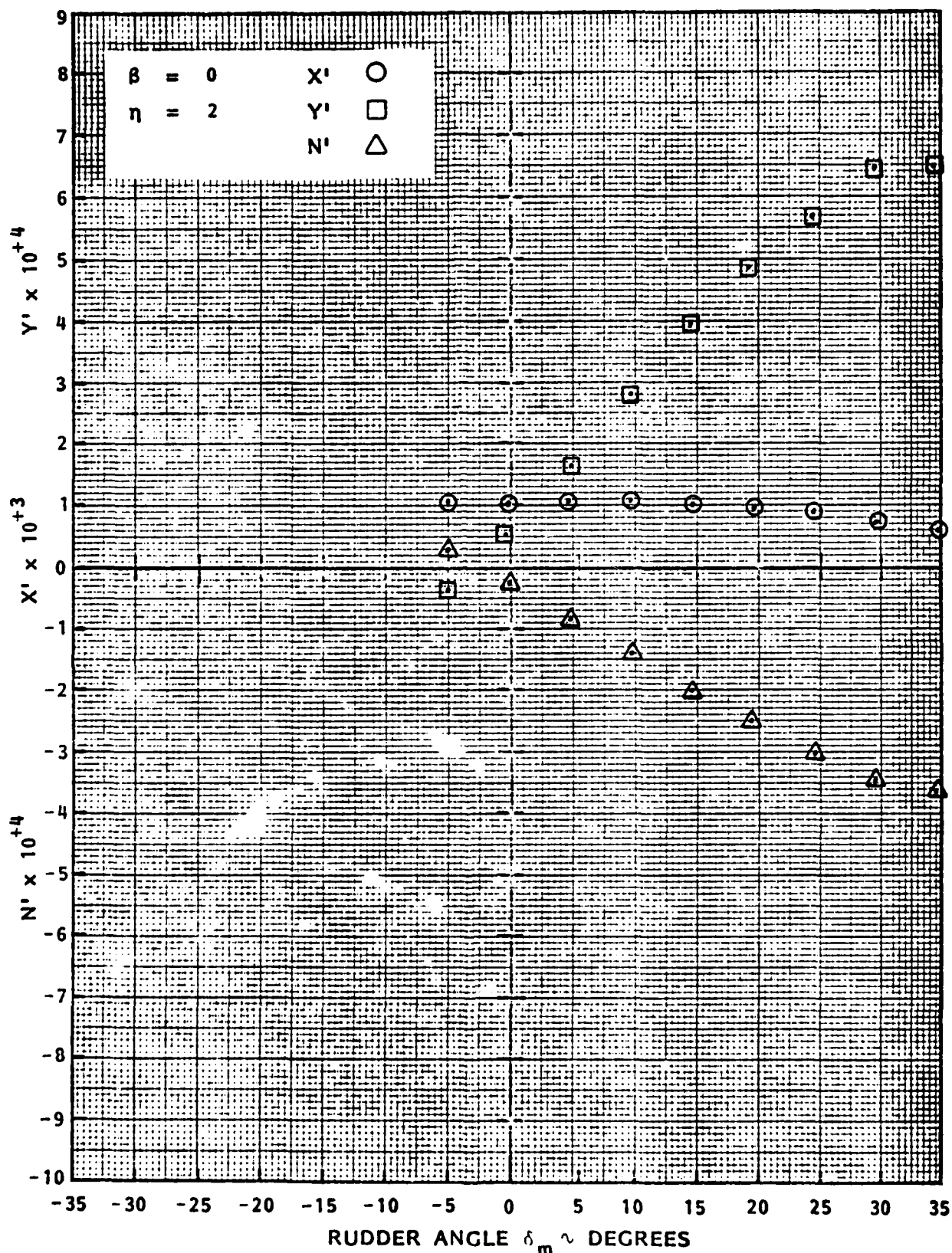
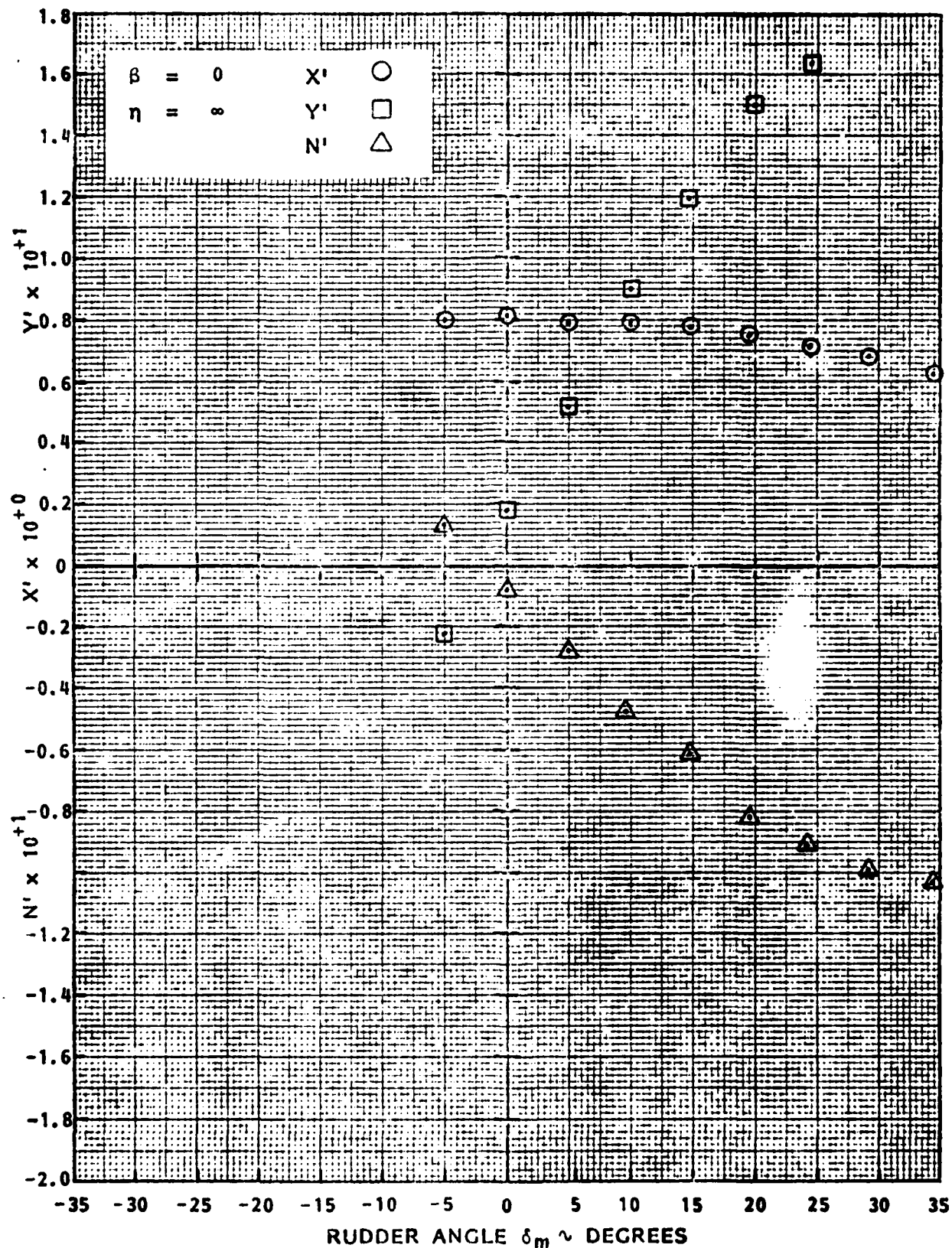


FIGURE A.11 - AXIAL FORCE, LATERAL FORCE AND YAW MOMENT COEFFICIENTS AS FUNCTIONS OF MAIN RUDDER ANGLE δ_m FOR AHEAD MOTION AT $\eta = 2$ IN DEEP WATER



RUDDER ANGLE δ_m ~ DEGREES

FIGURE A.12 - AXIAL FORCE, LATERAL FORCE AND YAW MOMENT COEFFICIENTS AS FUNCTIONS OF MAIN RUDDER ANGLE δ_m FOR ZERO SPEED AT $\eta = \infty$ (AHEAD THRUST) IN DEEP WATER

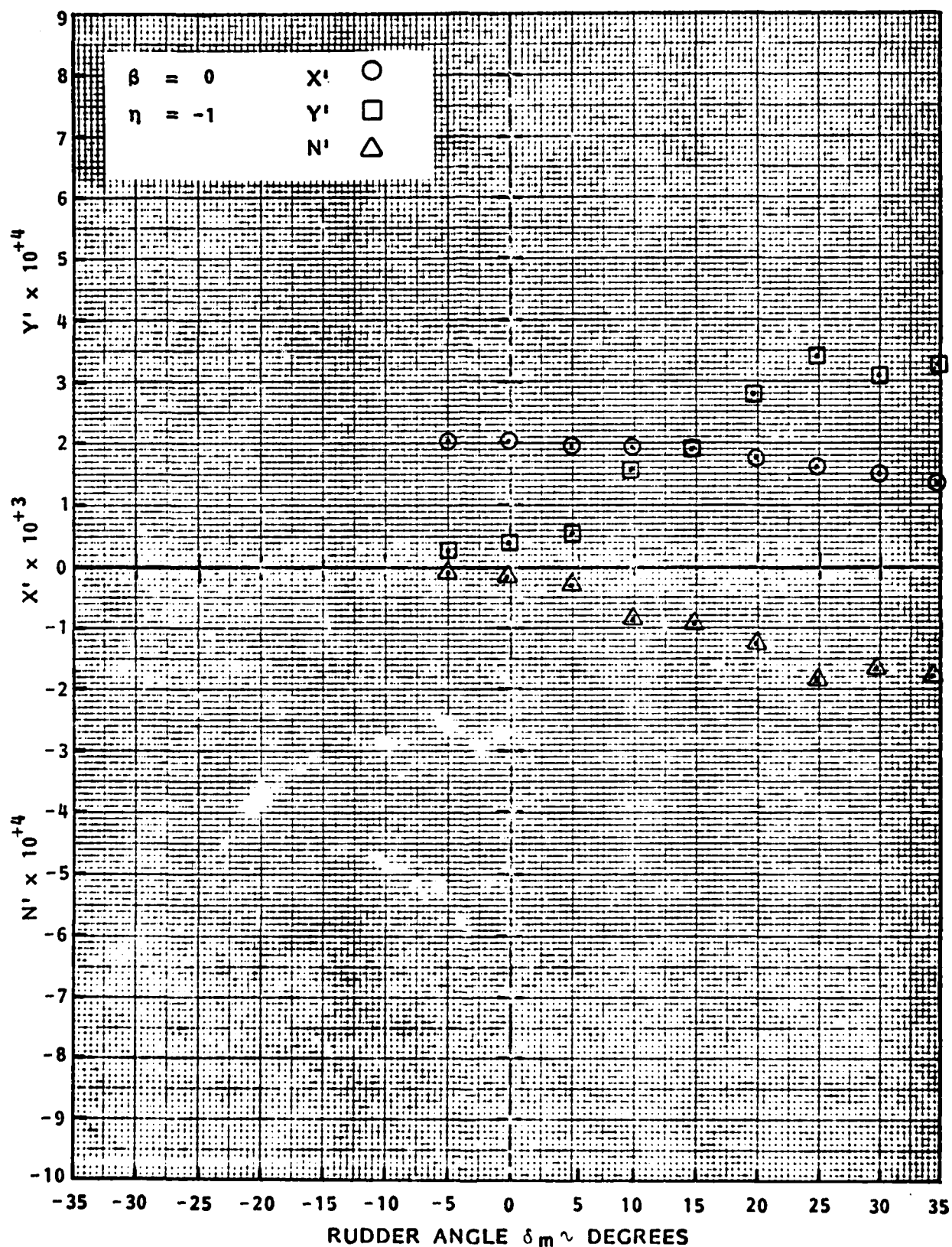


FIGURE A.13 - AXIAL FORCE, LATERAL FORCE AND YAW MOMENT COEFFICIENTS AS FUNCTIONS OF MAIN RUDDER ANGLE δ_m FOR ASTERN MOTION AT $\eta = -1$ IN DEEP WATER

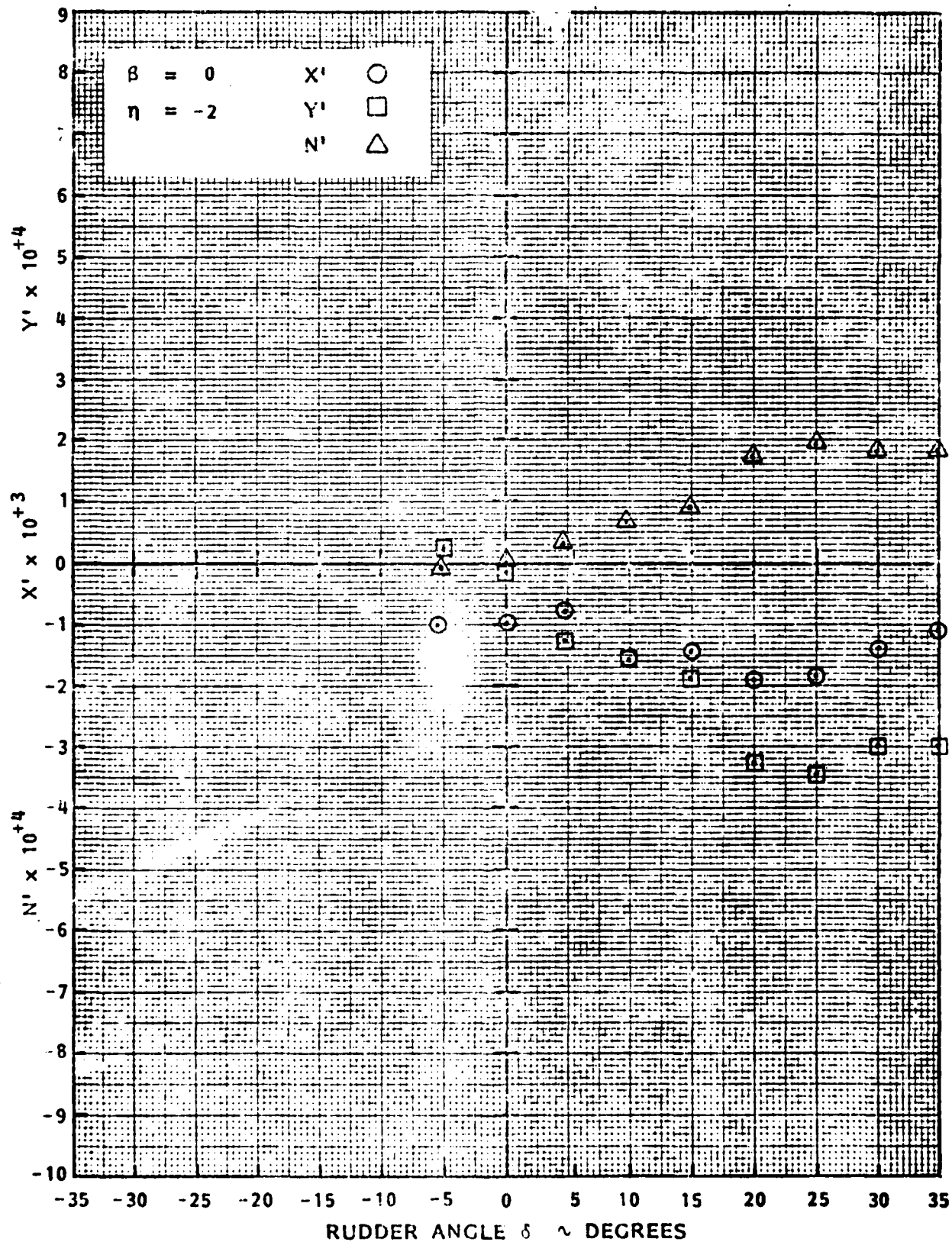


FIGURE A.14 - AXIAL FORCE, LATERAL FORCE AND YAW MOMENT COEFFICIENTS AS FUNCTIONS OF FLANKING RUDDER ANGLE δ_F FOR AHEAD MOTION AT $\eta = -2$ IN DEEP WATER

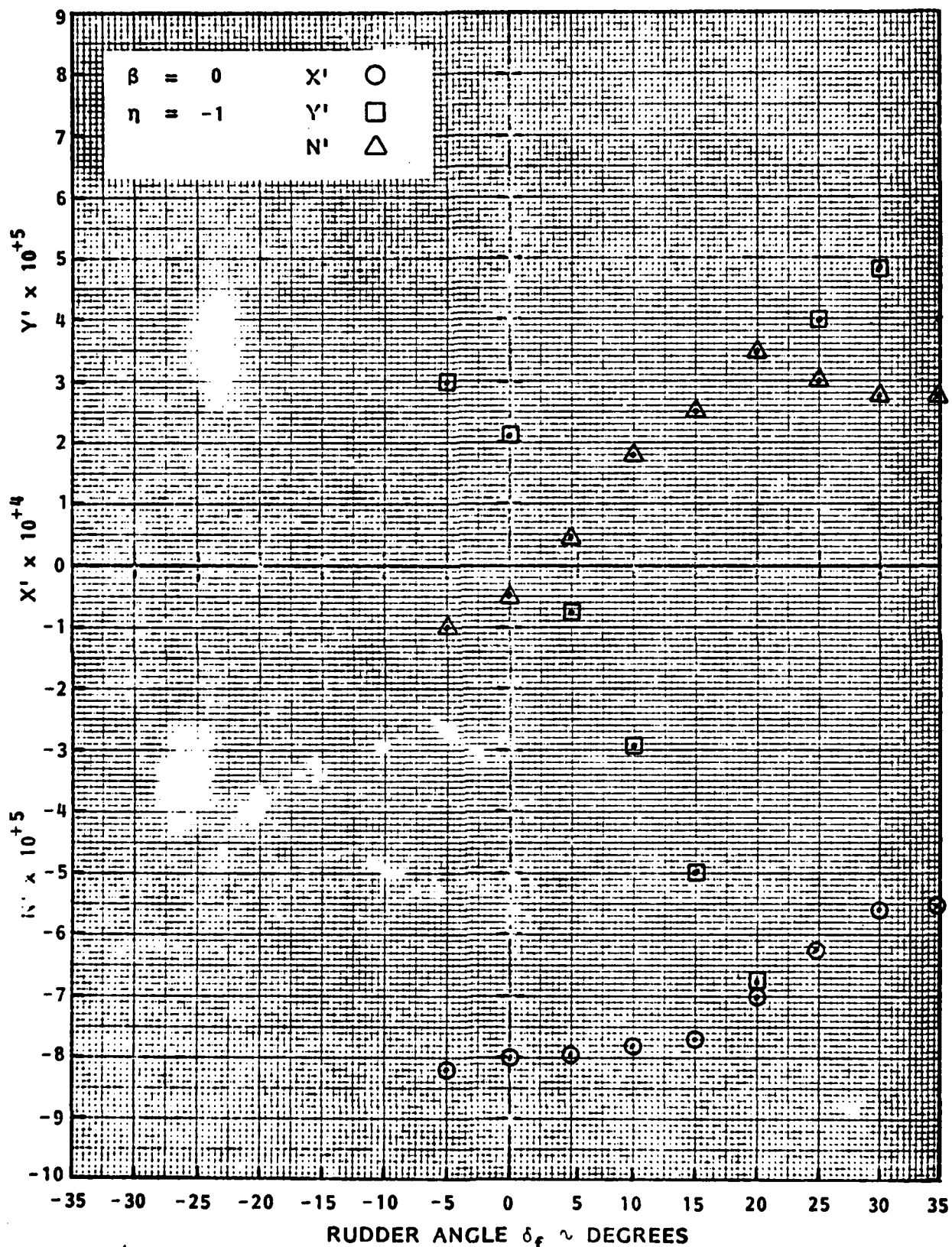


FIGURE A.15 - AXIAL FORCE, LATERAL FORCE AND YAW MOMENT COEFFICIENTS AS FUNCTIONS OF FLANKING RUDDER ANGLE δ_f FOR AHEAD MOTION AT $\eta = -1$ IN DEEP WATER

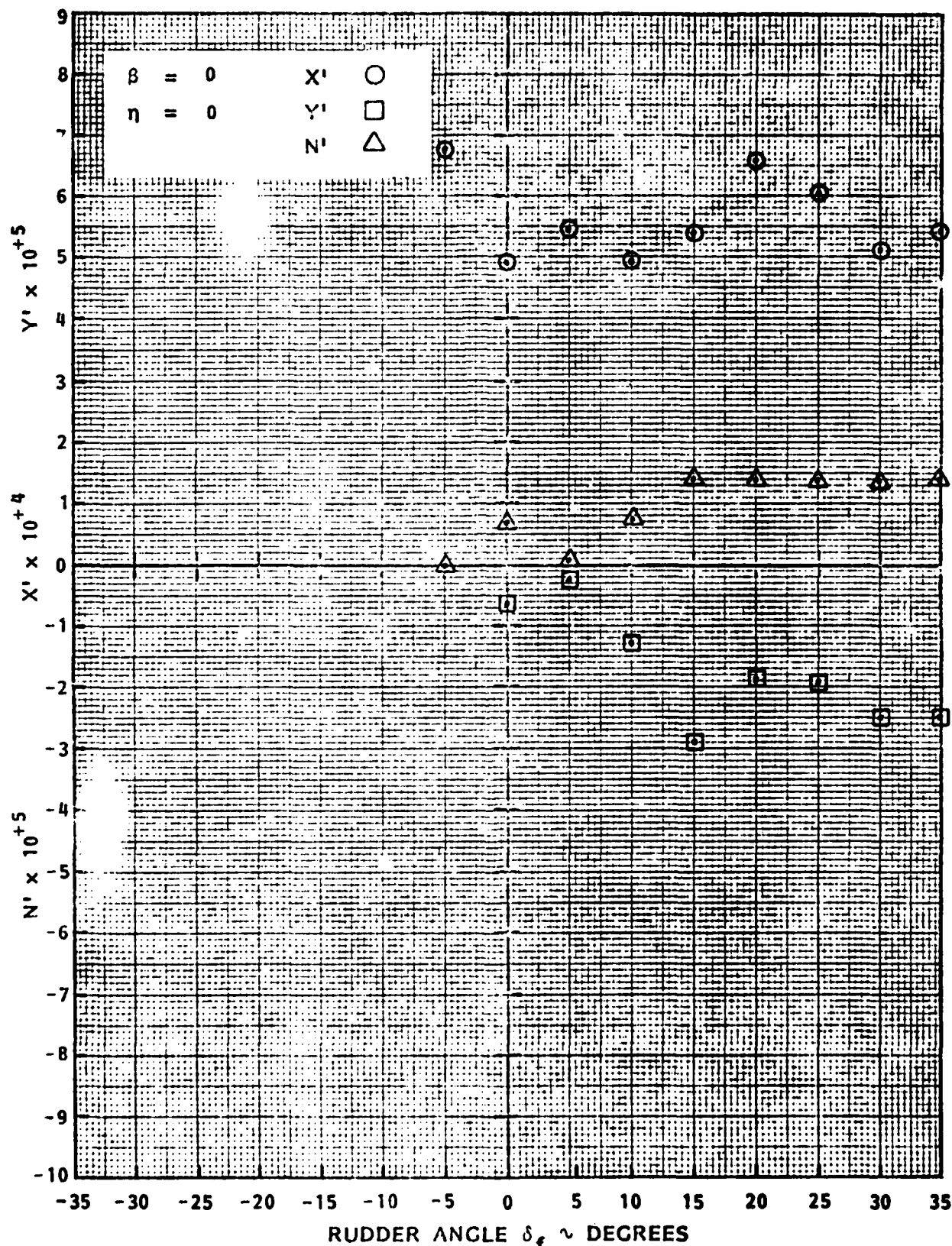


FIGURE A.16 - AXIAL FORCE, LATERAL FORCE AND YAW MOMENT COEFFICIENTS AS FUNCTIONS OF FLANKING RUDDER ANGLE δ_f FOR ASTERN MOTION AT $\eta = 0$ IN DEEP WATER

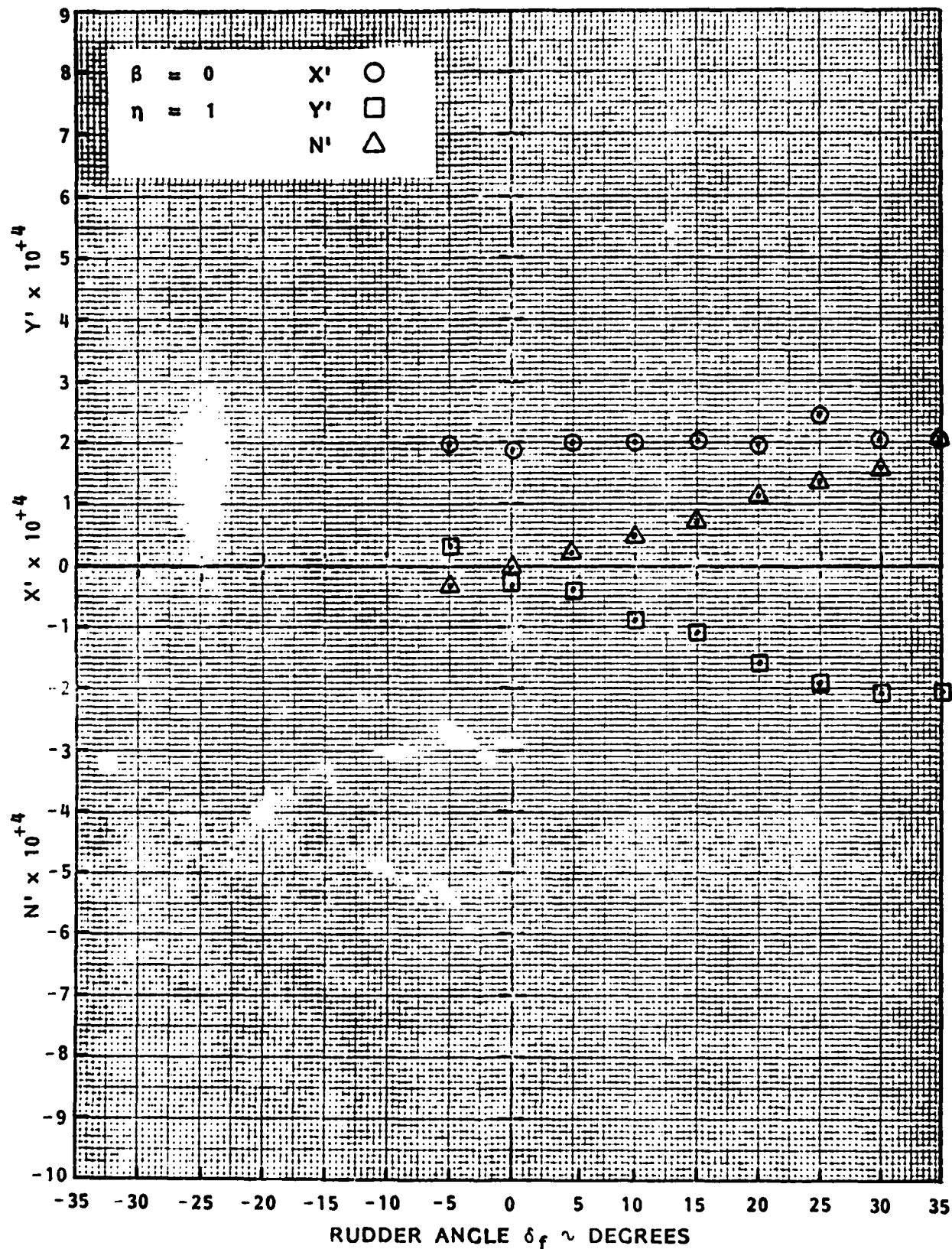


FIGURE A.17 - AXIAL FORCE, LATERAL FORCE AND YAW MOMENT COEFFICIENTS AS FUNCTIONS OF FLANKING RUDDER ANGLE δ_f FOR ASTERN MOTION AT $\eta = 1$ IN DEEP WATER

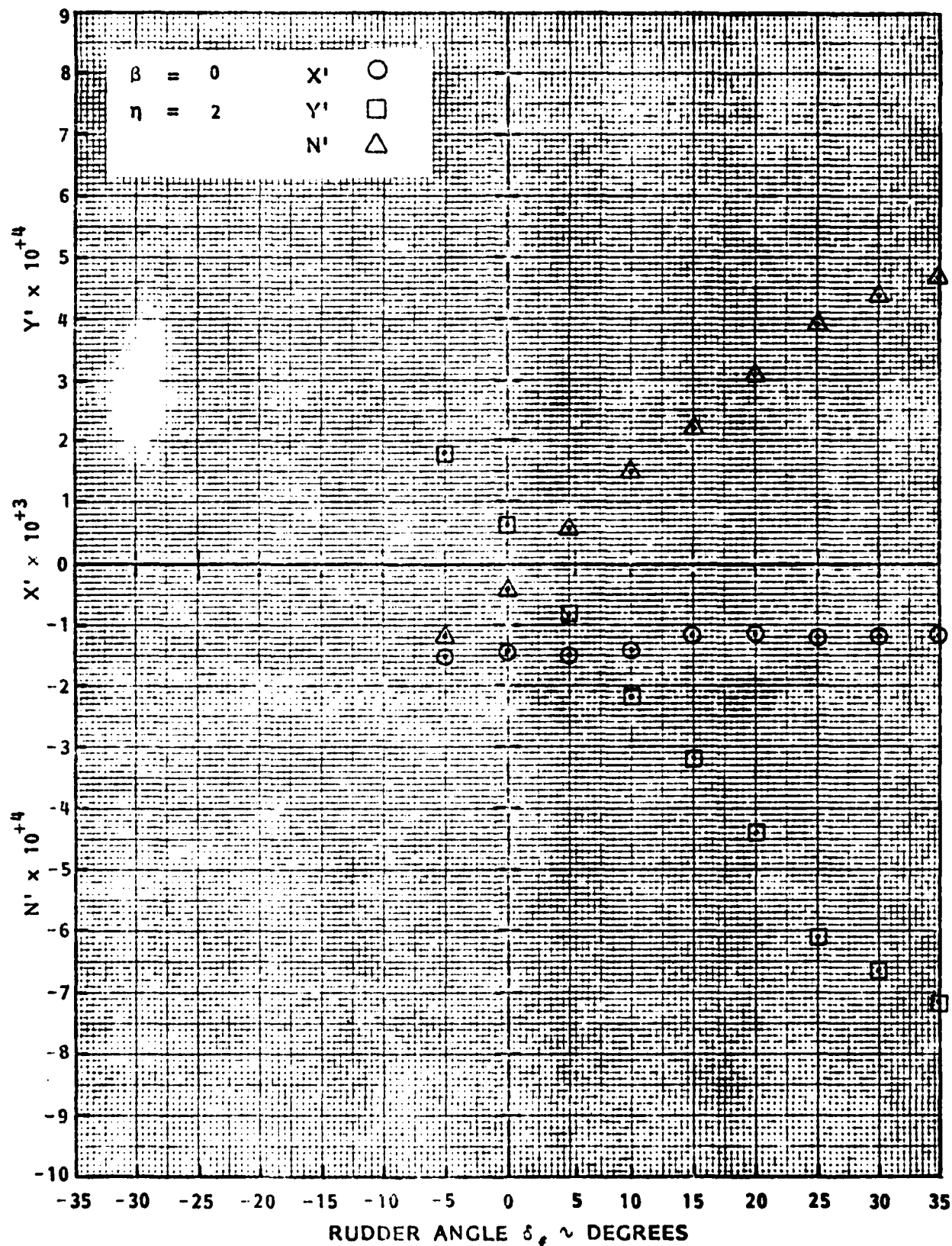


FIGURE A.18 - AXIAL FORCE, LATERAL FORCE AND YAW MOMENT COEFFICIENTS AS FUNCTIONS OF PLANKING RUDDER ANGLE δ_r FOR ASTERN MOTION AT $\eta = 2$ IN DEEP WATER

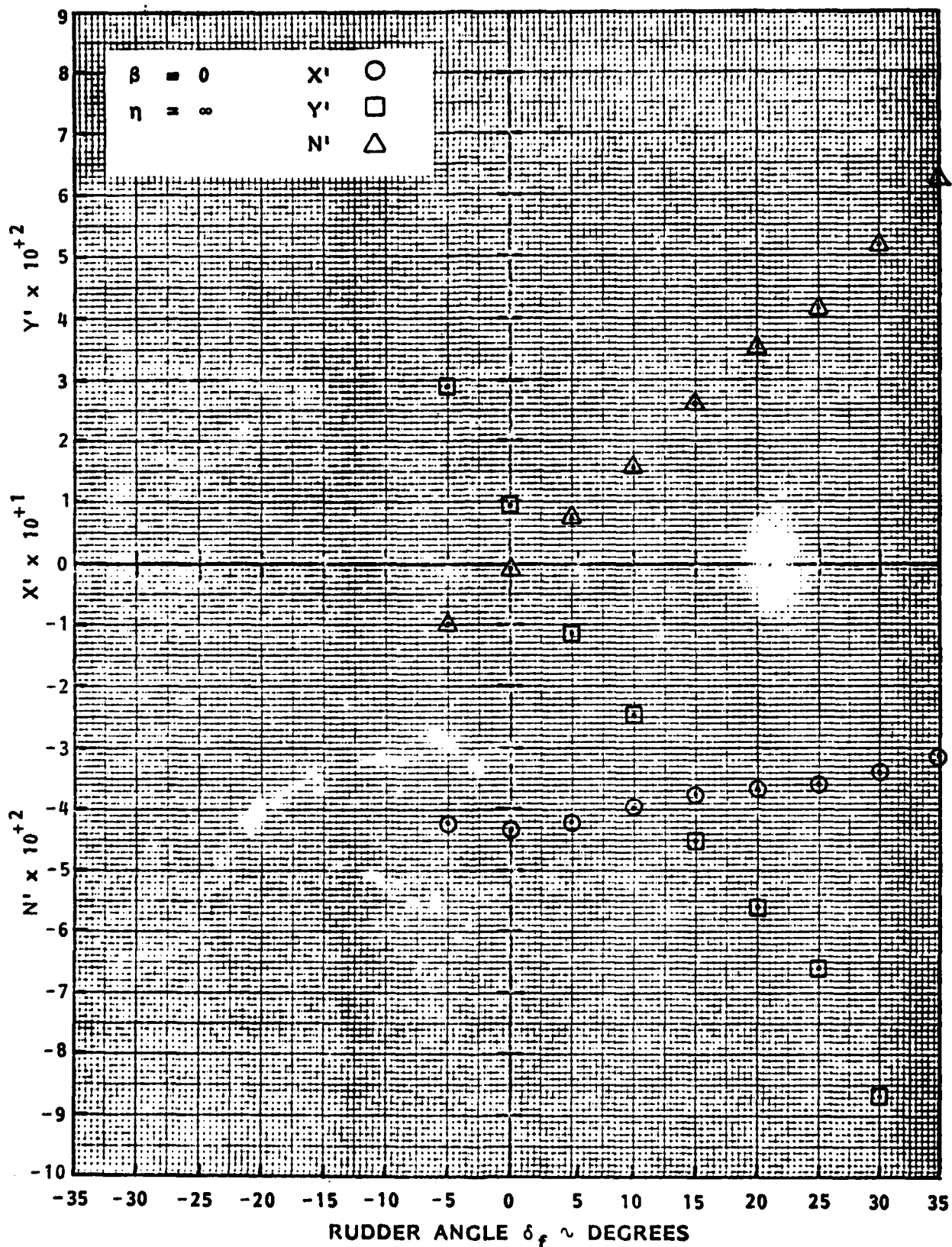


FIGURE A.19 - AXIAL FORCE, LATERAL FORCE AND YAW MOMENT COEFFICIENTS AS FUNCTIONS OF FLANKING RUDDER ANGLE δ_F FOR ZERO SPEED AT $\eta = \infty$ (ASTERN THRUST) IN DEEP WATER

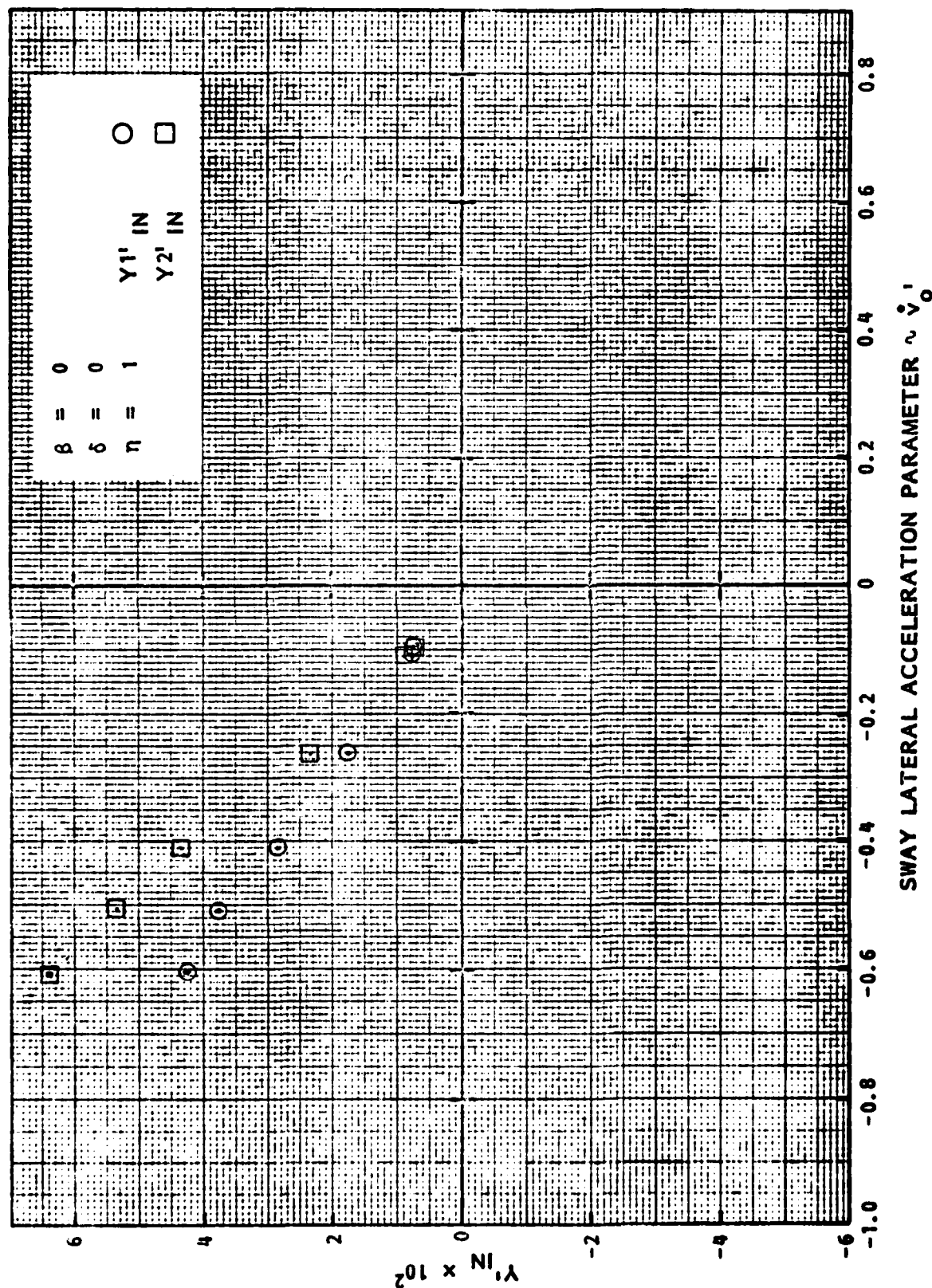


FIGURE A.20 - LATERAL FORCE GAGE IN-PHASE COEFFICIENTS
AS FUNCTIONS OF SWAY ACCELERATION FOR AHEAD
MOTION AT $\eta = 1$ IN DEEP WATER

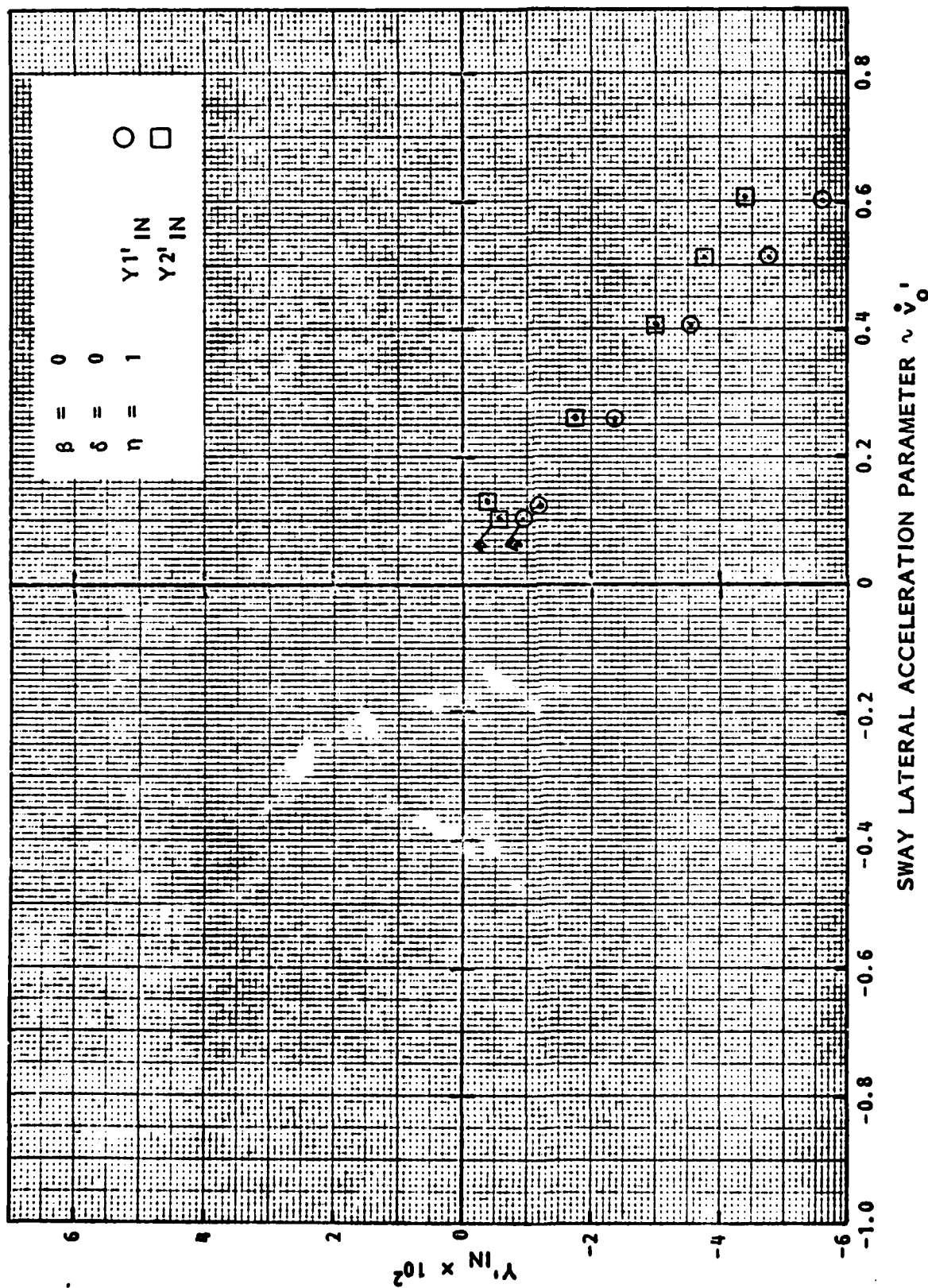


FIGURE A.21 - LATERAL FORCE GAGE IN-PHASE COEFFICIENTS
AS FUNCTIONS OF SWAY ACCELERATION FOR ASTERN
MOTION AT $\eta = 1$ IN DEEP WATER

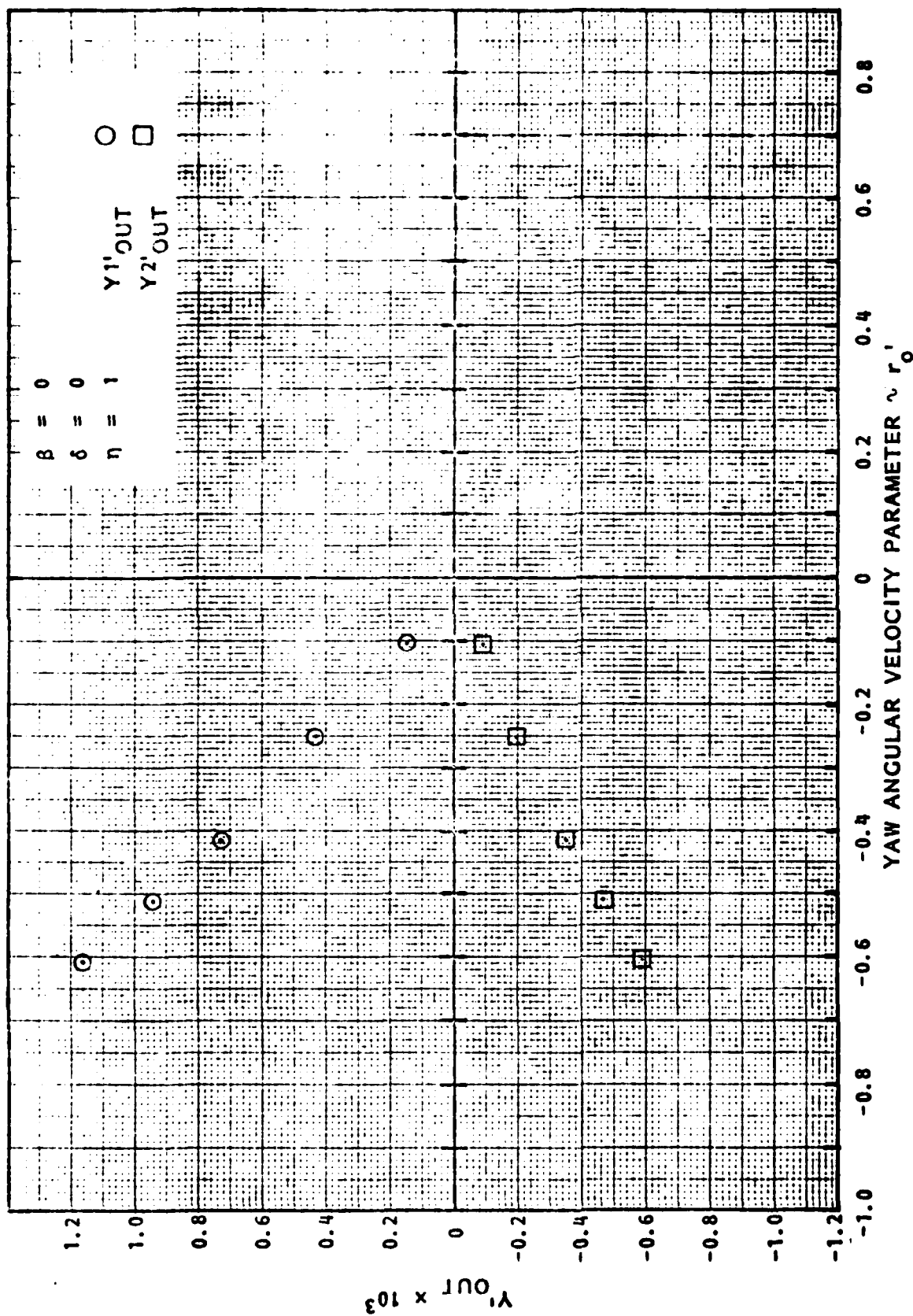


FIGURE A.22 - LATERAL FORCE GAGE OUT-OF-PHASE COEFFICIENTS
AS FUNCTIONS OF YAW ANGULAR VELOCITY FOR AHEAD
MOTION AT $\eta = 1$ IN DEEP WATER

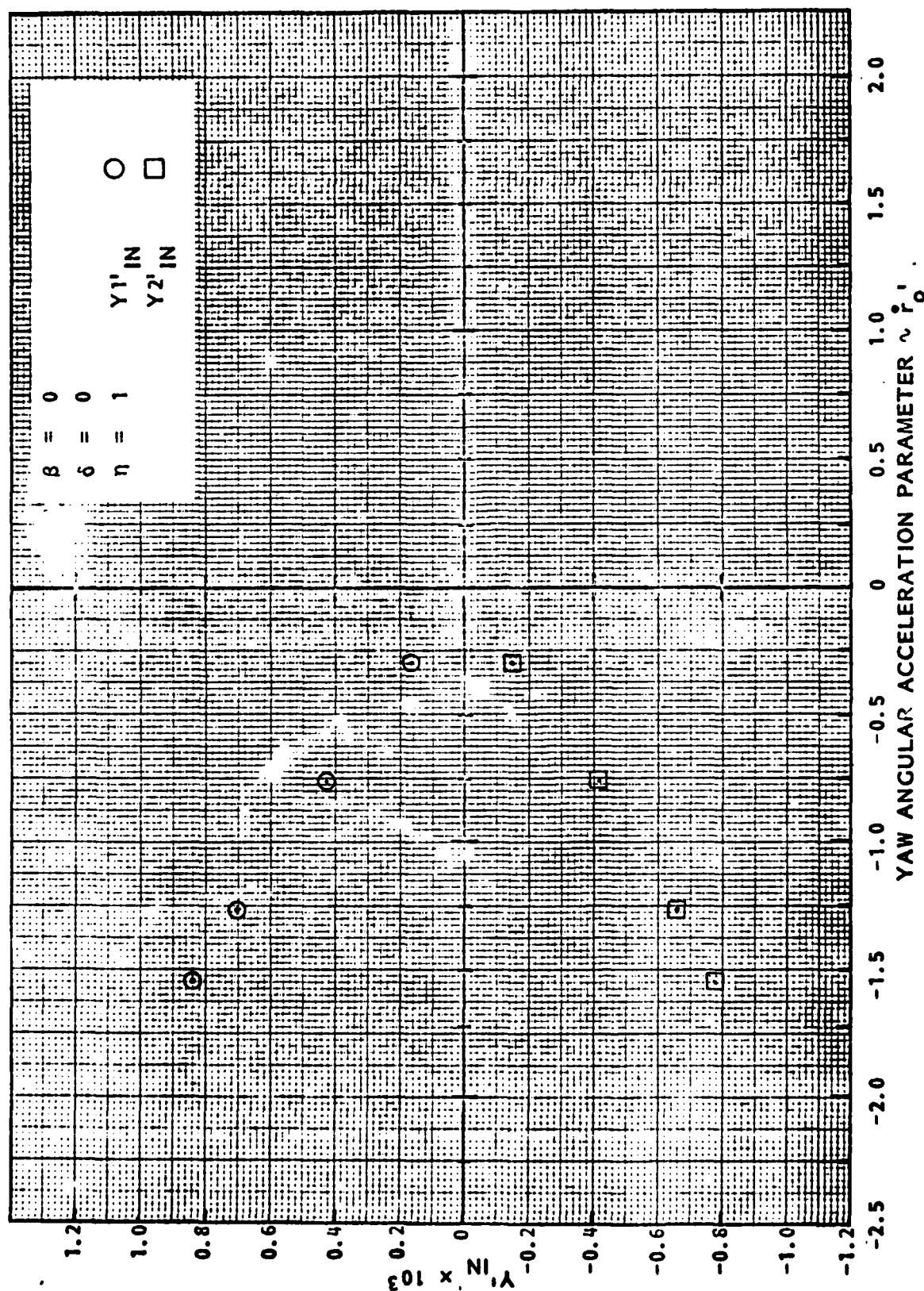


FIGURE A.23 - LATERAL FORCE GAGE IN-PHASE COEFFICIENTS
AS FUNCTIONS OF YAW ANGULAR ACCELERATION FOR
AHEAD MOTION AT $\eta = 1$ IN DEEP WATER

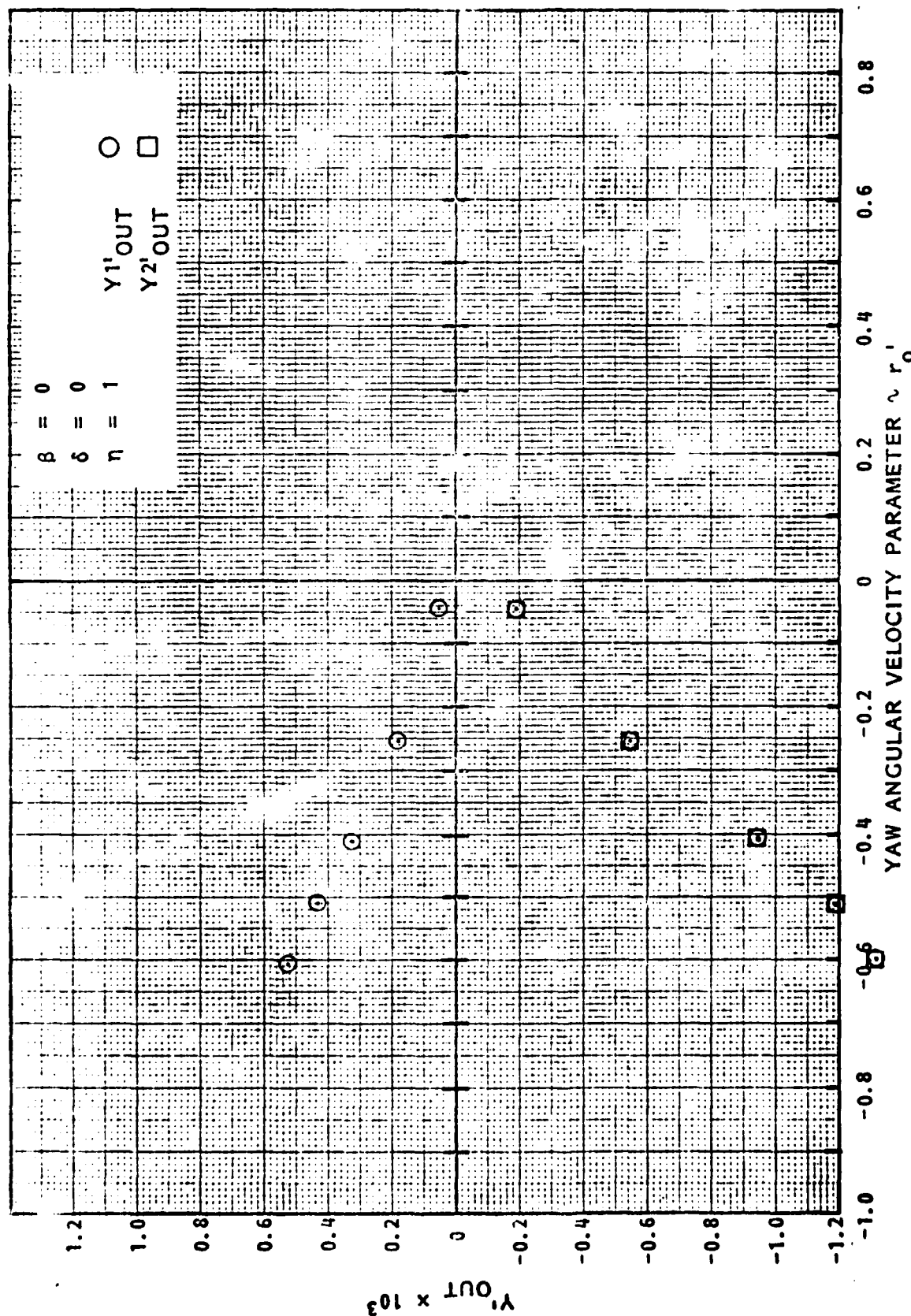


FIGURE A.24 - LATERAL FORCE GAGE OUT-OF-PHASE COEFFICIENTS
AS FUNCTIONS OF YAW ANGULAR VELOCITY FOR ASTERN
MOTION AT $\eta = 1$ IN DEEP WATER

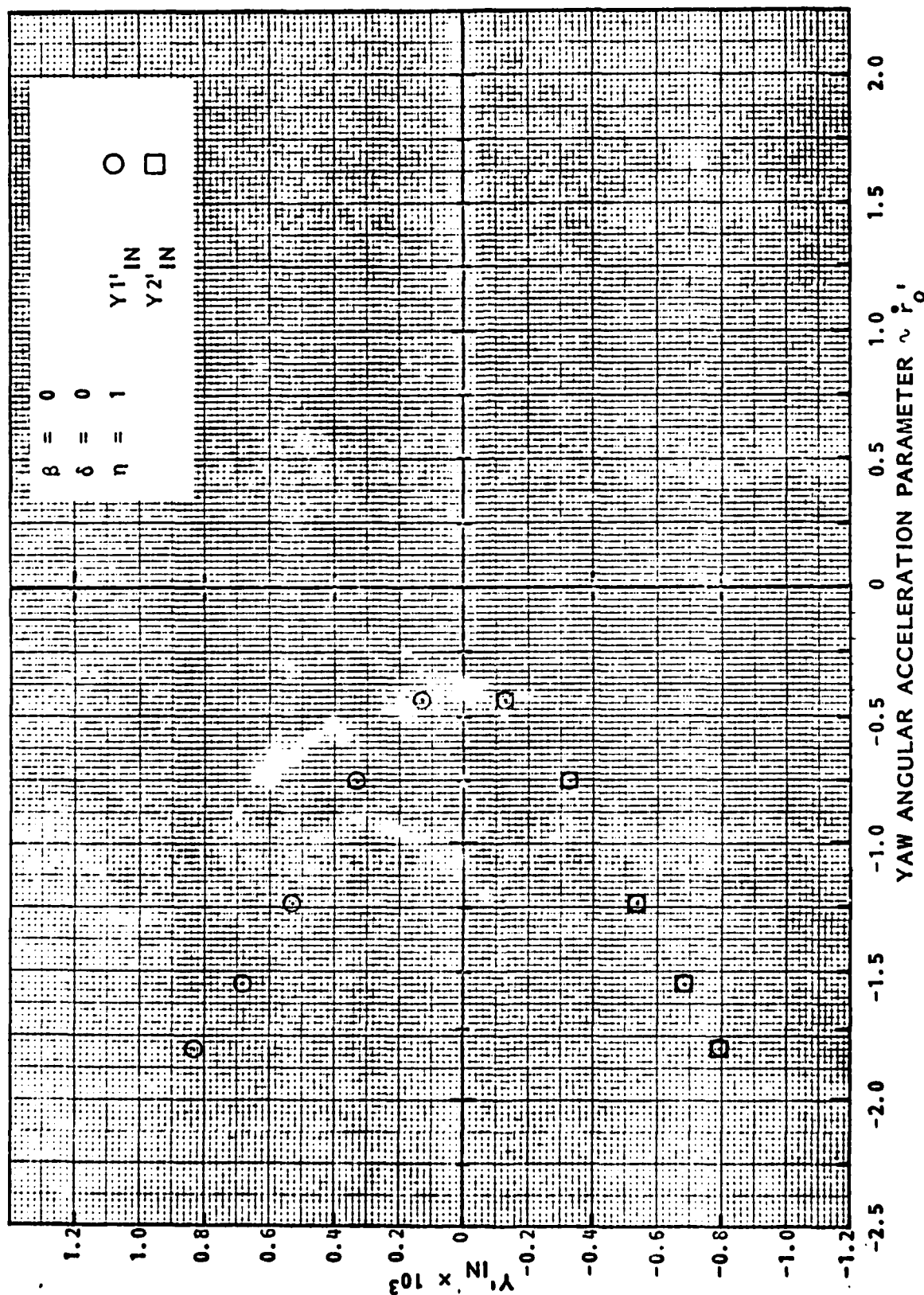


FIGURE A.25 - LATERAL FORCE GAGE IN-PHASE COEFFICIENTS AS FUNCTIONS OF YAW ANGULAR ACCELERATION FOR ASTERN MOTION AT $\eta = 1$ IN DEEP WATER

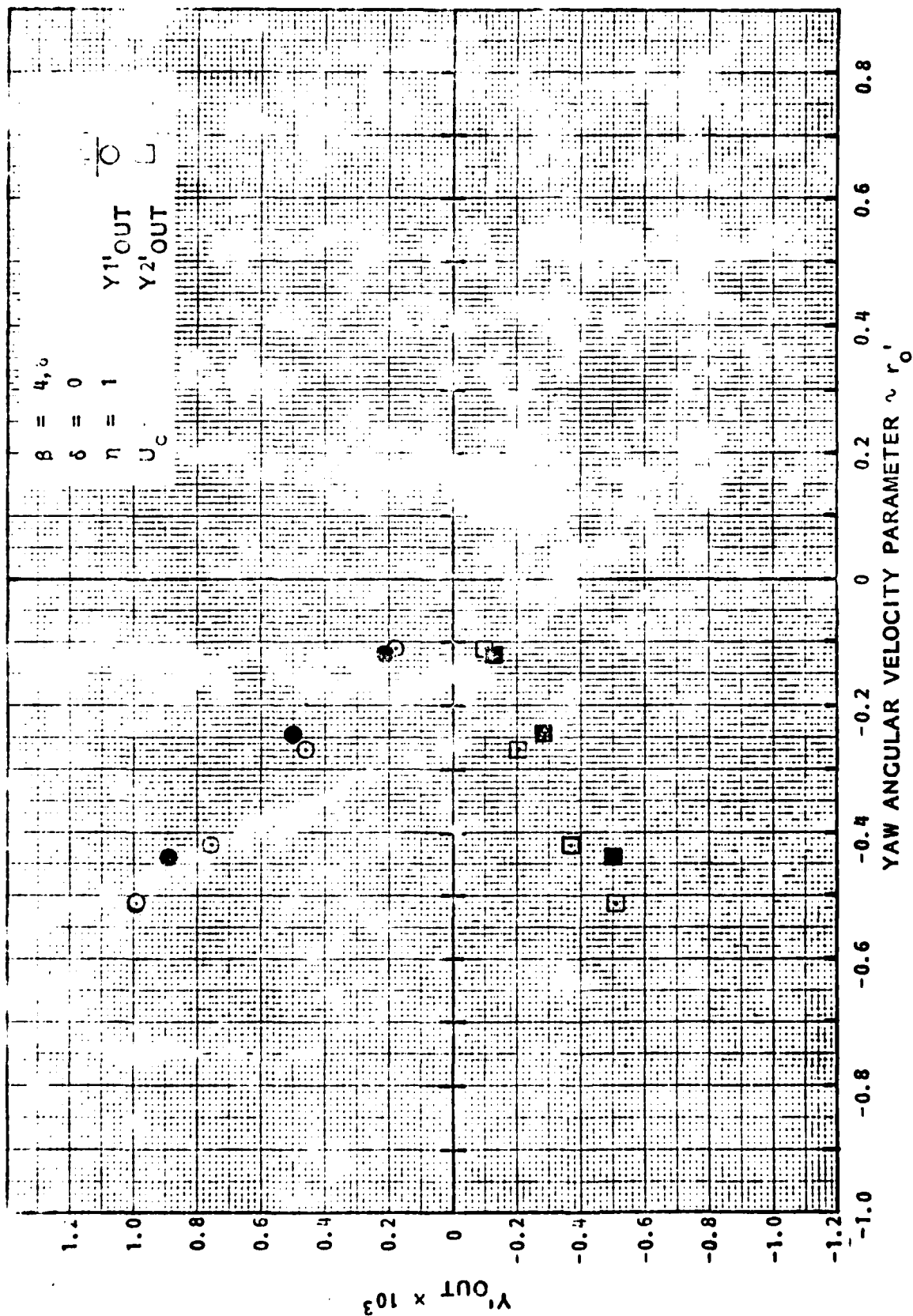


FIGURE A.26 - LATERAL FORCE GAUGE OUT-OF-PHASE COEFFICIENTS AS FUNCTIONS OF YAW ANGULAR VELOCITY AND DRIFT ANGLE FOR AHEAD MOTION AT $\eta = 1$ IN DEEP WATER

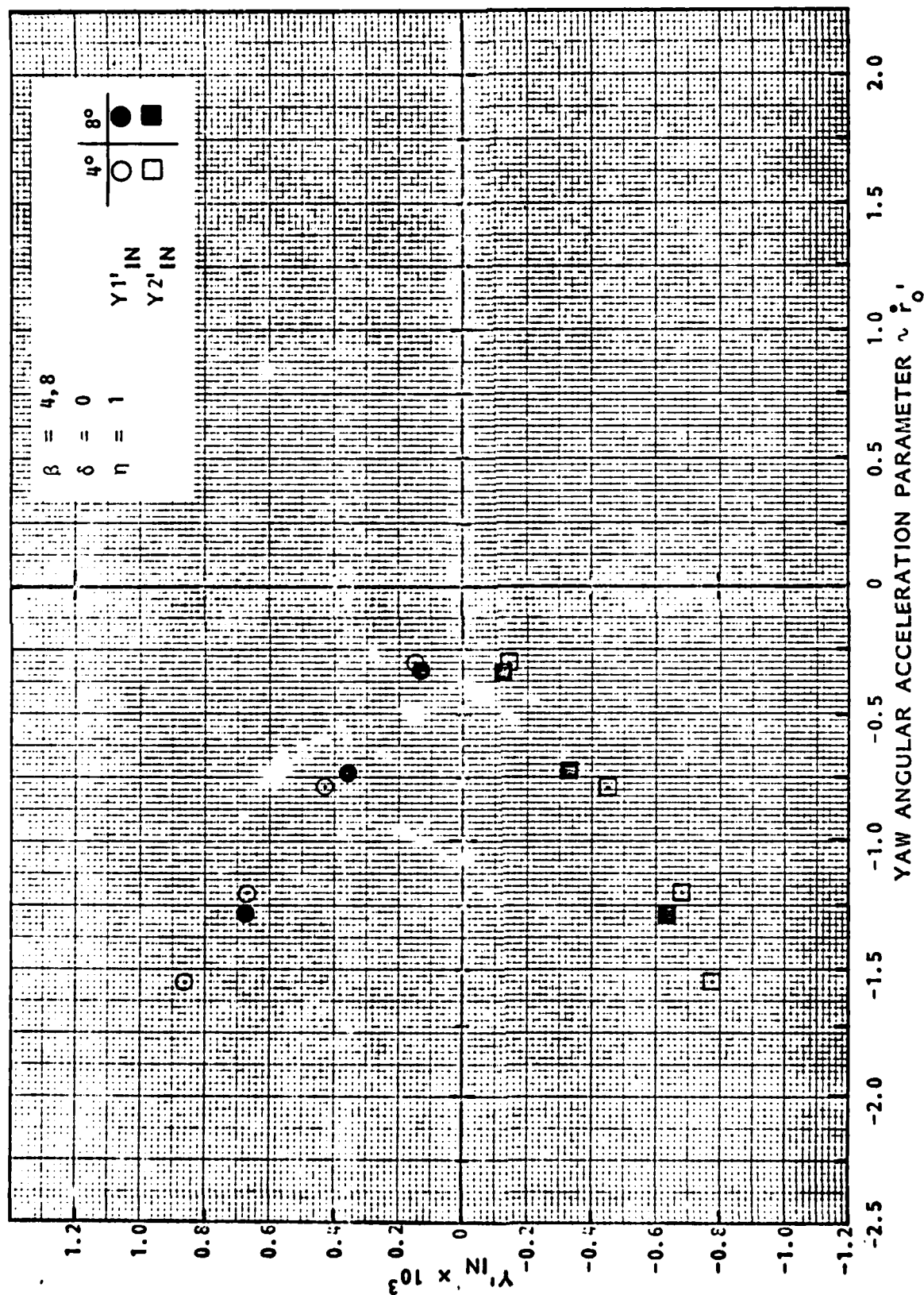


FIGURE A.27 - LATERAL FORCE GAGE IN-PHASE COEFFICIENTS AS FUNCTIONS OF YAW ANGULAR ACCELERATION AND DRIFT ANGLE FOR AHEAD MOTION AT $\eta = 1$ IN DEEP WATER

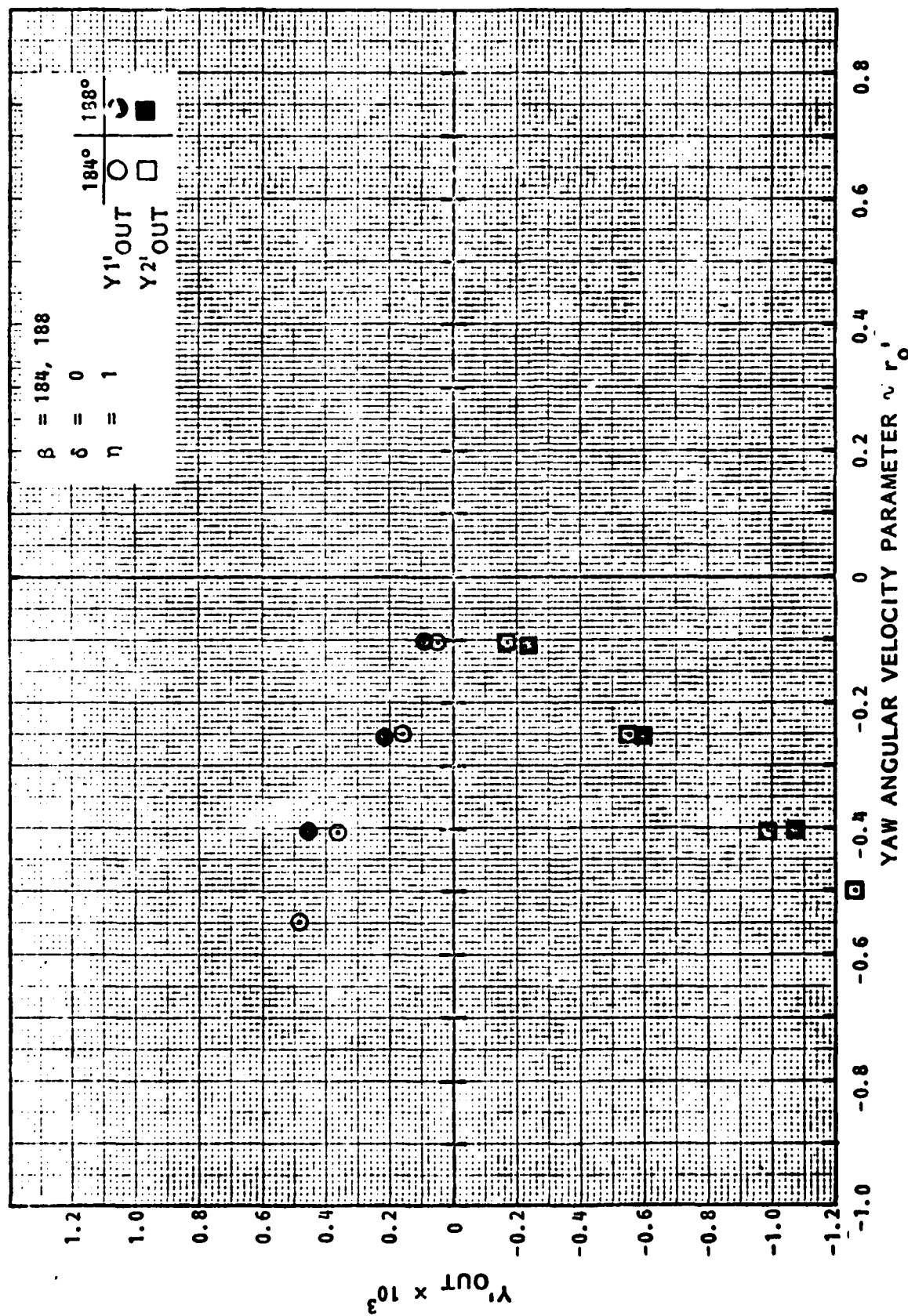


FIGURE A.28 - LATERAL FORCE GAGE OUT-OF-PHASE COEFFICIENTS AS FUNCTIONS OF YAW ANGULAR VELOCITY AND DRIFT ANGLE FOR ASTERN MOTION AT $\eta = 1$ IN DEEP WATER

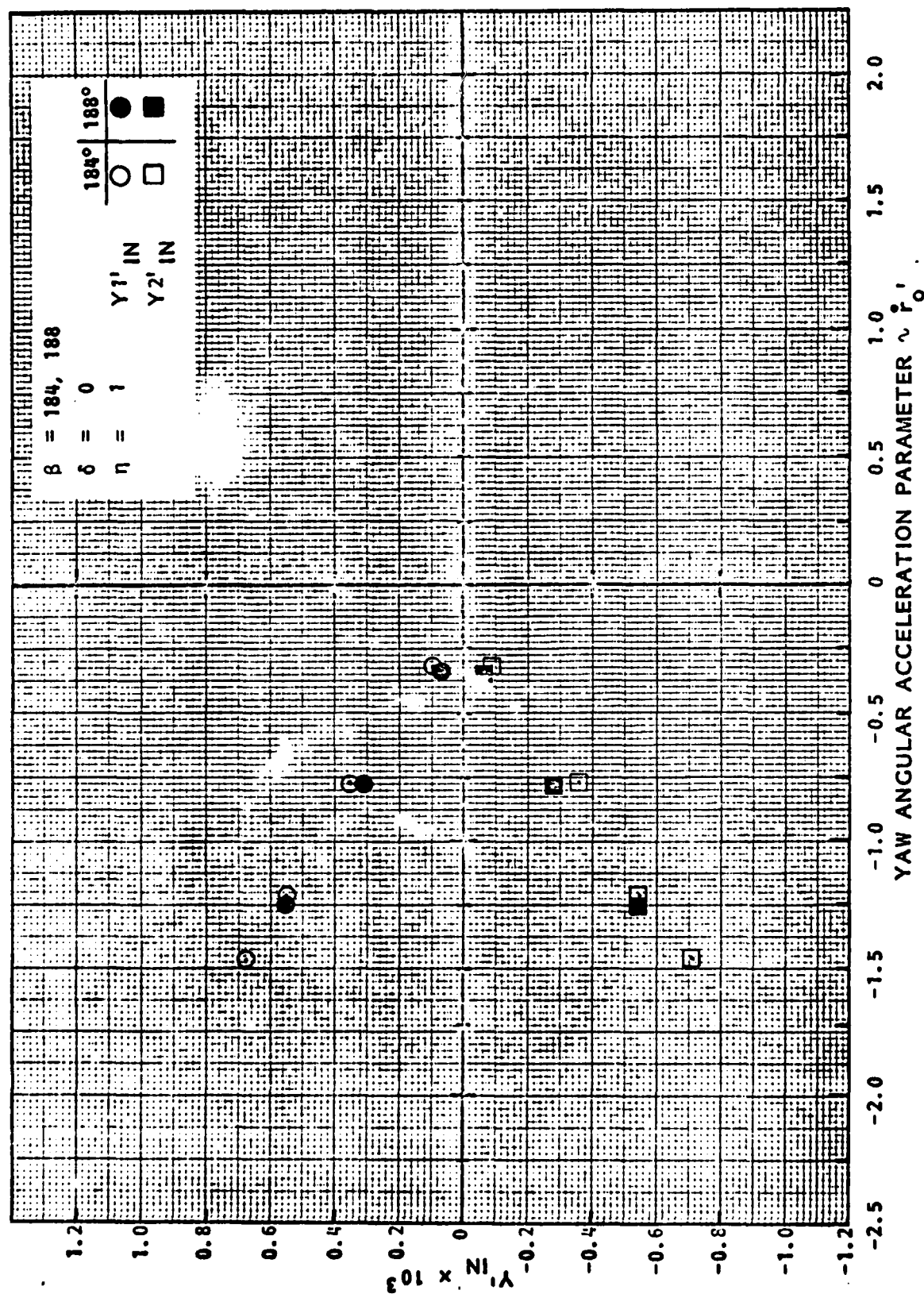


FIGURE A.29 - LATERAL FORCE GAGE IN-PHASE COEFFICIENTS AS FUNCTIONS OF YAW ANGULAR ACCELERATION AND DRIFT ANGLE FOR ASTERN MOTION AT $\eta = 1$ IN DEEP WATER

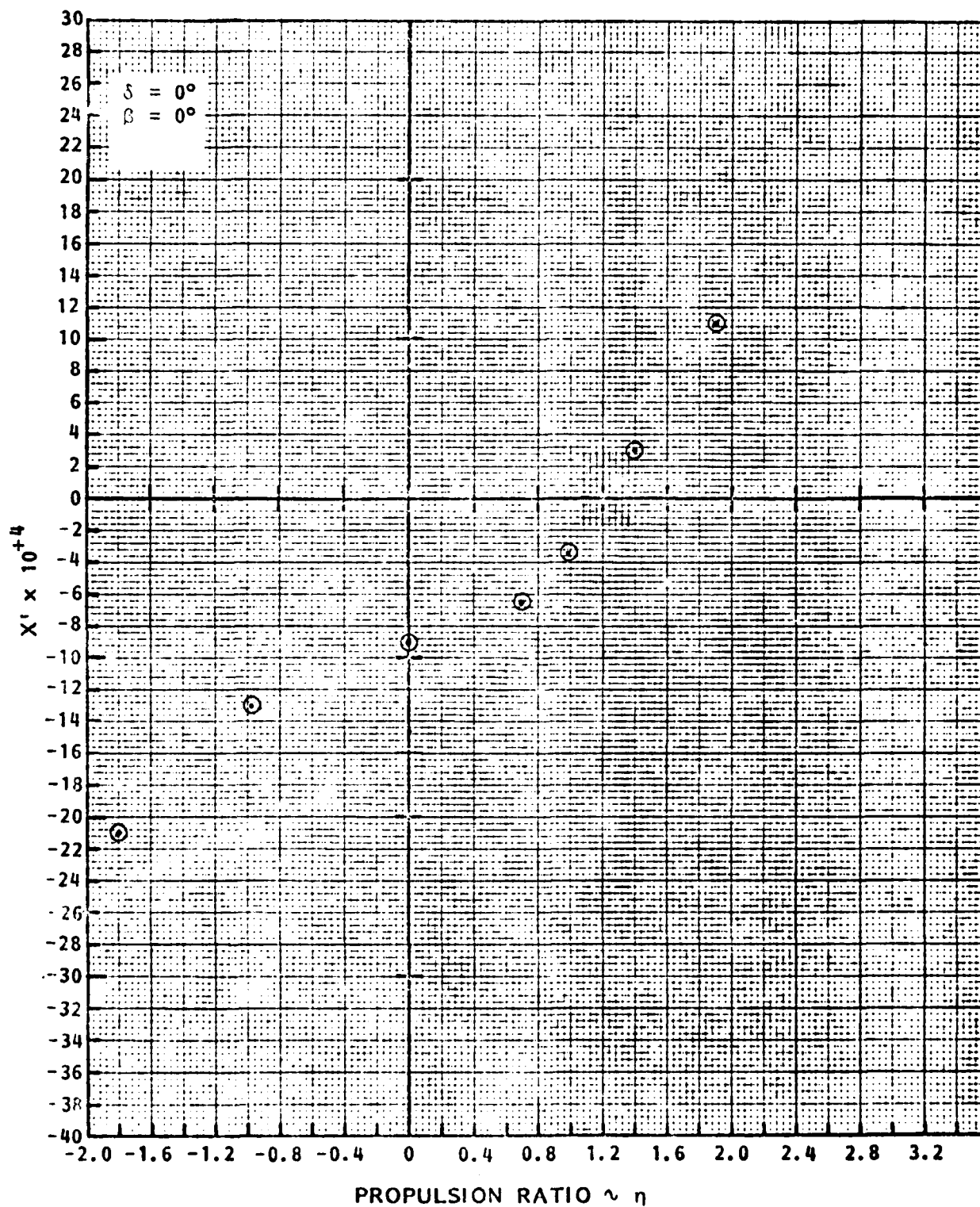


FIGURE A.30 - AXIAL FORCE COEFFICIENT AS FUNCTION OF PROPULSION RATIO η FOR AHEAD MOTION IN SHALLOW WATER, $H/T = 1.50$

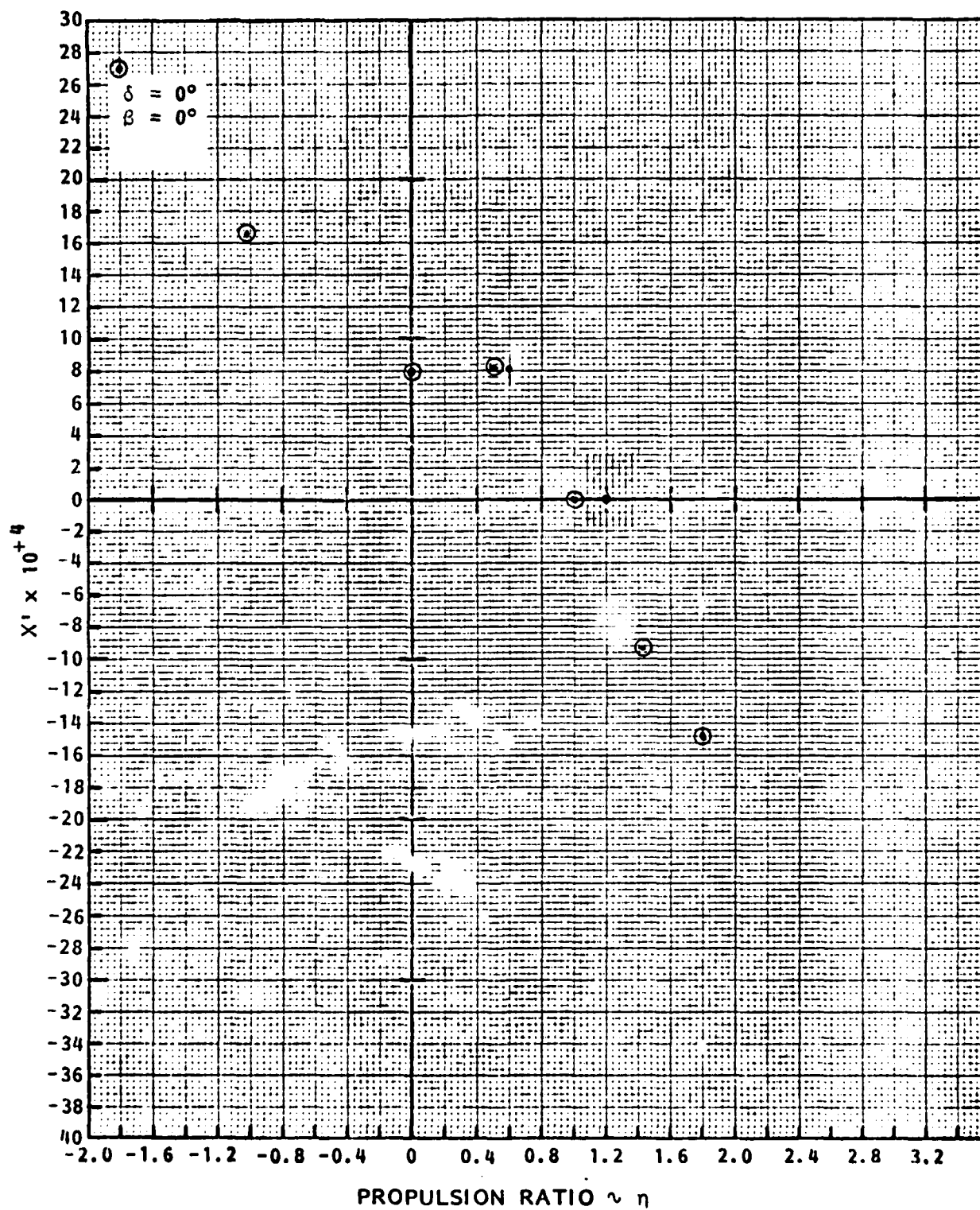


FIGURE A.31 - AXIAL FORCE COEFFICIENT AS FUNCTION OF PROPULSION RATIO η FOR ASTERN MOTION IN SHALLOW WATER, $H/T = 1.50$

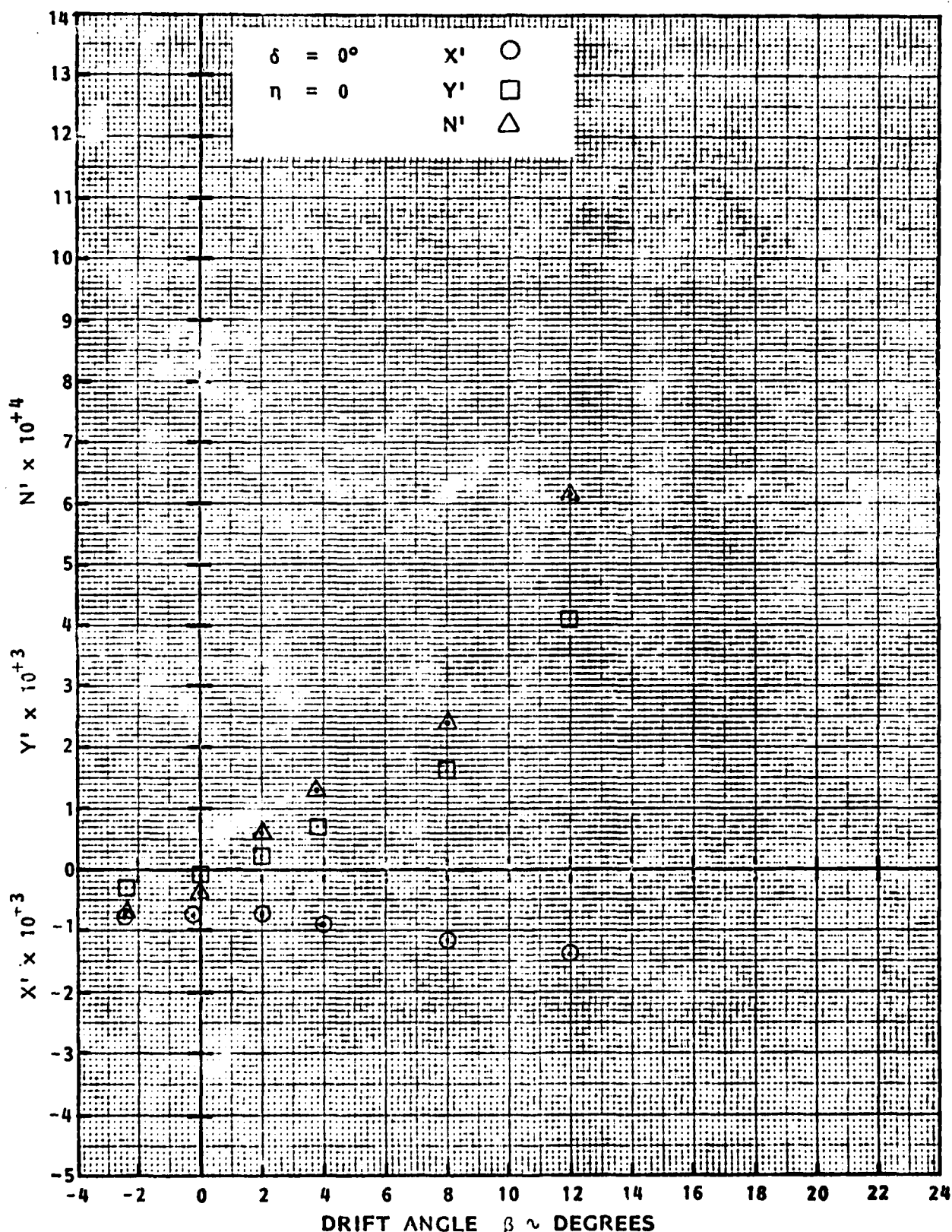


FIGURE A.32 - AXIAL FORCE, LATERAL FORCE, AND YAW MOMENT COEFFICIENTS AS FUNCTIONS OF DRIFT ANGLE β FOR AHEAD MOTION AT $\eta = 0$ IN SHALLOW WATER, $H/T = 1.50$

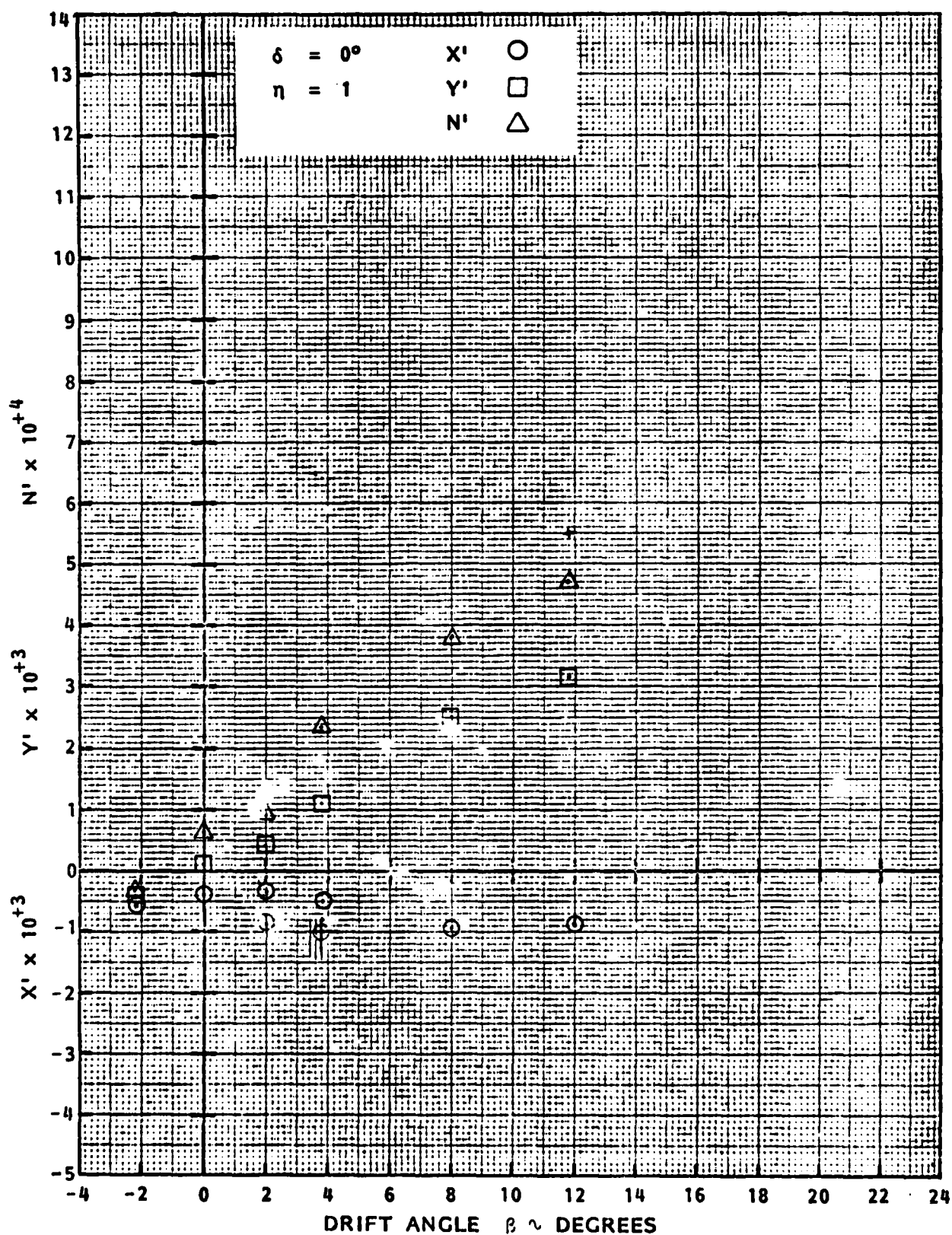


FIGURE A.33 - AXIAL FORCE, LATERAL FORCE, AND YAW MOMENT COEFFICIENTS AS FUNCTIONS OF DRIFT ANGLE β FOR AHEAD MOTION AT $\eta = 1$ IN SHALLOW WATER, $H/T = 1.50$

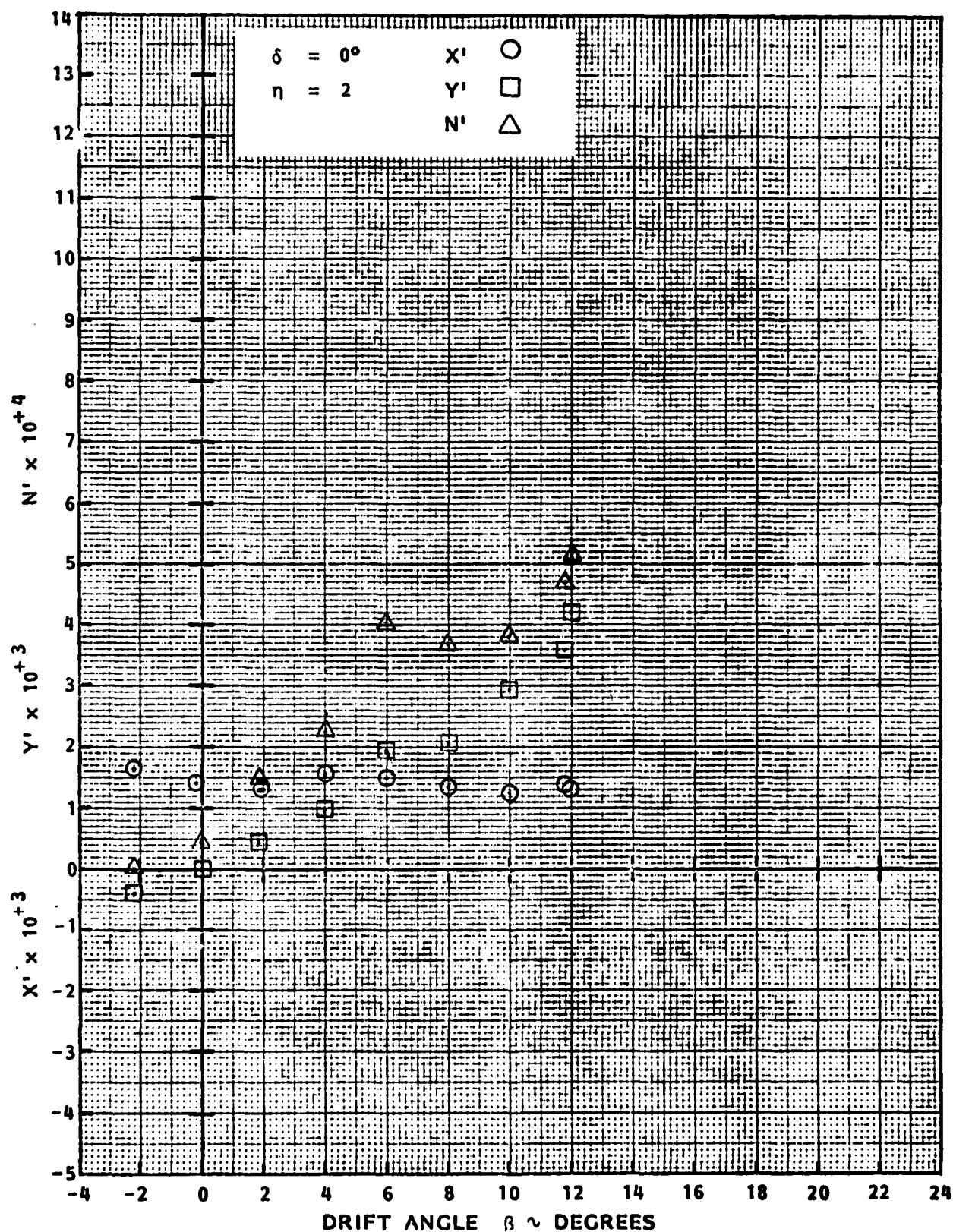


FIGURE A.34 - AXIAL FORCE, LATERAL FORCE, AND YAW MOMENT COEFFICIENTS AS FUNCTIONS OF DRIFT ANGLE β FOR AHEAD MOTION AT $\eta = 2$ IN SHALLOW WATER, $H/T = 1.50$

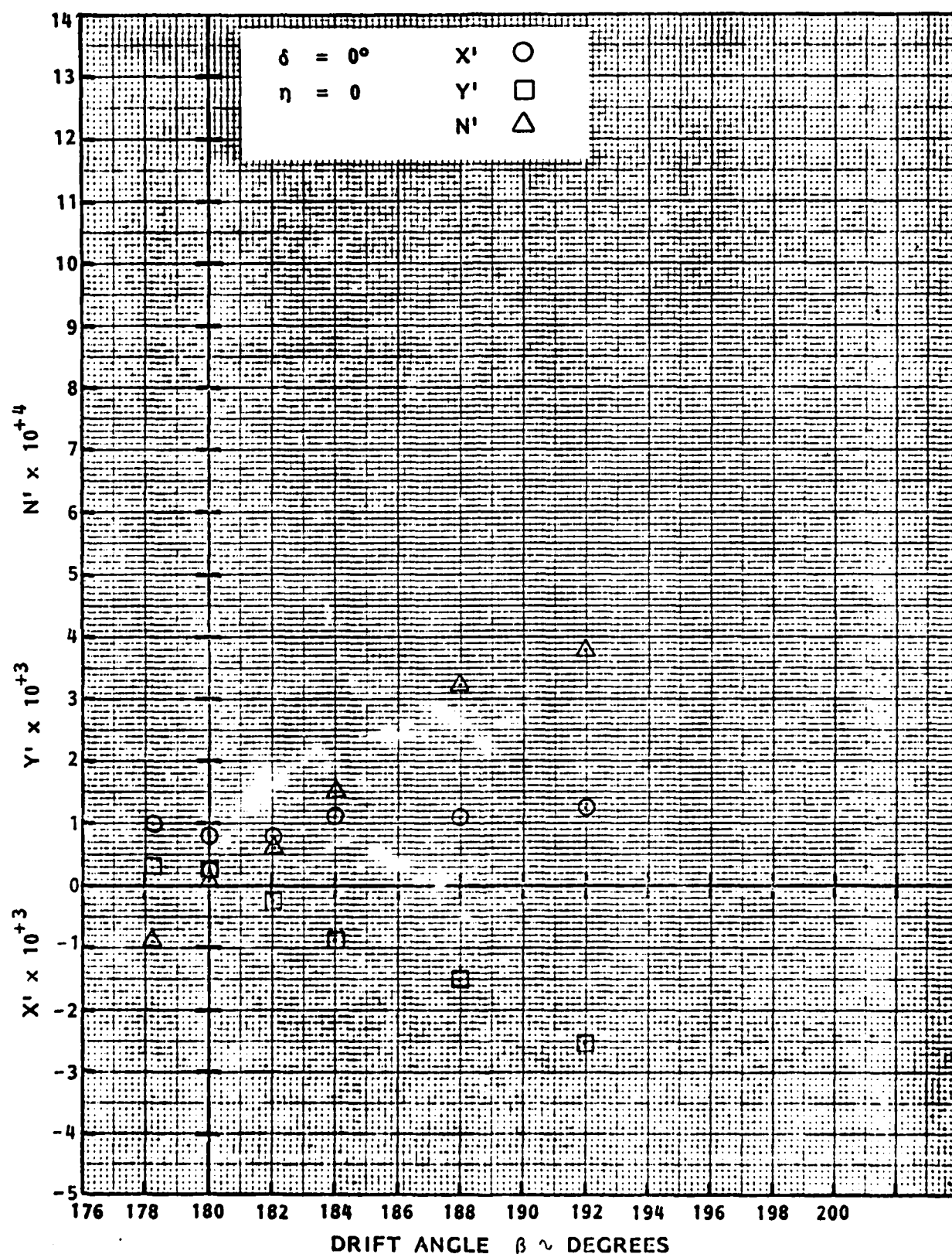


FIGURE A.35 - AXIAL FORCE, LATERAL FORCE, AND YAW MOMENT COEFFICIENTS AS FUNCTIONS OF DRIFT ANGLE β FOR ASTERN MOTION AT $\eta = 0$ IN SHALLOW WATER, $H/T = 1.50$

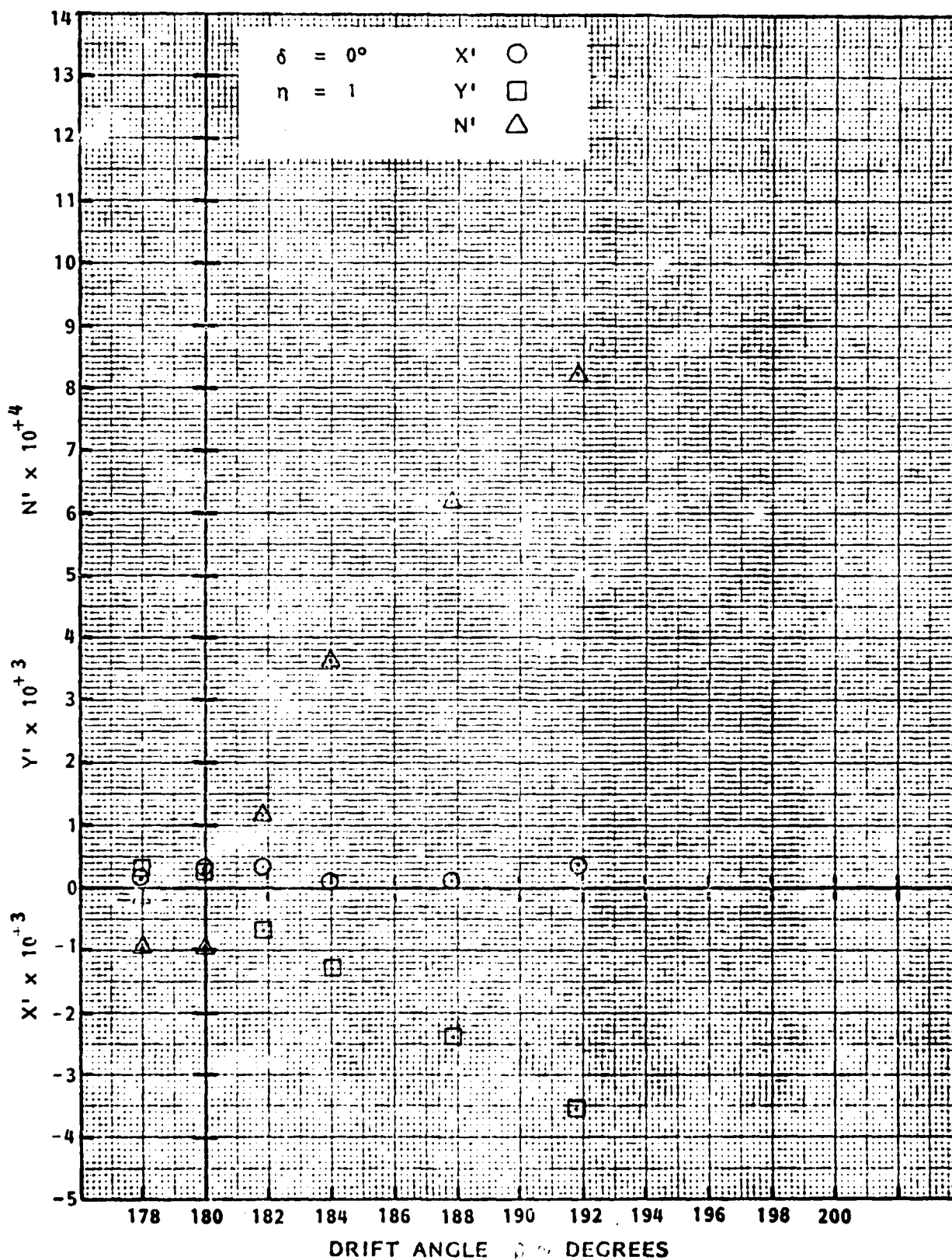


FIGURE A.36 - AXIAL FORCE, LATERAL FORCE, AND YAW MOMENT COEFFICIENTS AS FUNCTIONS OF DRIFT ANGLE δ FOR ASTERN MOTION AT $\eta = 1$ IN SHALLOW WATER, $H/T = 1.50$

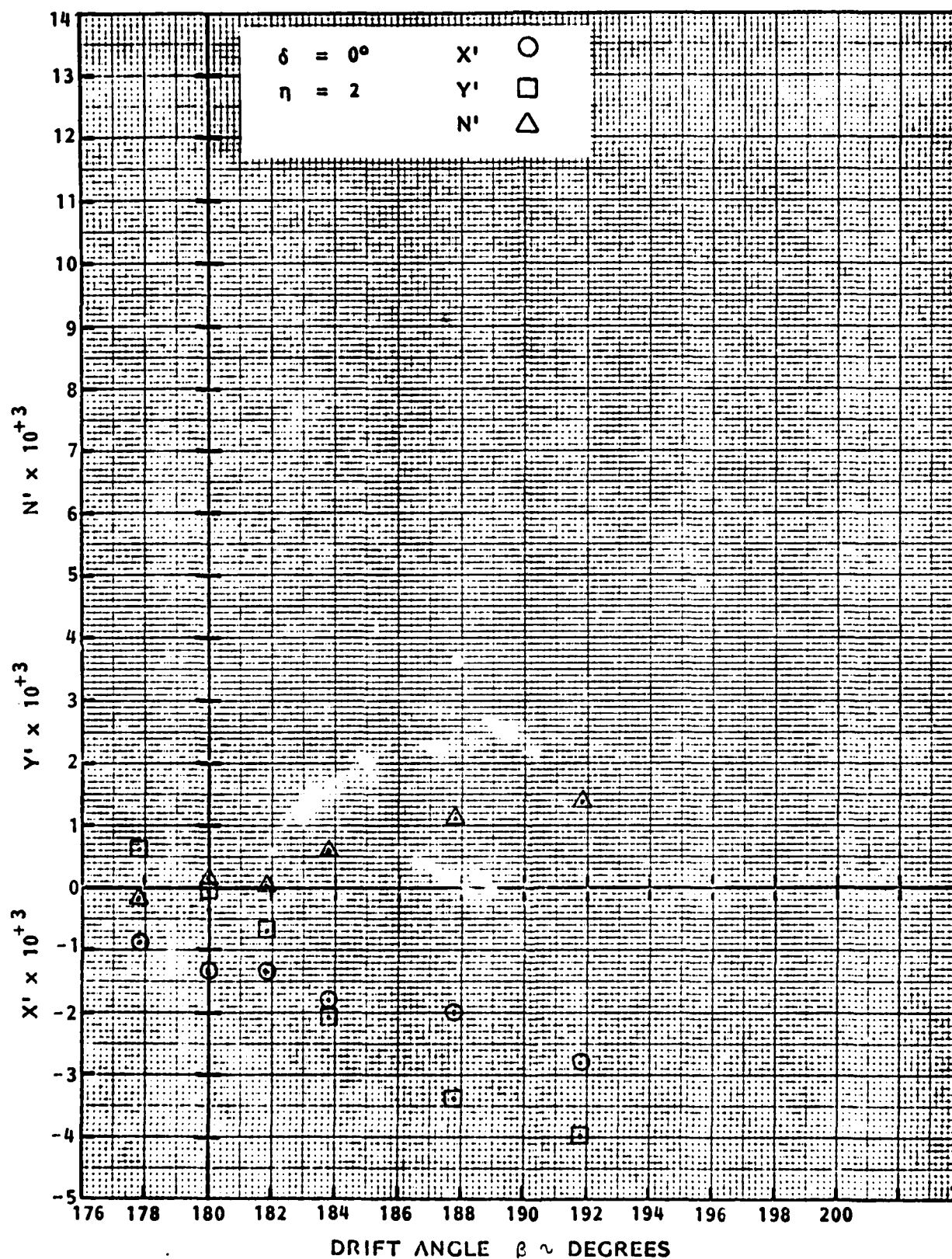


FIGURE A.37 - AXIAL FORCE, LATERAL FORCE, AND YAW MOMENT COEFFICIENTS AS FUNCTIONS OF DRIFT ANGLE β FOR ASTERN MOTION AT $\eta = 2$ IN SHALLOW WATER, $H/T = 1.50$

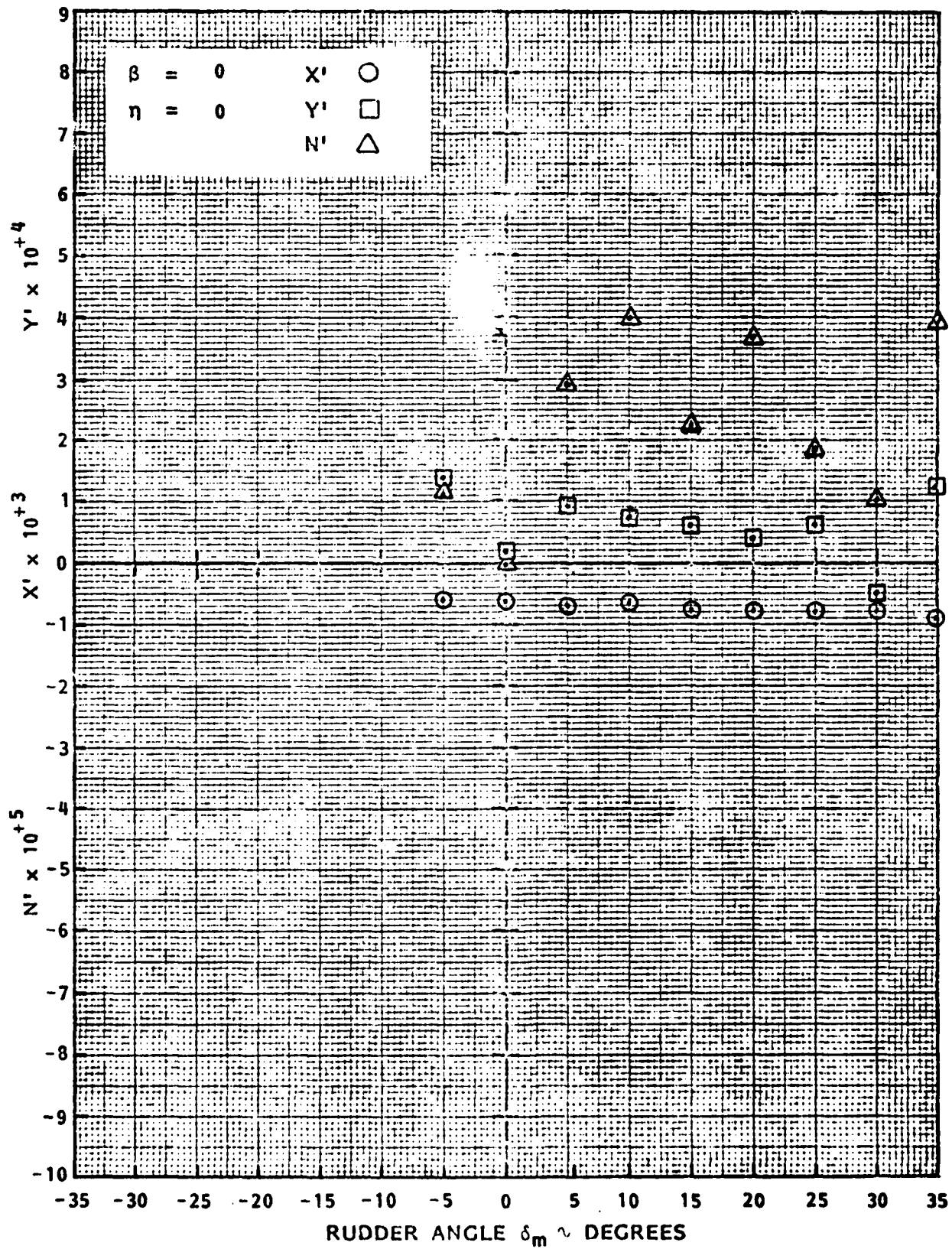


FIGURE A.38 - AXIAL FORCE, LATERAL FORCE AND YAW MOMENT COEFFICIENTS AS FUNCTIONS OF MAIN RUDDER ANGLE δ_m FOR AHEAD MOTION AT $\eta = 0$ IN SHALLOW WATER, $H/T = 1.50$

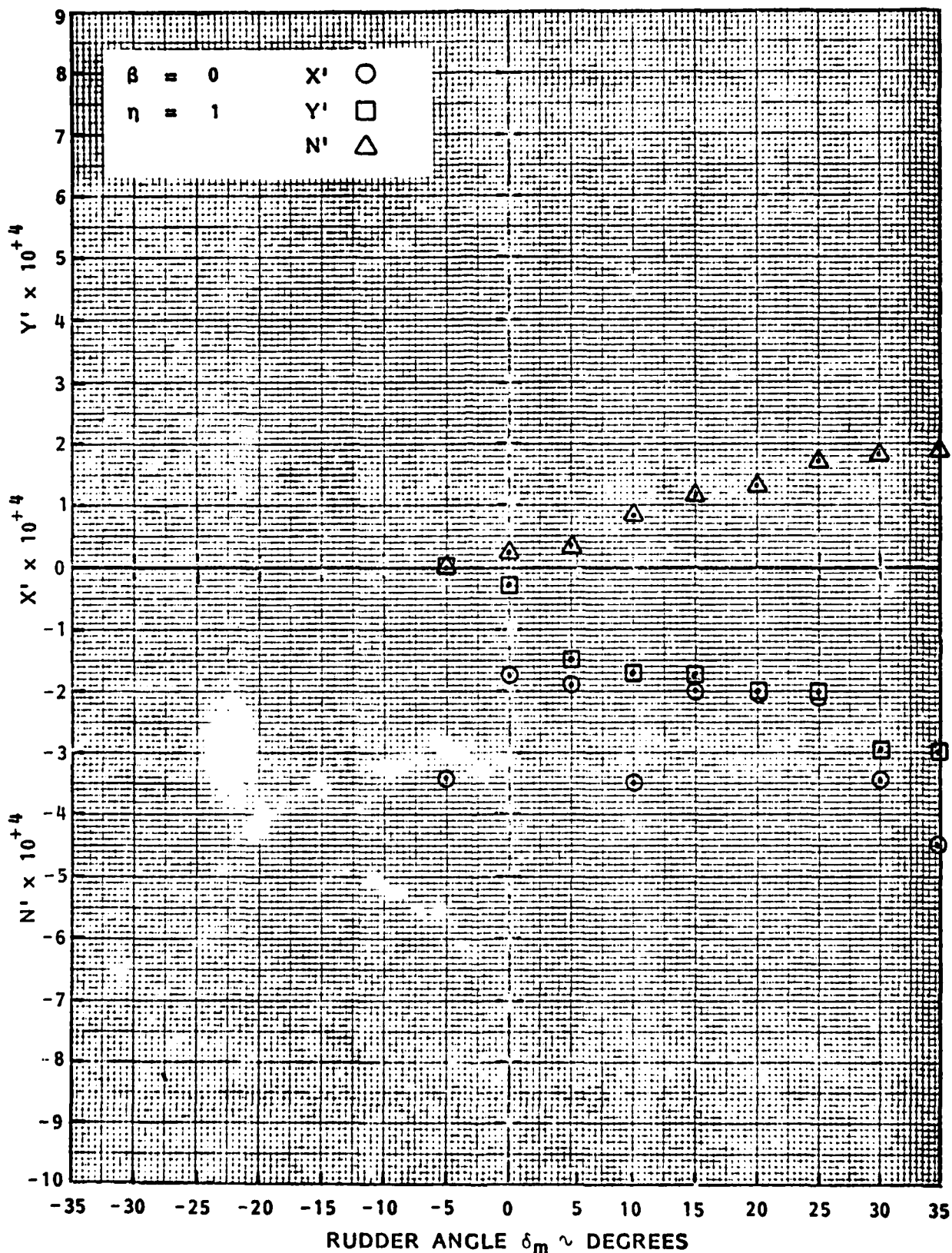


FIGURE A.39 - AXIAL FORCE, LATERAL FORCE AND YAW MOMENT COEFFICIENTS AS FUNCTIONS OF MAIN RUDDER ANGLE δ_m FOR AHEAD MOTION AT $\eta = 1$ IN SHALLOW WATER, $H/T = 1.50$

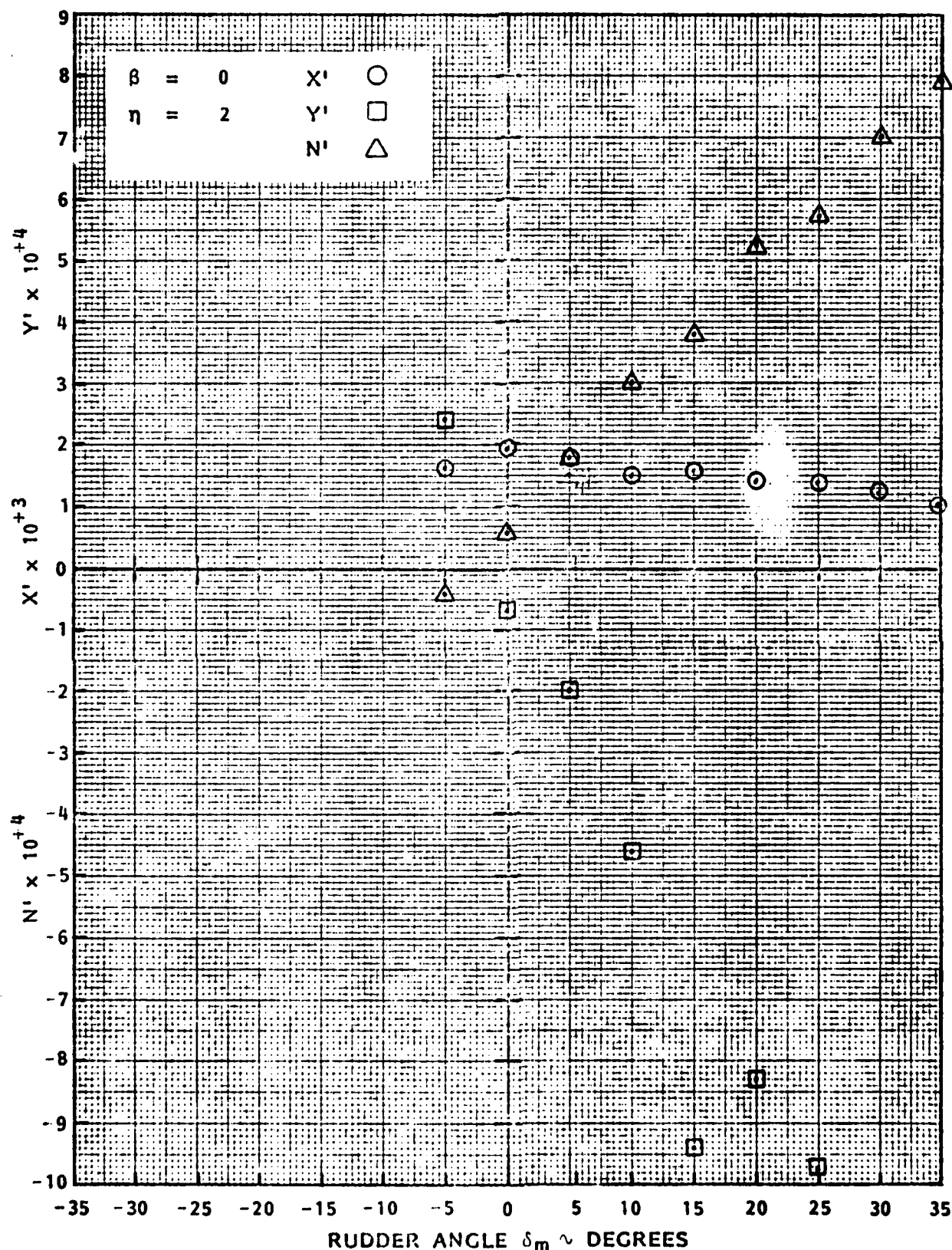


FIGURE A.40 - AXIAL FORCE, LATERAL FORCE AND YAW MOMENT COEFFICIENTS AS FUNCTIONS OF MAIN RUDDER ANGLE δ_m FOR AHEAD MOTION AT $\eta = 2$ IN SHALLOW WATER, $H/T = 1.50$

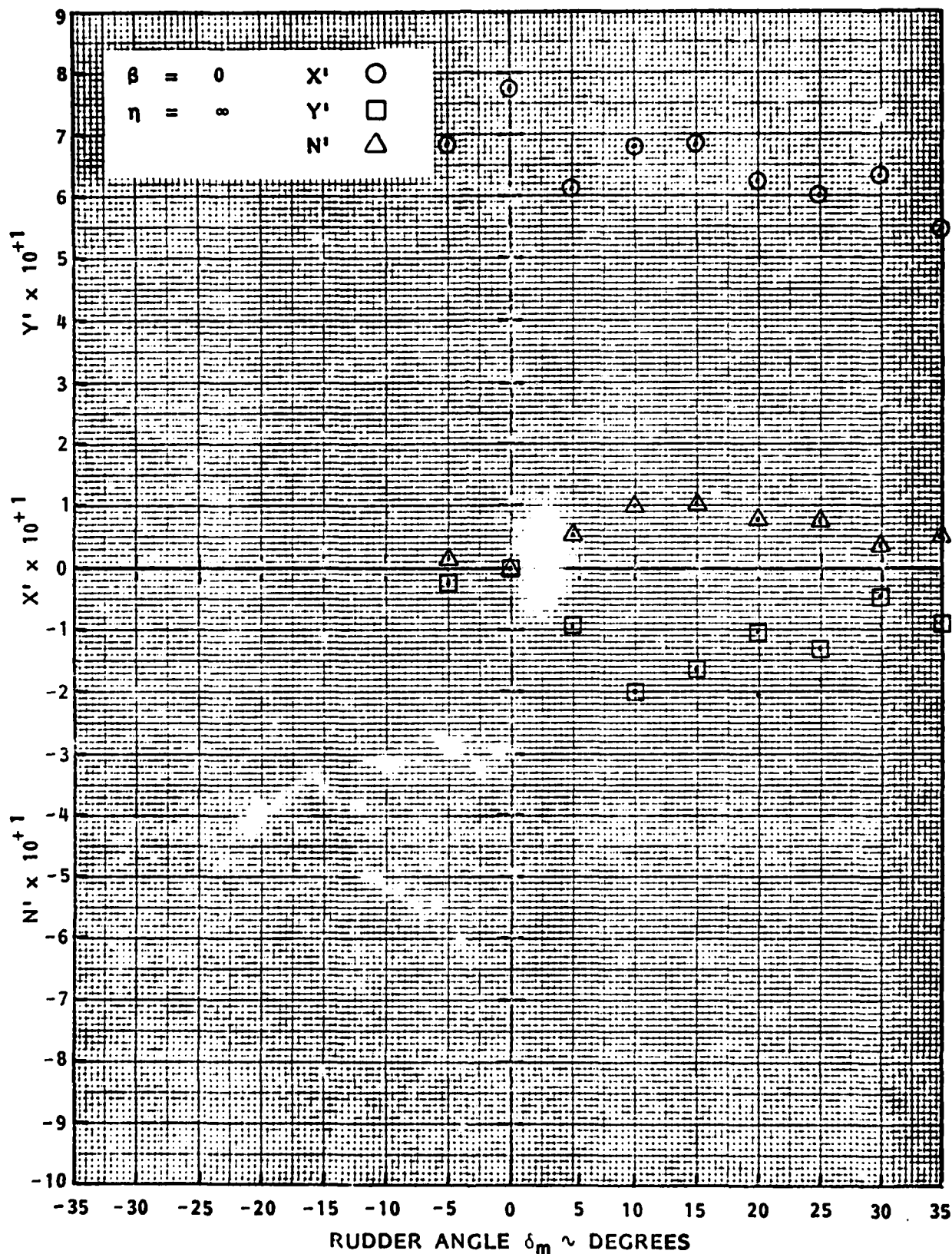


FIGURE A.41 - AXIAL FORCE, LATERAL FORCE AND YAW MOMENT COEFFICIENTS AS FUNCTIONS OF MAIN RUDDER ANGLE δ_m FOR ZERO SPEED AT $\eta = \infty$ (AHEAD THRUST) IN SHALLOW WATER, $H/T = 1.50$

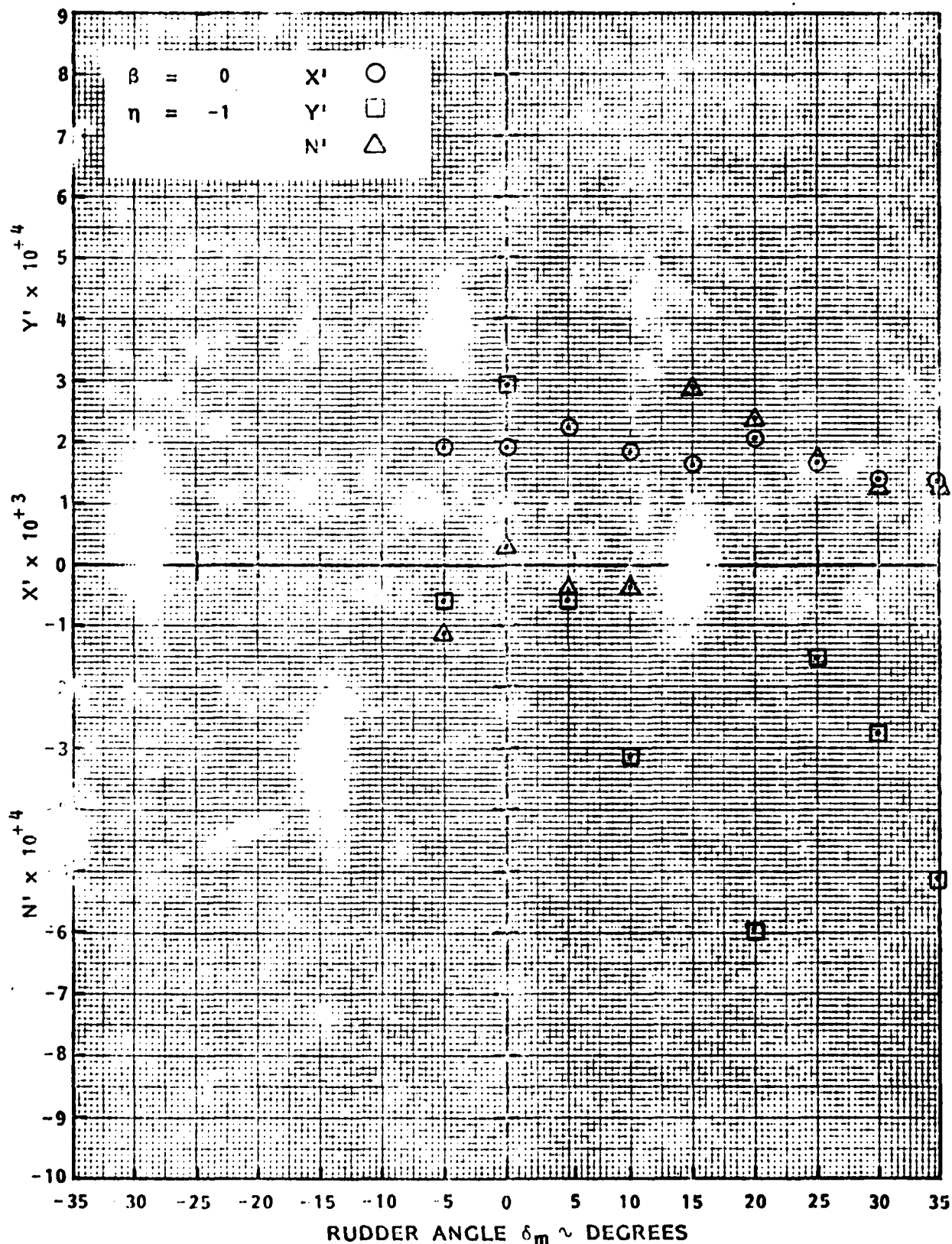


FIGURE A.42 - AXIAL FORCE, LATERAL FORCE AND YAW MOMENT COEFFICIENTS AS FUNCTIONS OF MAIN RUDDER ANGLE δ_m FOR ASTERN MOTION AT $\eta = -1$ IN SHALLOW WATER, $H/T = 1.50$

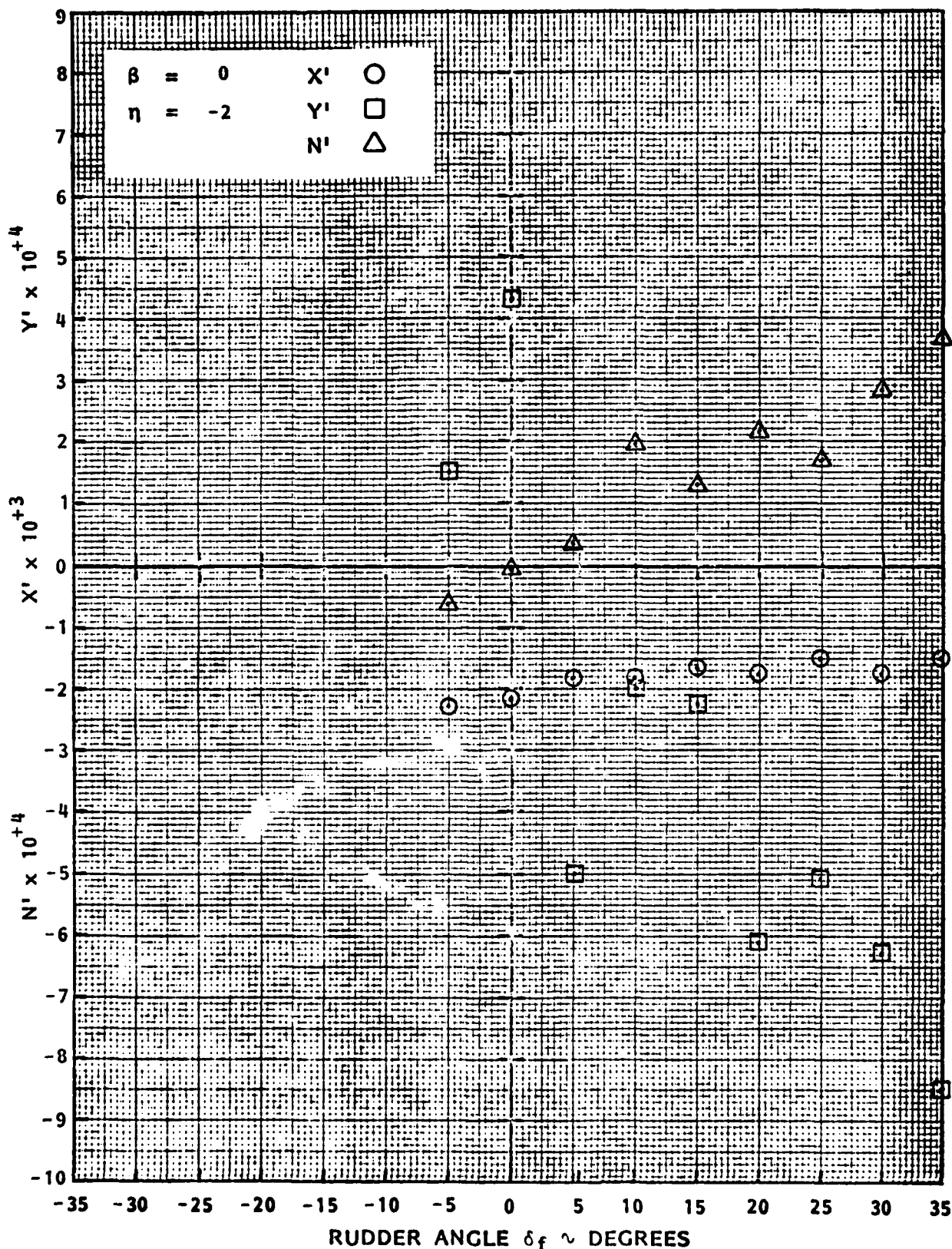


FIGURE A.43 - AXIAL FORCE, LATERAL FORCE AND YAW MOMENT COEFFICIENTS AS FUNCTIONS OF FLANKING RUDDER ANGLE δ_f FOR AHEAD MOTION AT $\eta = -2$ IN SHALLOW WATER, $H/T = 1.50$

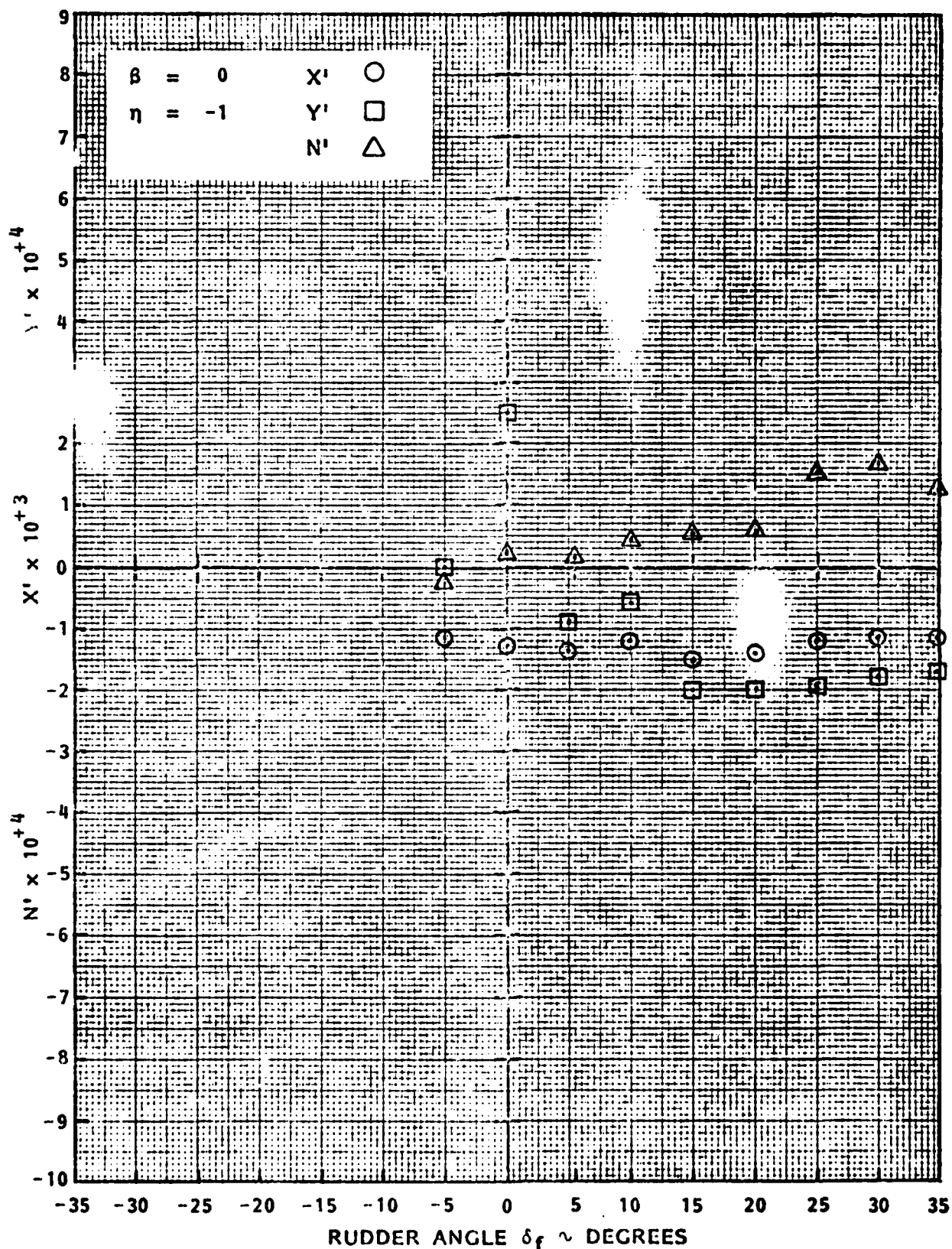


FIGURE A.44 - AXIAL FORCE, LATERAL FORCE AND YAW MOMENT COEFFICIENTS AS FUNCTIONS OF FLANKING RUDDER ANGLE δ_f FOR AHEAD MOTION AT $\eta = -1$ IN SHALLOW WATER, $H/T = 1.50$

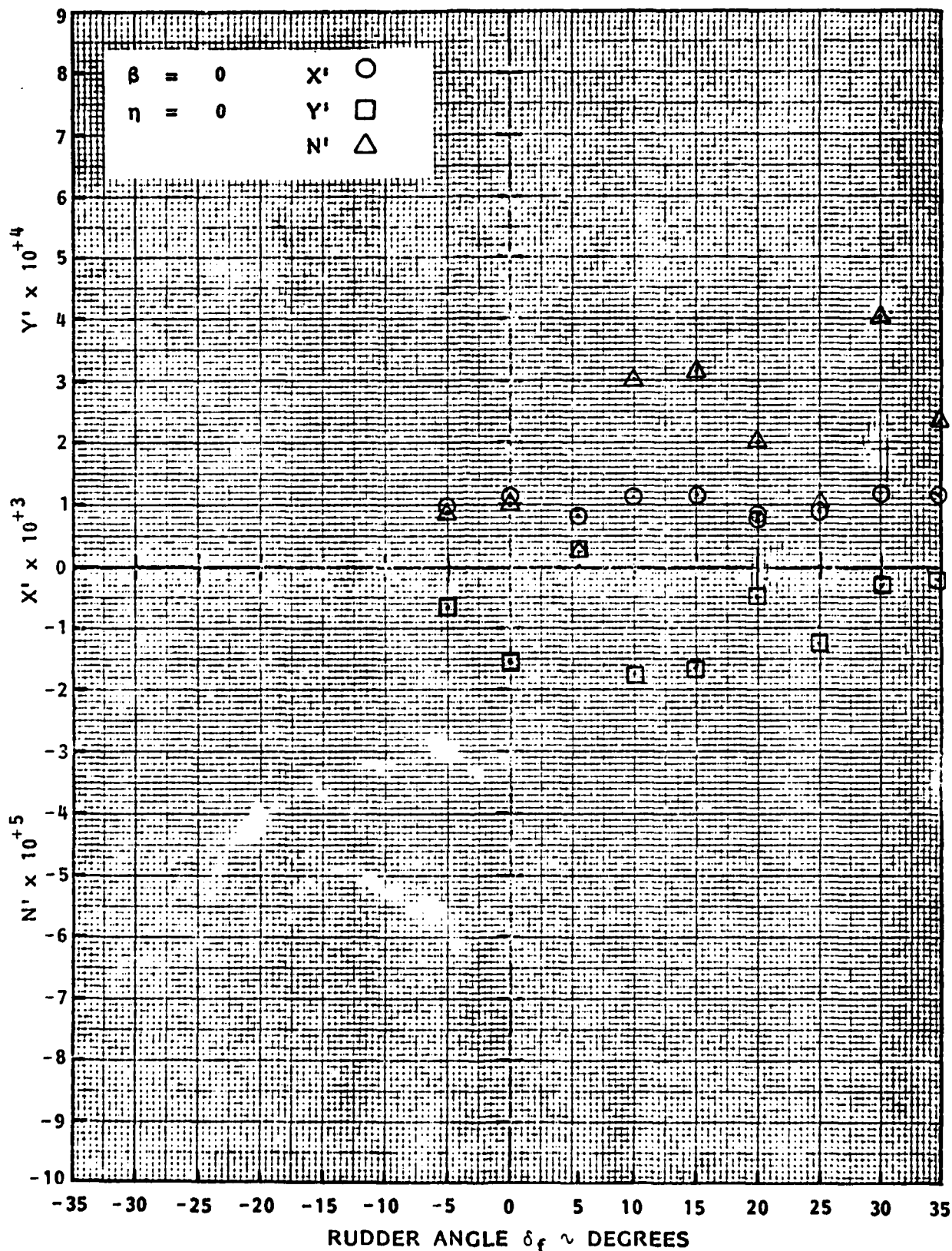


FIGURE A.45 - AXIAL FORCE, LATERAL FORCE AND YAW MOMENT COEFFICIENTS AS FUNCTIONS OF FLANKING RUDDER ANGLE δ_f FOR ASTERN MOTION AT $\eta = 0$ IN SHALLOW WATER, $H/T = 1.50$

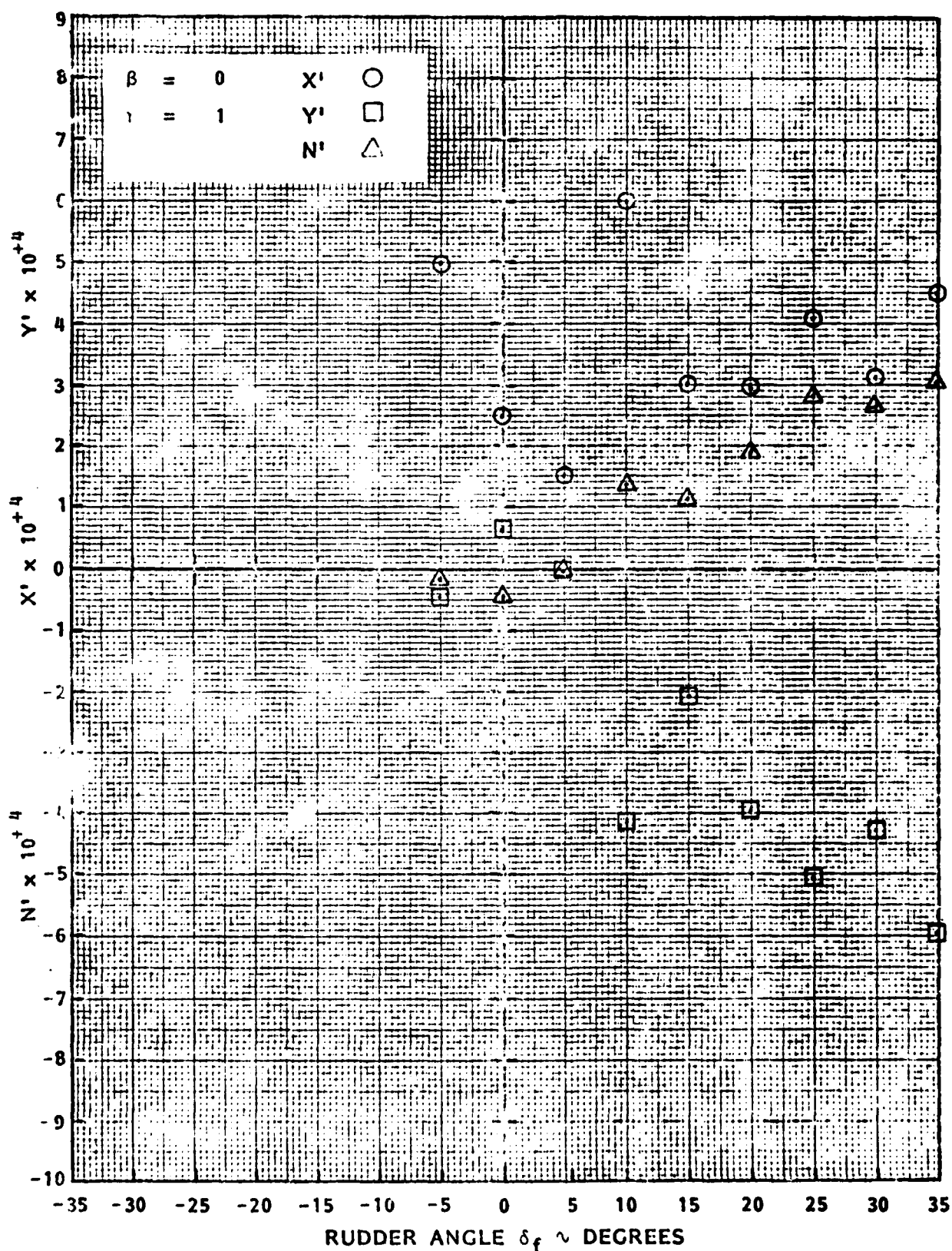


FIGURE A.46 - AXIAL FORCE, LATERAL FORCE AND YAW MOMENT COEFFICIENTS AS FUNCTIONS OF FLANKING RUDDER ANGLE δ_f FOR ASTERN MOTION AT $\eta = 1$

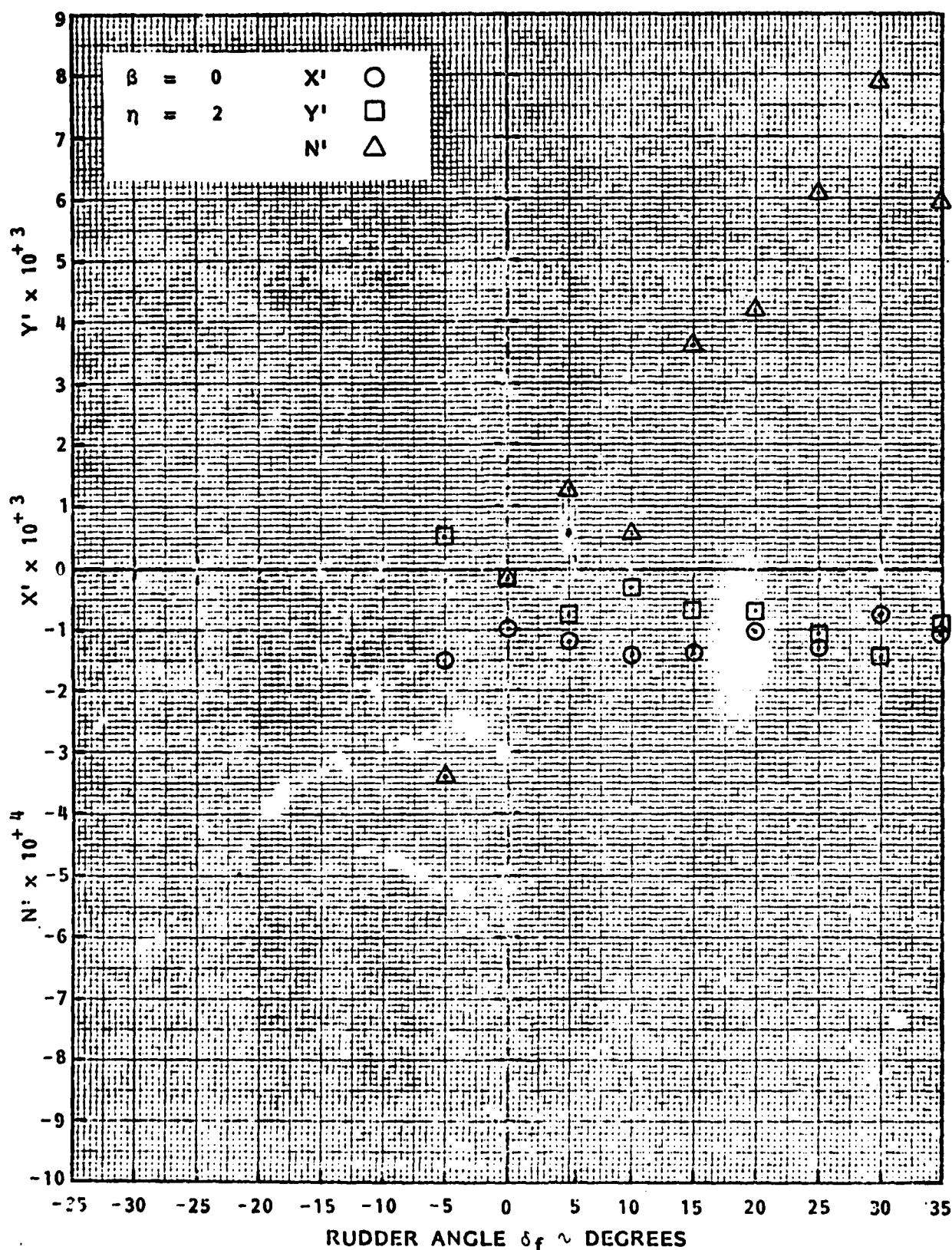


FIGURE A.47 - AXIAL FORCE, LATERAL FORCE AND YAW MOMENT COEFFICIENTS AS FUNCTIONS OF FLANKING RUDDER ANGLE δ_f FOR ASTERN MOTION AT $\eta = 2$ IN SHALLOW WATER $H/T = 1.50$

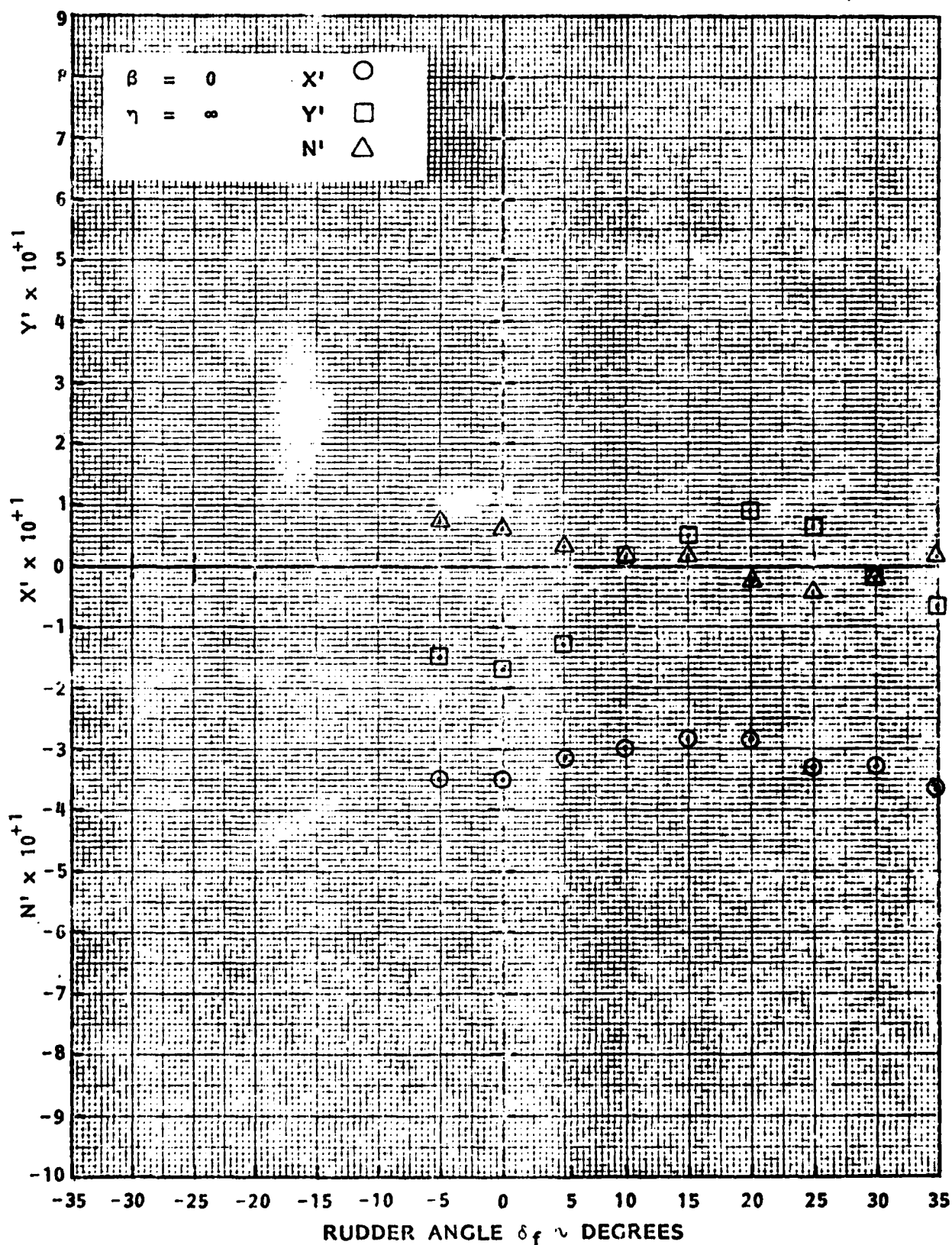


FIGURE A.48 - AXIAL FORCE, LATERAL FORCE AND YAW MOMENT COEFFICIENTS AS FUNCTIONS OF FLANKING RUDDER ANGLE δ_f FOR ZERO SPEED AT $\eta = \infty$ (ASTERN THRUST) IN SHALLOW WATER, $H/T = 1.50$

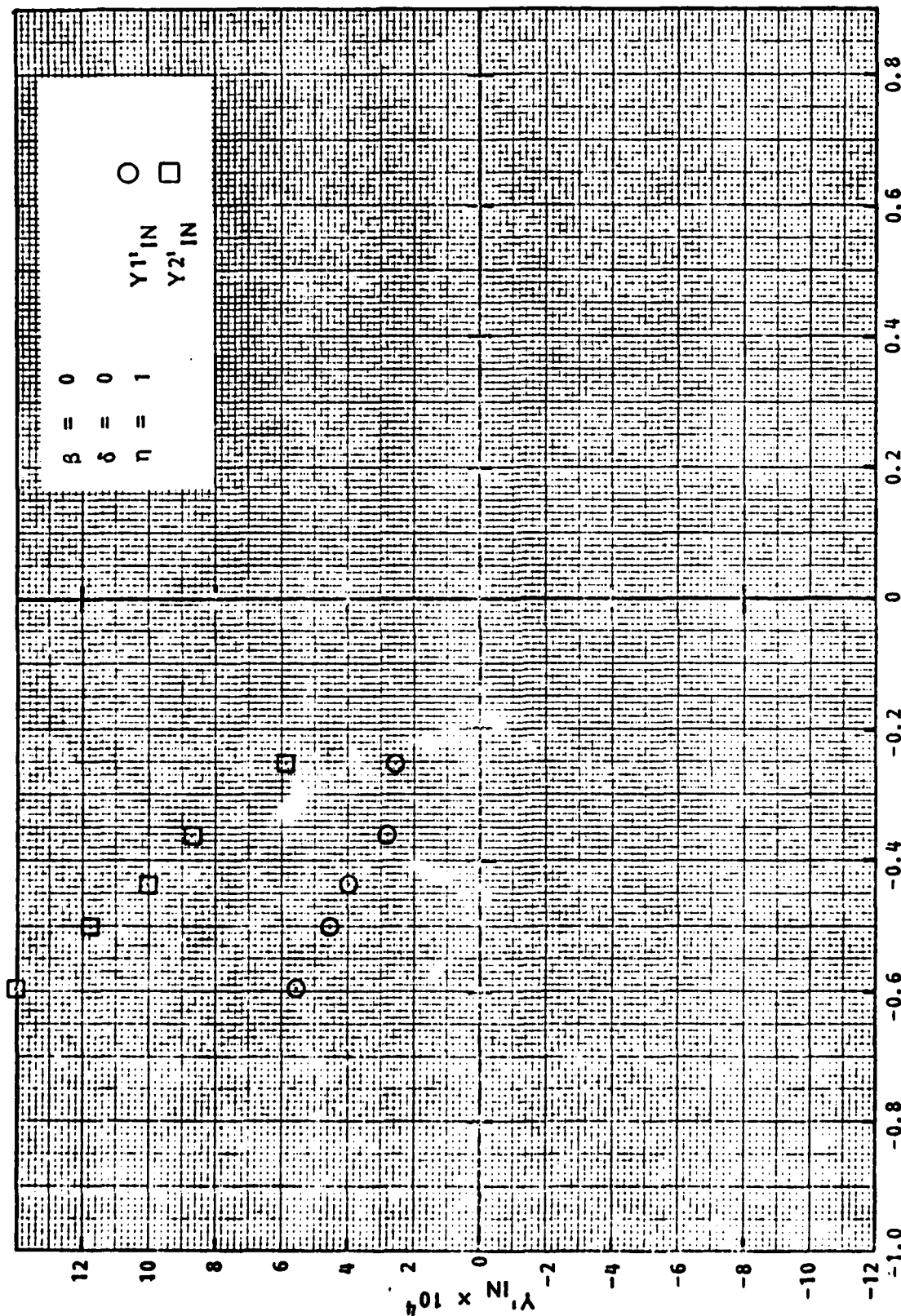


FIGURE A.49 - LATERAL FORCE GAGE IN-PHASE COEFFICIENTS
AS FUNCTIONS OF SWAY ACCELERATION FOR
AHEAD MOTION AT $\eta = 1$ IN SHALLOW WATER,
 $H/T = 1.50$

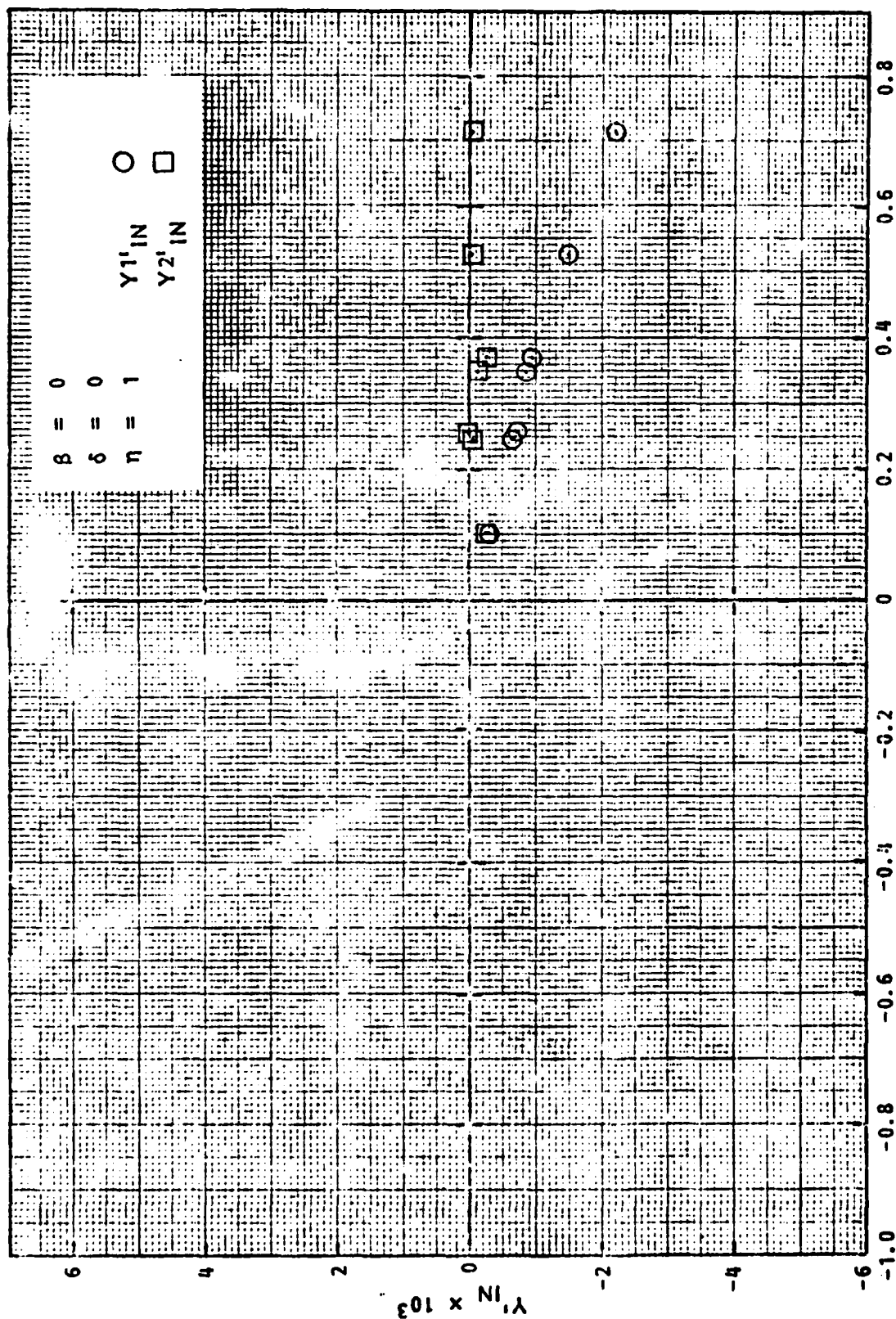


FIGURE A.50 - LATERAL FORCE GAGE IN-PHASE COEFFICIENTS AS FUNCTIONS OF SWAY ACCELERATION FOR ASTERN MOTION AT $\eta = 1$ IN SHALLOW WATER, $H/T = 1.50$

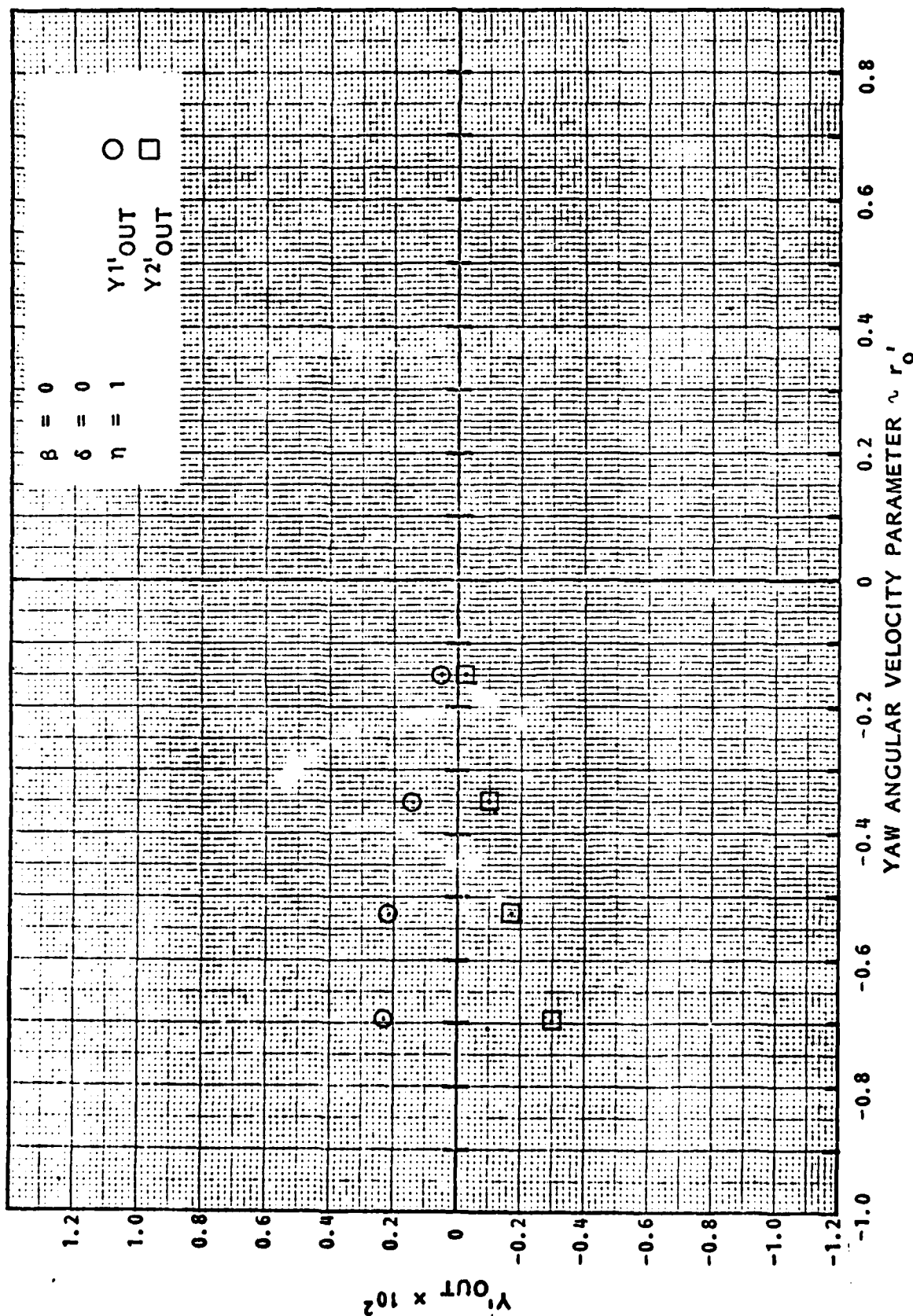


FIGURE A.51 - LATERAL FORCE GAGE OUT-OF-PHASE COEFFICIENTS
AS FUNCTIONS OF YAW ANGULAR VELOCITY FOR
AHEAD MOTION AT $\eta = 1$ IN SHALLOW WATER,
 $H/T = 1.50$

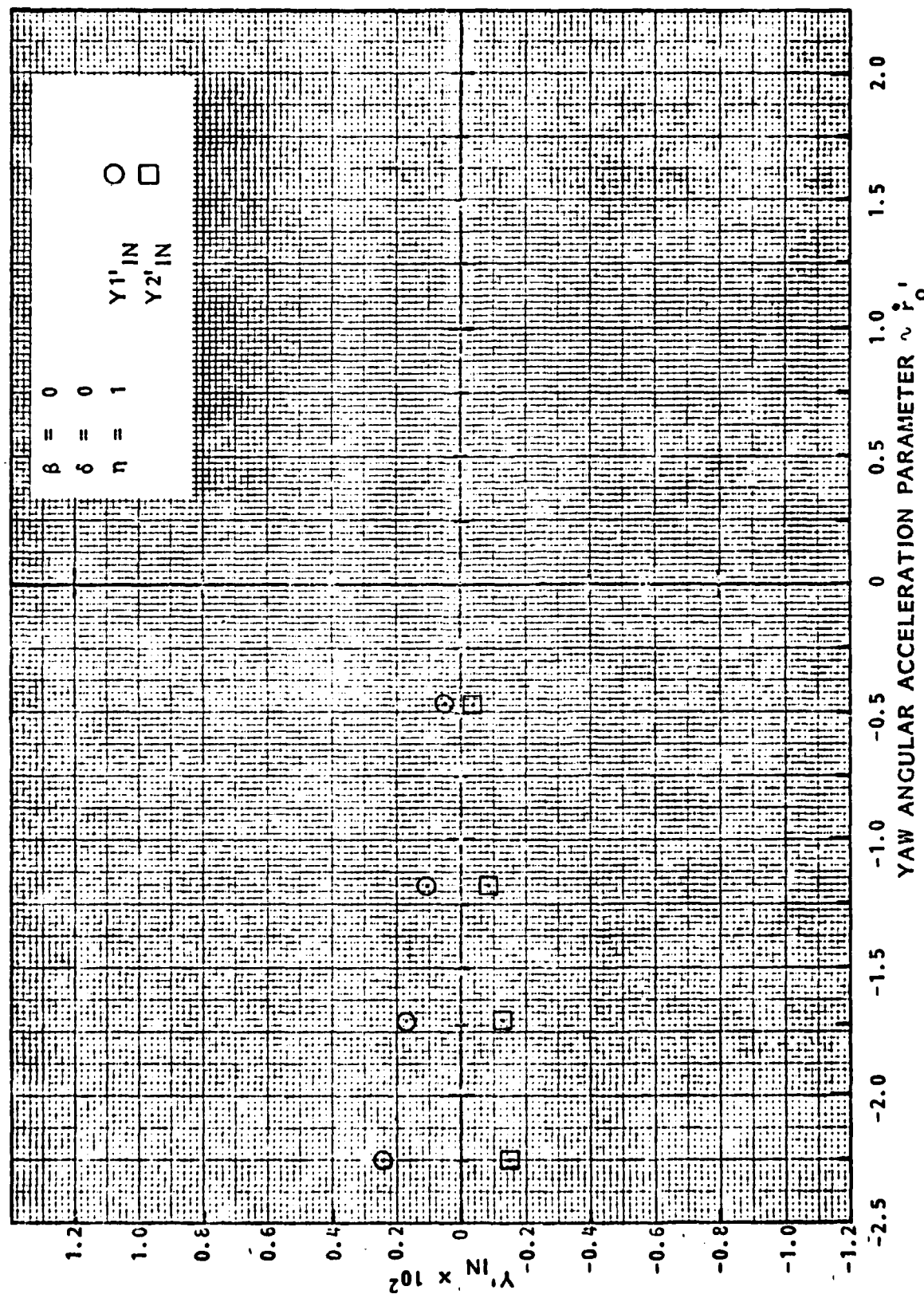
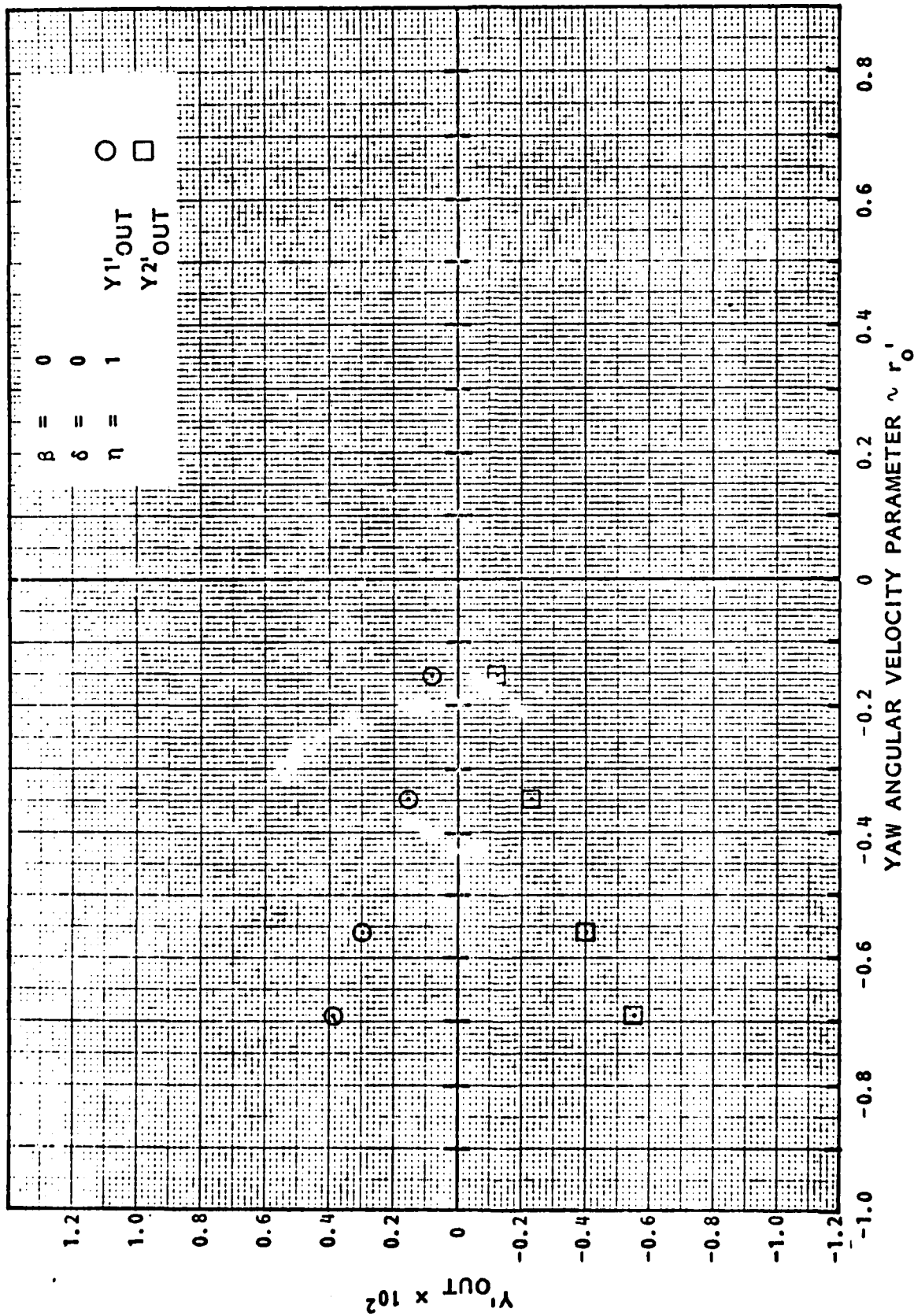


FIGURE A.52 - LATERAL FORCE GAGE IN-PHASE COEFFICIENTS AS FUNCTIONS OF YAW ANGULAR ACCELERATION FOR AHEAD MOTION AT $\eta = 1$ IN SHALLOW WATER, $H/T = 1.50$



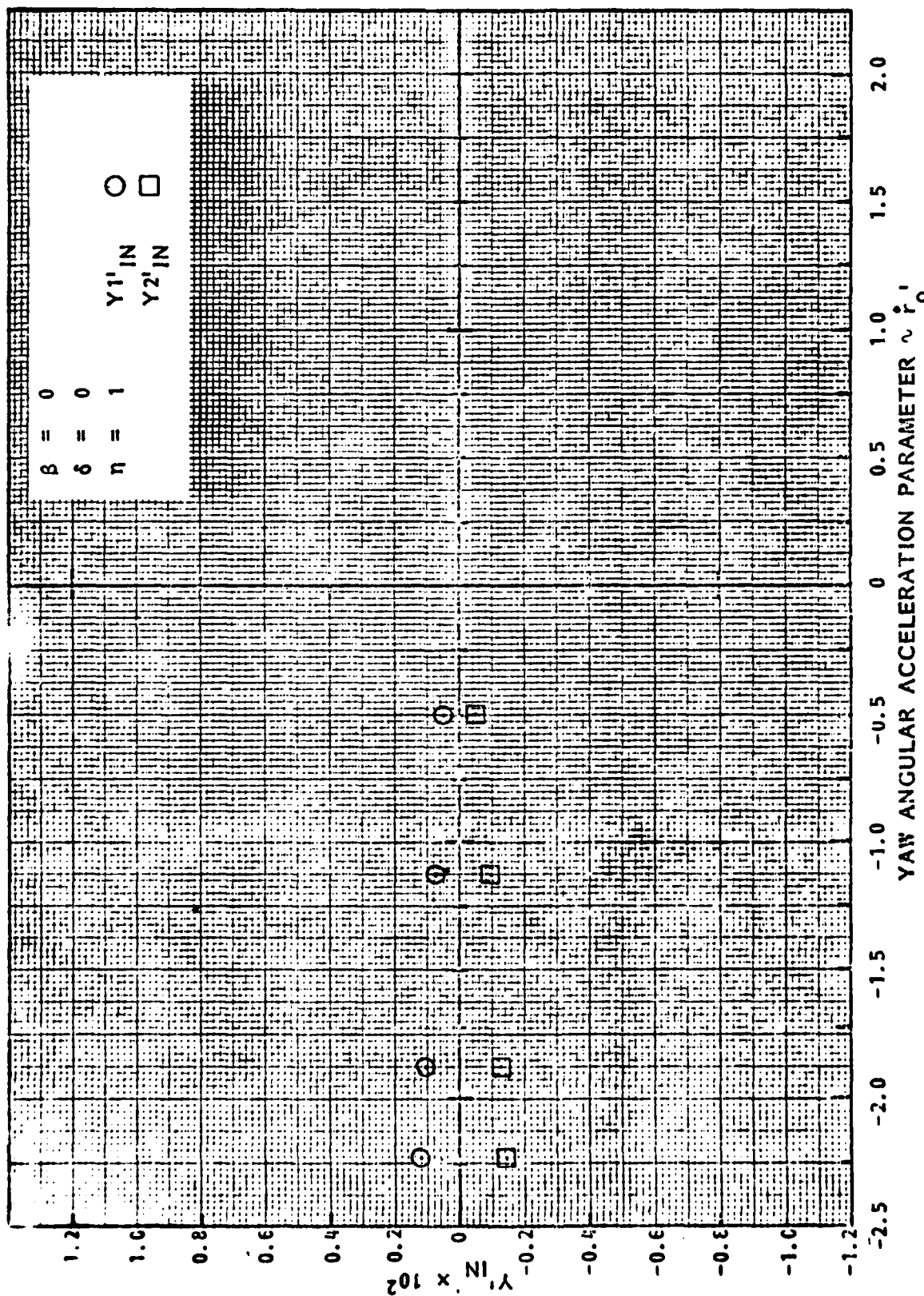


FIGURE A.54 - LATERAL FORCE GAGE IN-PHASE COEFFICIENTS
AS FUNCTIONS OF YAW ANGULAR ACCELERATION FOR
ASTERION MOTION AT $\eta = 1$ IN SHALLOW WATER,
 $H/T = 1.50$

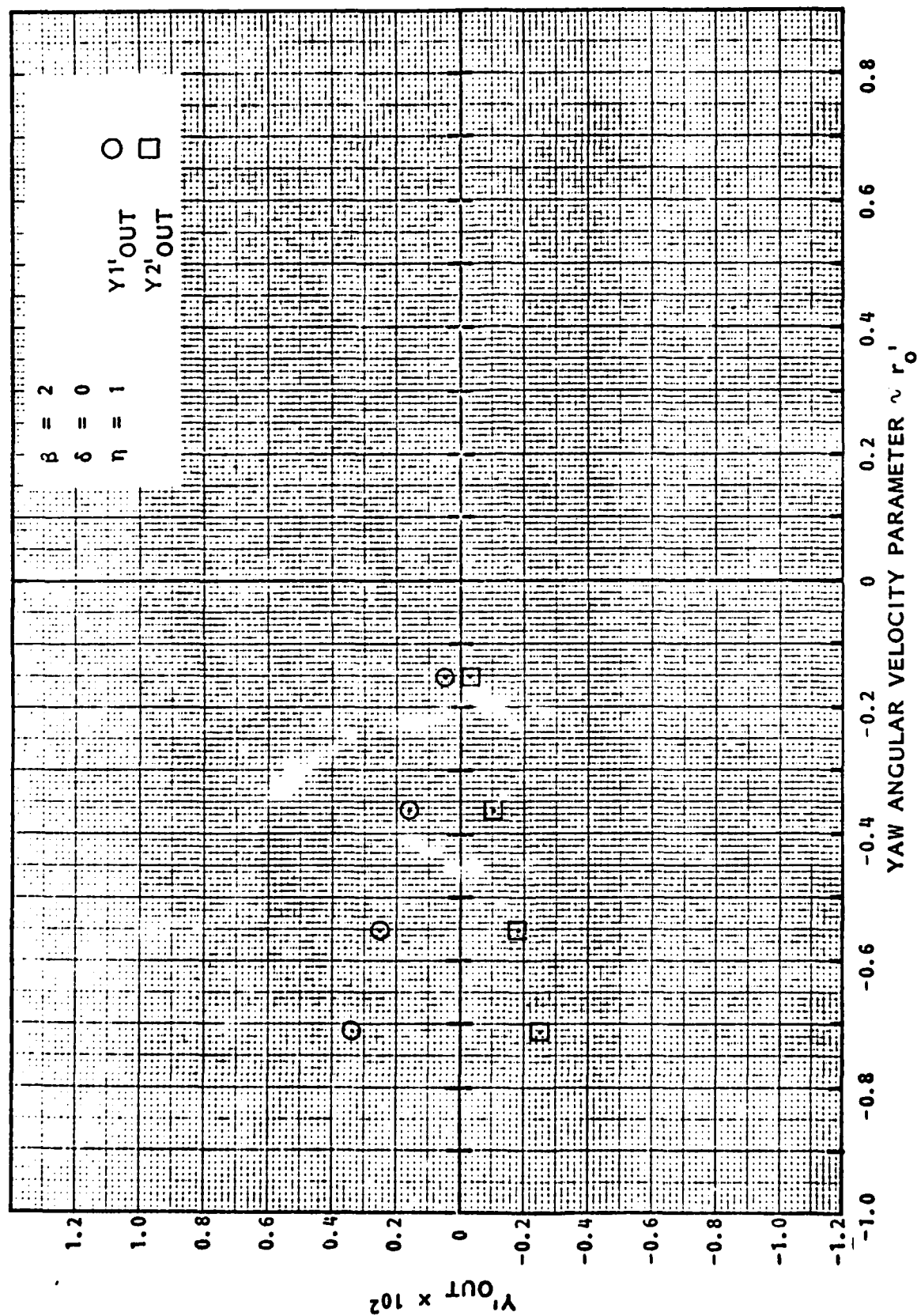


FIGURE A.55 - LATERAL FORCE GAGE OUT-OF-PHASE COEFFICIENTS
AS FUNCTIONS OF YAW ANGULAR VELOCITY AT DRIFT
ANGLE $\beta = 2$ DEGREES FOR AHEAD MOTION AT $\eta = 1$
IN SHALLOW WATER, $H/T = 1.50$

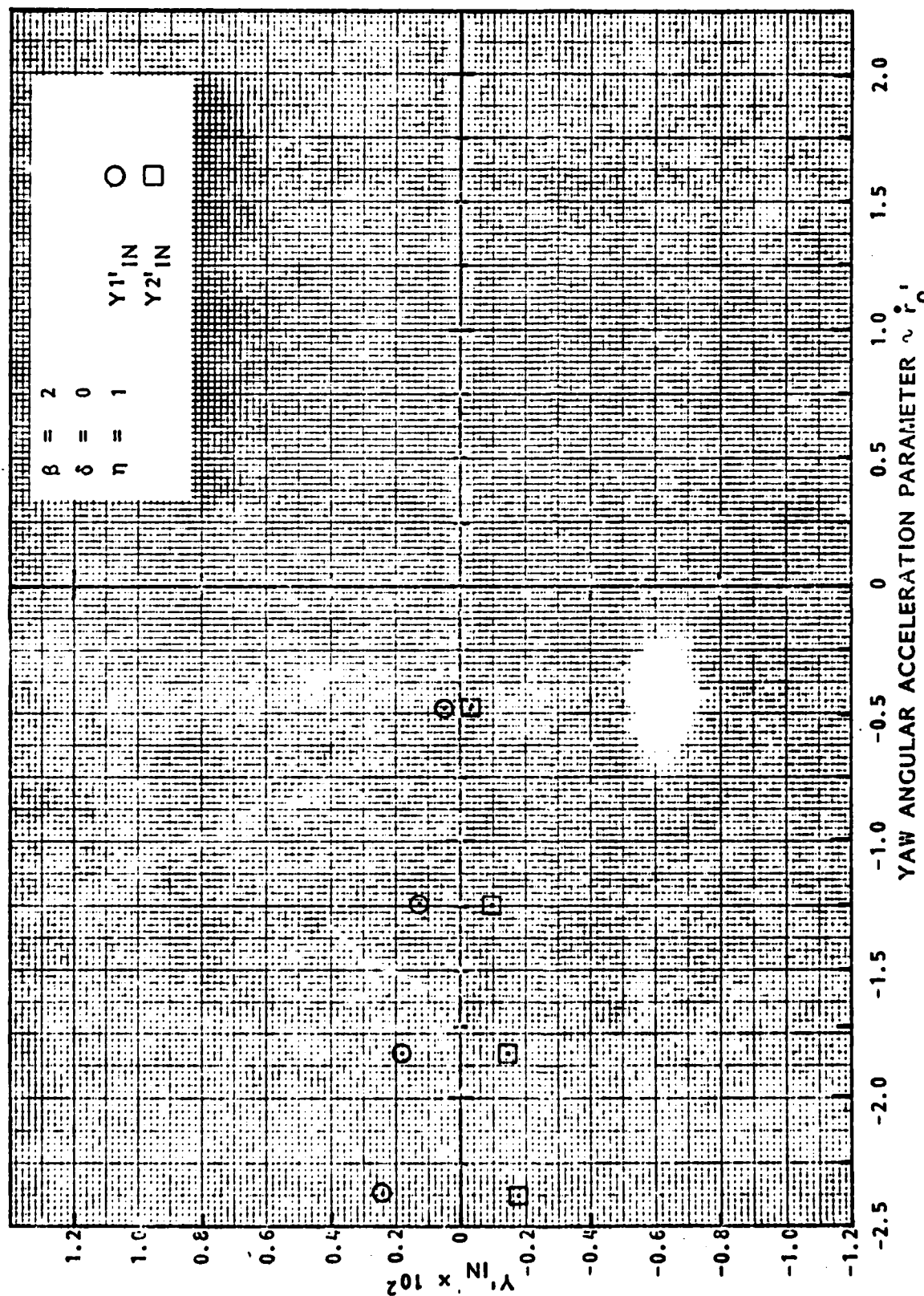


FIGURE A.56 - LATERAL FORCE GAGE IN-PHASE COEFFICIENTS AS FUNCTIONS OF YAW ANGULAR ACCELERATION AT DRIFT ANGLE $\beta = 2$ DEGREES FOR AHEAD MOTION AT $\eta = 1$ IN SHALLOW WATER, $H/T = 1.50$

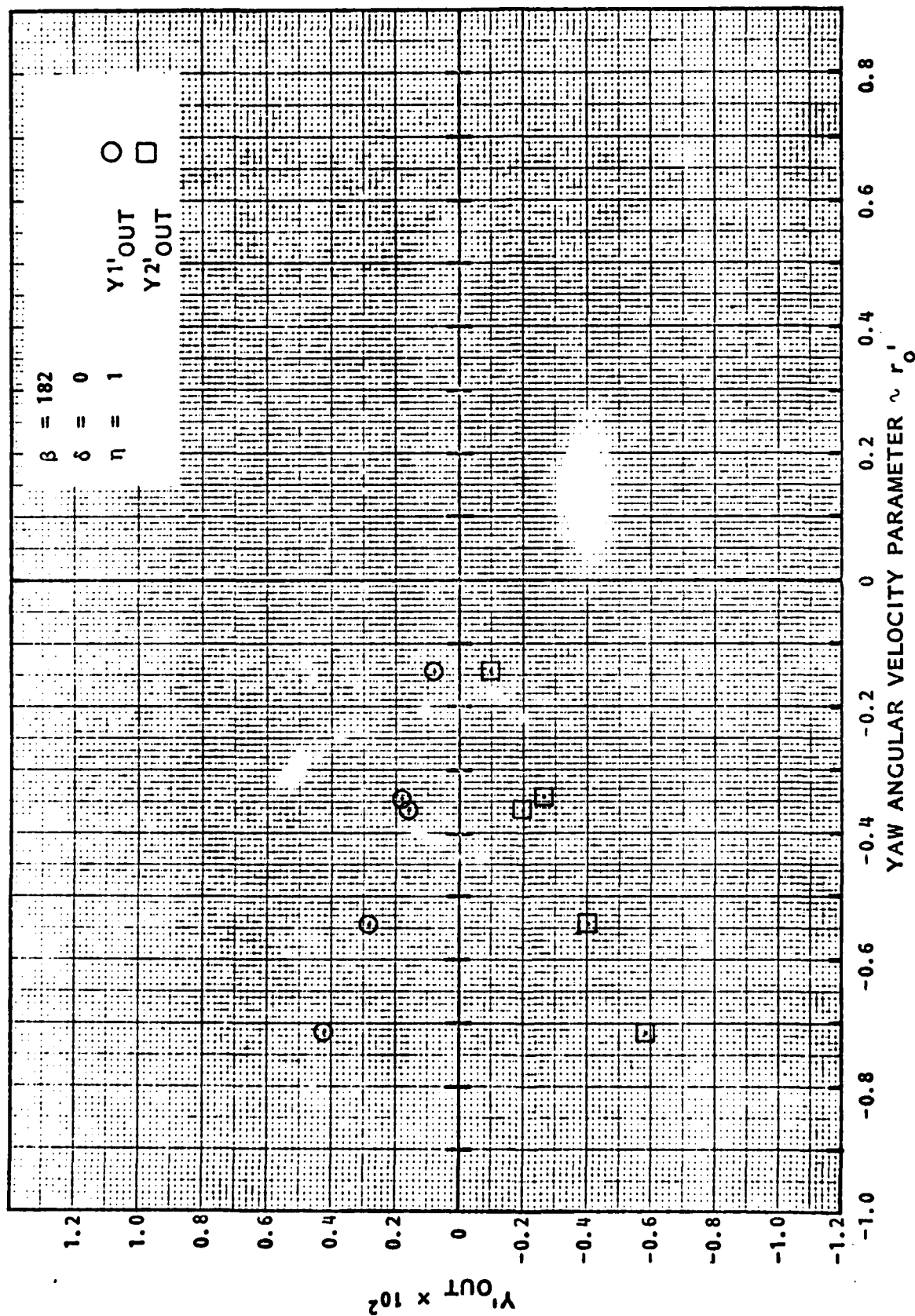


FIGURE A.57 - LATERAL FORCE GAGE OUT-OF-PHASE COEFFICIENTS AS FUNCTIONS OF YAW ANGULAR VELOCITY AT DRIFT ANGLE $\beta = 182$ DEGREES FOR ASTERN MOTION AT $\eta = 1$ IN SHALLOW WATER, $H/T = 1.50$

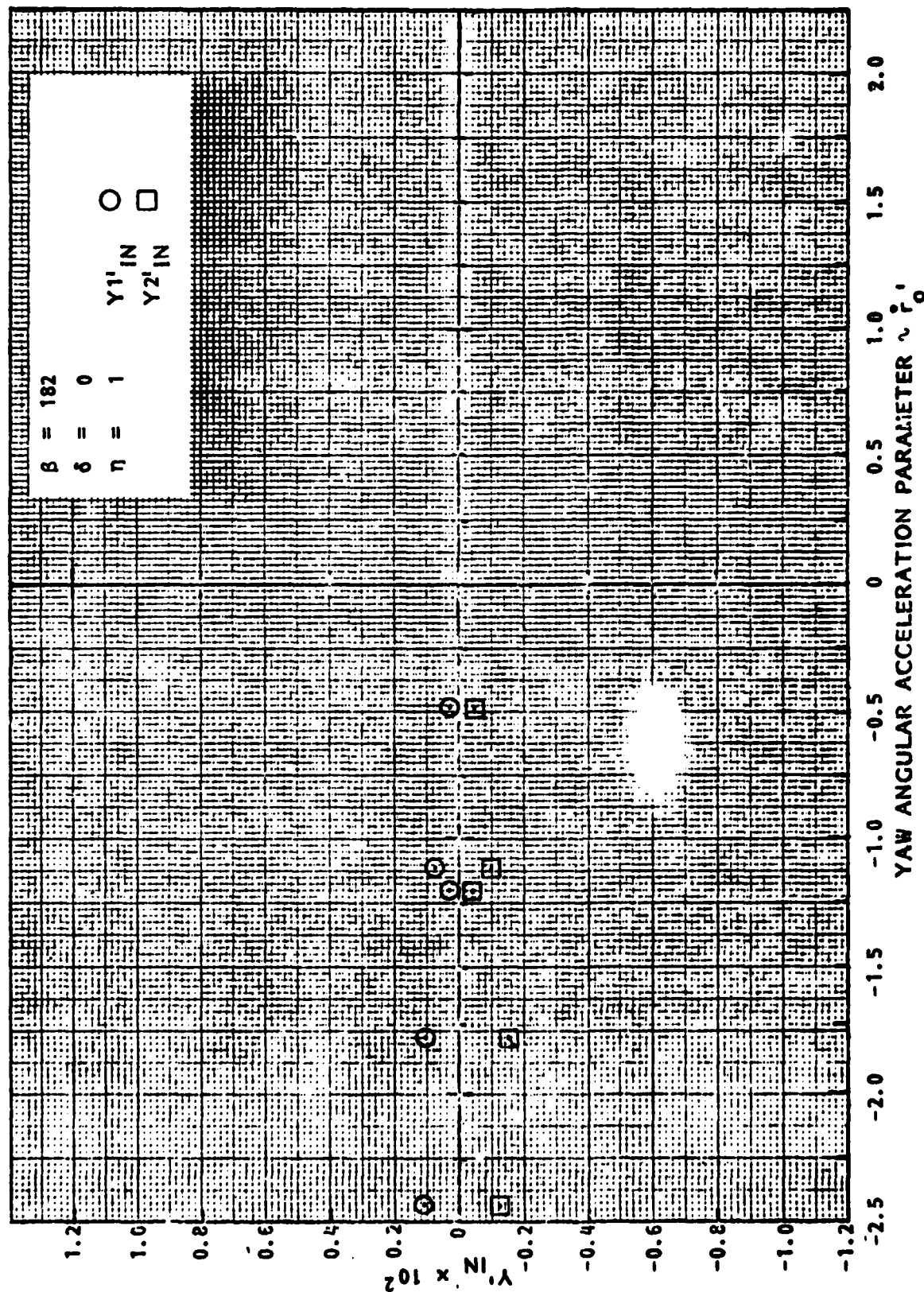


FIGURE A.58 - LATERAL FORCE GAGE IN-PHASE COEFFICIENTS AS FUNCTIONS OF YAW ANGULAR ACCELERATION AT DRIFT ANGLE $\beta = 182$ DEGREES FOR ASTERN MOTION AT $\eta = 1$ IN SHALLOW WATER, $H/T = 1.50$

Tracor Hydronautics

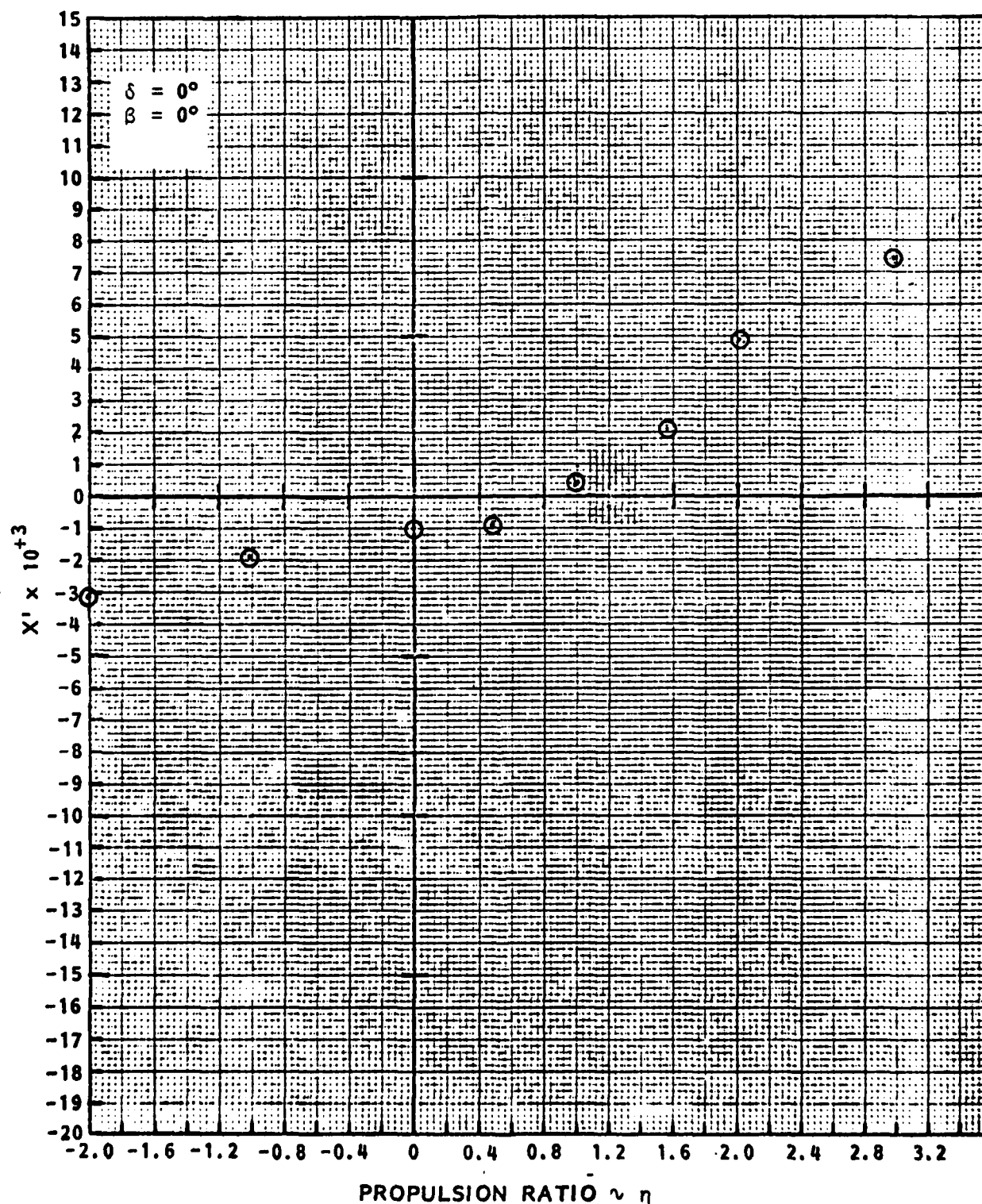


FIGURE A.59 - AXIAL FORCE COEFFICIENT AS FUNCTION OF PROPULSION RATIO η FOR AHEAD MOTION IN SHALLOW WATER, $H/T = 1.17$

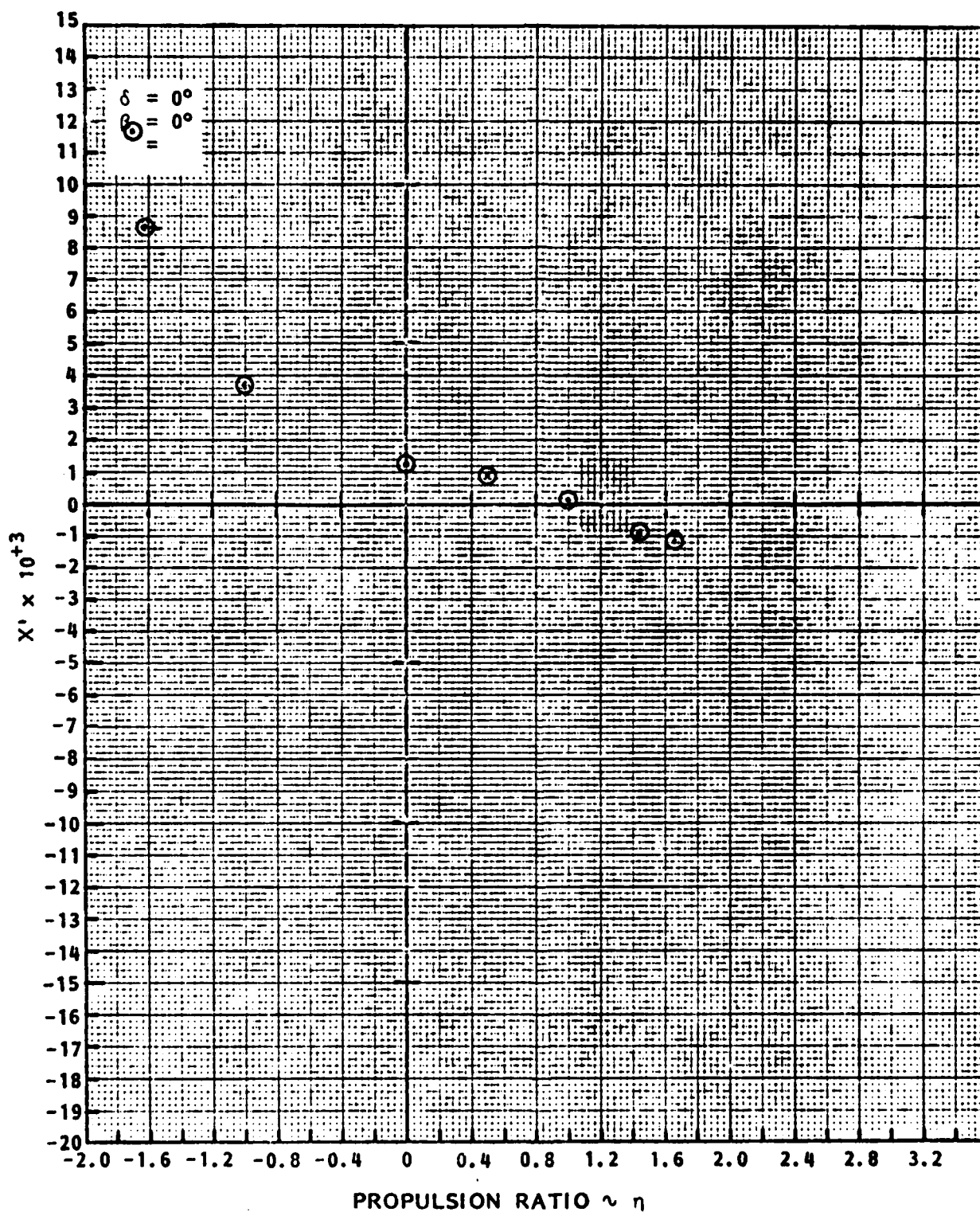


FIGURE A.60 - AXIAL FORCE COEFFICIENT AS FUNCTION OF PROPULSION RATIO η FOR ASTERN MOTION IN SHALLOW WATER, $H/T = 1.17$

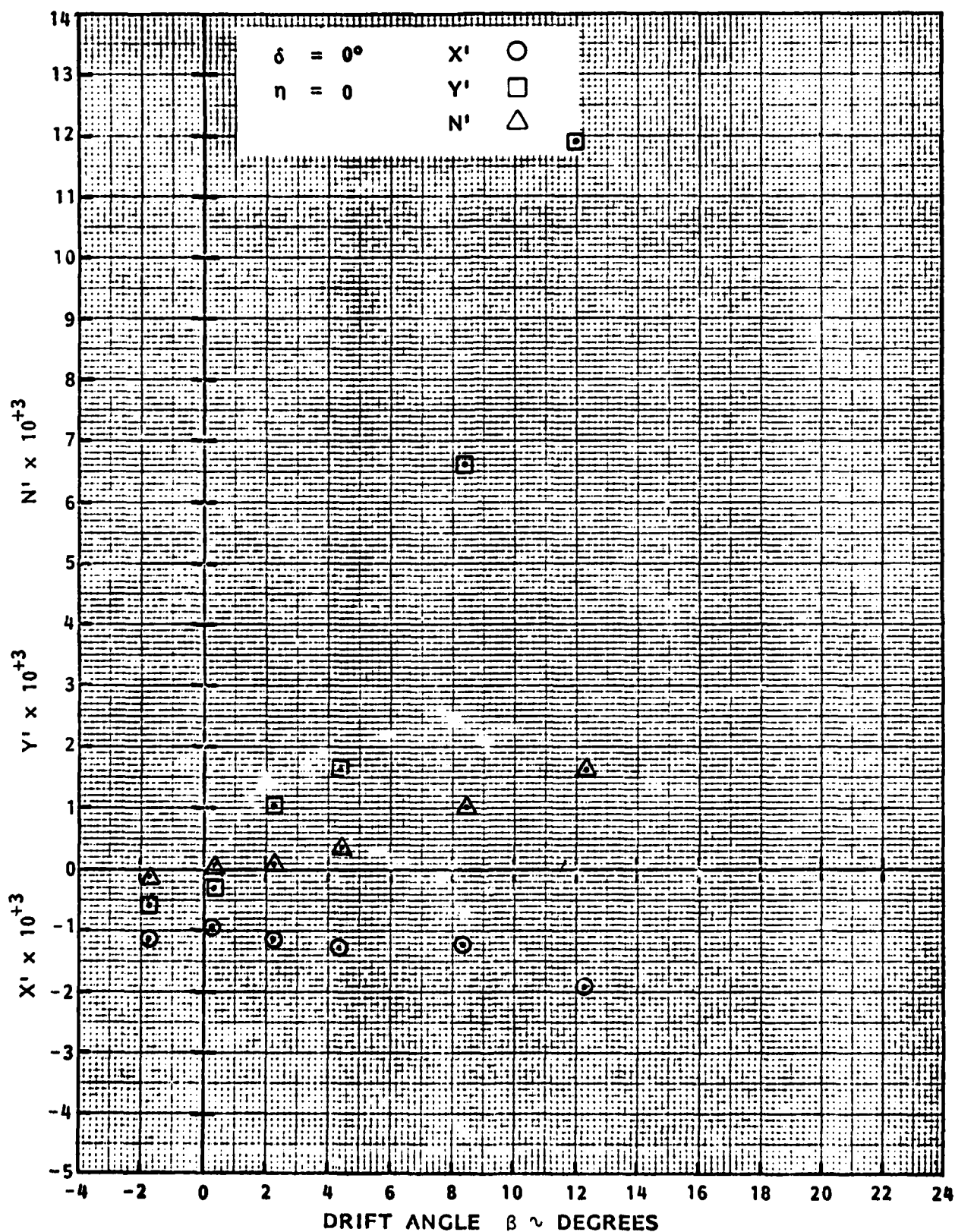


FIGURE A.61 - AXIAL FORCE, LATERAL FORCE, AND YAW MOMENT COEFFICIENTS AS FUNCTIONS OF DRIFT ANGLE β FOR AHEAD MOTION AT $\eta = 0$ IN SHALLOW WATER, $H/T = 1.17$

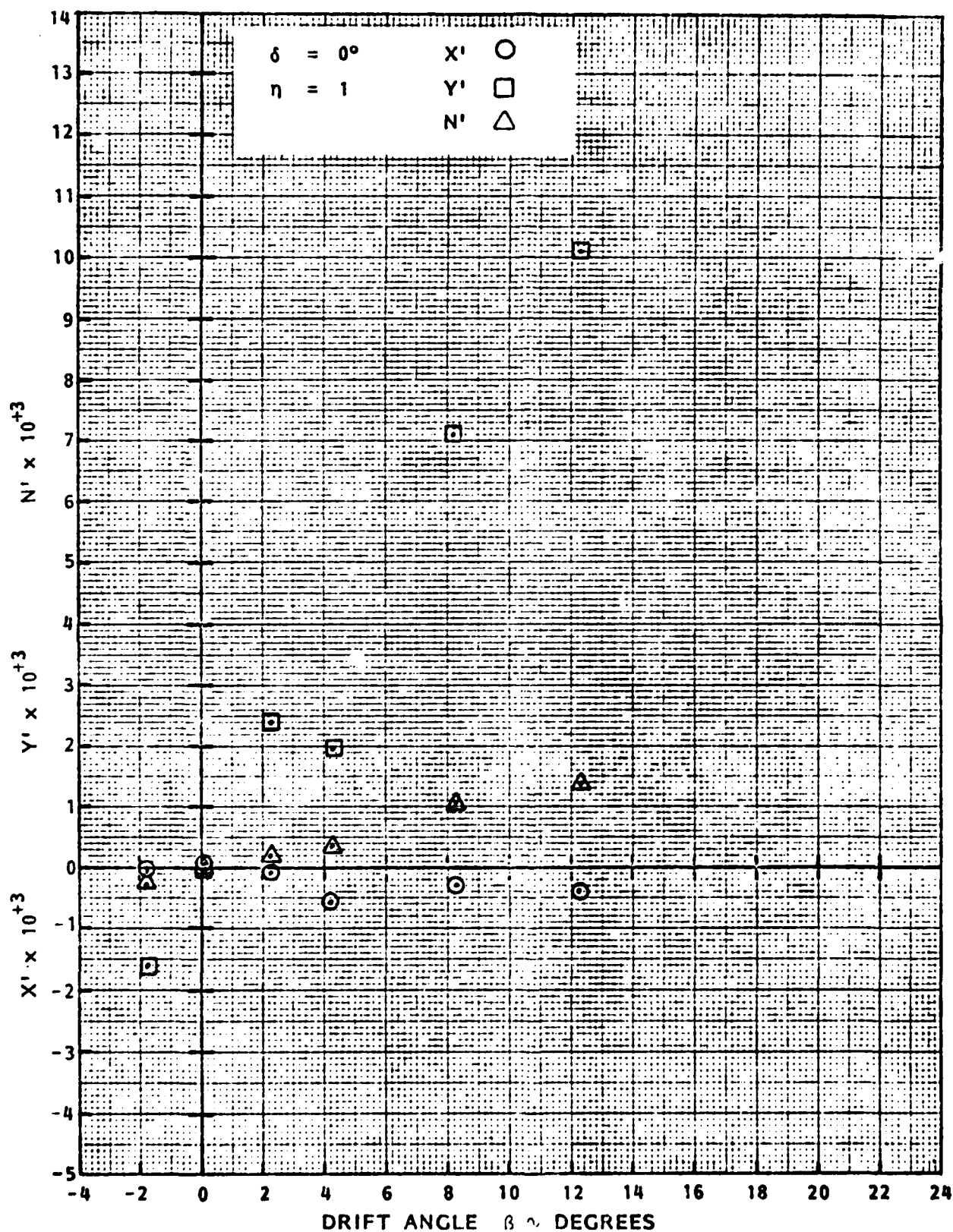


FIGURE A.62 - AXIAL FORCE, LATERAL FORCE, AND YAW MOMENT COEFFICIENTS AS FUNCTIONS OF DRIFT ANGLE β FOR AHEAD MOTION AT $\eta = 1$ IN SHALLOW WATER, $H/T = 1.17$

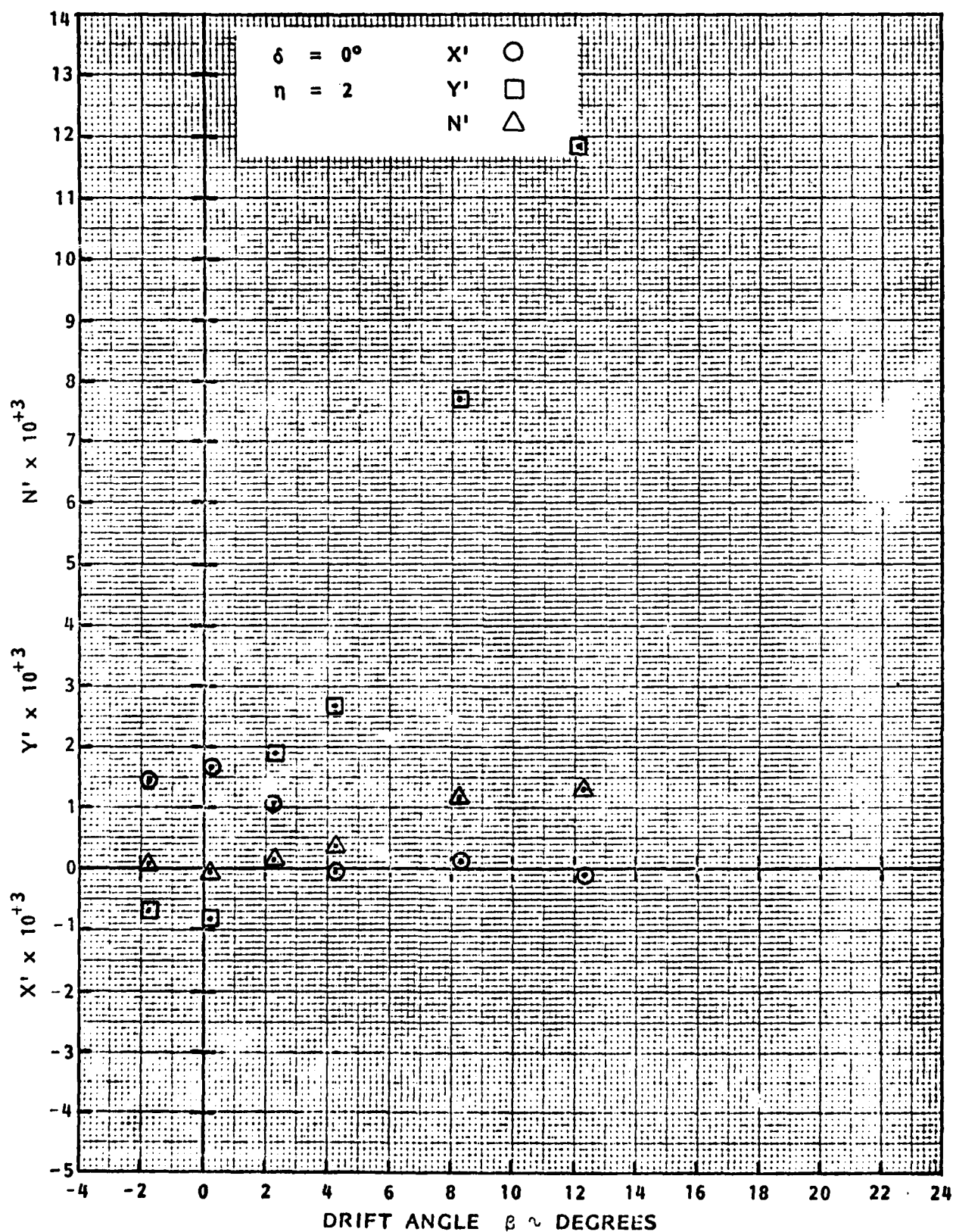


FIGURE A.63 - AXIAL FORCE, LATERAL FORCE, AND YAW MOMENT COEFFICIENTS AS FUNCTIONS OF DRIFT ANGLE β FOR AHEAD MOTION AT $\eta = 2$ IN SHALLOW WATER, $H/T = 1.17$

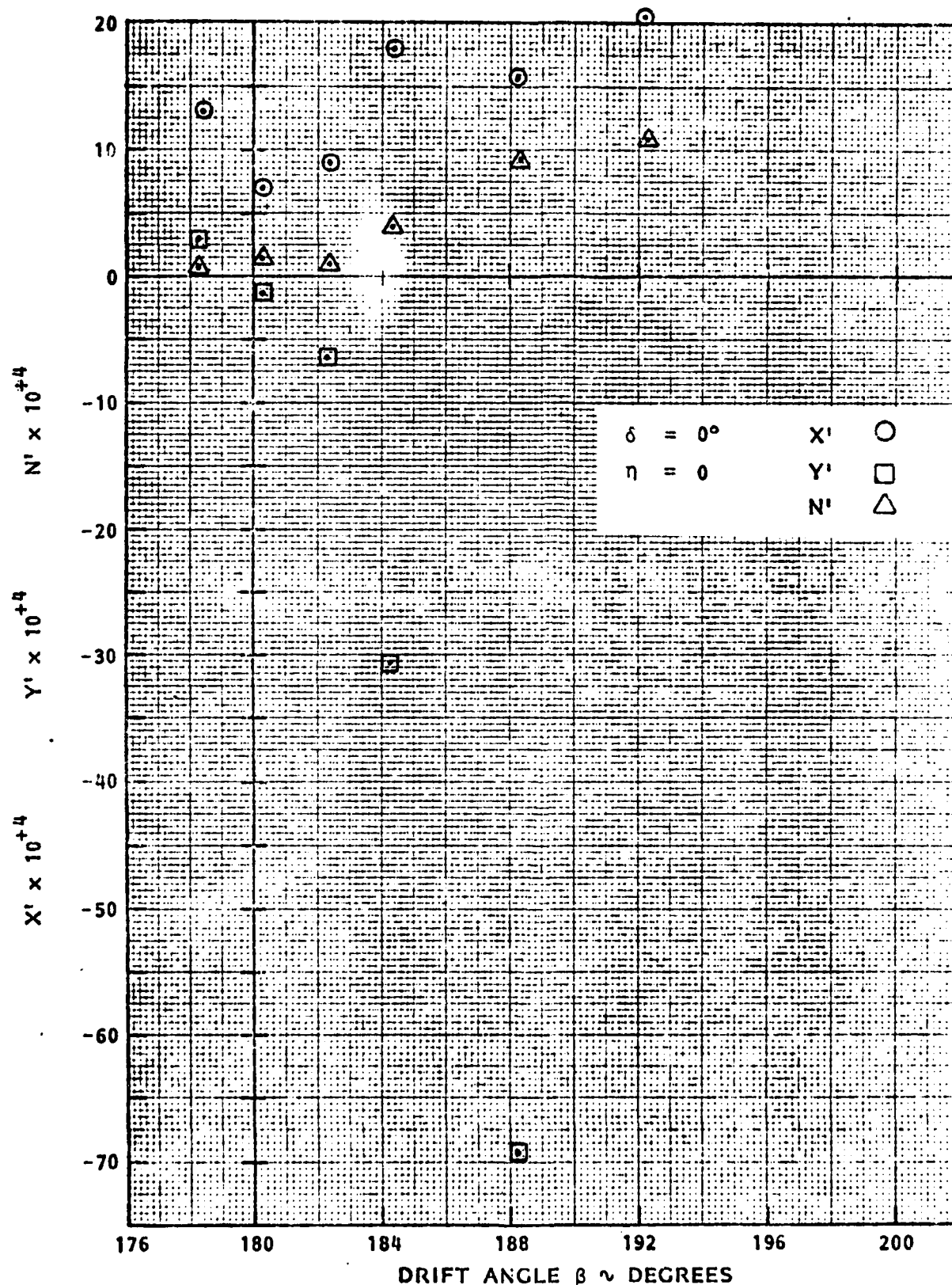


FIGURE A.64 - AXIAL FORCE, LATERAL FORCE, AND YAW MOMENT COEFFICIENTS AS FUNCTIONS OF DRIFT ANGLE β FOR ASTERN MOTION AT $\eta = 0$ IN SHALLOW WATER, $H/T = 1.17$

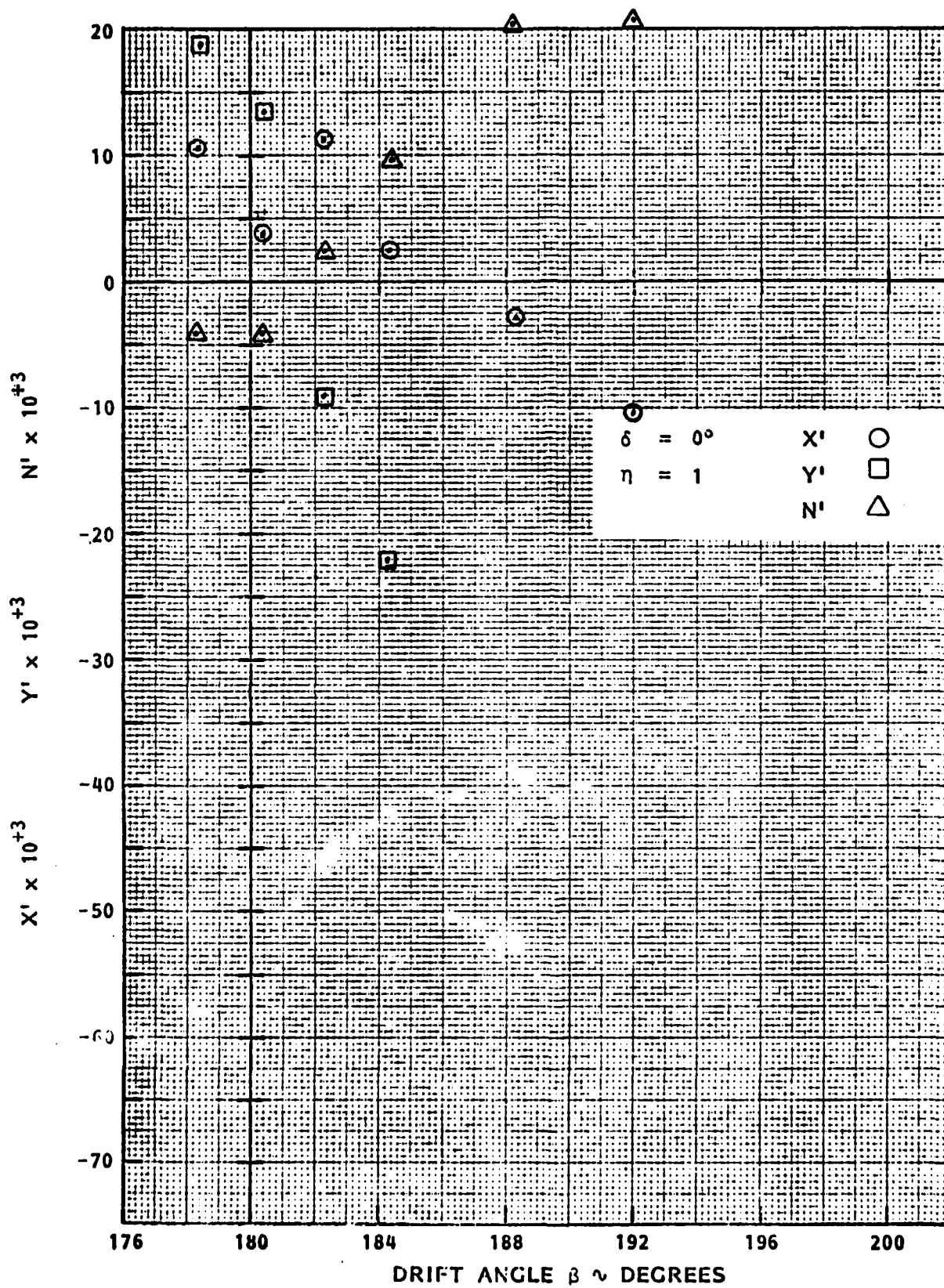


FIGURE A.65 - AXIAL FORCE, LATERAL FORCE, AND YAW MOMENT COEFFICIENTS AS FUNCTIONS OF DRIFT ANGLE β FOR ASTERN MOTION AT $\eta = 1$ IN SHALLOW WATER, $H/T = 1.17$

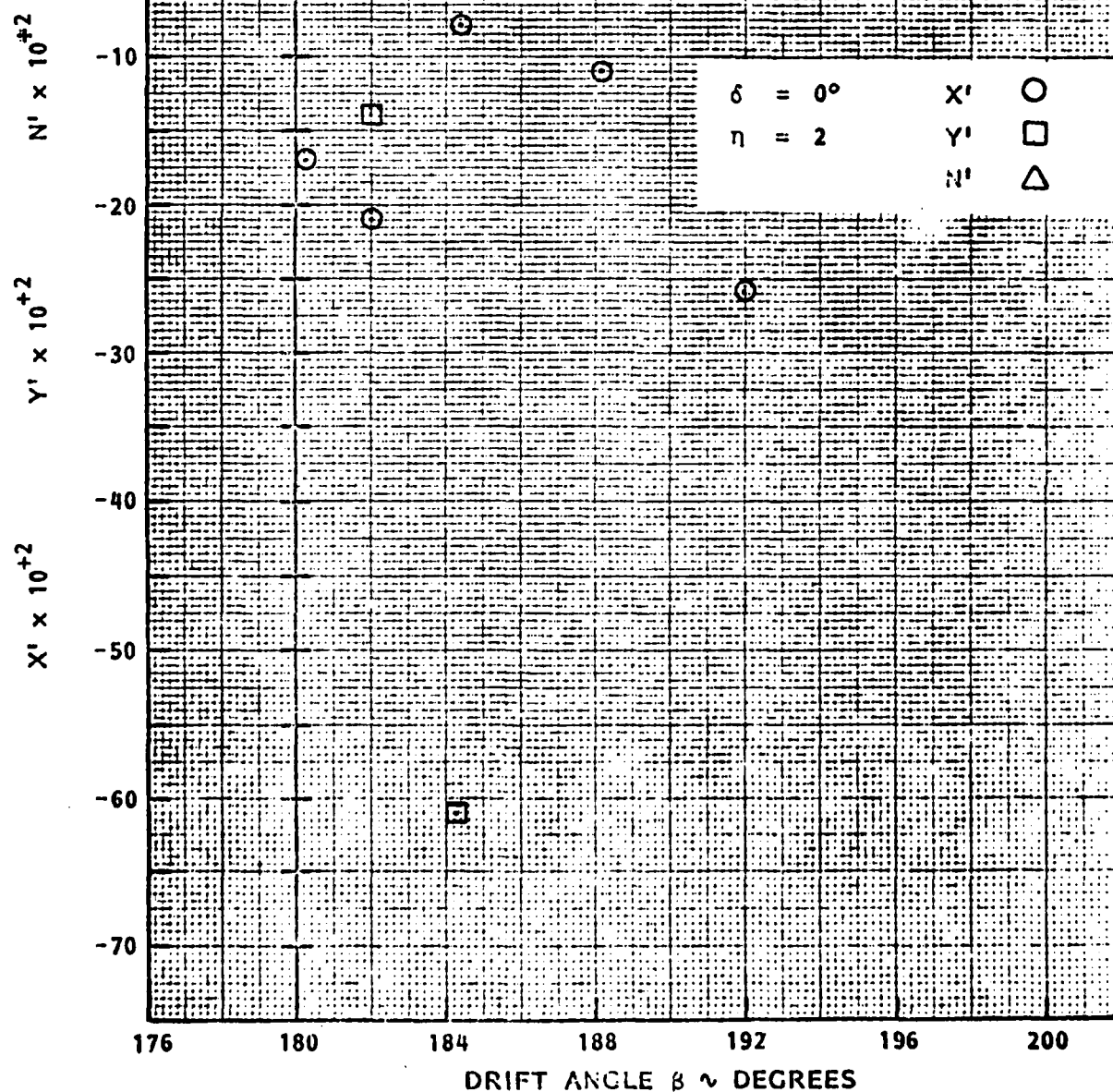


FIGURE A.66 - AXIAL FORCE, LATERAL FORCE, AND YAW MOMENT COEFFICIENTS AS FUNCTIONS OF DRIFT ANGLE β FOR ASTERN MOTION AT $\eta = 2$ IN SHALLOW WATER $H/T = 1.17$

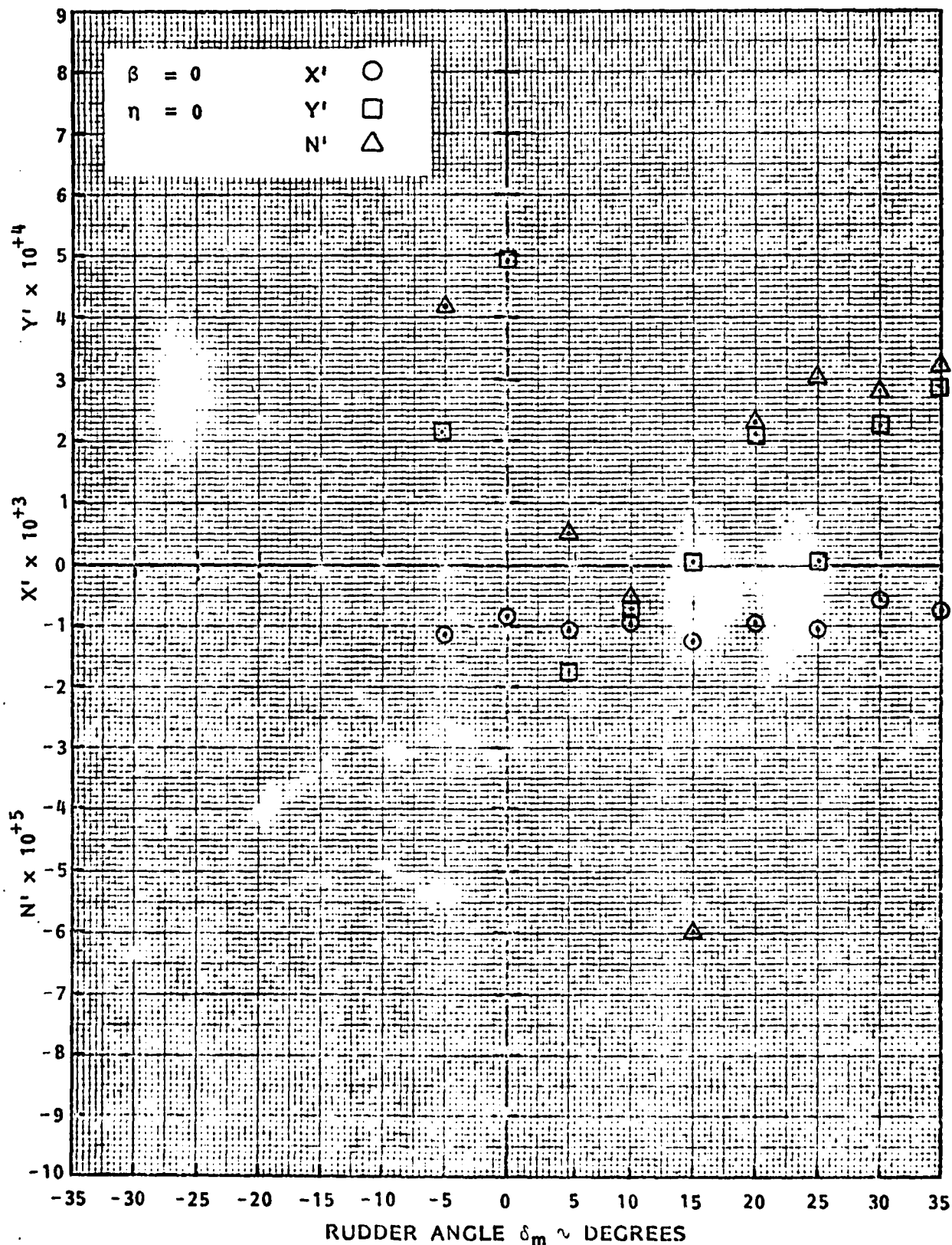


FIGURE A.67 - AXIAL FORCE, LATERAL FORCE AND YAW MOMENT COEFFICIENTS AS FUNCTIONS OF MAIN RUDDER ANGLE δ_m FOR AHEAD MOTION AT $\eta = 0$ IN SHALLOW WATER, $H/T = 1.17$

AD-A146 511

MODEL TESTS AND COMPUTER SIMULATIONS OF A 15-BARGE TOW
FOR THE UPPER MISS. (U) TRACOR HYDRONAUTICS INC LAUREL
MD R HATTON ET AL. JAN 84 TR-83011-2 USCG-D-10-84

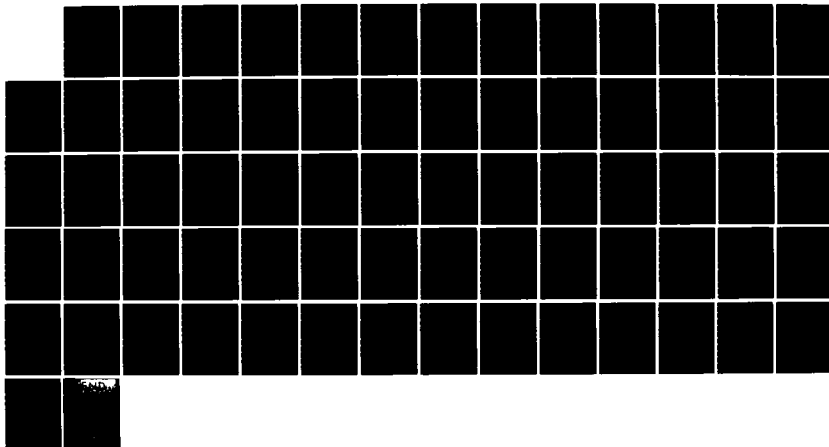
3/3

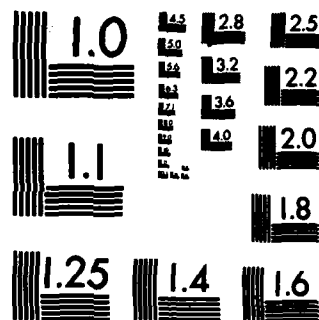
UNCLASSIFIED

DTCG23-82-C-20041

F/G 9/2

NL





COPY RESOLUTION TEST CHART

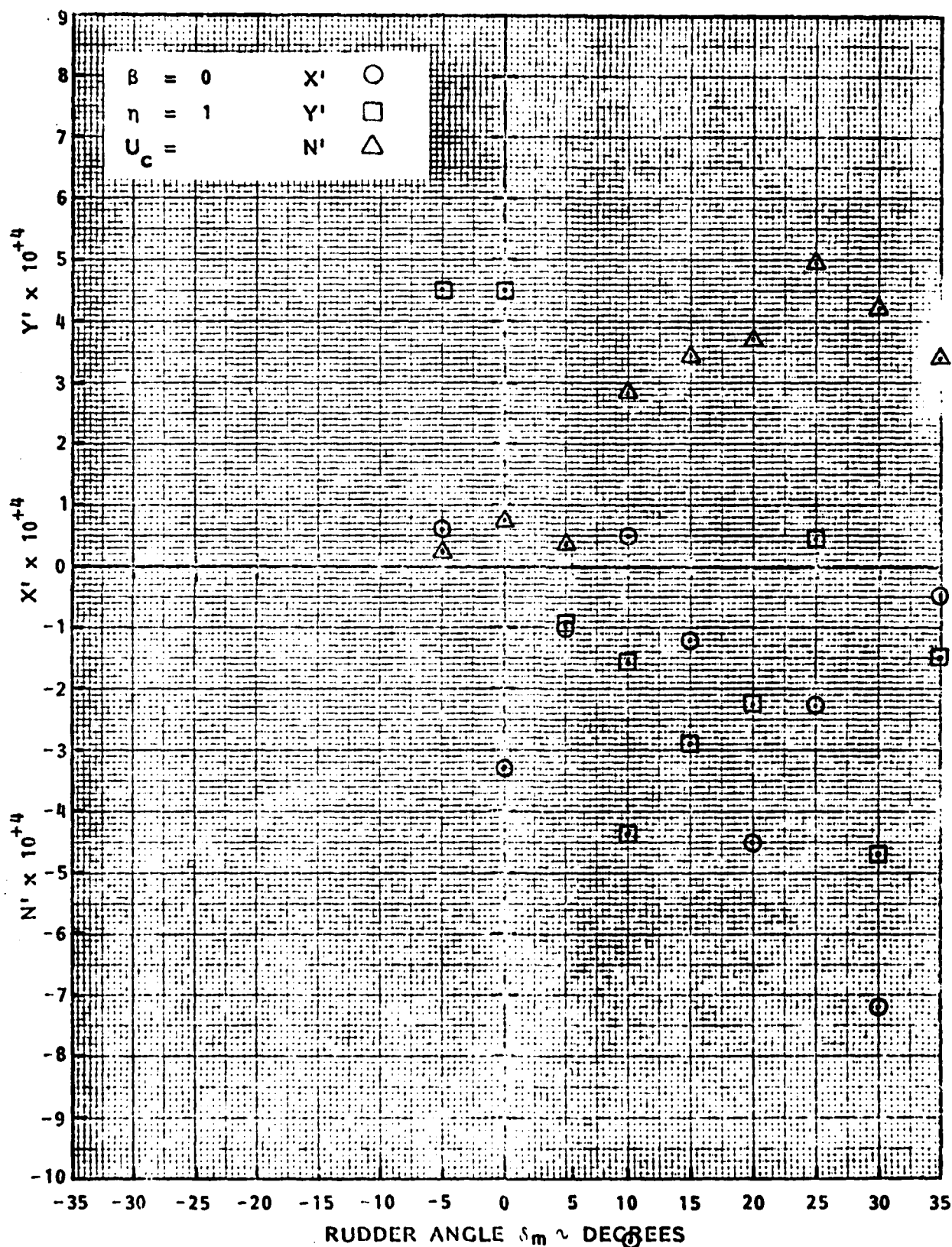


FIGURE A.68 - AXIAL FORCE, LATERAL FORCE AND YAW MOMENT COEFFICIENTS AS FUNCTIONS OF MAIN RUDDER ANGLE δ_m FOR AHEAD MOTION AT $\eta = 1$

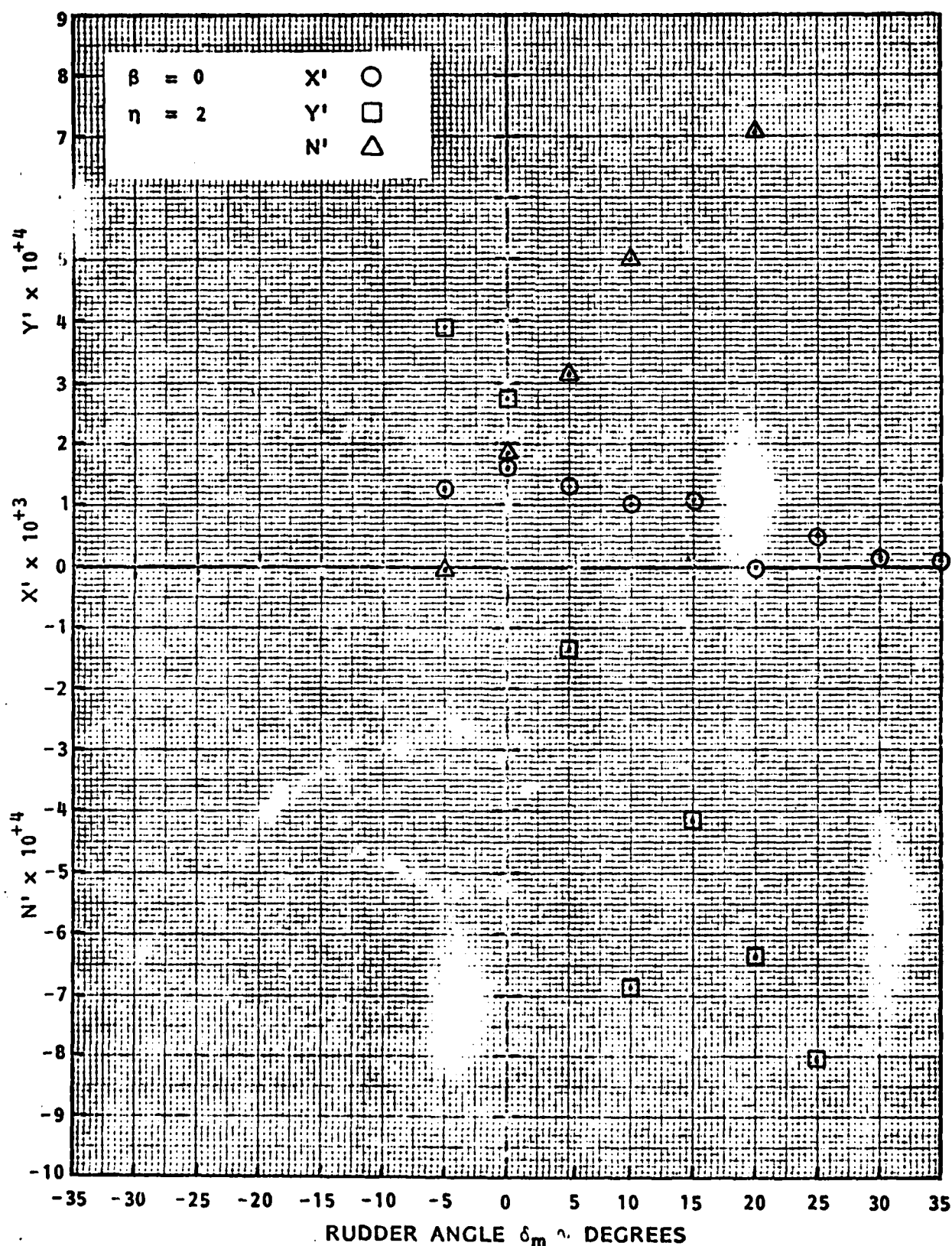


FIGURE A.69 - AXIAL FORCE, LATERAL FORCE AND YAW MOMENT COEFFICIENTS AS FUNCTION OF MAIN RUDDER ANGLE δ_m FOR AHEAD MOTION AT η = 2 IN SHALLOW WATER, H/T = 1.17

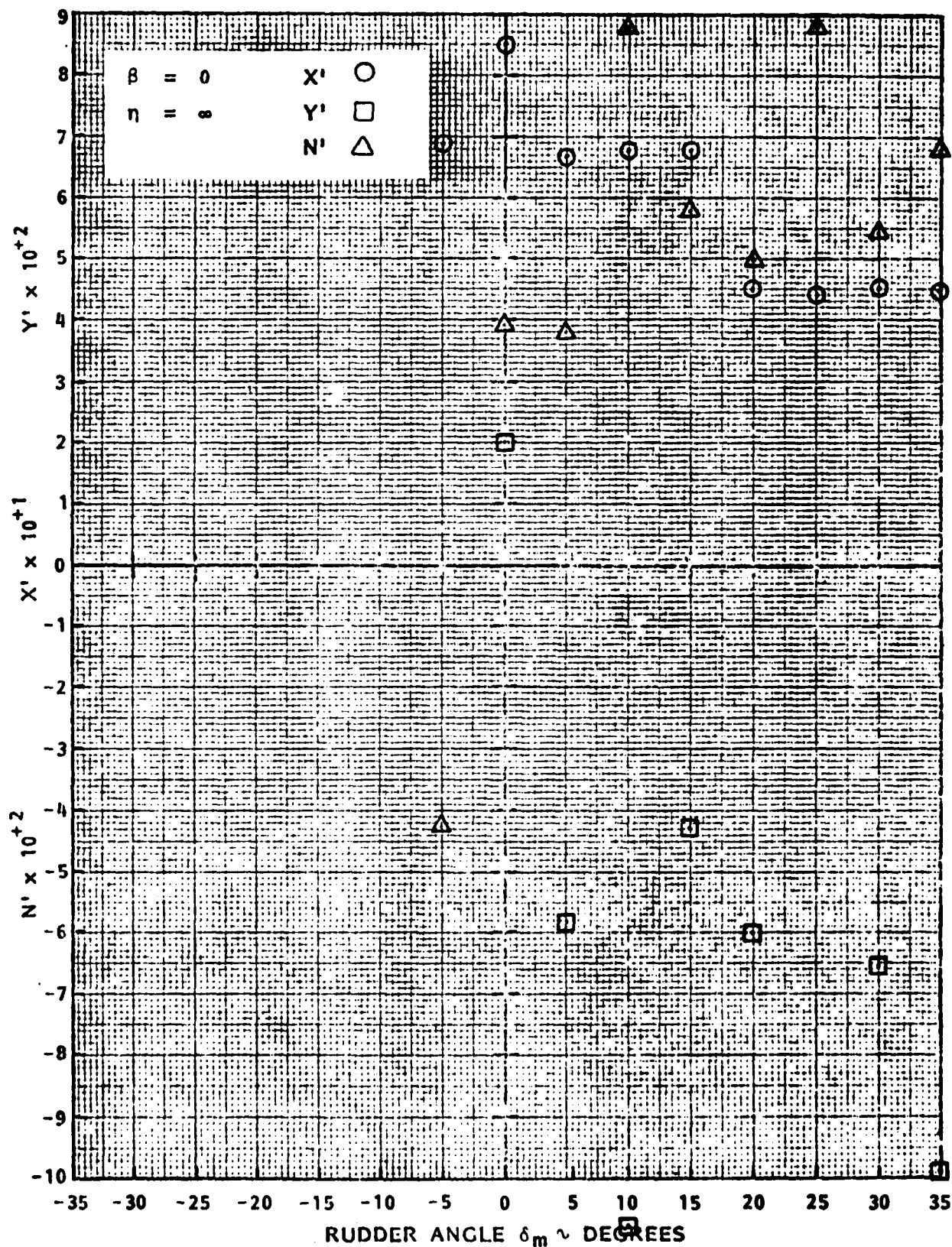


FIGURE A.70 - AXIAL FORCE, LATERAL FORCE AND YAW MOMENT COEFFICIENTS AS FUNCTIONS OF MAIN RUDDER ANGLE δ_m FOR ZERO SPEED AT $\eta = \infty$ (AHEAD THRUST) IN SHALLOW WATER, $H/T = 1.17$

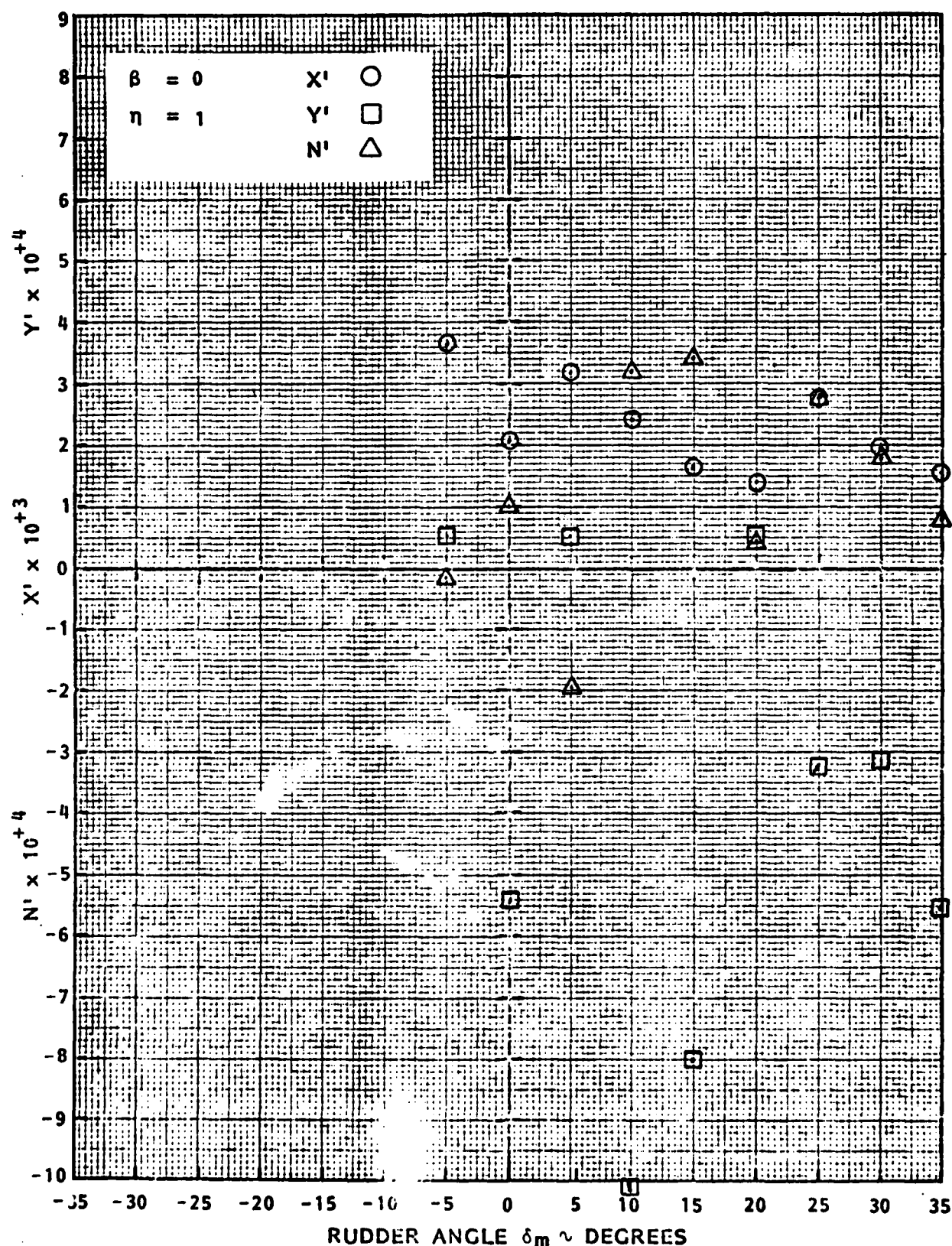


FIGURE A.71 - AXIAL FORCE, LATERAL FORCE AND YAW MOMENT COEFFICIENTS AS FUNCTIONS OF MAIN RUDDER ANGLE δ_m FOR ASTERN MOTION AT $\eta = -1$ IN SHALLOW WATER. $H/T = 1.17$

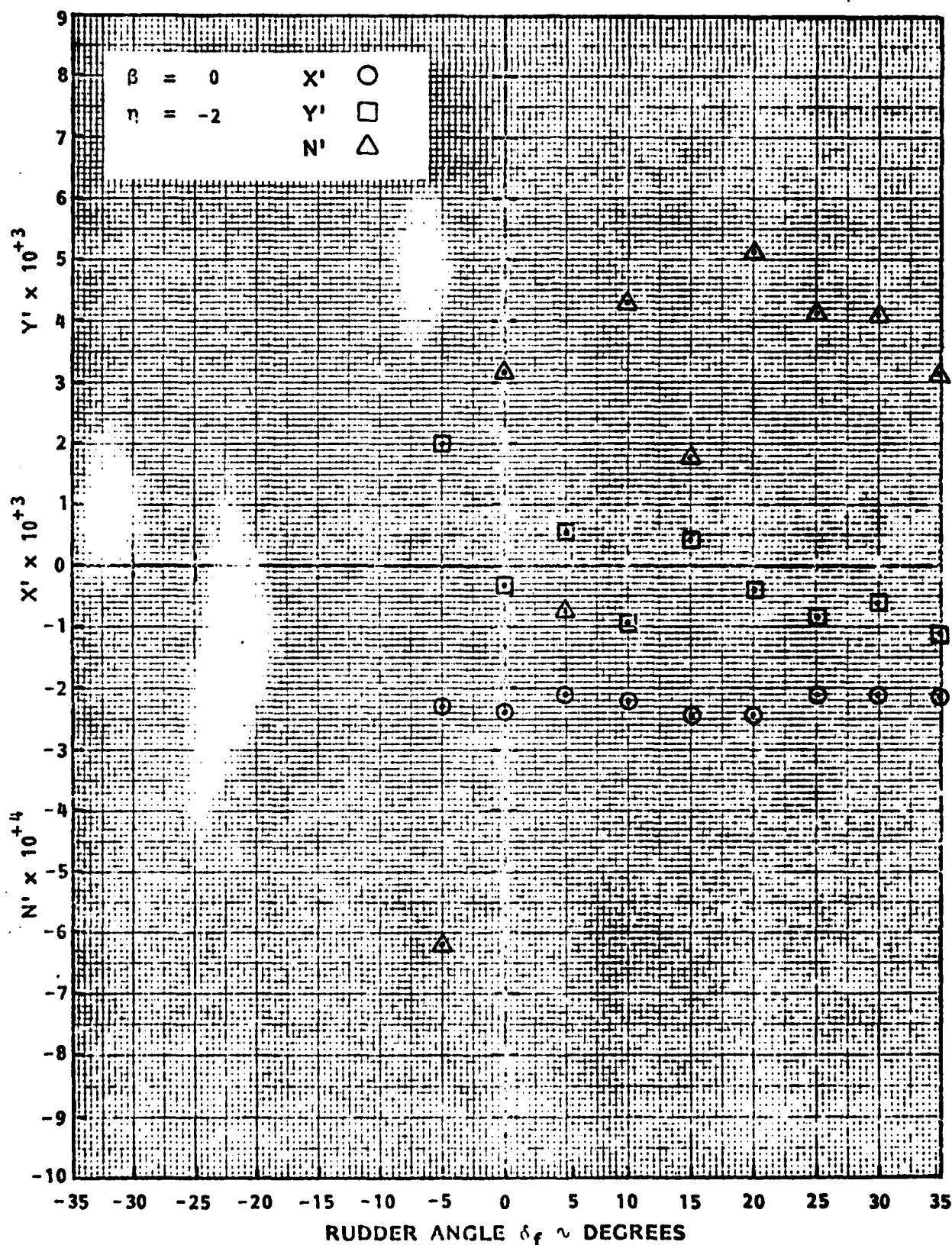


FIGURE A.72 - AXIAL FORCE, LATERAL FORCE AND YAW MOMENT COEFFICIENTS AS FUNCTIONS OF FLANKING RUDDER ANGLE δ_f FOR AHEAD MOTION AT $\eta = -2$ IN SHALLOW WATER, $H/T = 1.17$

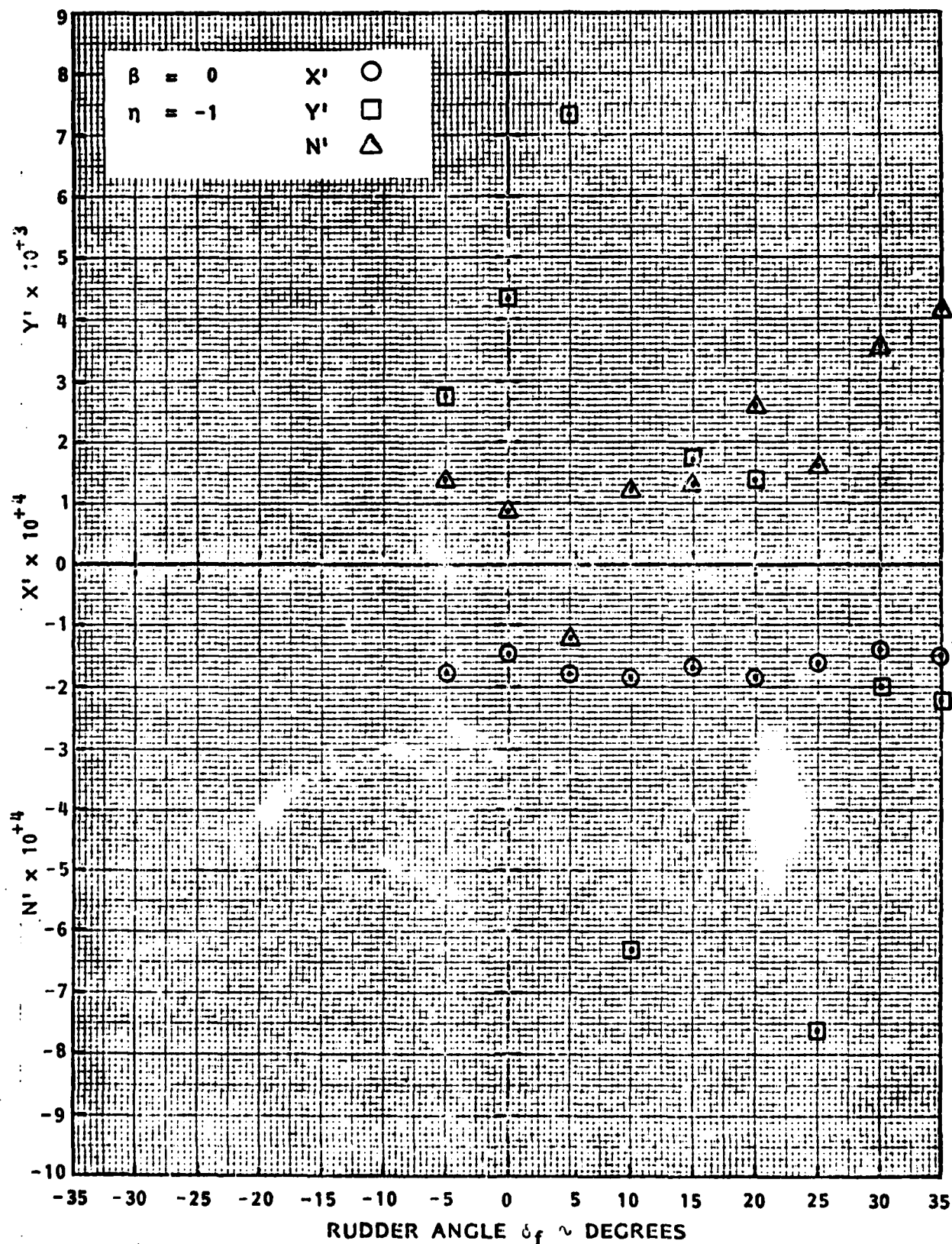


FIGURE A.73 - AXIAL FORCE, LATERAL FORCE AND YAW MOMENT COEFFICIENTS AS FUNCTIONS OF FLANKING RUDDER ANGLE δ_f FOR AHEAD MOTION AT $\eta = -1$ IN SHALLOW WATER, $H/T = 1.17$

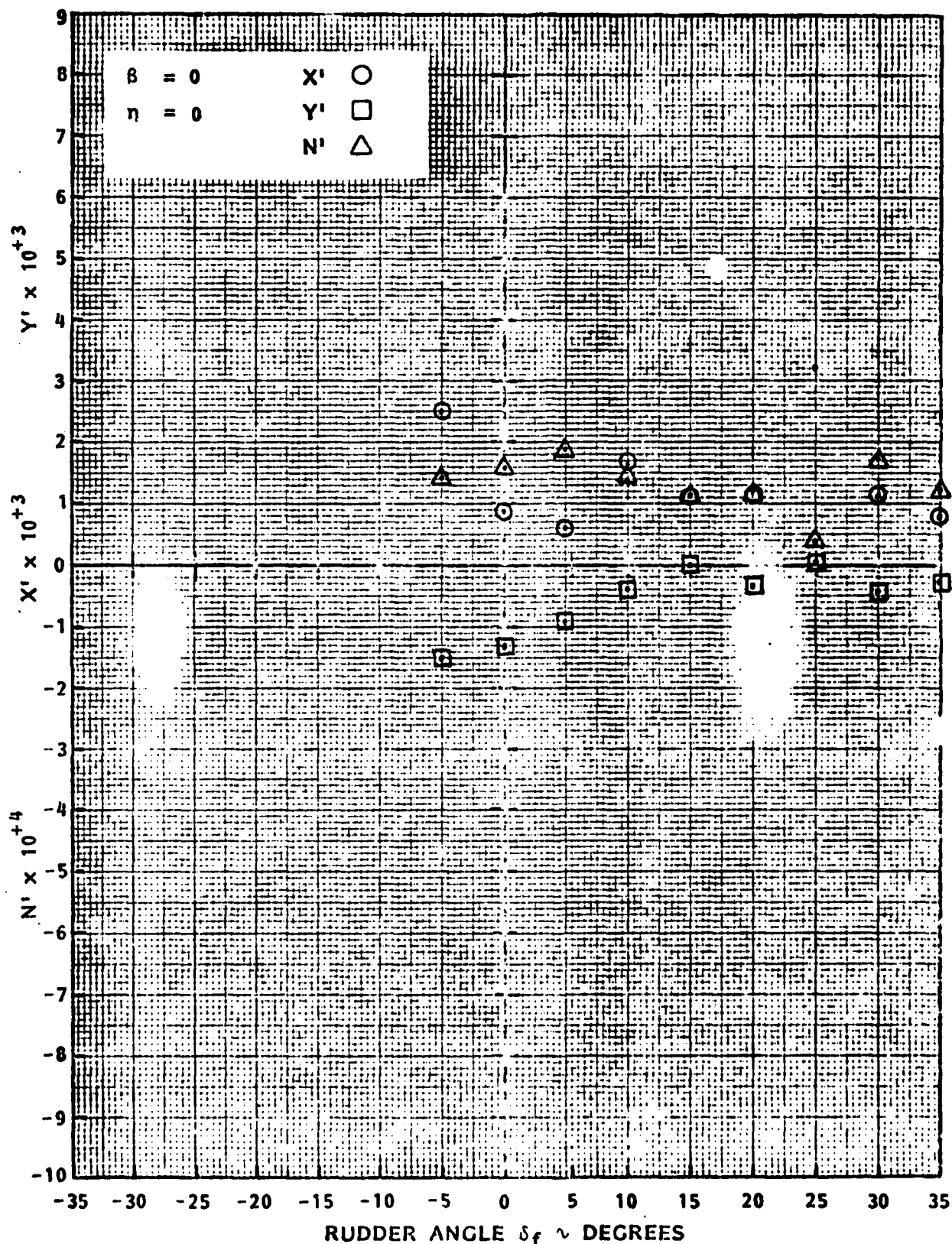


FIGURE A.74 - AXIAL FORCE, LATERAL FORCE AND YAW MOMENT COEFFICIENTS AS FUNCTIONS OF FLANKING RUDDER ANGLE δ_f FOR ASTERN MOTION AT $\eta = 0$ IN SHALLOW WATER, $H/T = 1.17$

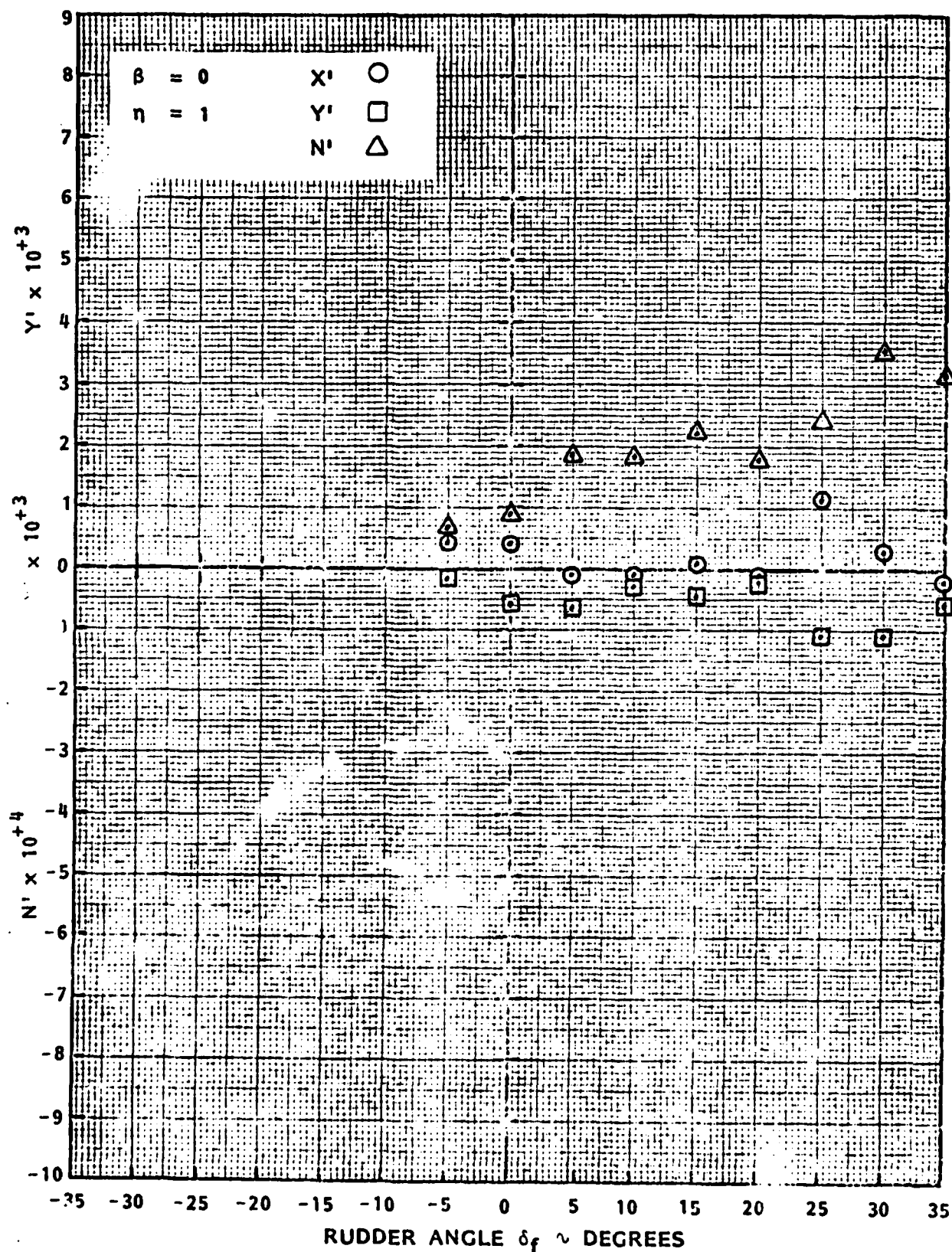


FIGURE A.75 - AXIAL FORCE, LATERAL FORCE AND YAW MOMENT COEFFICIENTS AS FUNCTIONS OF FLANKING RUDDER ANGLE δ_f FOR ASTERN MOTION AT $\eta = 1$ IN SHALLOW WATER, $H/T = 1.17$

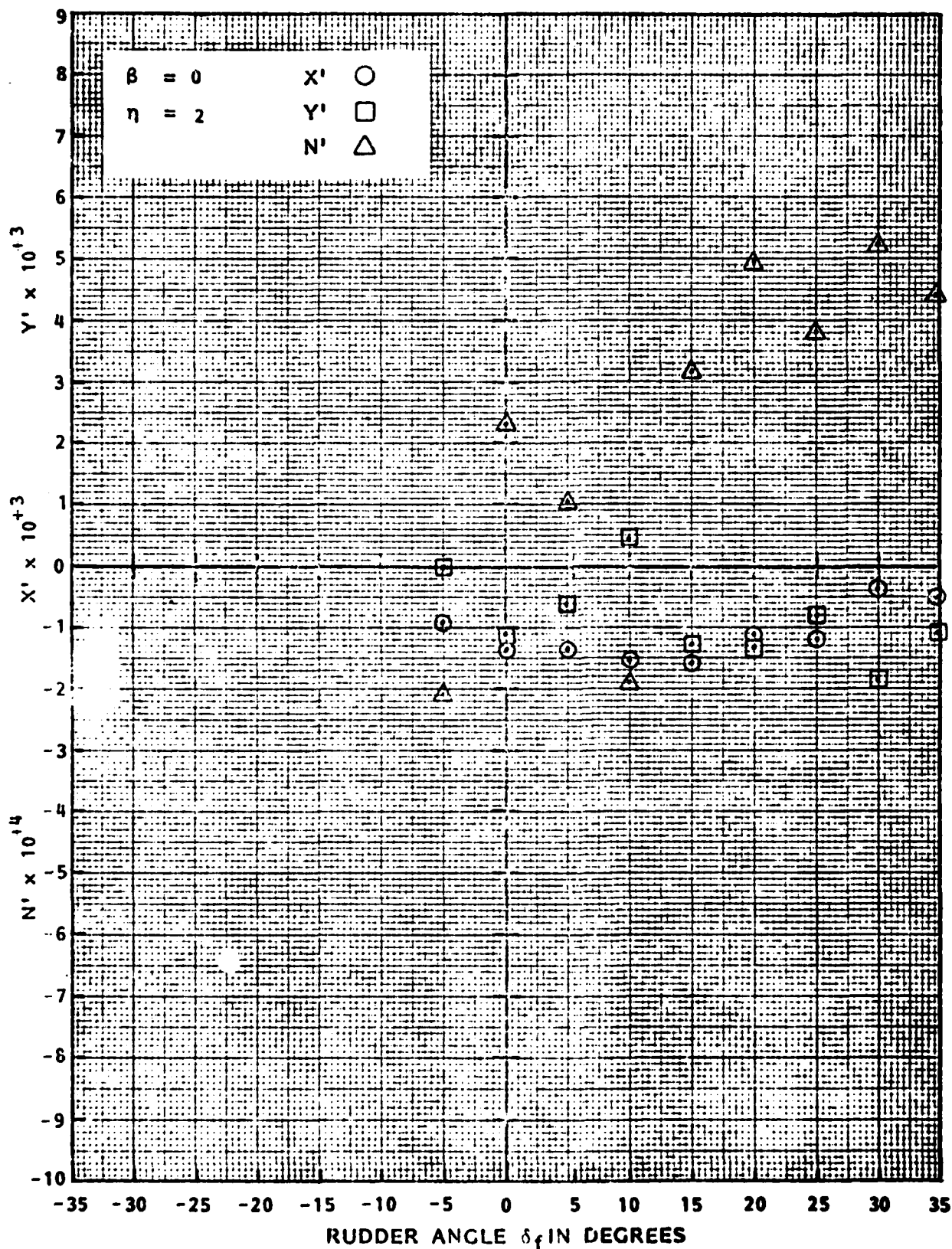


FIGURE A.76 - AXIAL FORCE, LATERAL FORCE AND YAW MOMENT COEFFICIENTS AS FUNCTIONS OF FLANKING RUDDER ANGLE δ_f FOR ASTERN MOTION AT $n = 2$ IN SHALLOW WATER. $H/T = 1.17$

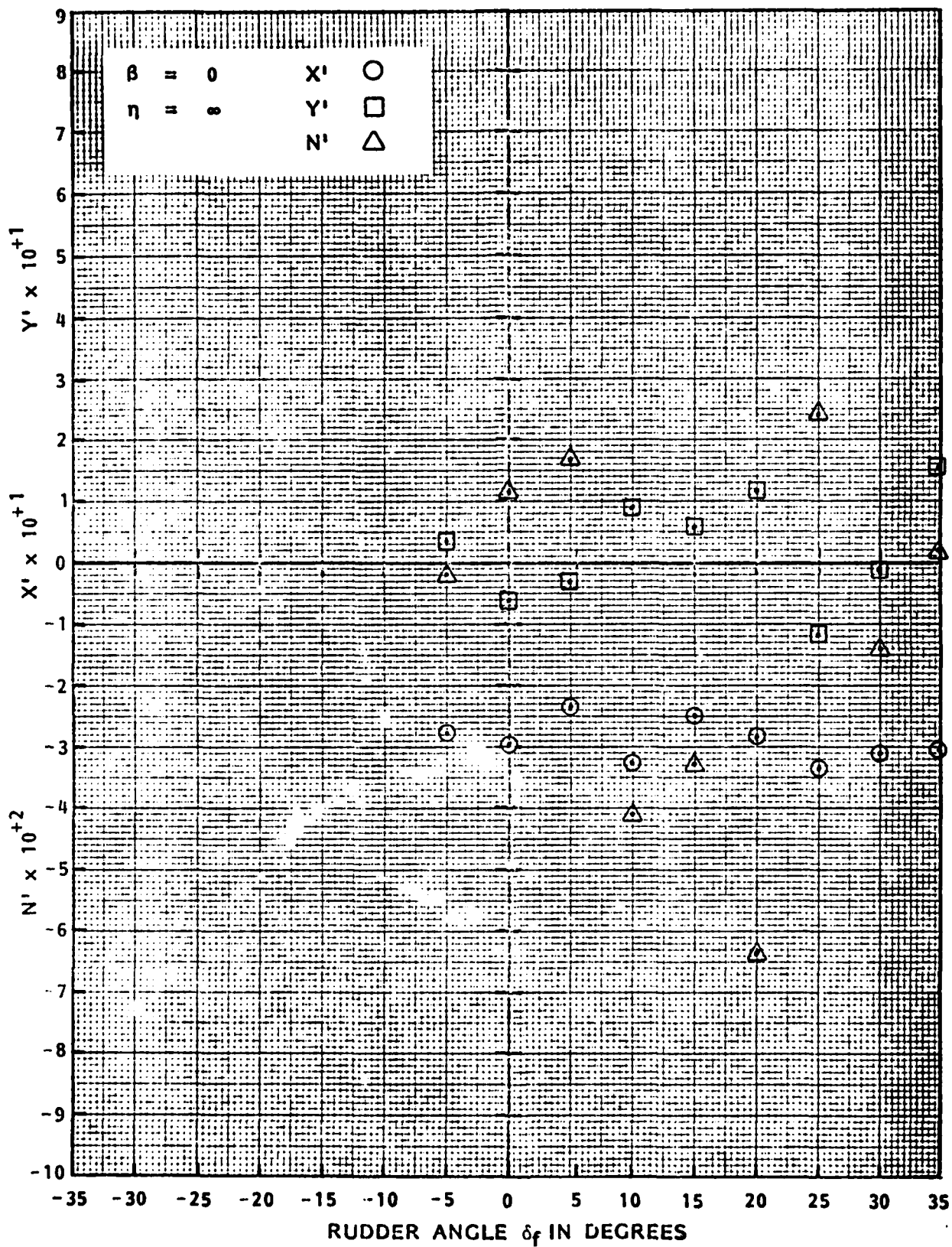


FIGURE A.77 - AXIAL FORCE, LATERAL FORCE AND YAW MOMENT COEFFICIENTS AS FUNCTIONS OF FLANKING RUDDER ANGLE δ_f FOR ZERO SPEED AT $\eta = \infty$ (ASTERN THRUST) IN SHALLOW WATER, $H/T = 1.17$

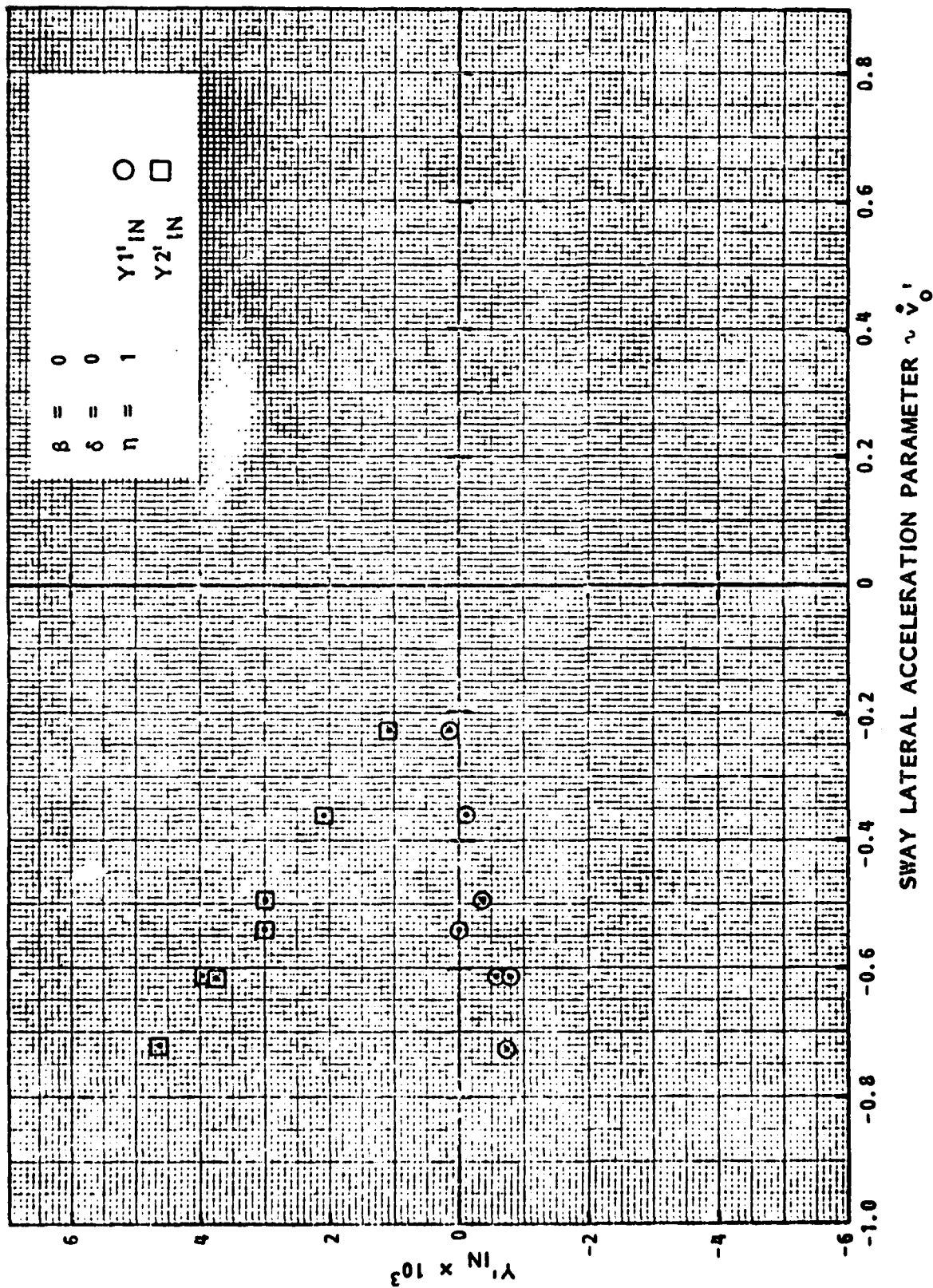
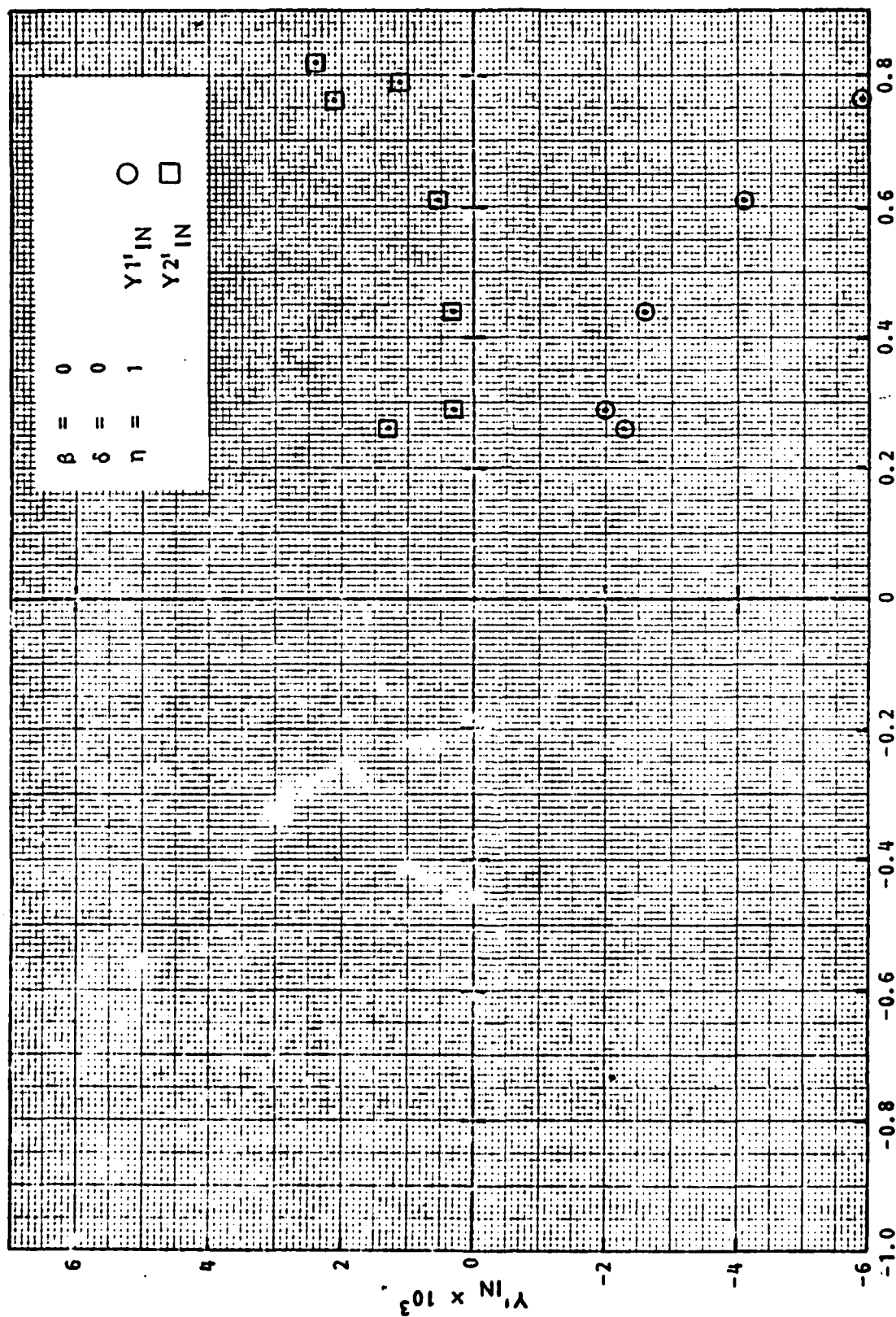


FIGURE A.78 - LATERAL FORCE GAGE IN-PHASE COEFFICIENTS
AS FUNCTIONS OF SWAY ACCELERATION FOR
AHEAD MOTION AT $\eta = 1$ IN SHALLOW WATER,
 $H/T = 1.17$



SWAY LATERAL ACCELERATION PARAMETER $\sim \dot{v}_0'$

FIGURE A.79 - LATERAL FORCE GAGE IN-PHASE COEFFICIENTS AS FUNCTIONS OF SWAY ACCELERATION FOR ASTERN MOTION AT $\eta = 1$ IN SHALLOW WATER, $H/T = 1.17$

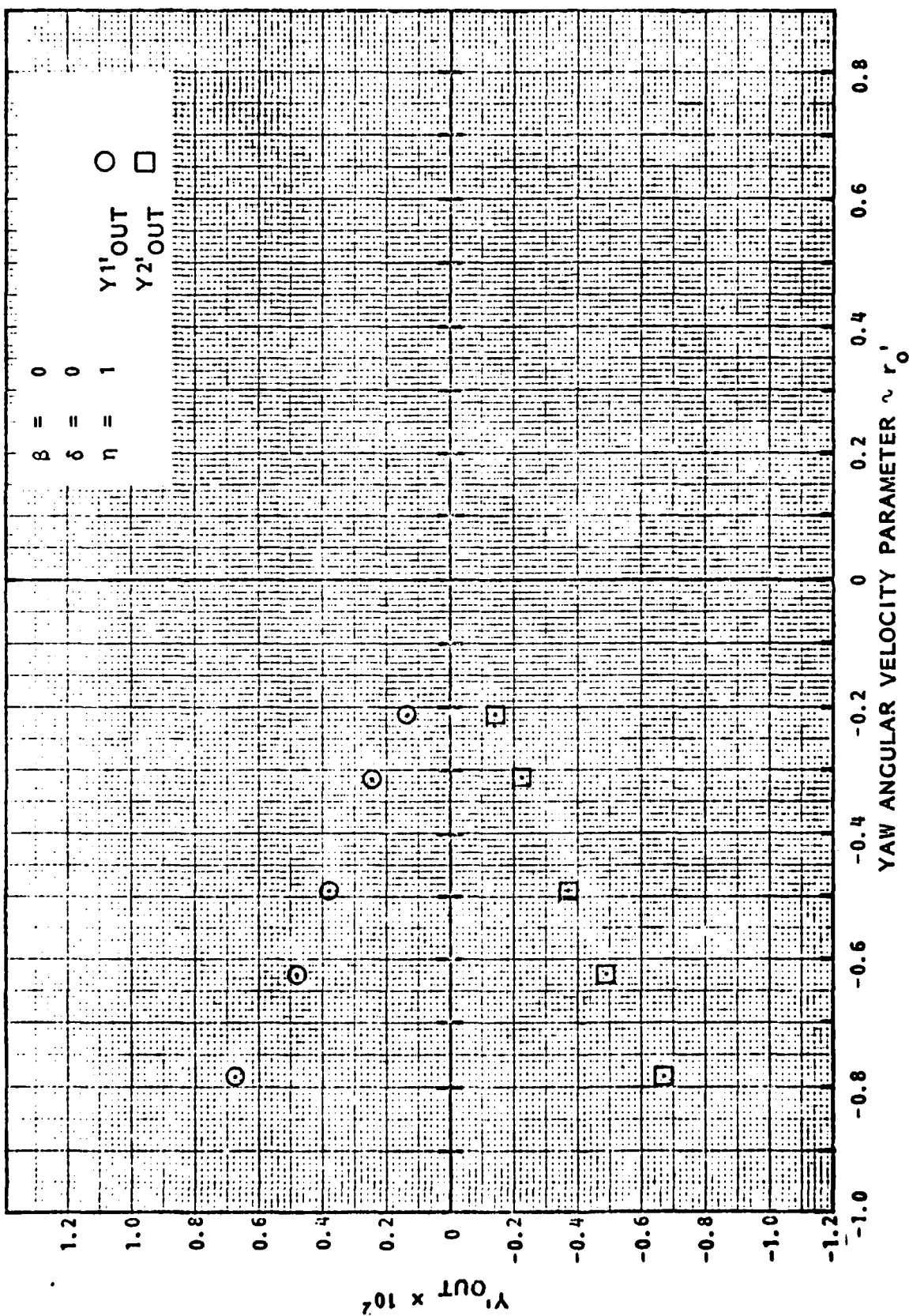


FIGURE A.80 - LATERAL FORCE GAGE OUT-OF-PHASE COEFFICIENTS AS FUNCTIONS OF YAW ANGULAR VELOCITY FOR AHEAD MOTION AT $\eta = 1$ IN SHALLOW WATER, $H/T = 1.17$

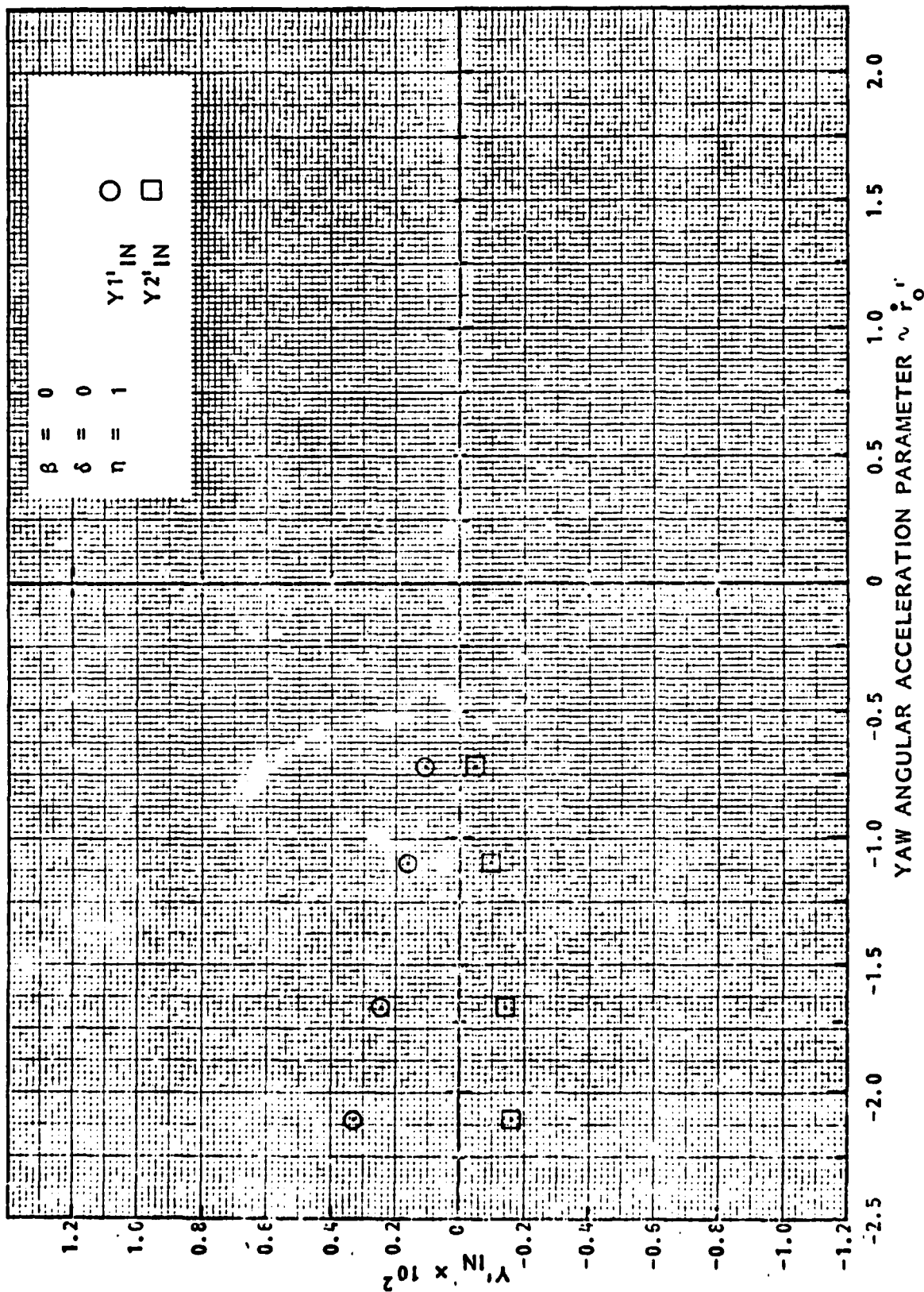


FIGURE A.81 - LATERAL FORCE GAGE IN-PHASE COEFFICIENTS AS FUNCTIONS OF YAW ANGULAR ACCELERATION FOR AHEAD MOTION AT $\eta = 1$ IN SHALLOW WATER, $H/T = 1.17$

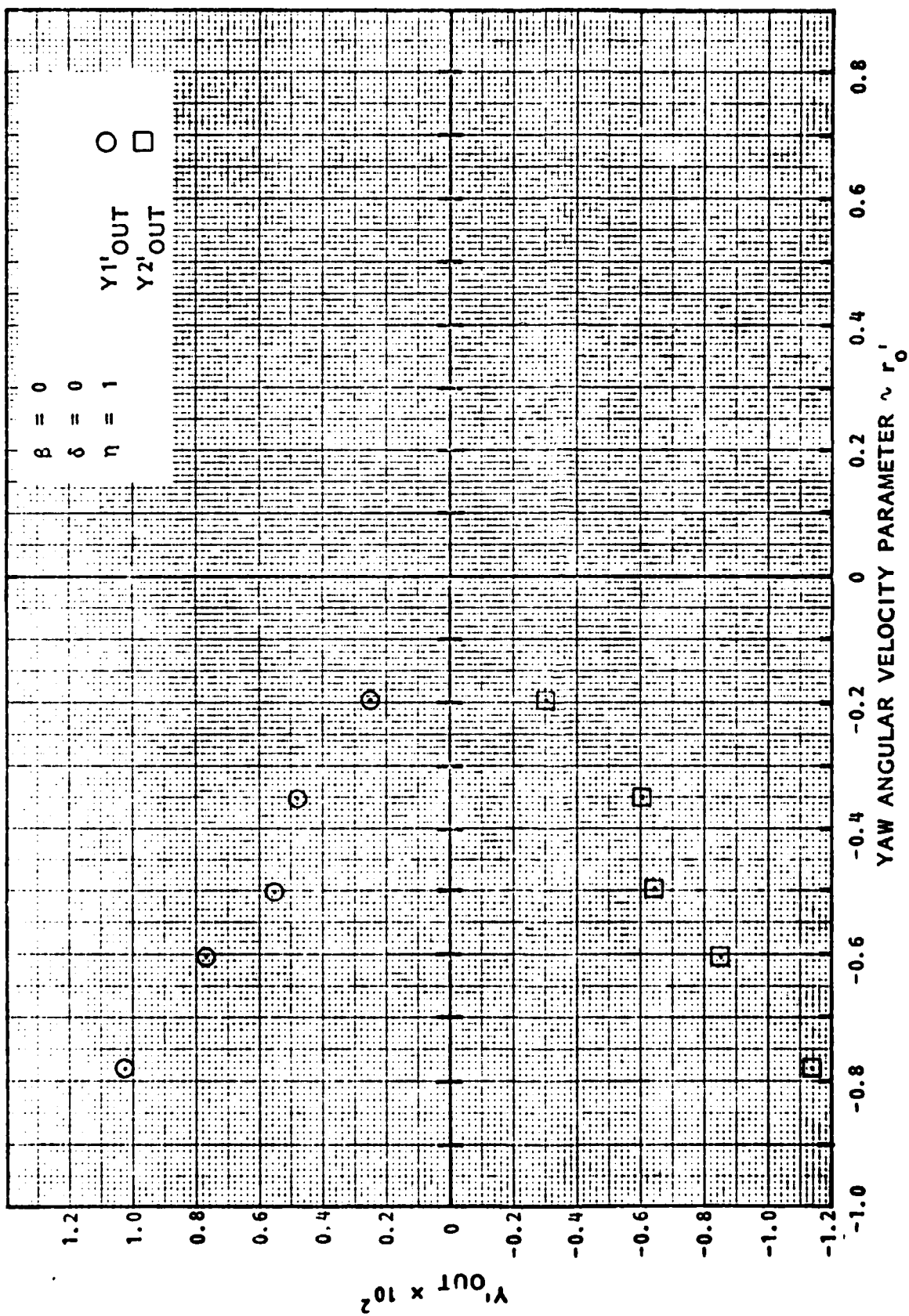


FIGURE A.82 - LATERAL FORCE GAGE OUT-OF-PHASE COEFFICIENTS AS FUNCTIONS OF YAW ANGULAR VELOCITY FOR ASTERN MOTION AT $\eta = 1$ IN SHALLOW WATER, $H/T = 1.17$

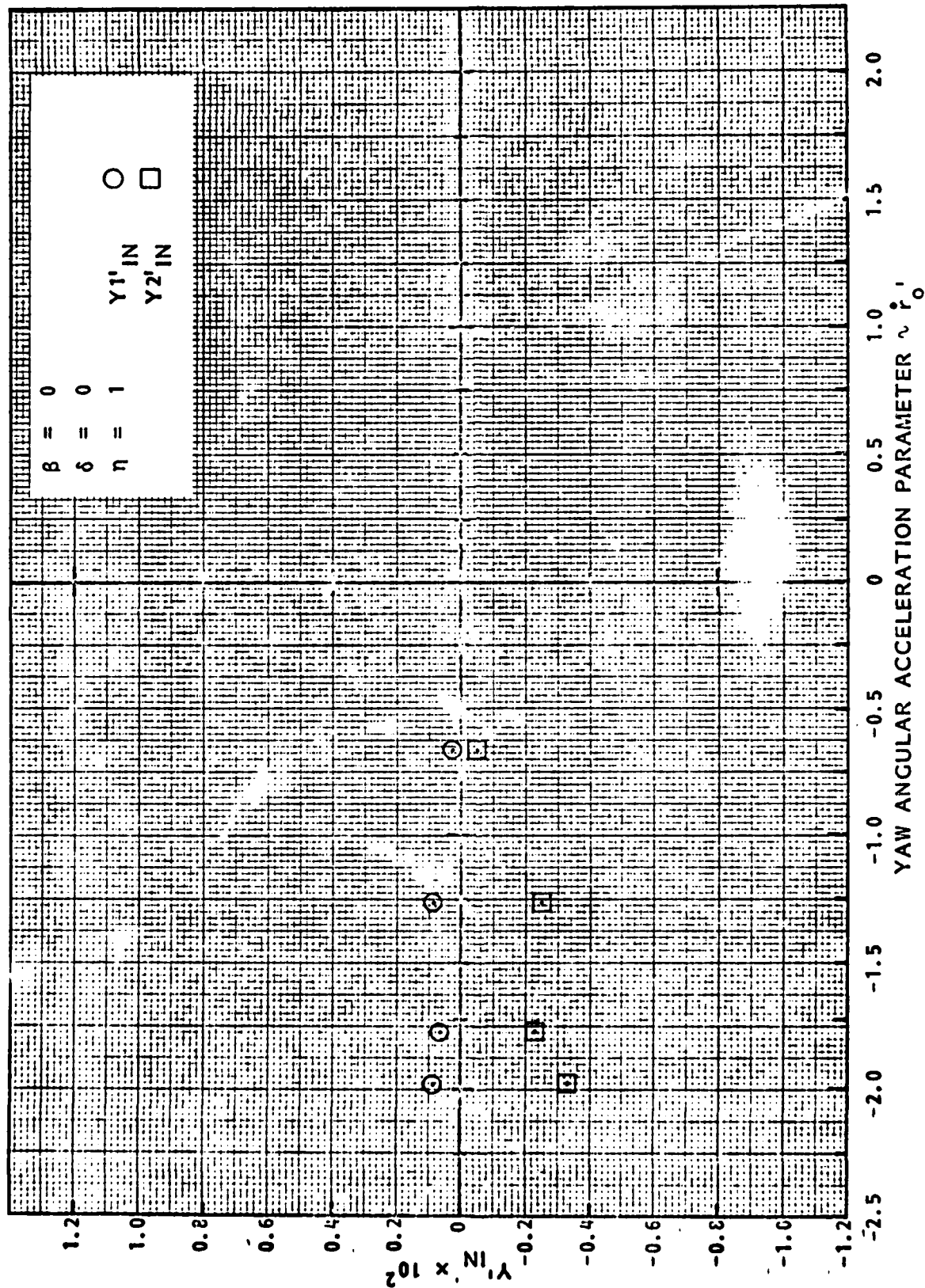


FIGURE A.83 - LATERAL FORCE GAGE IN-PHASE COEFFICIENTS AS FUNCTIONS OF YAW ANGULAR ACCELERATION FOR ASTERN MOTION AT $\eta = 1$ IN SHALLOW WATER, $H/T = 1.17$

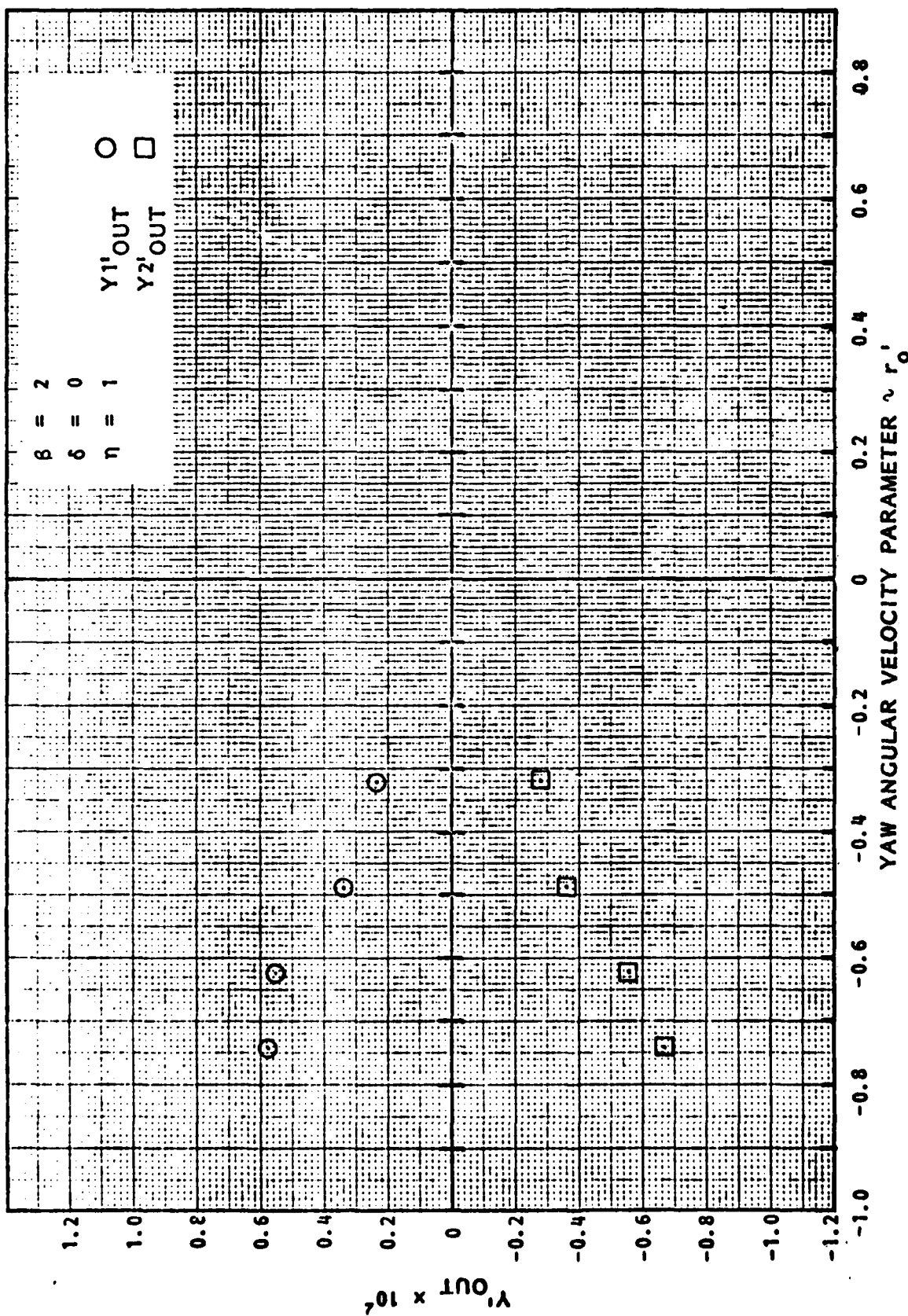


FIGURE A.84 - LATERAL FORCE GAGE OUT-OF-PHASE COEFFICIENTS AS FUNCTIONS OF YAW ANGULAR VELOCITY AT DRIFT ANGLE $\beta = 2$ DEGREES FOR AHEAD MOTION AT $\eta = 1$ IN SHALLOW WATER, $h/T = 1.17$

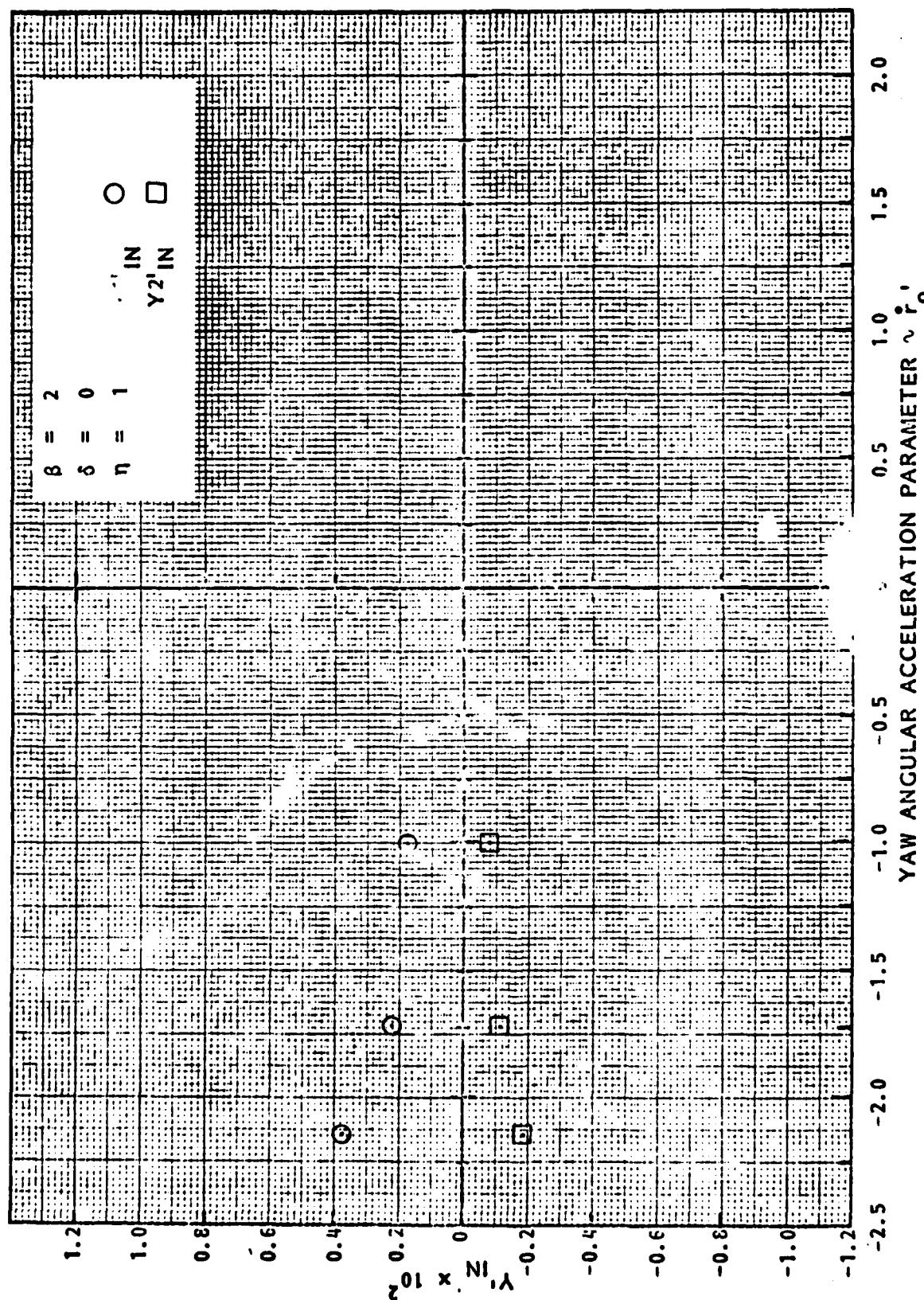


FIGURE A.85 - LATERAL FORCE GAGE IN-PHASE COEFFICIENTS AS FUNCTIONS OF YAW ANGULAR ACCELERATION AT DRIFT ANGLE $\beta = 2$ DEGREES FOR AHEAD MOTION AT $\eta = 1$ IN SHALLOW WATER, $H/T = 1.17$

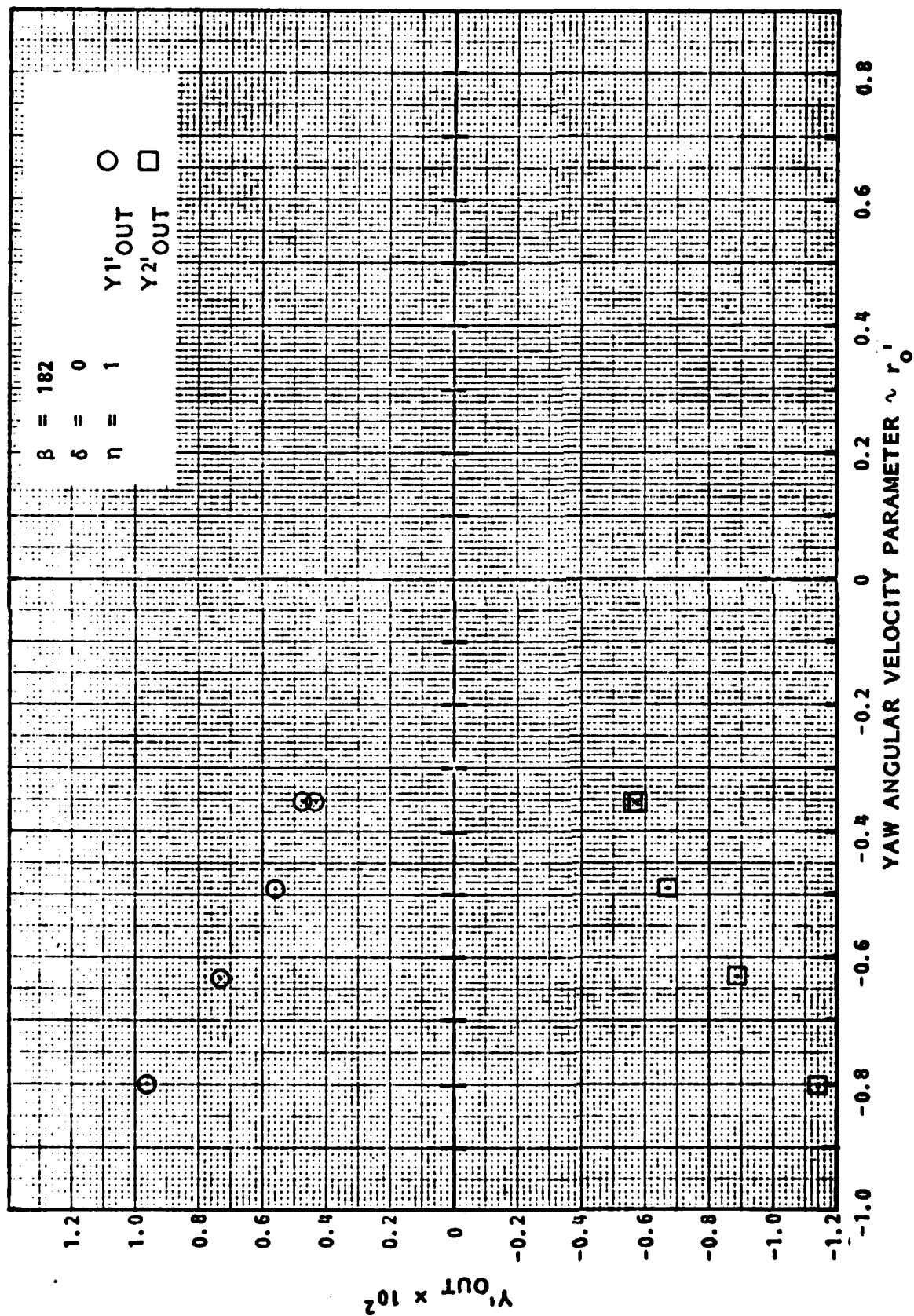


FIGURE A.86 - LATERAL FORCE GAGE OUT-OF-PHASE
 COEFFICIENTS AS FUNCTIONS OF YAW ANGULAR
 VELOCITY AT DRIFT ANGLE $\beta = 182$ DEGREES FOR
 ASTERN MOTION AT $\eta = 1$ IN SHALLOW WATER,
 $H/T = 1.17$

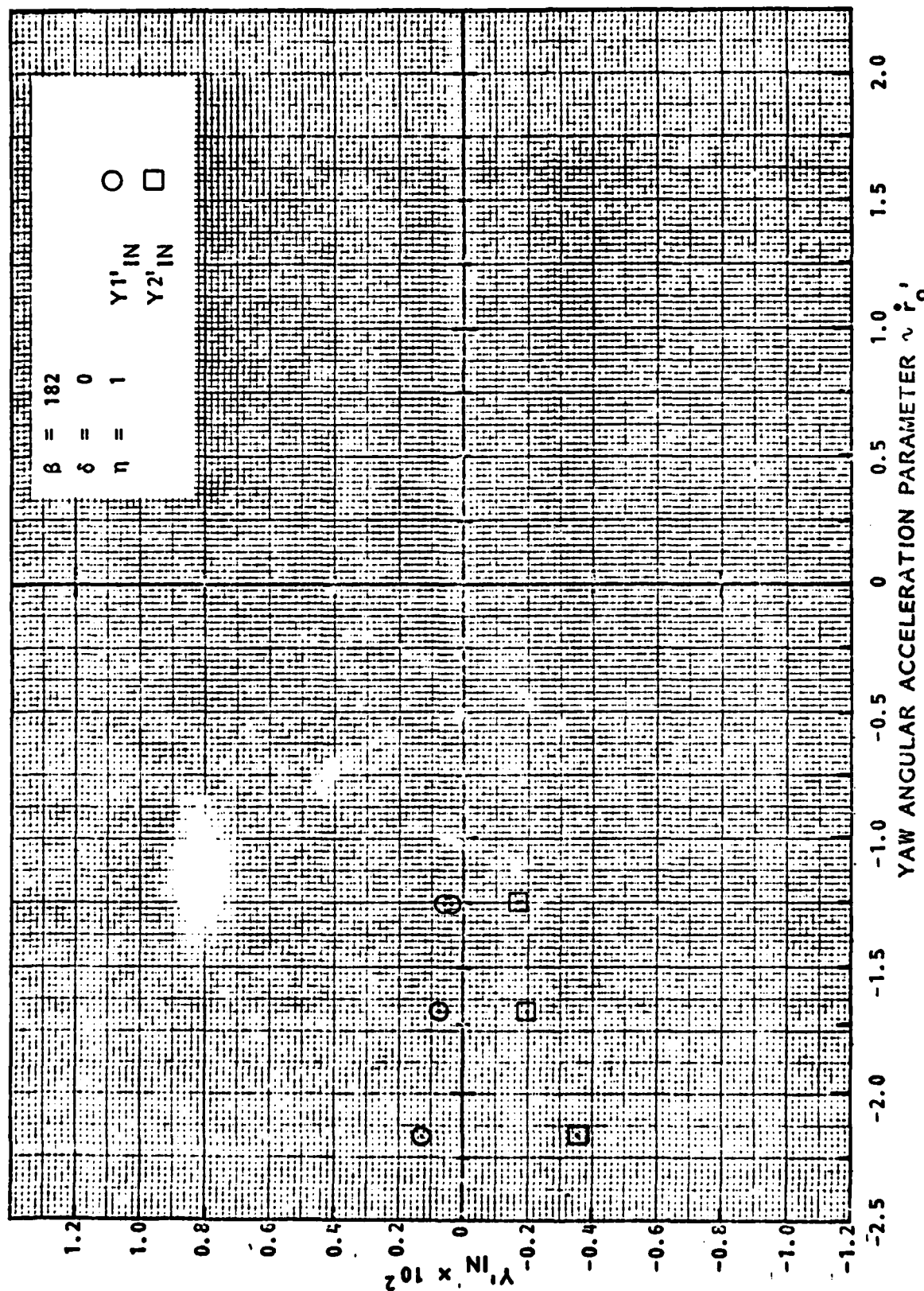


FIGURE A.87 - LATERAL FORCE GAGE IN-PHASE COEFFICIENTS AS FUNCTIONS OF YAW ANGULAR ACCELERATION AT DRIFT ANGLE $\beta = 182$ DEGREES FOR ASTERN MOTION AT $\eta = 1$ IN SHALLOW WATER, $H/T = 1.17$

Tracor Hydronautics

APPENDIX B

**PLANAR MOTION MECHANISM TEST DATA FOR 9.0 FOOT (PROTOTYPE) DRAFT
TOWBOAT WITH 15-BARGE TRAIN IN DEEP AND SHALLOW WATER**

Tracor Hydronautics

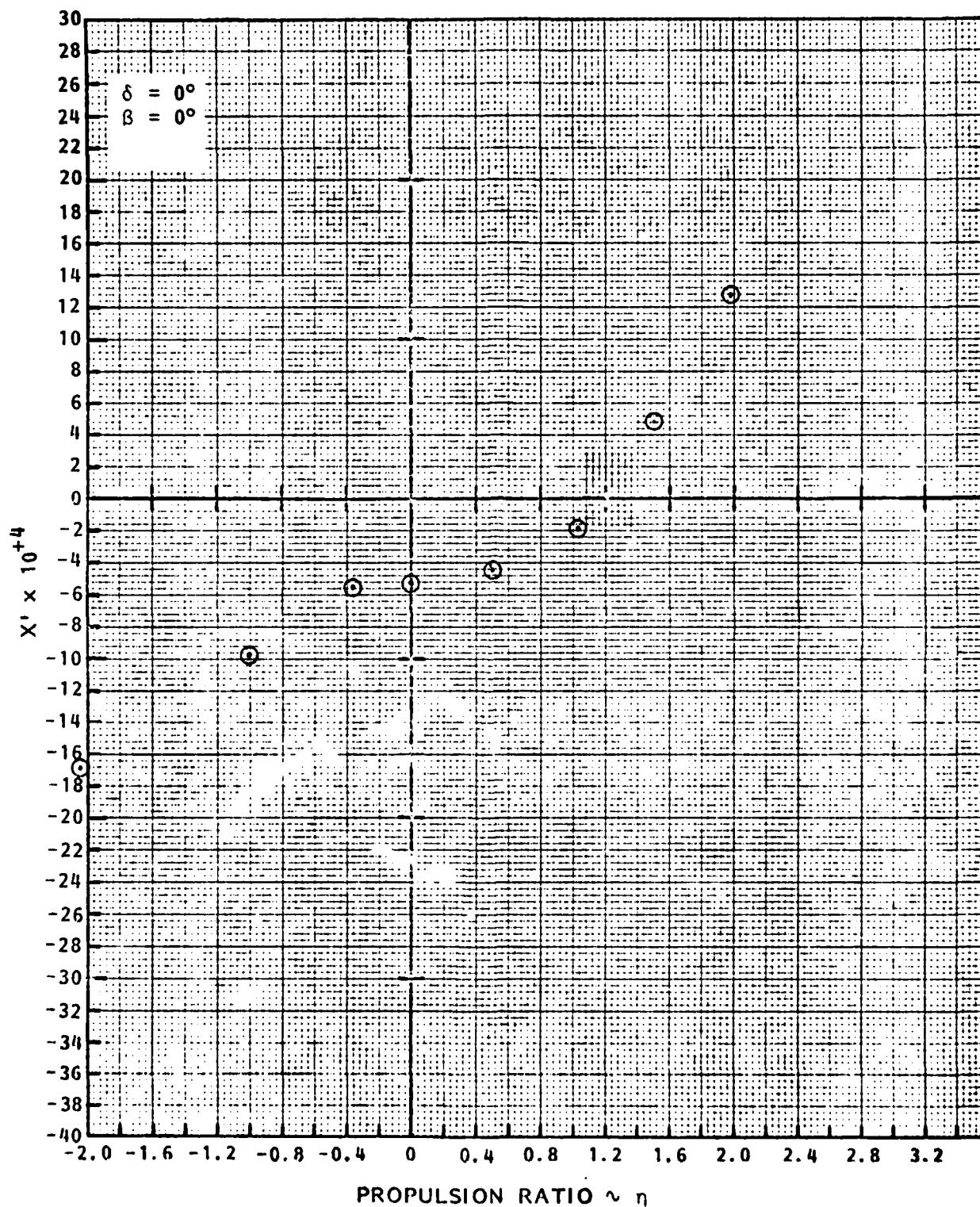


FIGURE B.1 - AXIAL FORCE COEFFICIENT AS FUNCTION OF PROPULSION RATIO η FOR AHEAD MOTION IN DEEP WATER

Tracor Hydronautics

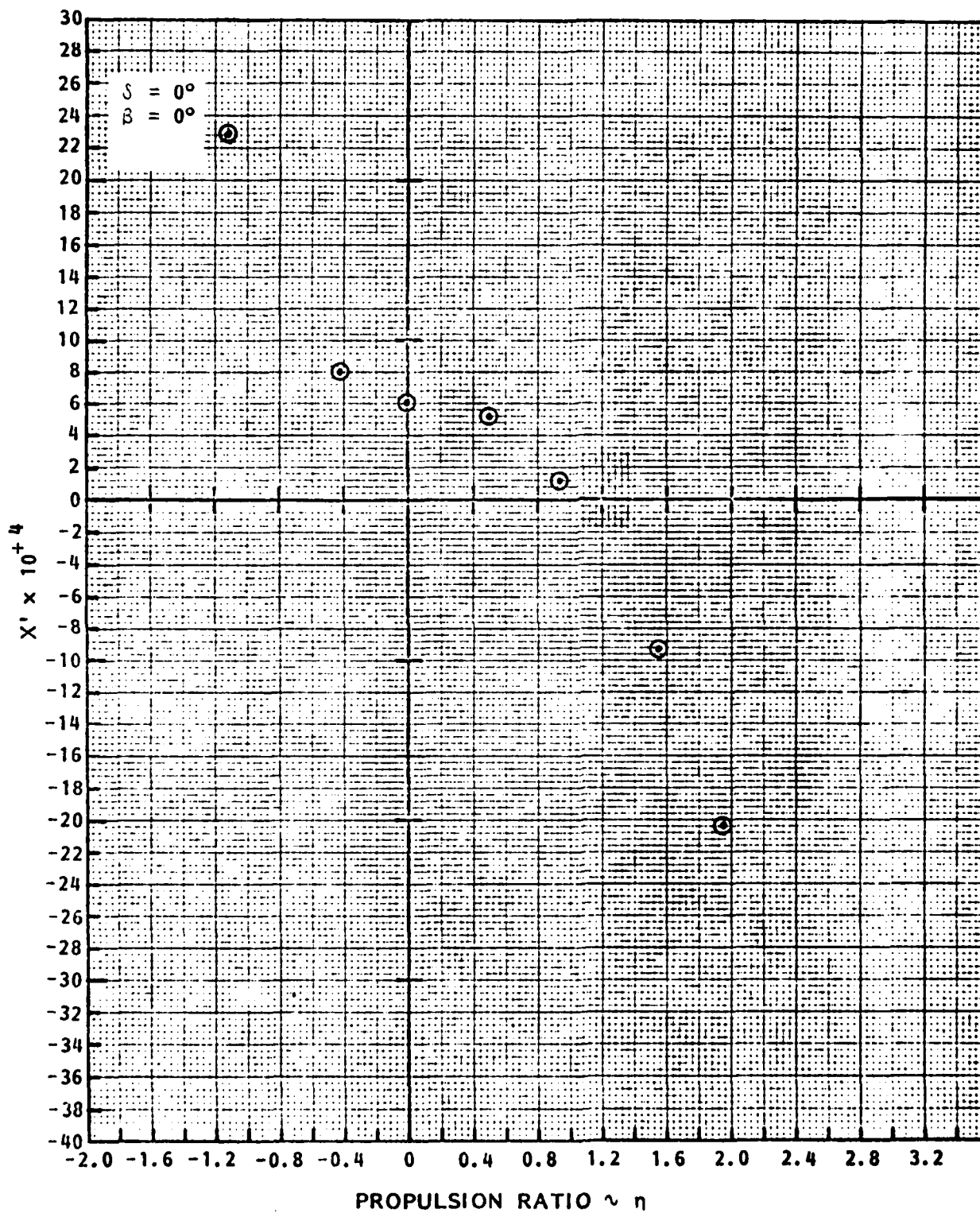


FIGURE B.2 - AXIAL FORCE COEFFICIENT AS FUNCTION OF PROPULSION RATIO η FOR ASTERN MOTION IN DEEP WATER

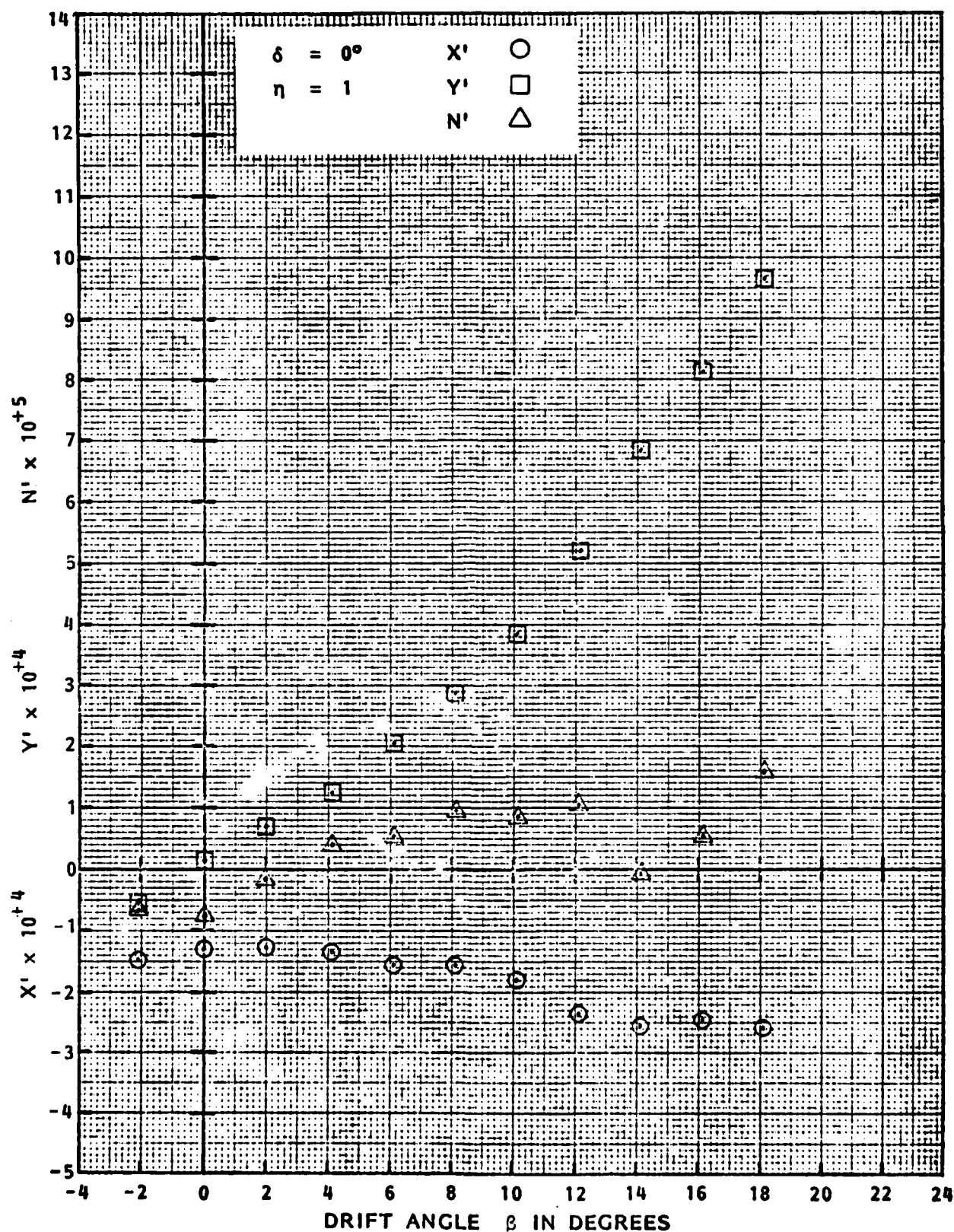


FIGURE B.3 - AXIAL FORCE, LATERAL FORCE, AND YAW MOMENT COEFFICIENTS AS FUNCTIONS OF DRIFT ANGLE β FOR AHEAD MOTION AT $\eta = 1$ IN DEEP WATER

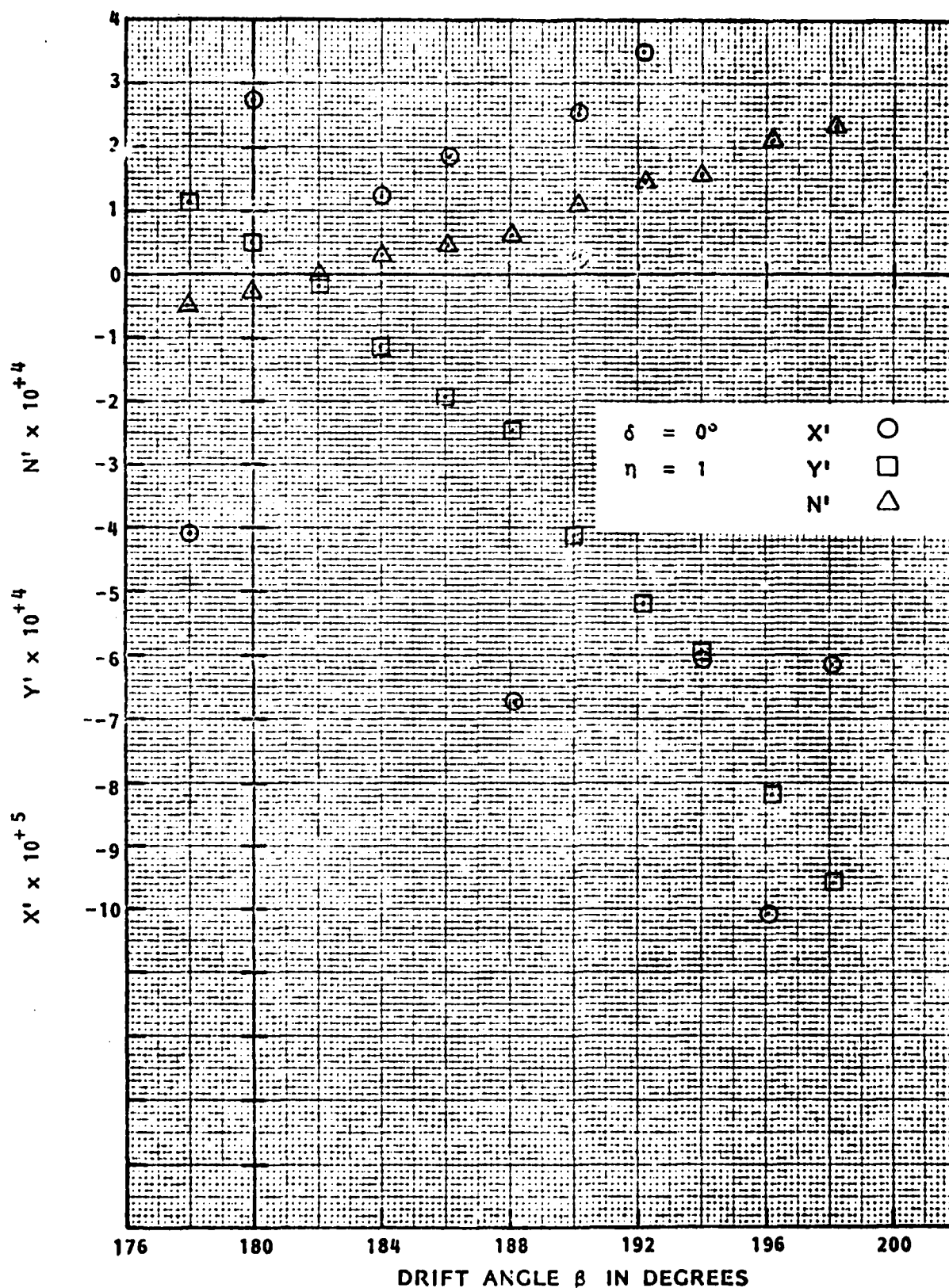


FIGURE B.4 - AXIAL FORCE, LATERAL FORCE, AND YAW MOMENT COEFFICIENTS AS FUNCTIONS OF DRIFT ANGLE β FOR ASTERN MOTION AT $\eta = 1$ IN DEEP WATER

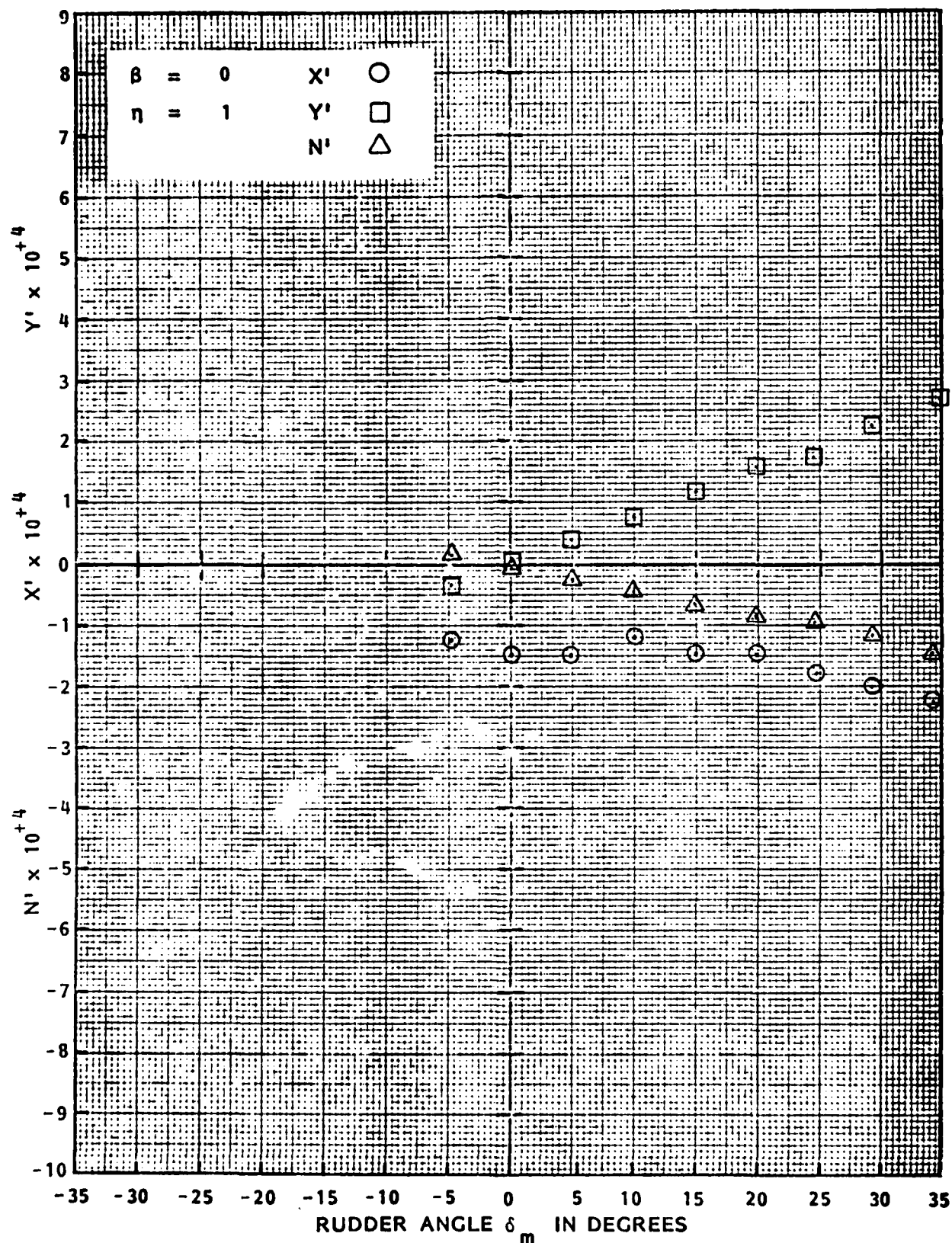


FIGURE B.5 - AXIAL FORCE, LATERAL FORCE AND YAW MOMENT COEFFICIENTS AS FUNCTIONS OF MAIN RUDDER ANGLE δ_m FOR AHEAD MOTION AT $\eta = 1$ IN DEEP WATER

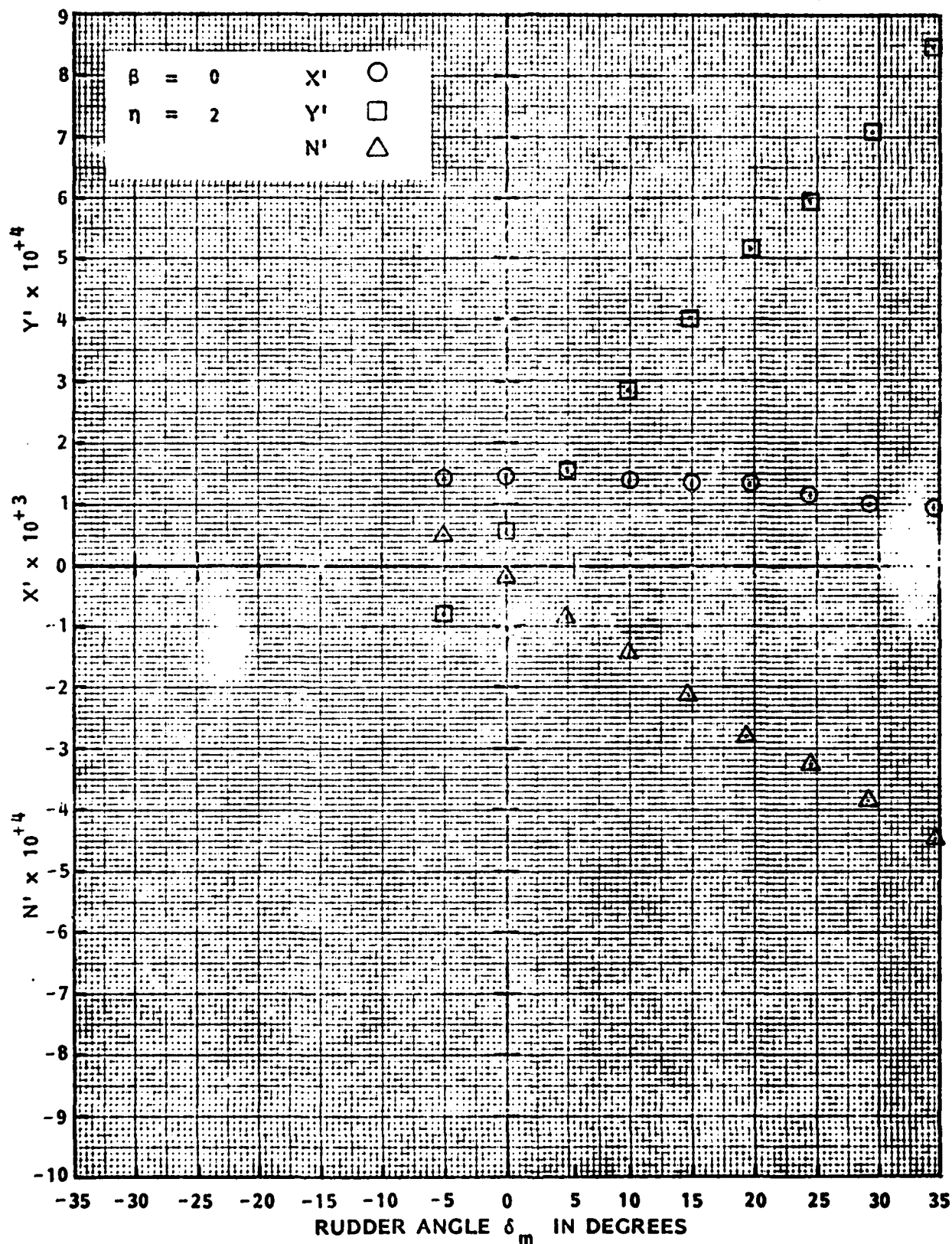


FIGURE B.6 - AXIAL FORCE, LATERAL FORCE AND YAW MOMENT COEFFICIENTS AS FUNCTIONS OF MAIN RUDDER ANGLE δ_m FOR AHEAD MOTION AT $\eta = 2$ IN DEEP WATER

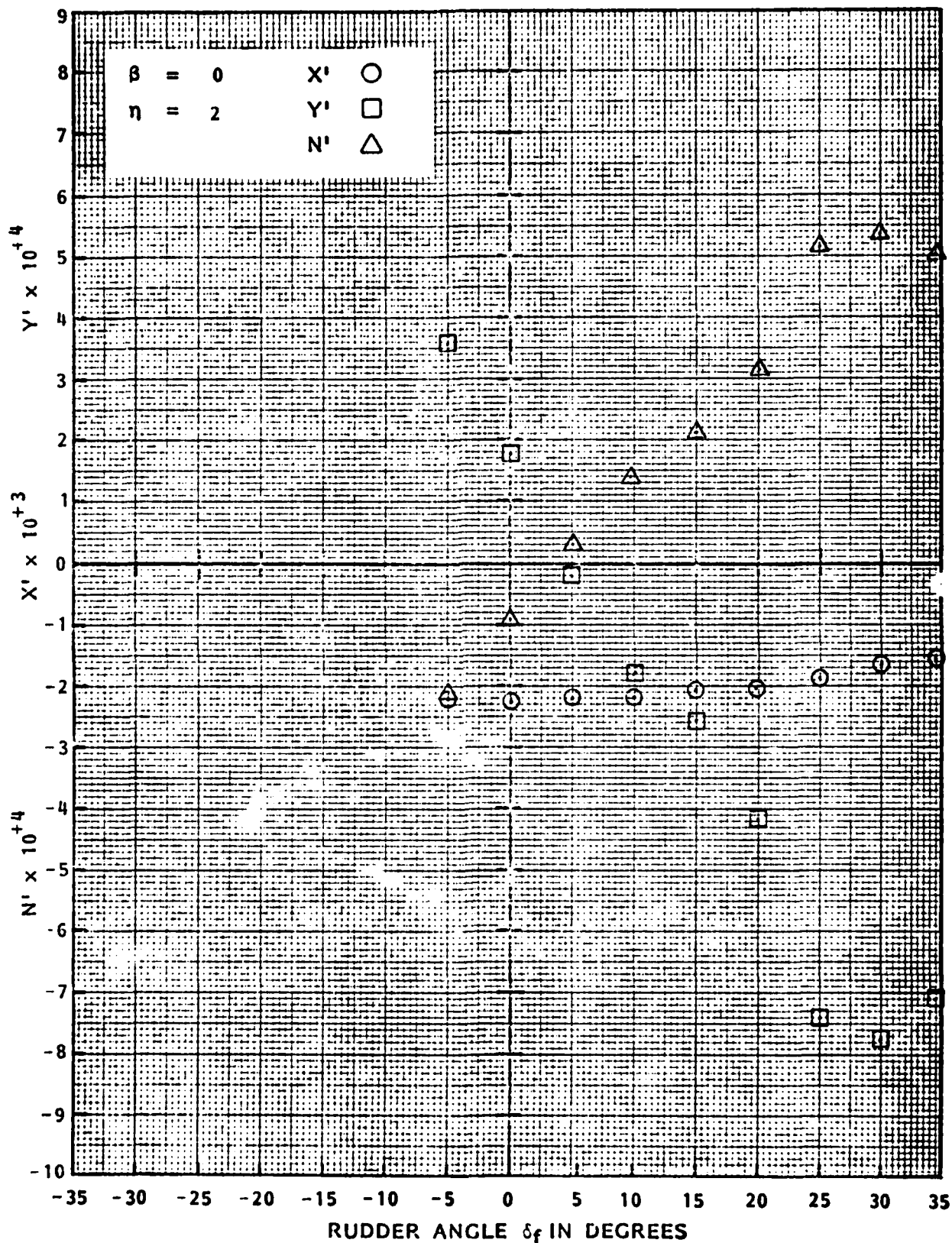


FIGURE B.7 - AXIAL FORCE, LATERAL FORCE AND YAW MOMENT COEFFICIENTS AS FUNCTIONS OF FLANKING RUDDER ANGLE δ_f FOR ASTERN MOTION AT $\eta = 2$ IN DEEP WATER

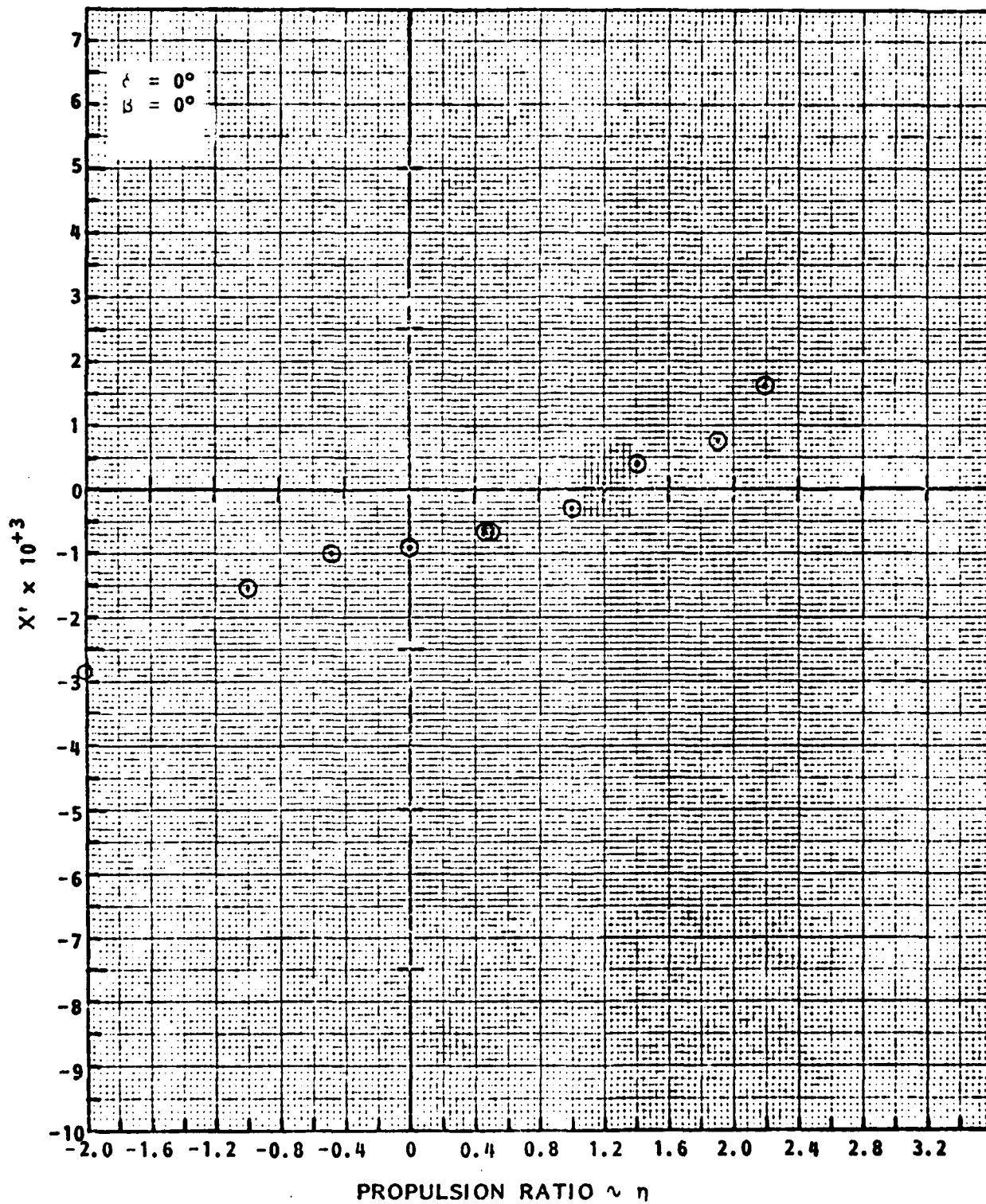


FIGURE B.8 - AXIAL FORCE COEFFICIENT AS FUNCTION OF PROPULSION RATIO η FOR AHEAD MOTION IN SHALLOW WATER, $H/T = 1.17$

Tracor Hydronautics

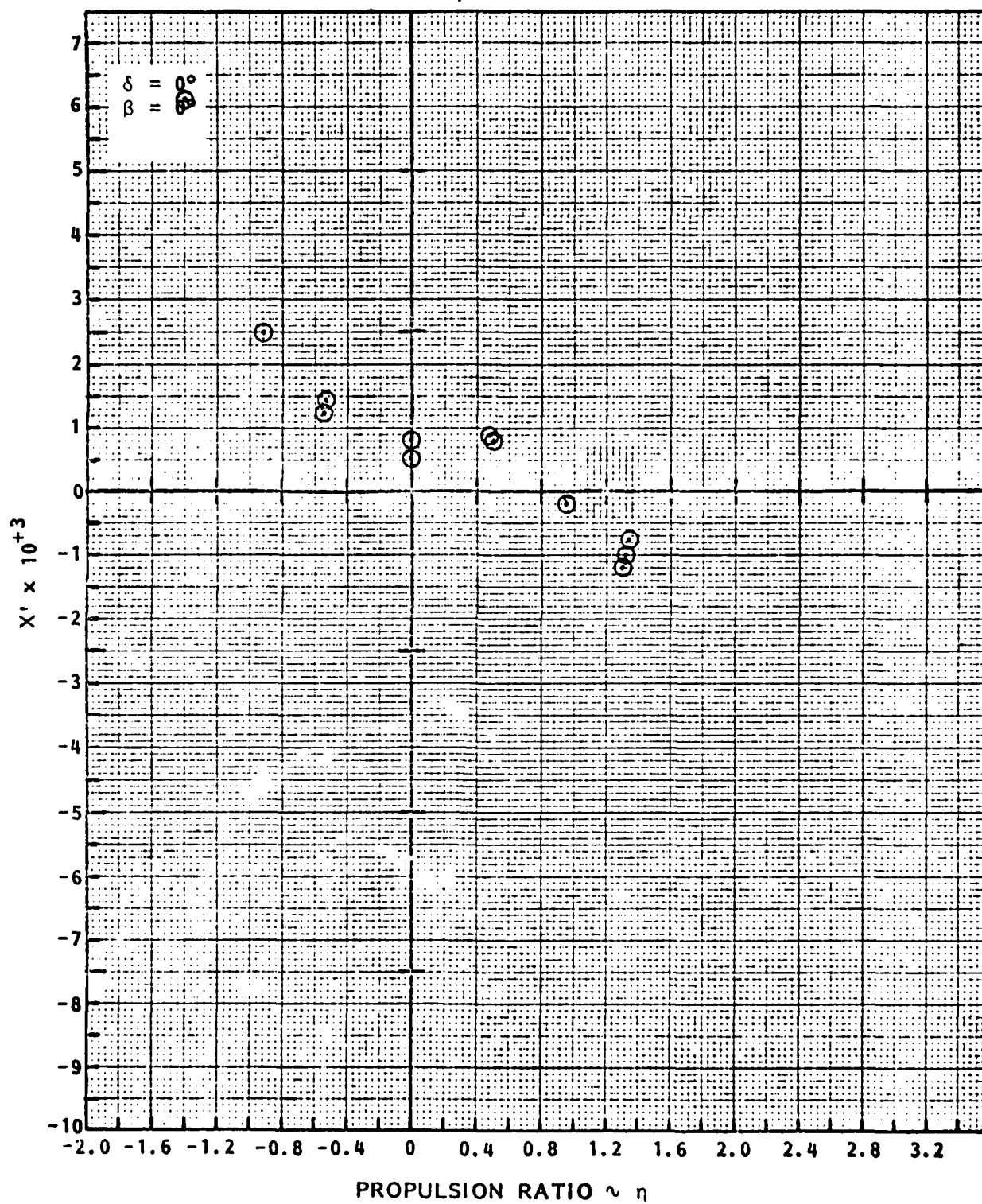


FIGURE B.9 - AXIAL FORCE COEFFICIENT AS FUNCTION OF PROPULSION RATIO η FOR ASTERN MOTION IN SHALLOW WATER, $H/T = 1.17$

Tracer Hydrodynamics

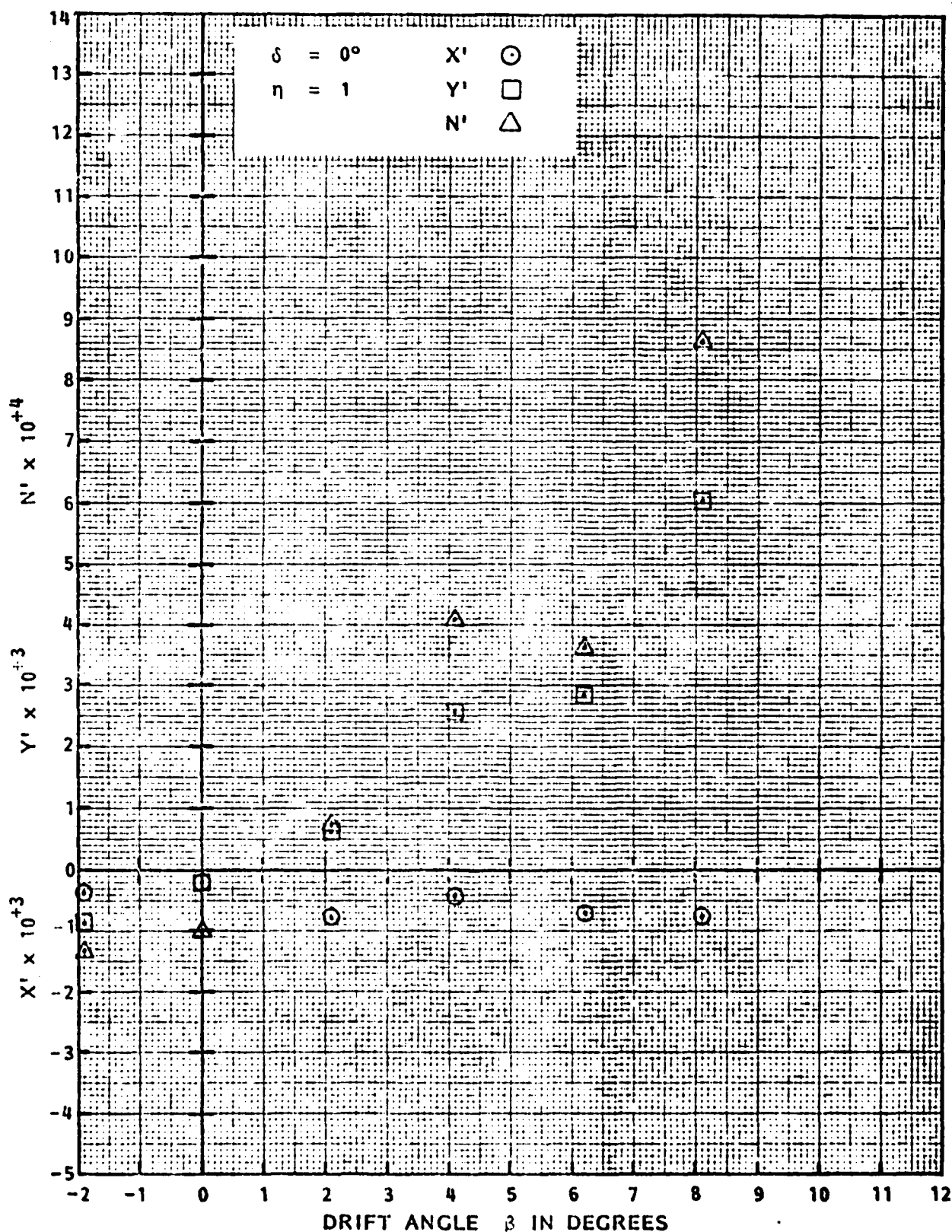


FIGURE B.10 - AXIAL FORCE, LATERAL FORCE, AND YAW MOMENT COEFFICIENTS AS FUNCTIONS OF DRIFT ANGLE β FOR AHEAD MOTION AT $\eta = 1$ IN SHALLOW WATER, $H/T = 1.17$

Tracor Hydronautics

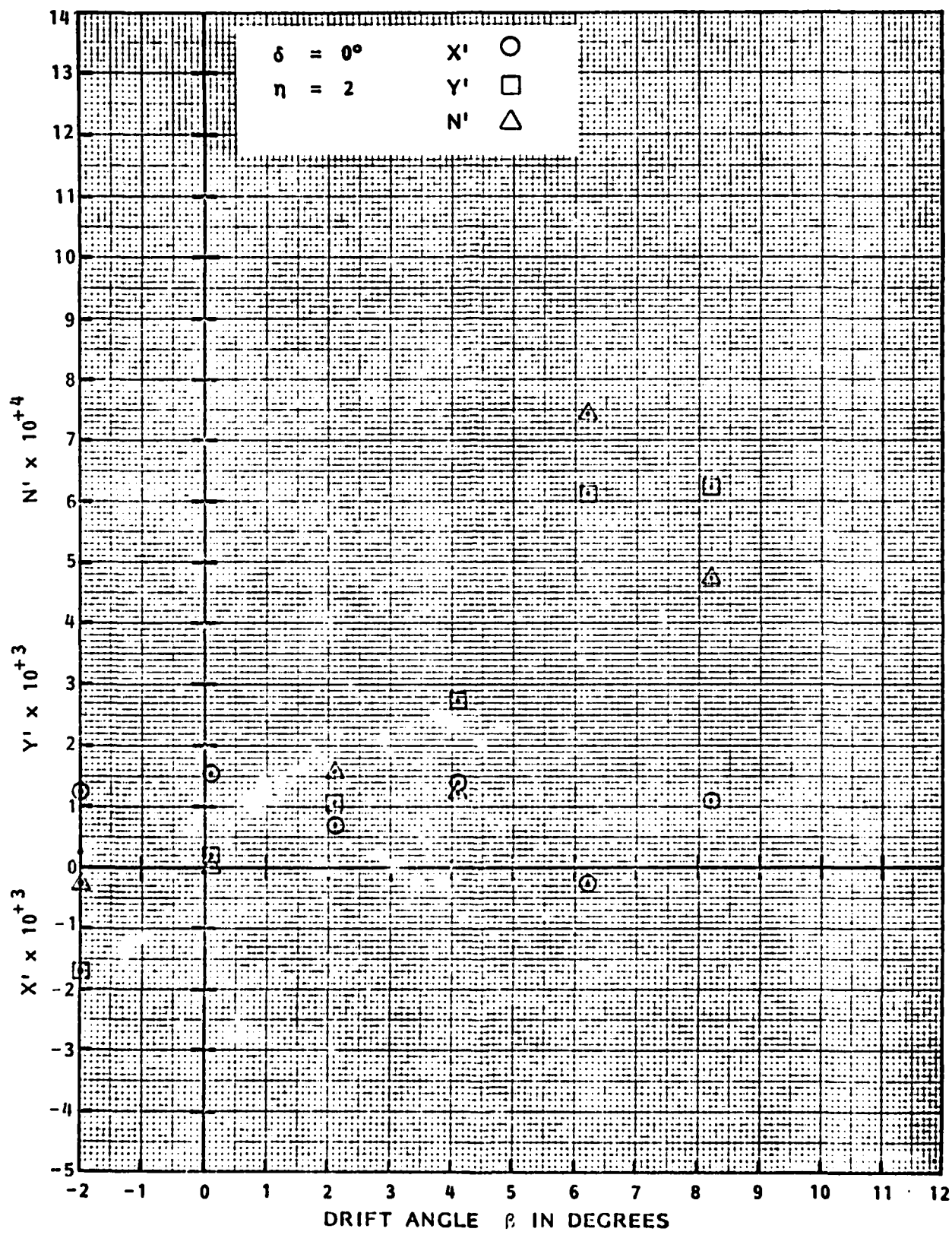


FIGURE B.11 - AXIAL FORCE, LATERAL FORCE, AND YAW MOMENT COEFFICIENTS AS FUNCTIONS OF DRIFT ANGLE β FOR AHEAD MOTION AT $\eta = 2$ IN SHALLOW WATER, $H/T = 1.17$

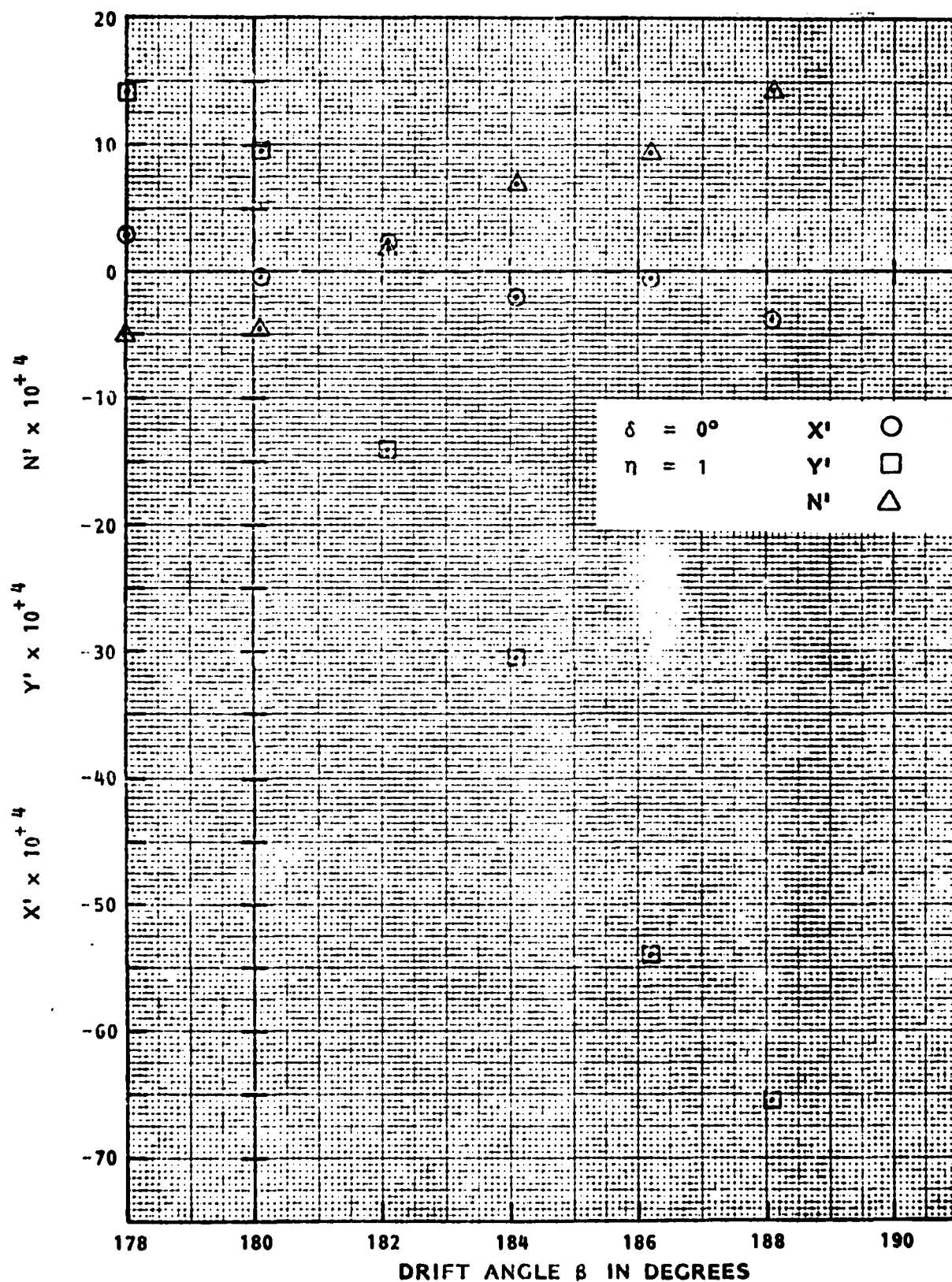


FIGURE B.12 - AXIAL FORCE, LATERAL FORCE, AND YAW MOMENT COEFFICIENTS AS FUNCTIONS OF DRIFT ANGLE β FOR ASTERN MOTION AT $\eta = 1$ IN SHALLOW WATER, $H/T = 1.17$

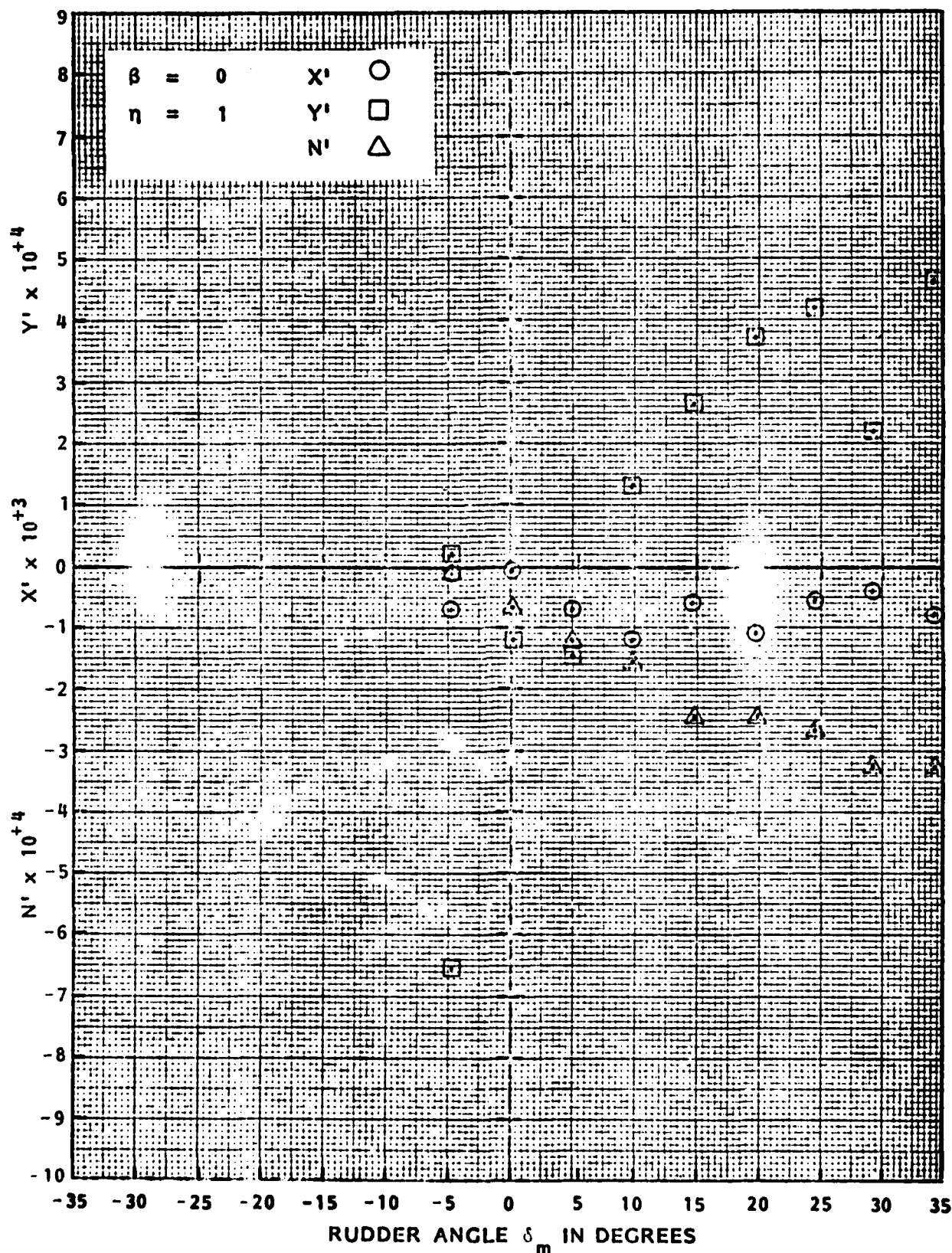


FIGURE B.13 - AXIAL FORCE, LATERAL FORCE AND YAW MOMENT COEFFICIENTS AS FUNCTIONS OF MAIN RUDDER ANGLE δ_m FOR AHEAD MOTION AT $\eta = 1$ IN SHALLOW WATER, $H/T = 1.17$

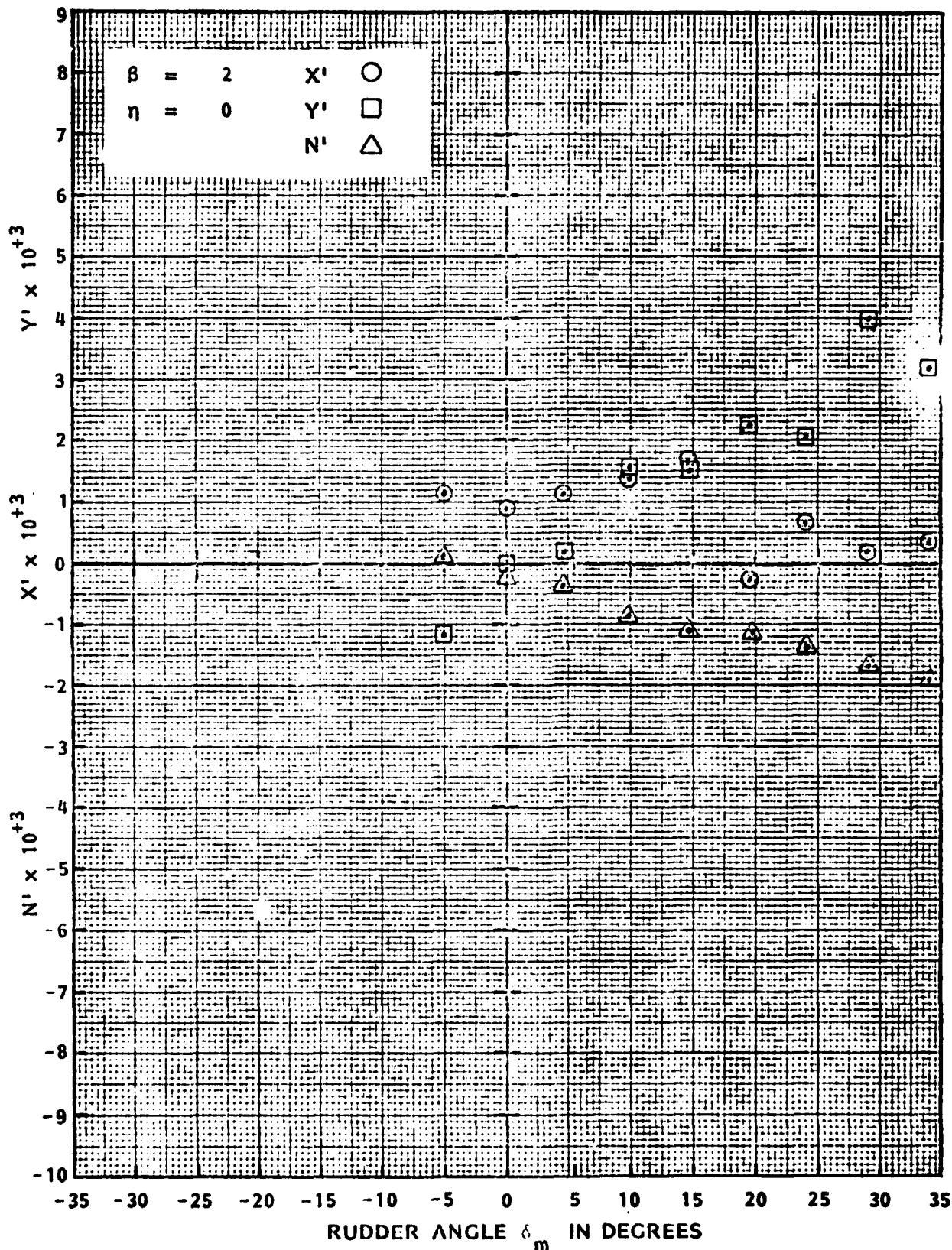


FIGURE B.14 - AXIAL FORCE, LATERAL FORCE AND YAW MOMENT COEFFICIENTS AS FUNCTIONS OF MAIN RUDDER ANGLE δ_m FOR AHEAD MOTION AT $\eta = 2$ IN SHALLOW WATER, $H/T = 1.17$

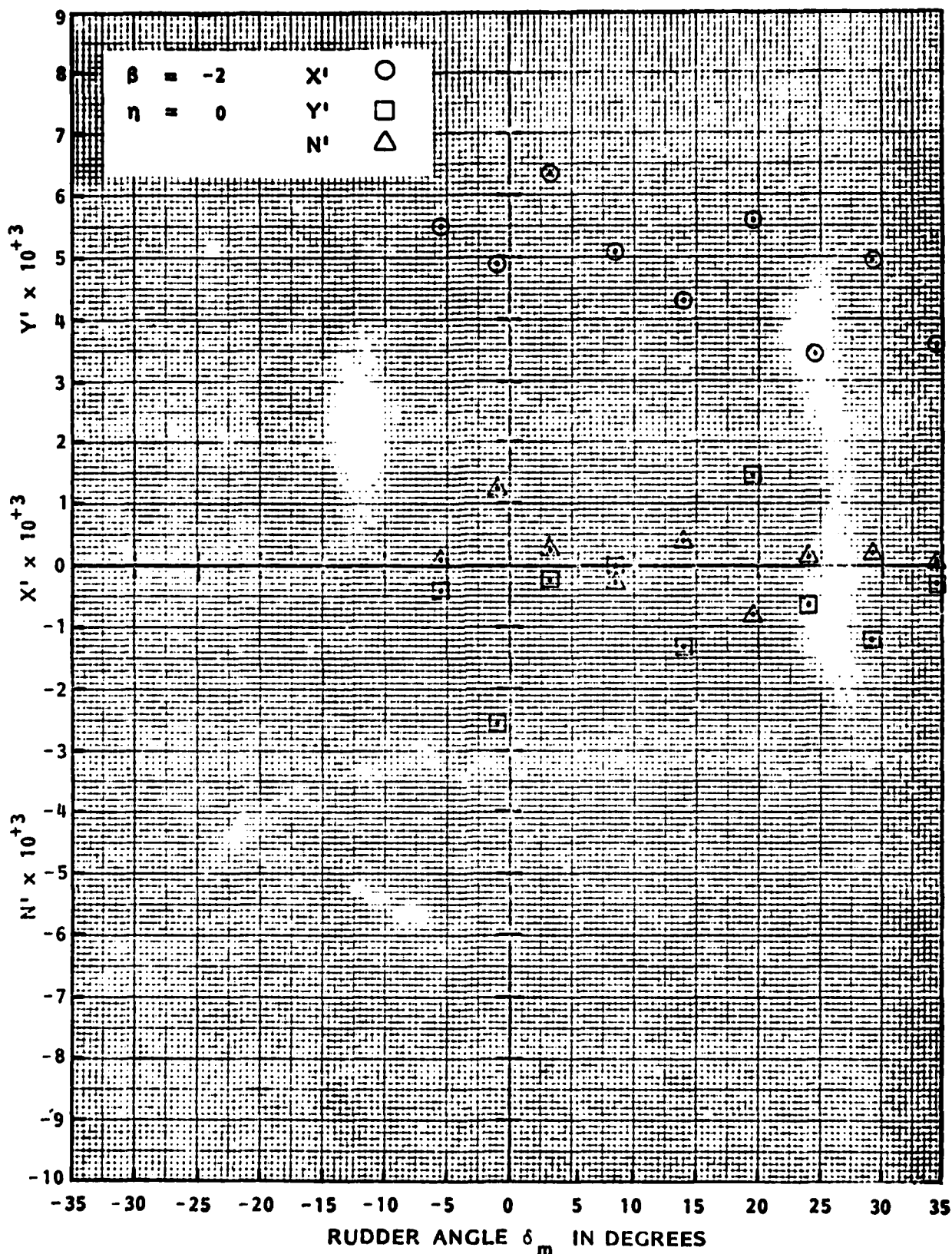


FIGURE B.15 - AXIAL FORCE, LATERAL FORCE AND YAW MOMENT COEFFICIENTS AS FUNCTIONS OF MAIN RUDDER ANGLE δ_m FOR ASTERN MOTION AT $\eta = -2$ IN SHALLOW WATER, $H/T = 1.17$

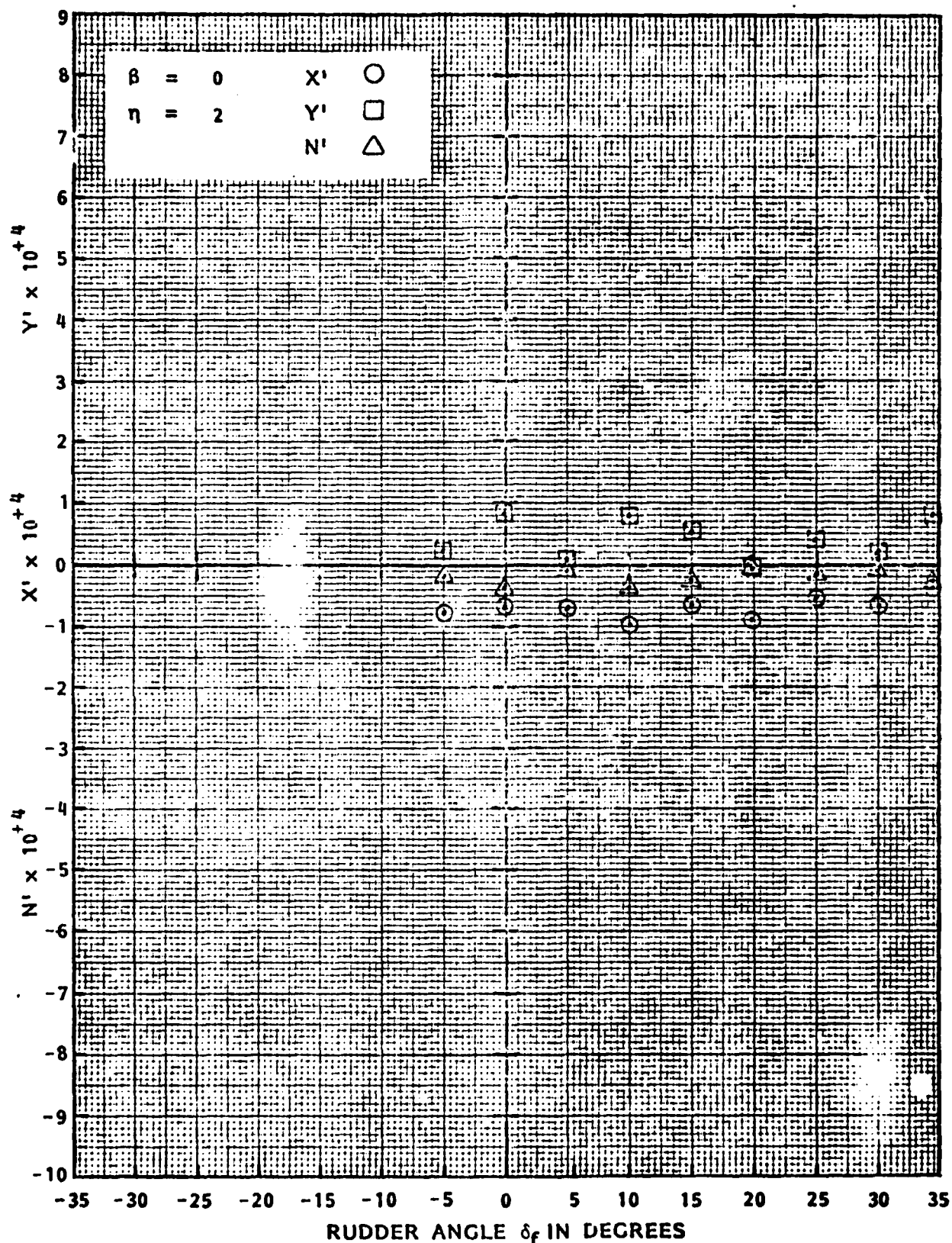


FIGURE B.16 - AXIAL FORCE, LATERAL FORCE AND YAW MOMENT COEFFICIENTS AS FUNCTIONS OF FLANKING RUDDER ANGLE δ_f FOR ASTERN MOTION AT $\eta = 2$ IN SHALLOW WATER, $H/T = 1.17$

Tracor Hydronautics

APPENDIX C

**MATHEMATICAL MODEL, NON-DIMENSIONAL HYDRODYNAMIC COEFFICIENTS,
AND METHODS OF ANALYSIS USED AT TRACOR HYDRONAUTICS FOR SURFACE
SHIP MANEUVERING PREDICTIONS**

APPENDIX C

MATHEMATICAL MODEL, NON-DIMENSIONAL HYDRODYNAMIC COEFFICIENTS, AND METHODS OF ANALYSIS USED AT TRACOR HYDRONAUTICS FOR SURFACE SHIP MANEUVERING PREDICTIONS

The mathematical model, non-dimensional hydrodynamic coefficients, and methods of analysis used at Tracor Hydronautics for surface ship maneuvering predictions are described in this appendix.

C.1 - Mathematical Model for Ship Maneuvering Simulation Studies

The basic mathematical model used for the maneuvering of twin-screw ships consists of coupled differential equations in three degrees of freedom (surge, sway, and yaw), which describe the motions in the x-y plane, and the complete set of hydrodynamic coefficients and external forces which are required to numerically integrate these equations. There are also auxiliary equations which describe the response of the steering and propulsion system to external inputs.

A complete set of three differential equations with all of the terms necessary to simulate normal maneuvers of surface ships is presented in Reference 3. These equations are based on a full six degree of freedom set of equations developed by the U. S. Navy for the simulation of submarine motions. For maneuvering studies of twin-screw ships in the presence of current and wind, this basic surface ship maneuvering simulation

Tracor Hydronautics

was modified as described in Reference 8 to include the following additional features:

- a. Simulation of ahead and astern motions with continuous operation through zero speed;
- b. Representation of both steering and flanking rudders;
- c. Representation of twin propellers with differential thrust;
- d. Special attention to low speed hydrodynamics including rudder propeller interactions, such as the rudder kick effect;
- e. Spatially varying current;
- f. Wind; and
- g. Simplified representations of propulsion and steering gear dynamics.

Sign conventions, a simulation program flow diagram, and notation are given in Figures C.1 and C.2, and the report NOTATION section.

Relative velocities ($U_R = U - U_C$, $V_R = V - V_C$) and relative yaw rate ($r_R = r - r_C$) can be calculated by the vector addition of the inertial velocities (U , V) and inertial yaw rate (r), and the current velocities (U_C , V_C) and current yaw rate (r_C). In the numerical integration a matrix of current speeds (U_{Cij}) and directions (ψ_{Cij}) at points on the X , Y plane is defined. Based on the location of the bow (X_B , Y_B) midships (X_M , Y_M) and stern (X_S , Y_S) of the ship, an interpolation in the current speed and direction matrix is carried out to obtain the current speed and direction at the bow (U_{CB} , ψ_{CB}), midships (U_{CM} , ψ_{CM}), and stern (U_{CS} , ψ_{CS}). The following relationships then apply:

Tracor Hydronautics

$$\begin{aligned}
 u_{CB} &= U_{CB} \cos (\psi_{CB} - \psi) & v_{CB} &= U_{CB} \sin (\psi_{CB} - \psi) \\
 u_{CM} &= U_{CM} \cos (\psi_{CM} - \psi) & v_{CM} &= U_{CM} \sin (\psi_{CM} - \psi) \\
 u_{CS} &= U_{CS} \cos (\psi_{CS} - \psi) & v_{CS} &= U_{CS} \sin (\psi_{CS} - \psi) \\
 u_C &= \frac{u_{CB} + u_{CM} + u_{CS}}{3} & v_C &= \frac{v_{CB} + v_{CM} + v_{CS}}{3} \quad [C-1]
 \end{aligned}$$

$$r_C = \frac{v_{CB} - v_{CS}}{L}$$

$$u_R = u - u_C \quad v_R = v - v_C \quad r_R = r - r_C$$

In Equation set [C-1] the mean longitudinal and lateral current velocities in the body axis system are obtained from the average of values at the bow, midships and stern. The variation of lateral velocity along the ship is accounted for by an apparent current yaw rate defined by the difference in the lateral velocities at the bow and stern divided by length. This assumed the lateral velocity varies linearly from bow to stern.

The equations of motion formulated for the ship are as follows:

$$U_R = \sqrt{u_R^2 + v_R^2} \quad [C-2]$$

$$v_R = -U_R \sin \beta_R \quad [C-3]$$

$$u_R = U_R \cos \beta_R \quad [C-4]$$

$$\beta_R = \arctan \left(\frac{v_R}{u_R} \right) \quad [C-5]$$

AXIAL FORCE

$$\begin{aligned}
 m(\dot{u}-v\dot{r}-x_G\dot{r}^2) = & \frac{\rho}{2} L^3 [(X_0'\dot{u}_R + (X_{VR}'|\cos \beta_R| - X_0' |\sin \beta_R|) v_R \dot{r}_R)] + \frac{\rho}{2} L^4 (X_{rr}' \dot{r}_R^2) \\
 & + \frac{\rho}{2} L^2 (X_{VV}' v_R^2) + \frac{\rho}{2} L^2 u_R^2 \left(a_i + \frac{b_i}{2} \eta_s + \frac{c_i}{2} \eta_s^2 + \frac{b_i}{2} \eta_s + \frac{c_i}{2} \eta_p^2 \right) \\
 & + \frac{\rho}{2} L^2 \left[\frac{X_{VV}\eta'}{2} (\eta_s - 1) + \frac{X_{VV}\eta'}{2} (\eta_p - 1) \right] v_R^2 \\
 & + \frac{\rho}{2} L^2 X_A' u_A^2 + \frac{\rho}{2} L^2 \left[u_P^2 \left(\frac{X_{RUD}' \delta_S^2 + X_{\delta_F \delta_F}' \delta_f^2}{2} \right) + u_{PS}^2 \left(\frac{X_{RUD}' \delta_S^2 + X_{\delta_F \delta_F}' \delta_f^2}{2} \right) \right] \quad [C-6]
 \end{aligned}$$

where:

$$X_{RUD}' = X_{\delta_S \delta_S}' (1 + \bar{v}_{RUD} \cdot Y_{\delta_S} |v|' / Y_{\delta_S}') \quad [C-7]$$

$$\bar{v}_{RUD} = |v_R + r_R X_S| u_R / u_{RUD}^2 \quad [C-8]$$

$$u_{RUD}^2 = u^2 + (v + r X)^2 \quad [C-9]$$

$$X_S = L N_{\delta_S}' / Y_{\delta_S}' \quad [C-10]$$

LATERAL FORCE

$$\begin{aligned}
 m(\dot{\phi} + u\dot{r} + x_G \ddot{t}) = & \frac{\rho}{2} L^4 (Y_{\dot{r}}' \ddot{r} + Y_{\dot{r}}' \dot{r} |r| + \frac{\rho}{2} L^3 (Y_{\dot{\phi}}' \dot{\phi} \\
 & + \frac{\rho}{2} L^3 (Y_{\dot{r}}' u_R \dot{r} + Y_{\dot{v}}' v_R |r| + \frac{\rho}{2} L^2 v_A^2 Y_A' + \frac{\rho}{2} L^4 (Y_{v\dot{r}}'^2 v_R \dot{r}^2 / u_R) \\
 & + \frac{\rho}{2} L^2 (Y_{\dot{v}}' u_R v_R + Y_{\dot{v}}' v_R |v| + Y_{v\dot{v}}' u_R v_R (\frac{\eta_S + \eta_D}{2} - 1)) \\
 & + \frac{\rho}{2} L^2 [Y_{\dot{v}}' v |v| \eta + v_R |v_R| (\frac{\eta_S + \eta_D}{2} - 1)] + \frac{\rho}{2} L^3 Y_{\dot{r}}' \eta u_R \dot{r} (\frac{\eta_S + \eta_D}{2} - 1) \\
 & + \frac{\rho}{2} L^2 [u_{pP}^2 \cdot (\frac{Y_{RUC}' \delta_S + Y_{\delta_F}' \delta_F}{2} + u_{pS}^2 (\frac{Y_{RUD}' \delta_S + Y_{\delta_F}' \delta_F}{2}))] \\
 & + \frac{\rho}{2} L^2 [w_{pP}^2 (\frac{Y_{\dot{r}}'}{2}) + w_{pS}^2 (\frac{Y_{\dot{r}}'}{2})]
 \end{aligned}
 \tag{C-11}$$

where:

$$Y_{RUD}' = Y_{\delta_S}' + \bar{v}_{RUD} Y_{\delta_S}' |v|'$$

[C-12]

$$u_p^2 = (du_{RUD}^2 + eDn u_{RUD} + fD^2 n^2) \text{ where } n = \text{Prop RPM}$$

[C-13]

$$\eta = \text{Propulsion Ratio} = (n/u_R)/(n_C/u_C)$$

[C-14]

$$w_p^2 = (a_w u_{RUD} + b_w Dn u_{RUD} + c_w D^2 n^2)$$

[C-15]

YAWING MOMENT

$$\begin{aligned}
 I_z \ddot{\phi} + m x_G (\dot{\phi} - u r) = & \frac{\rho}{2} L^5 (N_z' \dot{\phi} + N_r' r + N_{rr}' r^2) \left\{ 1 + 2 \left[1 - \tanh \left| \frac{2 u r}{r_L L} \right| \right] \right\} + \frac{\rho}{2} L^4 N_{\phi}'' \dot{\phi} \\
 & + \frac{\rho}{2} L^4 (N_z' u_r r + N_r' |v| r + N_{rr}' v r) + \frac{\rho}{2} L^5 (N_{v r^2}' v r^2 + N_{r r^2}' v r^2 / u_r \\
 & + \frac{\rho}{2} L^4 (N_{r r}'' u_r r) \left(\frac{\eta_S + \eta_P}{2} - 1 \right) \\
 & + \frac{\rho}{2} L^3 (N_{v r}'' u_r v + N_v' |v| v + N_{r r}' v r) \left(\frac{\eta_S + \eta_P}{2} - 1 \right) \\
 & + \frac{\rho}{2} L^3 \left[u_{p p}^2 \left(\frac{N_{r u d}' \delta_S + N_{\phi_P}' \delta_P}{2} \right) + u_{p_S}^2 \left(\frac{N_{r u d}' \delta_S + N_{\phi_P}' \delta_P}{2} \right) \right] \\
 & + \frac{\rho}{2} L^3 (N_v' u_r v + N_v' |v| v + N_{r r}' v r) + \frac{\rho_A}{2} L^3 N_A'' u_A^2 \\
 & + \frac{\rho}{2} L^2 u_r^2 \left[- y_S \left(\frac{b_1}{2} \eta_S + \frac{c_1}{2} \eta_S^2 \right) + y_P \left(\frac{b_1}{2} \eta_P + \frac{c_1}{2} \eta_P^2 \right) \right] \\
 & + \frac{\rho}{2} L^3 \left[w_{p p}^2 \left(\frac{N_A''}{2} \right) + w_{p_S}^2 \left(\frac{N_A''}{2} \right) \right]
 \end{aligned}$$

where:

$$N_{r u d}' = N_{\phi_S}' + \bar{v}_{r u d} N_{\phi_S}' |v|$$

[C-16]

[C-17]

Tracor Hydronautics

Modifications to the equations of motion presented in Reference 3 which have been incorporated in the preceding equations primarily describe hull-propeller-rudder interactions. These effects are discussed in the following paragraphs.

Total rudder force and moment are calculated using the equation:

$$Y_{RUD} = \frac{\rho}{2} L^2 u_p^2 (Y_{\delta_s}' + Y_{\delta_s}|v|' \bar{V}_{RUD}) \quad [C-18]$$

where the velocity u_p , defined by:

$$u_p^2 = (dU_{RUD}^2 + eDnU_{RUD} + fD_2n^2) \quad [C-19]$$

is a function of the absolute velocity at the rudder location:

$$U_{RUD} = \sqrt{u_R^2 + (V_R + r_R X_s)^2} \quad [C-20]$$

as well as propeller RPS, r . Coefficients d , e , and f , in addition to coefficients $X_{\delta_s}\delta_s'$, Y_{δ_s}' , and N_{δ_s}' are obtained from curve fits of test data when ship drift angle and yaw rate are zero.

In realistic maneuvers, the ship may operate both ahead and astern and, in some cases, at very large drift angles. In order to properly represent the hydrodynamic forces and moments which act in such conditions, different sets of hydrodynamic coefficients are used depending on the relative drift angle β_R . These can be noted in Tables 10 to 16 in which the hydrodynamic coefficients from the model tests are presented. Most coefficients depend on both the direction of motion and the drift angle. In order to obtain a better representation of the steady side force and yawing moment at drift angles near 90 and 270 degrees, certain coefficients are given an addition value for large drift angles.

Tracor Hydronautics

The product of the coefficient $Y_{\delta_s|v}'$ and the non-dimensional velocity ratio:

$$\bar{V}_{RUD} = |v_R + r_R x_R| u_R / U_{RUD}^2 \quad [C-21]$$

represents the influence of cross flow on the rudder. This product is derived from test data at non-zero drift angles. It has been assumed that the rudder resistance due to the cross-flow will be proportional to this component of lateral rudder force.

The surge equation includes a term X_{rr}' , the longitudinal component of the hydrodynamic force due to yaw rate. This term is obtained from the PMM dynamic test data at pure yawing. The axial force equation of motion includes all the longitudinal forces while the ship is swaying and yawing (X_{vv}' , X_{vr}' , and X_{rr}'). Measurements conducted at DTNSRDC in the rotating arm facility on models at very large drift angles show that the value of X_{vr} is small in these regimes. Based on these data and on theoretical analysis the X_{vr} component is approximated by the sum:

$$X_{vr} = \frac{\rho}{2} L^3 [X_{vr}' |\cos \beta_R| - X_{\dot{u}}' |\sin \beta_R|] v_R r_R \quad [C-22]$$

which satisfactorily describes this force for all drift angles.

Asymmetric forces and moments defined by the non-dimensional coefficients Y_{\star}' and N_{\star}' are based on a velocity similar to that used for the rudder forces:

$$W_p^2 = a_w U_{RUD}^2 + b_w D n U_{RUD} + c_w D^2 n^2 \quad [C-23]$$

with the coefficients a_w , b_w , c_w determined from LAHPMM tests results. Coefficients a_w , b_w , c_w depend on the signs of both forward speed and propeller RPM.

Tracor Hydronautics

PMM tests conducted at zero speed yield non-linear damping coefficients $N_{r|r}'$ three to four times those determined from tests at finite forward speed. This behavior is reflected by a non-linear damping term in the yaw equation:

$$N_{r|r} = \frac{\rho}{2} L^5 \left[N_{r|r}' \cdot \left\{ 1 + 2 \left[1 - \tanh \left| \frac{2u_R}{Lr_R} \right| \right] \right\} \right] \quad [C-24]$$

This formula gives a value for the coefficient at zero speed equal to three times that for the case when the non-dimensional yawing rate, $r' = rL/u$ is less than one.

C-2. Non-Dimensional Hydrodynamic Coefficients

The procedures used to arrive at the numerical values for the sets of hydrodynamic coefficients in surge-sway-yaw differential equations given in Tables 10 to 16 are essentially the same as those described in References 3 and 8. In the interest of completeness the main features of the procedure are briefly repeated here.

In the lateral force and yawing moment equations, all terms except the "n dependent" terms are considered to constitute what have been designated as "reference" equations. As a matter of standard practice, the numerical values of the coefficients for the terms are derived from the reference LAHPMM tests, which are conducted for the case of $J = J_c$ at the ship-propulsion point defined as $\eta = 1.0$.

Non-dimensional test data Y' and N' are plotted and faired as functions of each of the appropriate non-dimensional kinematic variables such as v' , v'' , r' , and r'' . Finally, a least squares fit is applied to the faired data representing each of the functional relationships to obtain the desired non-dimensional coefficients.

Tracor Hydronautics

Certain of these functional relationships are known to be linear from considerations of theory, such as those related to acceleration, typified by $Y_{\dot{v}}'$, $Y_{\dot{r}}'$, $N_{\dot{r}}'$, and $N_{\dot{v}}'$. In such cases, only a straight-line fit is made, and the resulting numerical values can be used interchangeably as coefficients in the non-linear differential equations or as derivatives in the linearized equations of motion. A straight-line fit also is used in other cases where it is evident from the test data that the functional relationship can be closely approximated by such a fit over the entire range of practical interest. Here again, the resulting values can be treated either as first order coefficients or as derivatives. For nonlinear functional relationships, the least square fits are made to polynomials, typically carried up only to second order coefficients. (For such cases the numerical values of first order coefficients associated with second order fits are not the same as derivatives used in the linearized equations of motion.) It may be noted that many of the second order coefficients in the reference equations involve the use of absolute values of certain kinematic variables. This is done to assure proper signs in the computer representations, and is comparable to the use of third order coefficients for odd functions in the Taylor expansion method. Values of some coupling coefficients in the reference equations, such as $Y_v|r|'$ and $N_v|r|'$, can be derived by applying first order least square fits to plots of Y' and N' versus the products $v'|r|$ and $|v'|r'$, respectively. However, recent analyses of model test data from deep and shallow water programs has shown that better curve fits are provided by coefficients of the form $Y|v|r'$, Y_{vr^2}' , $N|v|r'$, and N_{vr^2}' . In both cases the data are acquired from LAHPMM yawing tests in which the model is maintained at a constant drift angle β to the oscillatory path.

Tracor Hydronautics

All of the coefficients of the n -dependent terms in the lateral force and yawing moment equations are considered to be of first order. Their values are based on linear fits to non-dimensional Y -force and N -moment plots as functions of $(n - 1)$, derived from the overload and underload PMM tests. In the axial force equations, coefficients X_{vv}' and $X_{vv\eta}'$ are derived by a process similar to that for the corresponding lateral force coefficients. The values of X_u' and X_{vr}' are estimated using PMM data obtained from other test programs. The procedure for obtaining the values of the coefficients a_i , b_i , and c_i from the net force curve, X' versus n , is described in Reference 3. Basically, these values of a_i , b_i , and c_i are generated by applying quadratic fits to the X' curve in four segments of n .

Coefficients $X_{\delta s \delta s}'$, $Y_{\delta s}'$ and $N_{\delta s}'$, as well as coefficients d , e , and f in the expression of the squared velocity:

$$U_p^2 = (d U_R^2 + e D n U_R + f D^2 n^2) \quad [C-25]$$

are derived from appropriate curve fits to the tested data.

The complete set of hydrodynamic coefficients for the ship are presented in Tables 5 to 11 for both ahead and astern motions. As noted previously some coefficients have multiple values depending on direction of motion, relative drift angle and propeller rotation. The hydrodynamic coefficients are assigned values in accordance with the following rules.

- a. The following coefficients have one of two values depending on $u_R > 0$ (+) or $u_R < 0$ (-):

$$X_u', X_{vr}', X_{vv}', X_{vv\eta}', Y_{\dot{t}}', Y_r', Y_{r|r}', Y_{|v|r}', Y_{vr}^2', \\ Y_{r\eta}', Y_{\dot{v}}', N_{\dot{t}}', N_r', N_{r|r}', N_{\dot{v}}', N_{|v|r}', N_{r\eta}', N_{vr}^2'$$

Tracor Hydronautics

- b. The following coefficients have one of four values depending on relative drift angle β_R :

$$|\beta_R| < \pm 30^\circ, 30^\circ < \beta_R < 150^\circ, 150^\circ < \beta < 210^\circ,$$

$$210^\circ < \beta_R < 330^\circ.$$

$$Y_v', Y_{v|v}|', Y_{v\eta}', Y_{v|v|\eta}', N_v', N_{v|v}|', N_{v\eta}', N_{v|v|\eta}'$$

- c. The following coefficients have one of four values depending on u_R and direction of propeller rotation, n .

$$u_R > 0, n > 0; u_R > 0, n < 0; u_R < 0, n > 0; u_R < 0, n < 0$$

$$X_{\delta_S \delta_S}', X_{\delta_F \delta_F}', Y_{\star}', Y_{\delta_S}', Y_{\delta_F}', N_{\star}', N_{\delta_F}', N_{\delta_F}',$$

$$Y_{\delta_S|v}|', N_{\delta_S|v}|'$$

$$d_i, e_i, f_i \text{ in calculation of } u_p^2.$$

$$a_w, b_w, c_w \text{ in calculation of } w_p^2.$$

- d. The following coefficients have one of eight values depending on the signs of u_R and n .

$$u_R + \text{ or } - \text{ and } -\infty < \eta < -1; -1 < \eta < 0; 0 < \eta < 1, 1 < \eta < \infty$$

$$a_i, b_i, c_i \text{ in calculation of net thrust.}$$

C-3. Simulation Procedure

The simulation program can be operated in two modes, fast time and real time. In the fast time mode, the equations are integrated as fast as possible by the computer and the rudder and propulsion system commands are controlled by some pre-determined logic. This mode is used to simulate the standard

Tracor Hydronautics

All of the coefficients of the η -dependent terms in the lateral force and yawing moment equations are considered to be of first order. Their values are based on linear fits to non-dimensional Y-force and N-moment plots as functions of $(\eta - 1)$, derived from the overload and underload PMM tests. In the axial force equations, coefficients X_{vv}' and $X_{vv\eta}'$ are derived by a process similar to that for the corresponding lateral force coefficients. The values of X_u' and X_{vr}' are estimated using PMM data obtained from other test programs. The procedure for obtaining the values of the coefficients a_i , b_i , and c_i from the net force curve, X' versus η , is described in Reference 3. Basically, these values of a_i , b_i , and c_i are generated by applying quadratic fits to the X' curve in four segments of η .

Coefficients $X_{\delta s \delta s}'$, $Y_{\delta s}'$ and $N_{\delta s}'$, as well as coefficients d , e , and f in the expression of the squared velocity:

$$U_p^2 = (d U_R^2 + e D n U_R + f D^2 n^2) \quad [C-25]$$

are derived from appropriate curve fits to the tested data.

The complete set of hydrodynamic coefficients for the ship are presented in Tables 5 to 11 for both ahead and astern motions. As noted previously some coefficients have multiple values depending on direction of motion, relative drift angle and propeller rotation. The hydrodynamic coefficients are assigned values in accordance with the following rules.

- a. The following coefficients have one of two values depending on $u_R > 0$ (+) or $u_R < 0$ (-):

$$X_{\dot{u}}', X_{vr}', X_{vv}', X_{vv\eta}', Y_{\dot{t}}', Y_r', Y_{r|r|}', Y_{|v|r|}', Y_{vr^2}'$$

$$Y_{rn}', Y_{\dot{\phi}}', N_{\dot{t}}', N_r', N_{r|r|}', N_{\dot{\phi}}', N_{|v|r|}', N_{rn}', N_{vr^2}'$$

Tracor Hydronautics

- b. The following coefficients have one of four values depending on relative drift angle β_R :

$$|\beta_R| < \pm 30^\circ, 30^\circ < \beta_R < 150^\circ, 150^\circ < \beta < 210^\circ,$$

$$210^\circ < \beta_R < 330^\circ.$$

$$Y_v', Y_{v|v}|', Y_{v\eta}', Y_{v|v}|\eta|', N_v', N_{v|v}|', N_{v\eta}', N_{v|v}|\eta|'$$

- c. The following coefficients have one of four values depending on u_R and direction of propeller rotation, n .

$$u_R > 0, n > 0; u_R > 0, n < 0; u_R < 0, n > 0; u_R < 0, n < 0$$

$$X_{\delta_S \delta_S}', X_{\delta_F \delta_F}', Y_{\delta_S}', Y_{\delta_S}', Y_{\delta_F}', N_{\delta_S}', N_{\delta_F}', N_{\delta_F}',$$

$$Y_{\delta_S|v}|', N_{\delta_S|v}|'$$

$$d_i, e_i, f_i \text{ in calculation of } u_p^2.$$

$$a_w, b_w, c_w \text{ in calculation of } w_p^2.$$

- d. The following coefficients have one of eight values depending on the signs of u_R and n .

$$u_R + \text{ or } - \text{ and } -\infty < \eta < -1; -1 < \eta < 0; 0 < \eta < 1, 1 < \eta < \infty$$

$$a_i, b_i, c_i \text{ in calculation of net thrust.}$$

C-3. Simulation Procedure

The simulation program can be operated in two modes, fast time and real time. In the fast time mode, the equations are integrated as fast as possible by the computer and the rudder and propulsion system commands are controlled by some pre-determined logic. This mode is used to simulate the standard

Tracor Hydronautics

definitive maneuvers including turns, zig-zags, and spirals. This mode also would be used for simulation of maneuvers controlled by some type of autopilot logic. In the real time mode the computer integrates equations at a rate which corresponds to real time and provides printed, plotted, or bridge simulator information on position, heading, rates, rudder angles and propeller RPM in real time. The simulation is controlled by a man in the loop making decisions based on the output information and providing input rudder and RPM commands via the analog to digital converter associated with the computer. The real time mode can be used in studies of complex maneuvers.

A flow diagram for a twin-screw ship maneuvering simulation program is presented in Figure C.2. The basic program logic is not complex. After the initial conditions are established, a loop is repeated each time step. The steps in the loop are: 1) the calculation of relative velocities, 2) the calculation of external forces, 3) the determination of control inputs, 4) the selection of the proper set of hydrodynamic coefficients, 5) the calculation of accelerations u , v , r from the equations of motion, 6) the calculation of updated velocities and positions and 7) the output of data on position velocities, etc.

The simulation program is written in FORTRAN IV and can operate on a minicomputer with 32K of core memory. In the fast time mode with a two second time step the program runs at about ten times faster than real time. Normally the results are documented by a summary of parameters at 10 second intervals and a plot showing the position every 30 seconds. Simulated maneuvers of the river tow referenced in this report were performed in the fast time mode, without current or wind, and without computer plotting.

Tracor Hydronautics

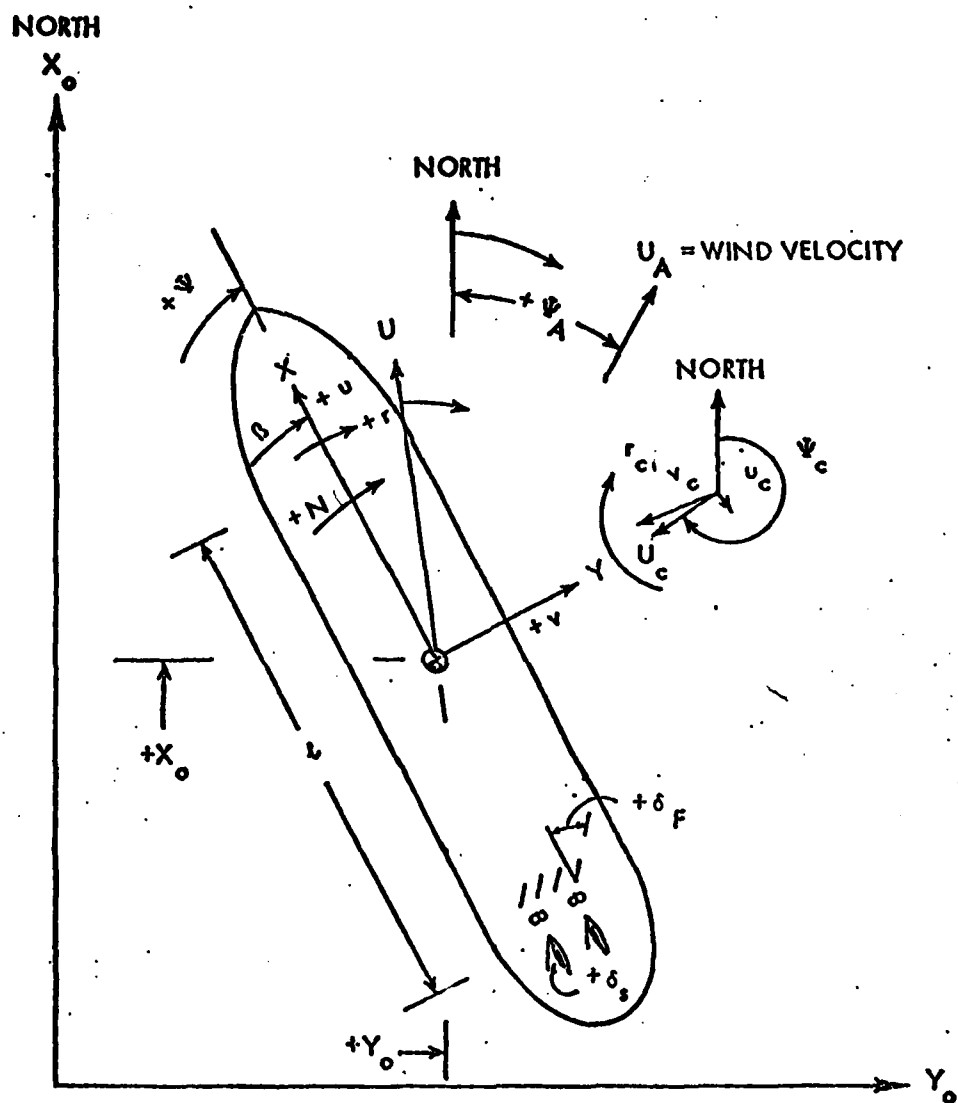


FIGURE -C.1 - SIGN CONVENTION FOR TWIN - SCREW SHIP MANEUVERING SIMULATION.

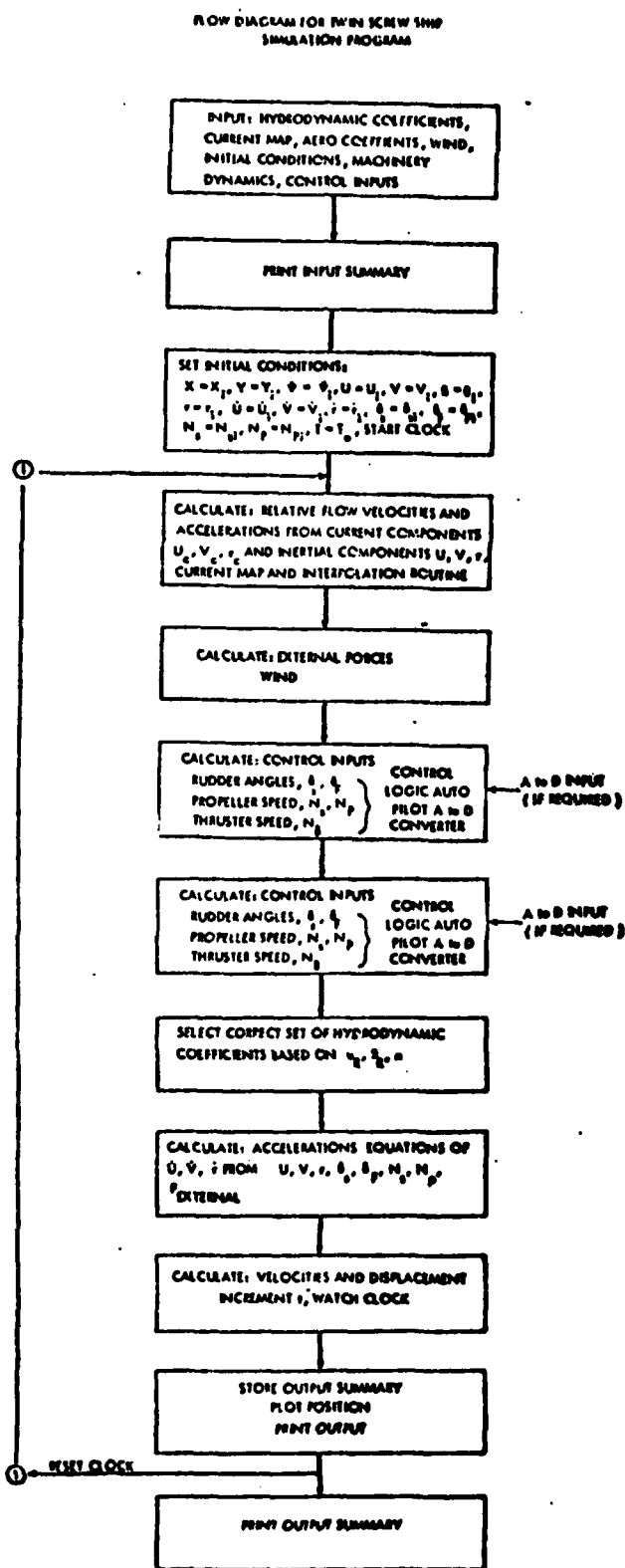


FIGURE C.2 - FLOW DIAGRAM FOR TWIN SCREW SHIP MANEUVERING SIMULATION PROGRAM

Tracor Hydronautics

APPENDIX D

NEAR-BANK AND WAVY-BOTTOM INTERACTION TEST DATA FOR 7.5 FOOT
(PROTOTYPE) DRAFT TOWBOAT WITH 15-BARGE TRAIN

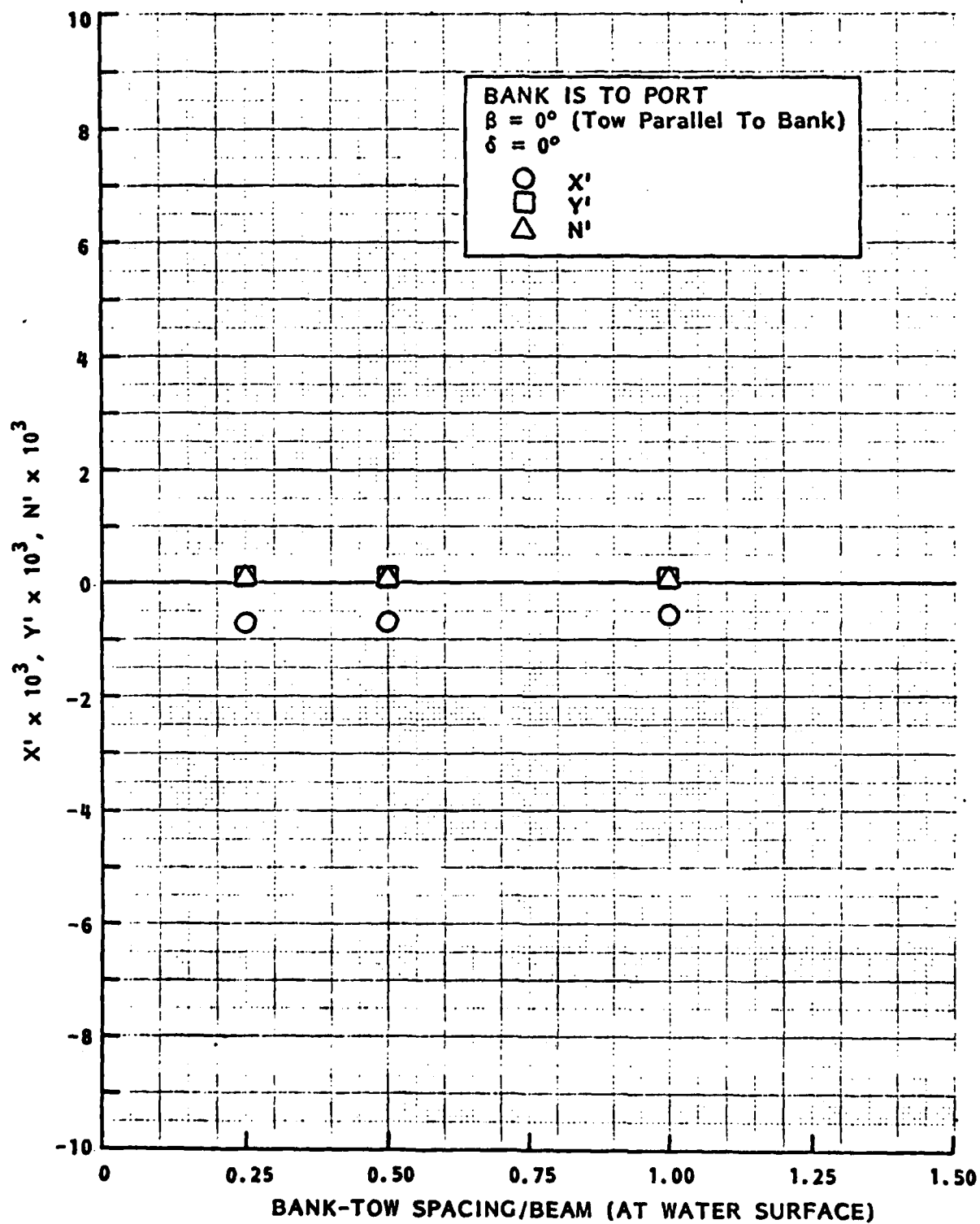


FIGURE D.1 - AXIAL FORCE, LATERAL FORCE AND YAW MOMENT COEFFICIENTS AS FUNCTIONS OF BANK-TOW SPACING FOR AHEAD MOTION AT $\eta = 1$ IN SHALLOW WATER, $H/T = 1.50$

Tracer Hydronautics

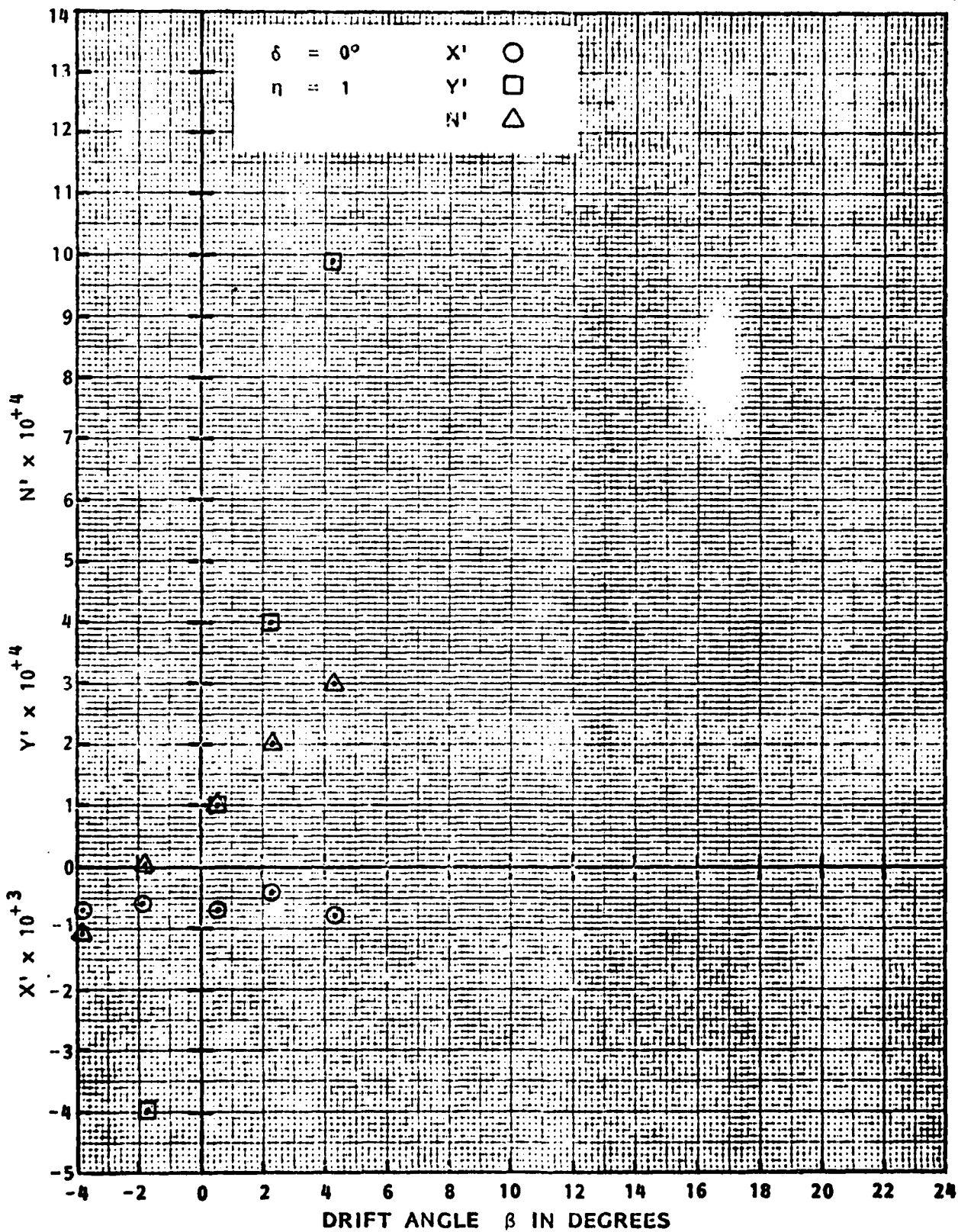


FIGURE D.2 - AXIAL FORCE, LATERAL FORCE, AND YAW MOMENT COEFFICIENTS AS FUNCTIONS OF DRIFT ANGLE β WITH BANK-TOW SPACING OF 0.50 BEAM. AHEAD MOTION AT $\eta = 1$ IN SHALLOW WATER, $H/T = 1.50$

Tractor Hydronautics

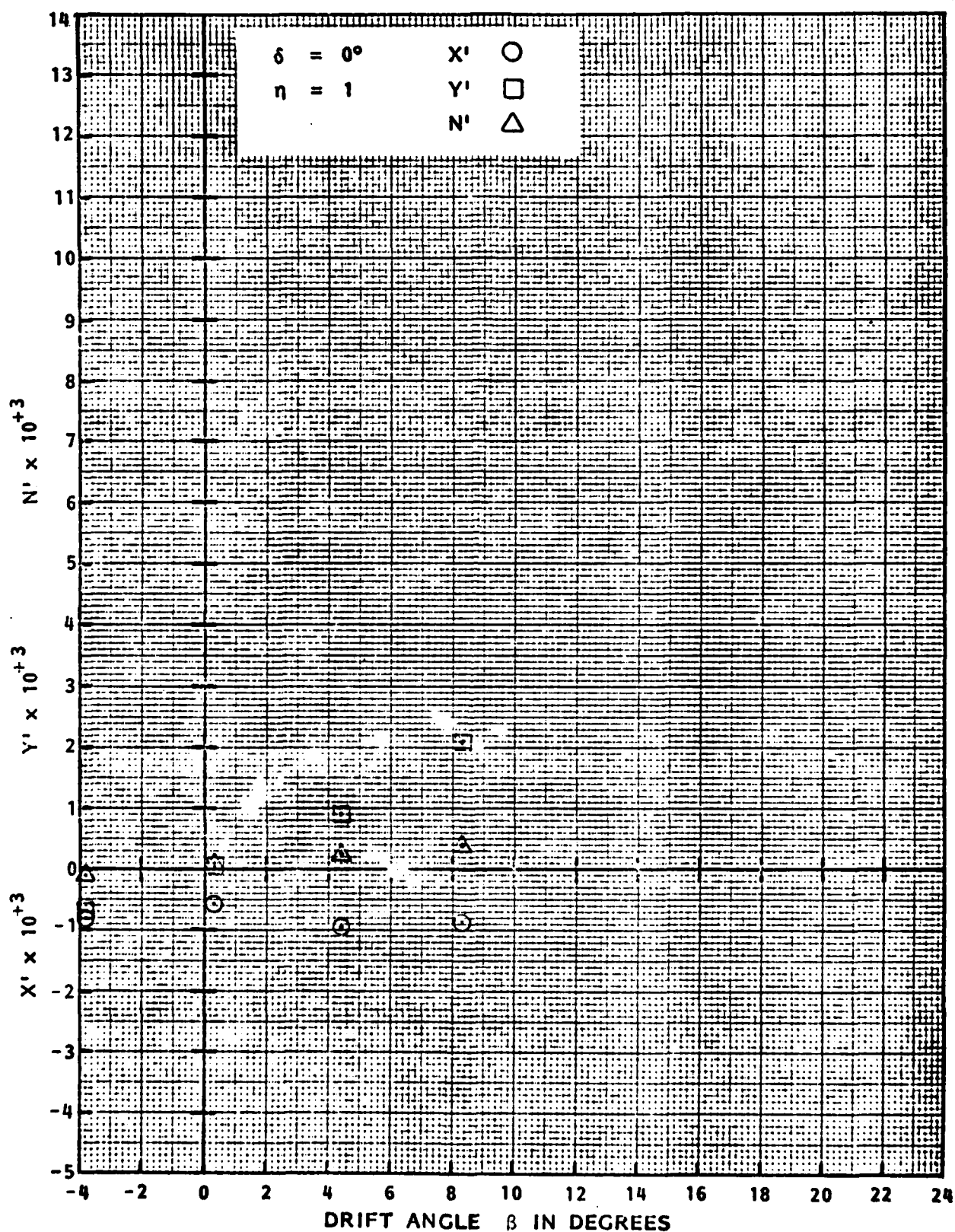


FIGURE D.3 - AXIAL FORCE, LATERAL FORCE, AND YAW MOMENT COEFFICIENTS AS FUNCTIONS OF DRIFT ANGLE β WITH BANK-TOW SPACING OF 1.00 BEAM. AHEAD MOTION AT $\eta = 1$ IN SHALLOW WATER, $H/T = 1.50$

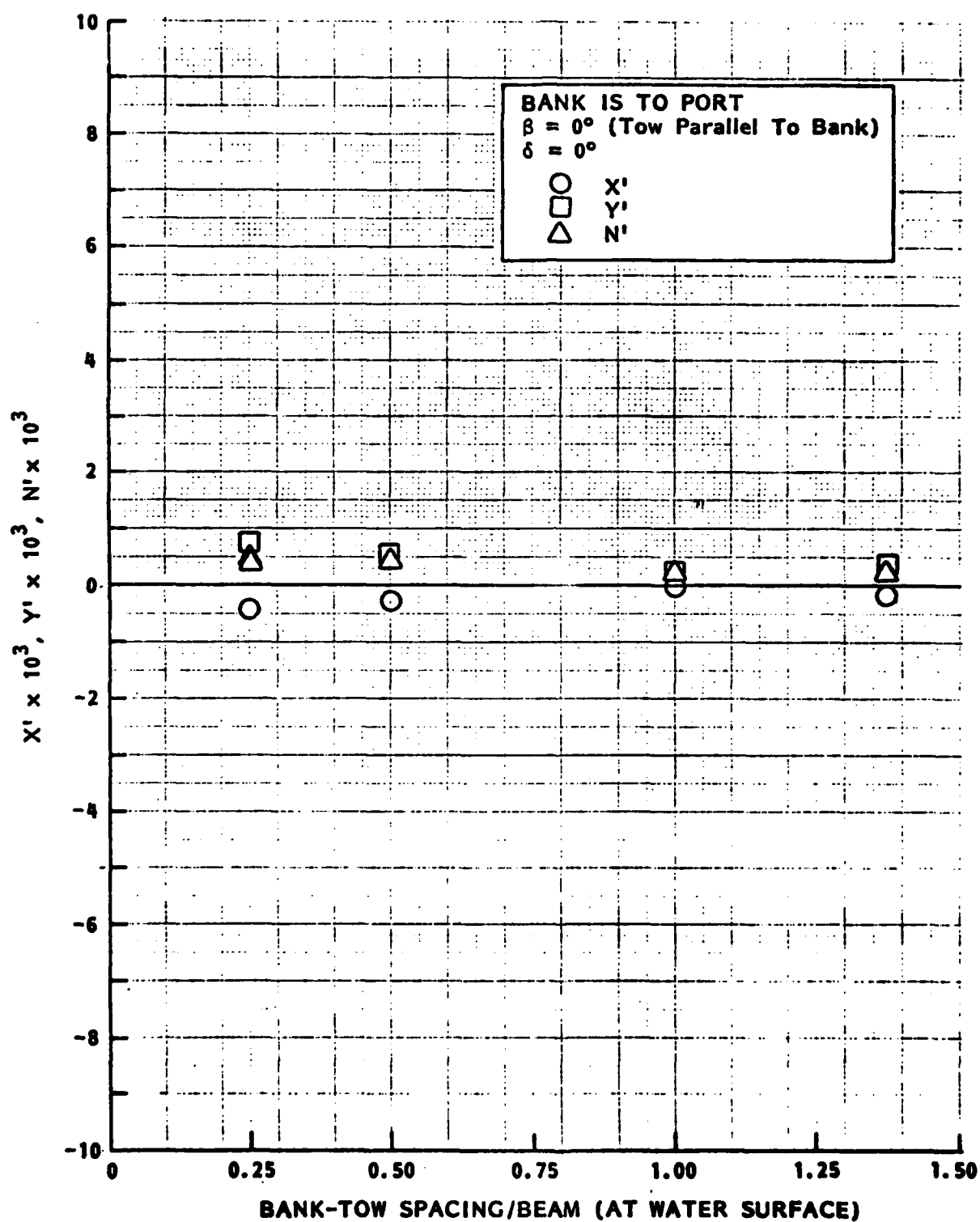


FIGURE D.4 - AXIAL FORCE, LATERAL FORCE AND YAW MOMENT COEFFICIENTS AS FUNCTIONS OF BANK-TOW SPACING FOR AHEAD MOTION AT $\eta = 1$ IN SHALLOW WATER, $H/T = 1.17$

Tracor Hydronautics

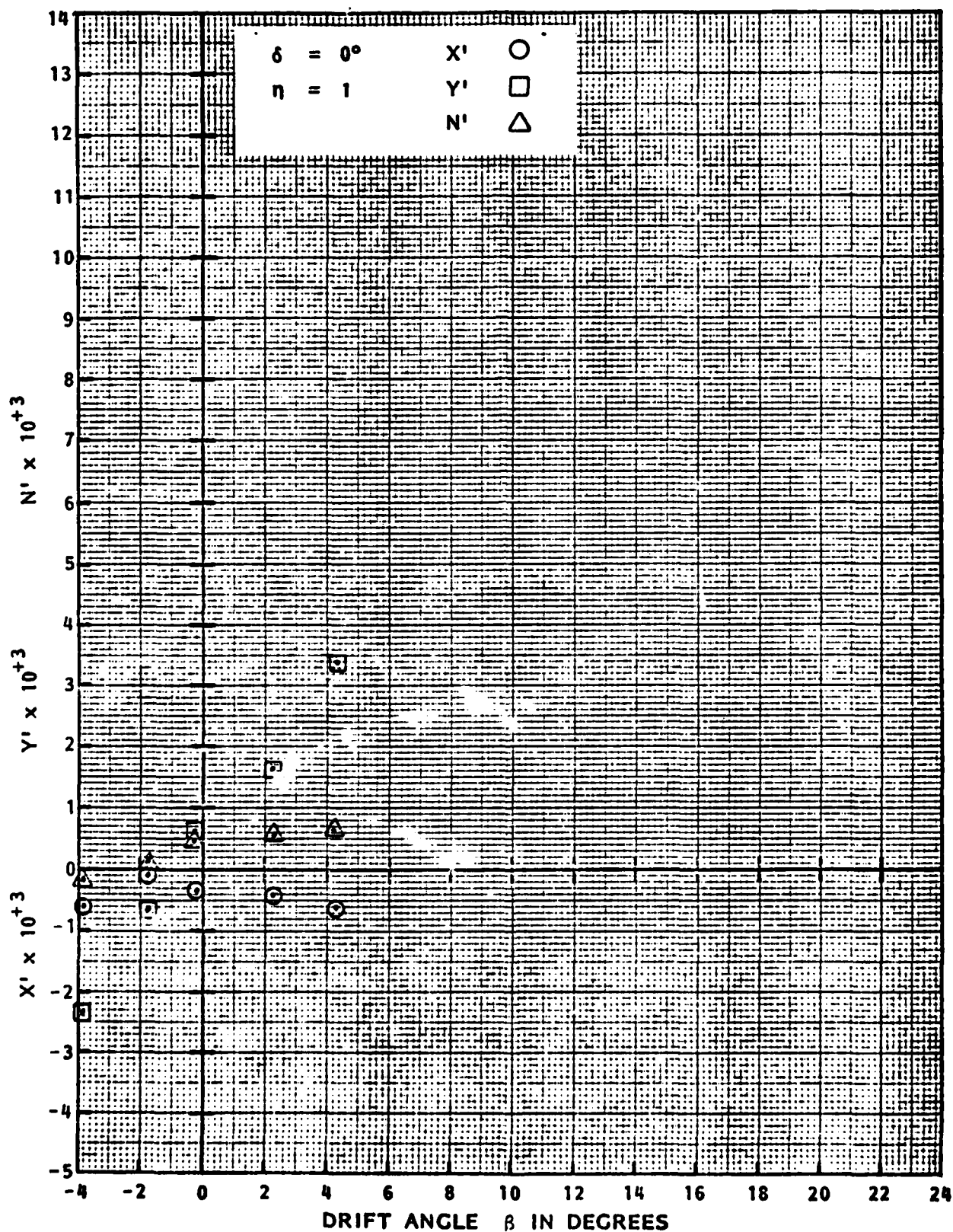


FIGURE D.5 - AXIAL FORCE, LATERAL FORCE, AND YAW MOMENT COEFFICIENTS AS FUNCTIONS OF DRIFT ANGLE β WITH BANK-TOW SPACING OF 0.50 BEAM. AHEAD

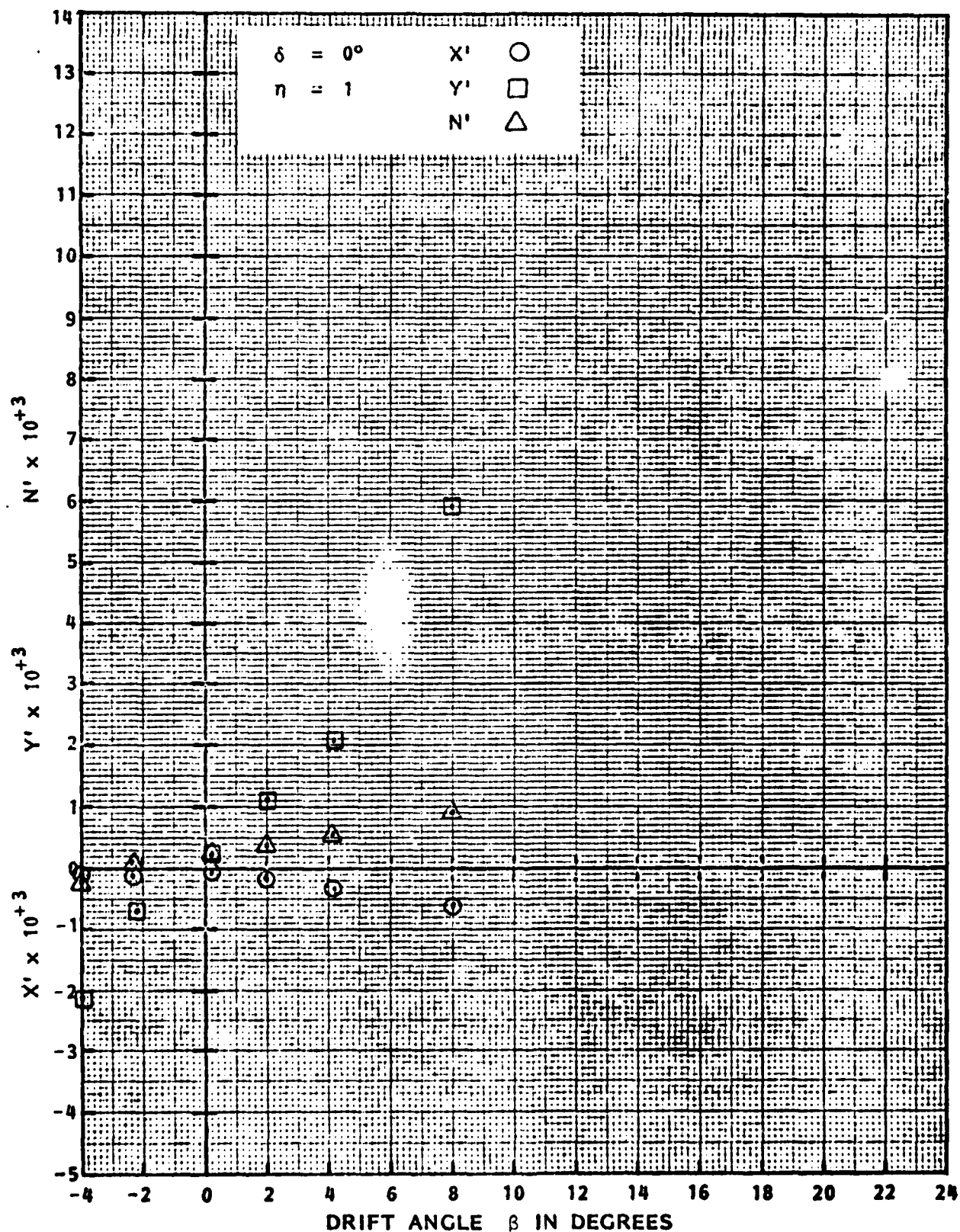


FIGURE D.6 - AXIAL FORCE, LATERAL FORCE, AND YAW MOMENT COEFFICIENTS AS FUNCTIONS OF DRIFT ANGLE β WITH BANK-TOW SPACING OF 1.00 BEAM. AHEAD MOTION AT $\eta = 1$ IN SHALLOW WATER, $H/T = 1.17$

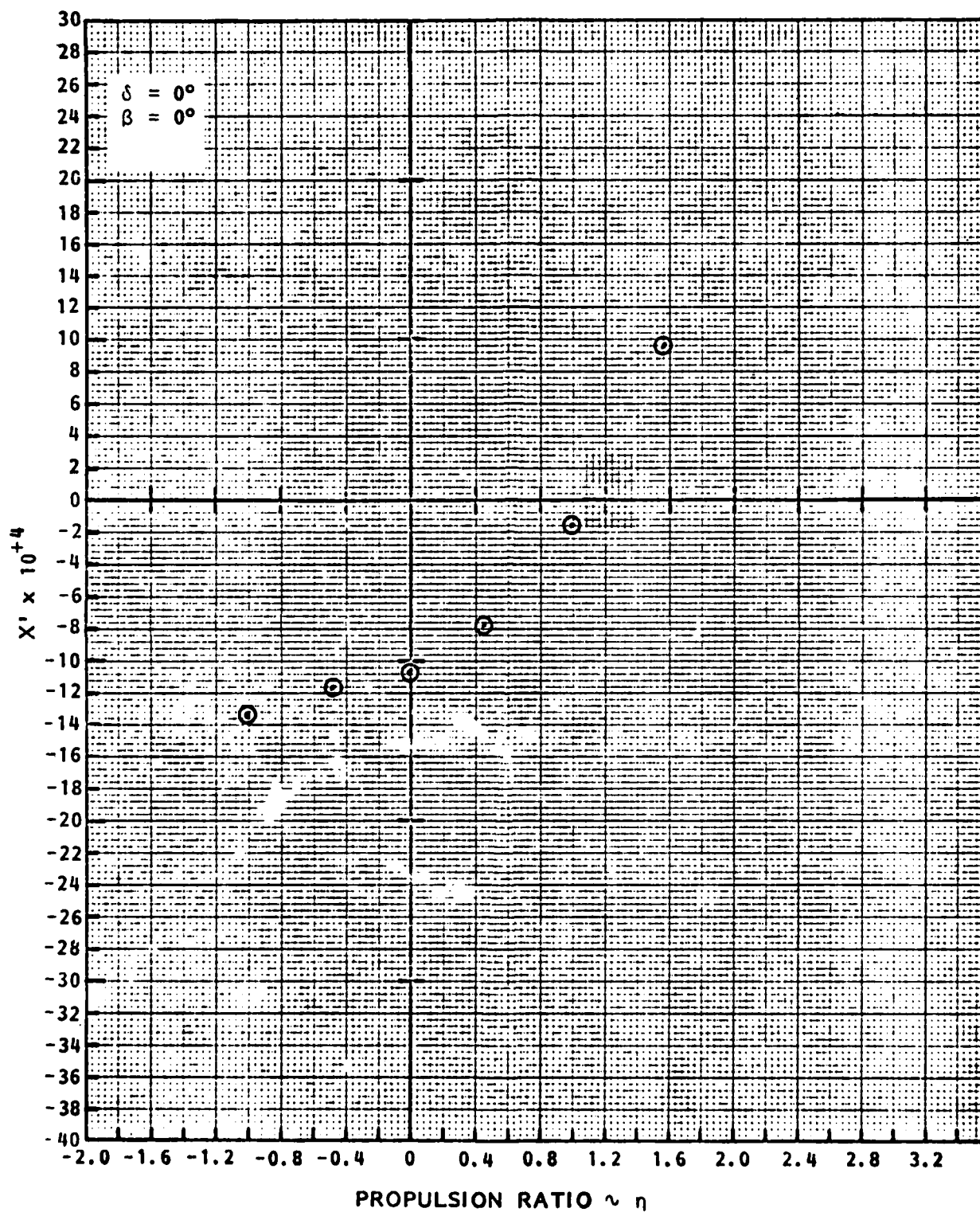


FIGURE D.7 - AXIAL FORCE COEFFICIENT AS FUNCTION OF PROPULSION RATIO η FOR AHEAD MOTION OVER IRREGULAR BOTTOM

Tracor Hydronautics

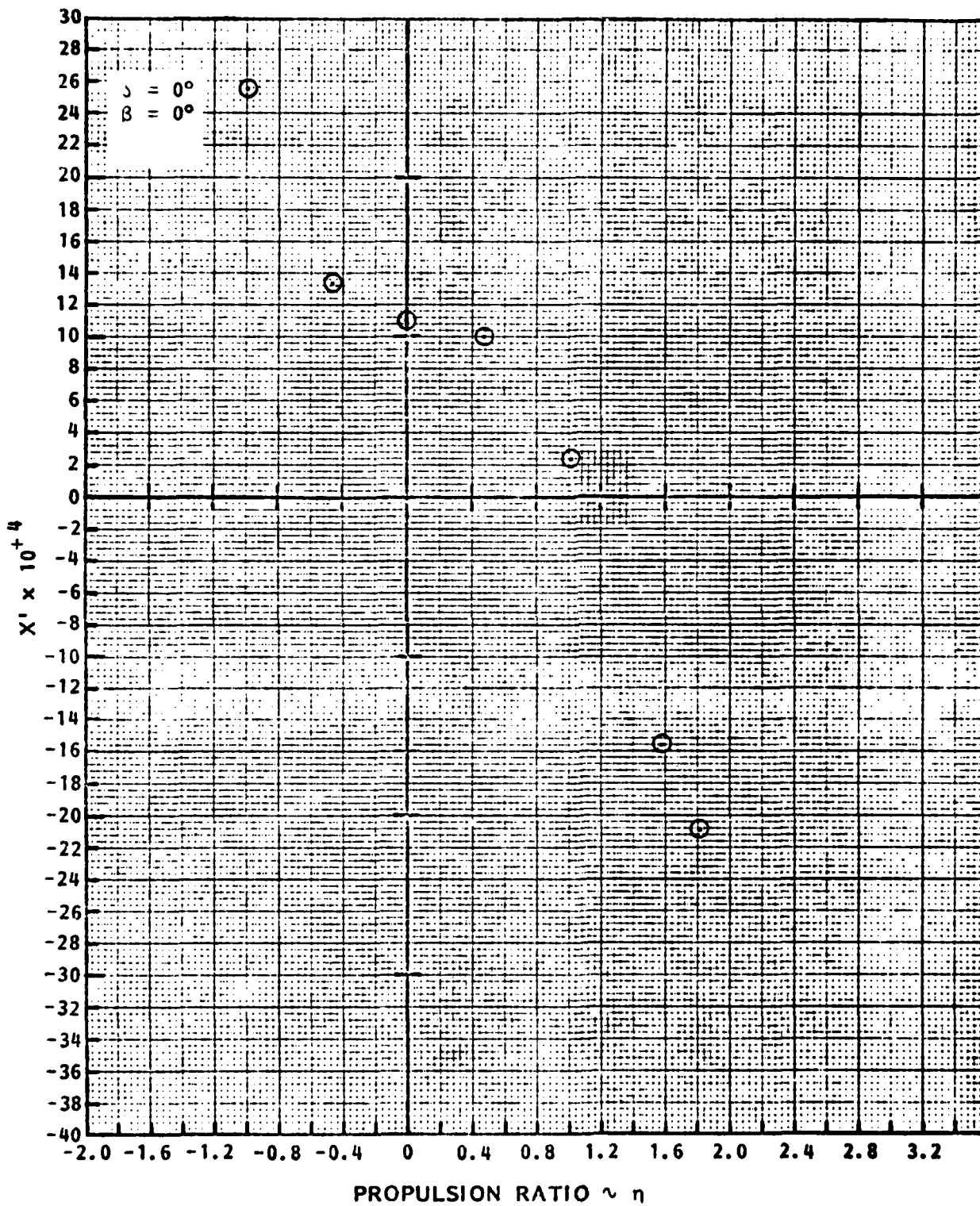


FIGURE D.8 - AXIAL FORCE COEFFICIENT AS FUNCTION OF PROPULSION RATIO η FOR ASTERN MOTION OVER IRREGULAR BOTTOM

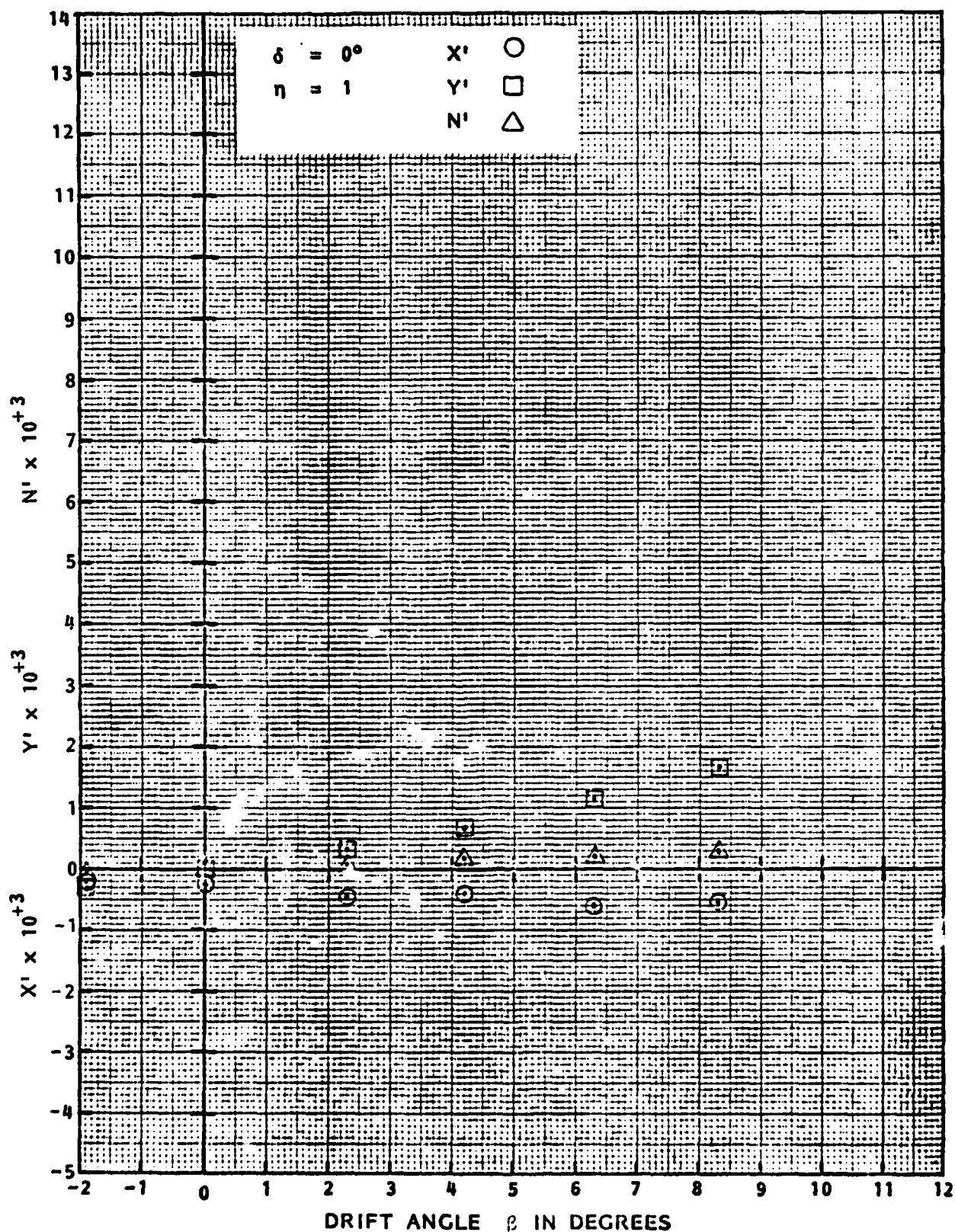


FIGURE D.9 - AXIAL FORCE, LATERAL FORCE, AND YAW MOMENT COEFFICIENTS AS FUNCTIONS OF DRIFT ANGLE β FOR AHEAD MOTION AT $\eta = 1$ OVER IRREGULAR BOTTOM

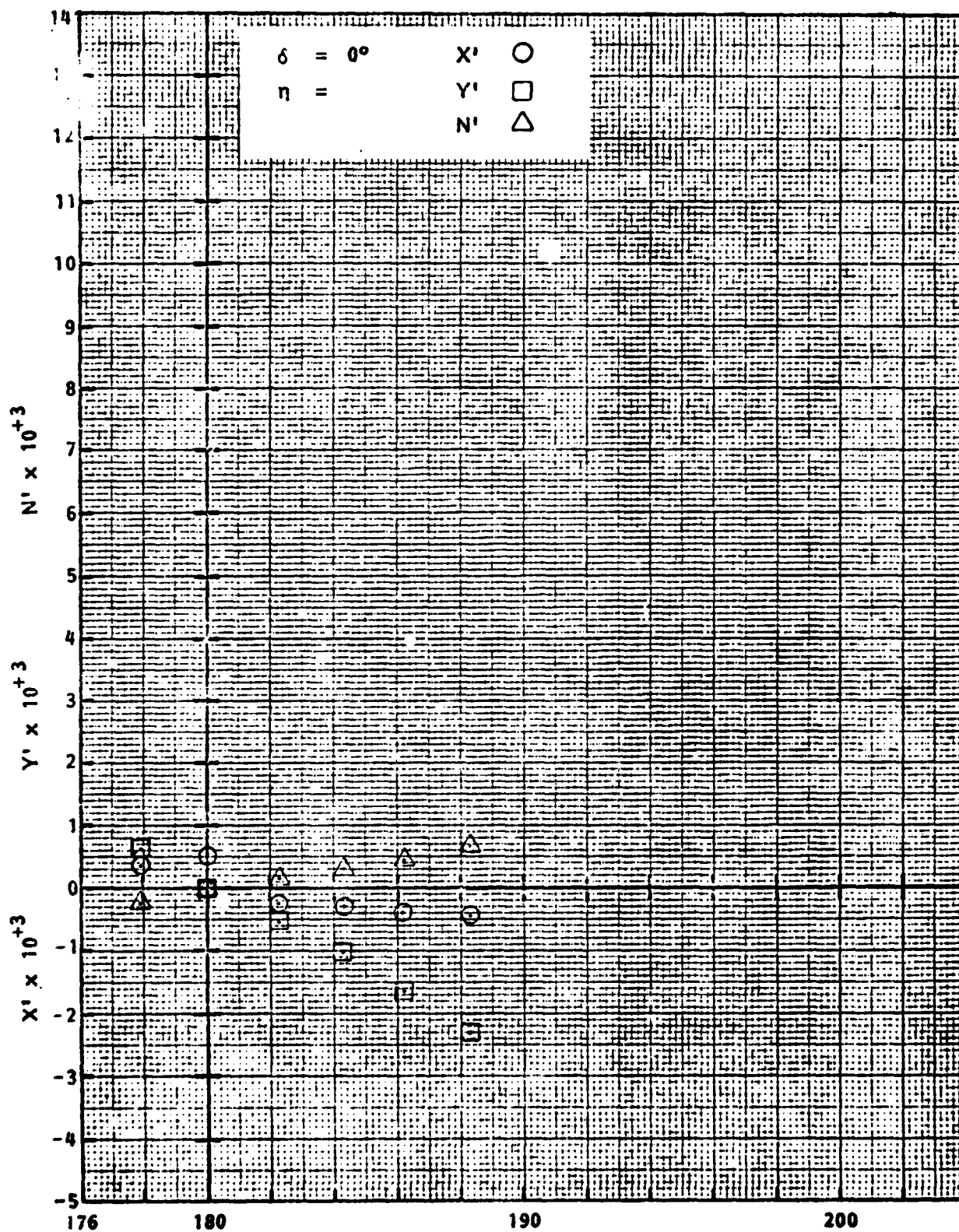


FIGURE D.10 - AXIAL FORCE, LATERAL FORCE, AND YAW MOMENT COEFFICIENTS AS FUNCTIONS OF DRIFT ANGLE β FOR ASTERN MOTION AT $\eta = 1$ OVER IRREGULAR BOTTOM

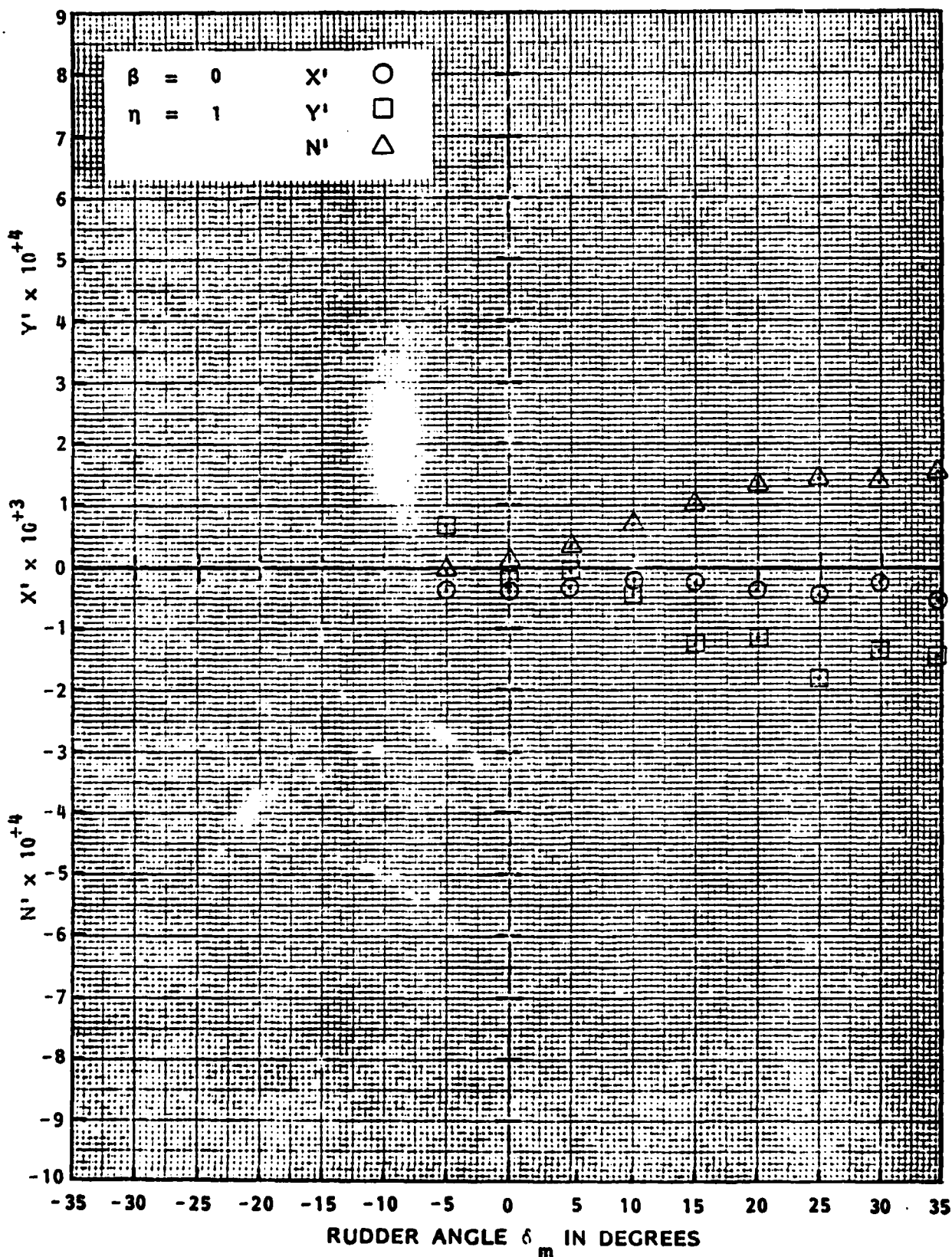


FIGURE D.11 - AXIAL FORCE, LATERAL FORCE AND YAW MOMENT COEFFICIENTS AS FUNCTIONS OF MAIN RUDDER ANGLE δ_m FOR AHEAD MOTION AT $\eta = 1$ OVER IRREGULAR BOTTOM

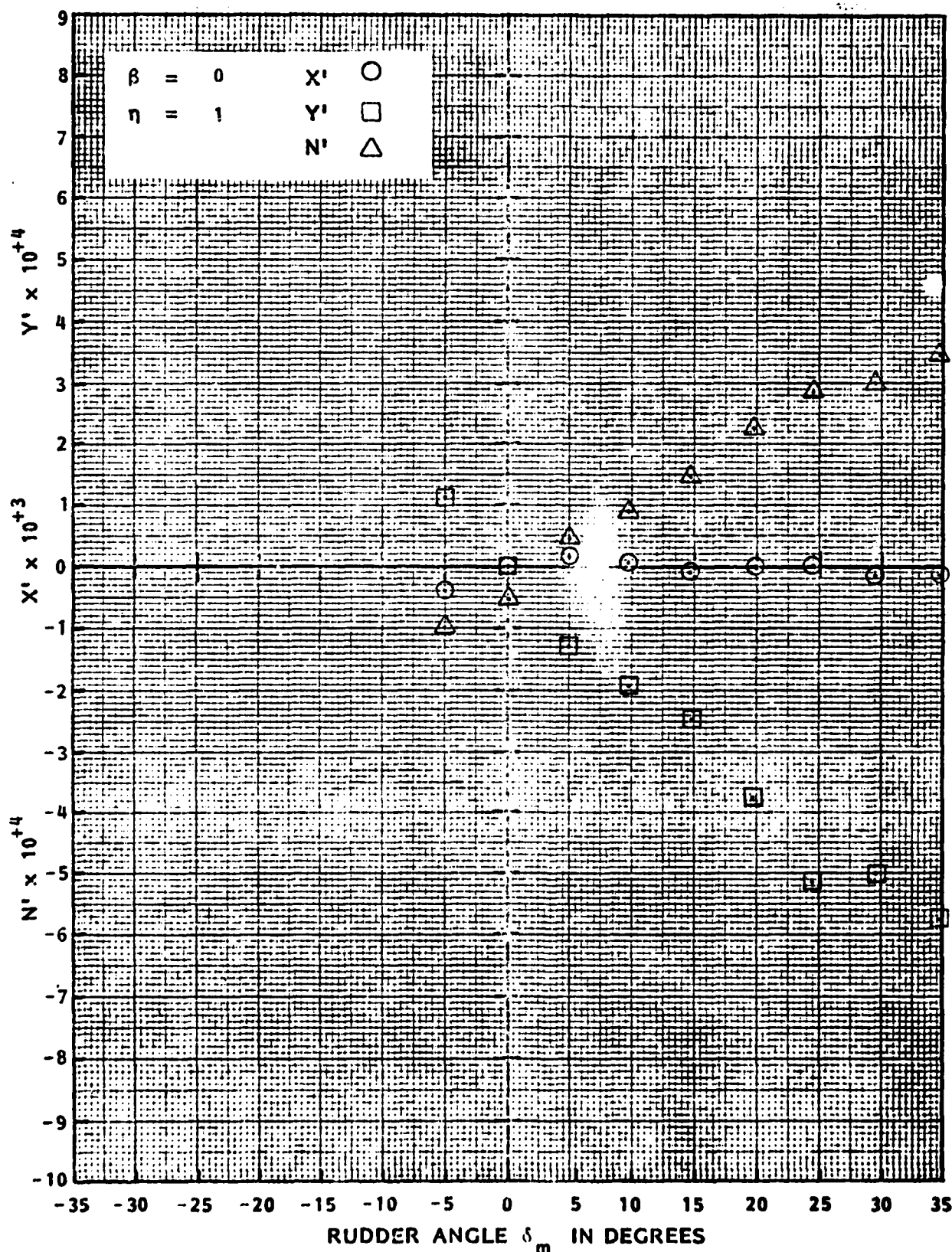


FIGURE D.12 - AXIAL FORCE, LATERAL FORCE AND YAW MOMENT COEFFICIENTS AS FUNCTIONS OF FLANKING RUDDER ANGLE δ_f FOR ASTERN MOTION AT $\eta = 1$ OVER IRREGULAR BOTTOM

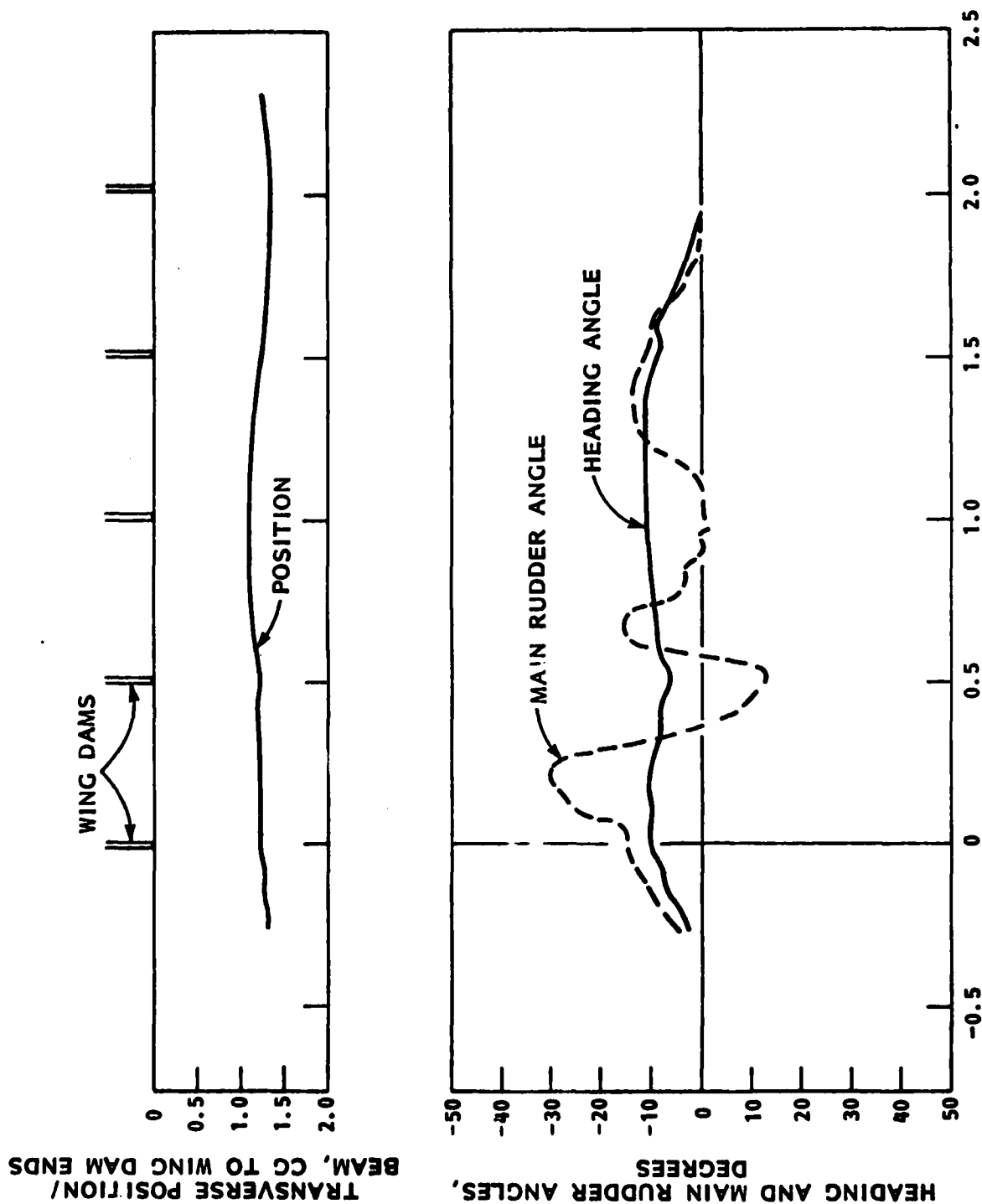


FIGURE D.13 - TRACK PLOT FOR FREE RUNNING TEST WITH WING DAMS, RUN NO. FW 1

END

FILMED

1-84

DTIC